JULY 1966

WDL-TR2962
VOLUME II
SIMULATION

FAN BEAM
NAVIGATION SATELLITE STUDY

NASA-CR-80025

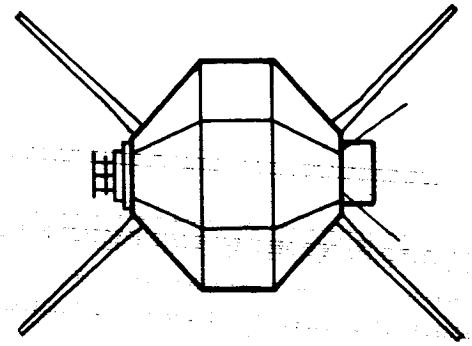

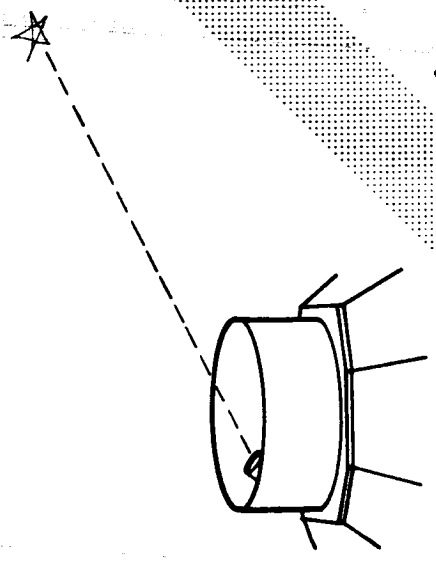

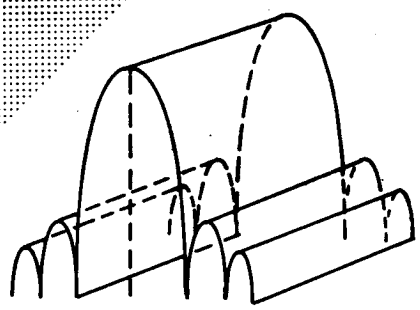

FACILITY FORM 602

N67-31489
(ACCESSION NUMBER)

197
(PAGES)

CR-80025
(NASA CR OR TMX OR AD NUMBER)

(THRU)
1
(CODE)
21
(CATEGORY)

CONTRACT
NUMBER
NASW-1368

Submitted to

HEADQUARTERS NATIONAL AERONAUTICS AND SPACE ADMINISTRATION
WASHINGTON, D.C.

PHILCO
A SUBSIDIARY OF Ford Motor Company
WDL DIVISION
PALO ALTO-CALIFORNIA
HOUSTON-TEXAS

WDL TECHNICAL REPORT 2962

FAN BEAM NAVIGATION SATELLITE STUDY

Volume II

SIMULATION STUDIES

13 July 1966

Contract No. NASW-1368

Submitted to:

Headquarters
National Aeronautics and Space Administration
Washington, D.C.

Prepared by

PHILCO CORPORATION
A Subsidiary of Ford Motor Company
WDL Division
Palo Alto, California

TABLE OF CONTENTS

TABLE OF CONTENTS (Continued)

LIST OF ILLUSTRATIONS

LIST OF ILLUSTRATIONS (Continued)

LIST OF ILLUSTRATIONS (Continued)

LIST OF ILLUSTRATIONS (Continued)

LIST OF ILLUSTRATIONS (Continued)

LIST OF TABLES

SECTION 1

INTRODUCTION AND SUMMARY

1.1 SIMULATION PROCEDURES

There are essentially two major types of computational processes needed to simulate the fan-beam navigation concept in action. First (A), on the basis of the dynamical model assumed, accurate digital calculations must be made for all time-varying quantities, to represent true states as they would occur in nature. Second (B), the important factors which influence the navigator's knowledge of the true state at any time must be applied singly and in combination, and the resultant effect on his position estimate determined.

The mathematics for the type (A) processes include: several transformations relating the various coordinate systems, satellite orbital motion as a function of time (requiring iterative solution of Kepler's equation), satellite attitude motion in closed form (a torque-free inertially symmetric spinning body is assumed), motion of the navigator relative to the earth, satellite antenna pattern, iterative procedures to compute time from prescribed conditions of state (needed to evaluate the times of the fan-beam passages at the navigator site).

Needed for the type (B) calculations are: delineation of the important sources of error in the position estimation (system motions, miscalibration of satellite angular velocity and antenna boom orientations, timing bias and noise, etc.); methods of impressing these errors on the system; consideration of types of calibration methods; "fix" computation methods; use of data smoothing techniques.

1.2 RESULTS OBTAINED

All simulations were performed for two satellite altitudes: 5000 and 19,311 n. miles. Various navigator locations relative to the satellite were assumed.

It was found that timing errors due to a finite (i.e. non-ideal planar) antenna pattern are correlated closely with the difference of the two fan-beam detection times, and are independent of particular navigator locations. These errors can thus be removed in calibration. Fix errors due to earth and satellite orbital motion and independent navigator motion appear to be insignificant except for the most demanding navigation requirements. For small errors in the navigator's knowledge of the satellite angular velocity vector direction, the consequent fix error varies linearly. A relatively simple type of calibration should make this effect inconsequential. Errors in knowledge of the orientations of the satellite antenna booms at prescribed reference times result in fix error curves somewhat different from those for angular velocity errors, and can cause more severe fix errors. For the same navigator site, the higher altitude satellite yields smaller fix errors than the lower for these studies in which no noise is assumed.

When N fixes in sequence are examined, it is found that typical fix error curves oscilate with a non-trivial amplitude, due to the changing satellite attitude. A single fix can easily "catch" the satellite in an unfavorable attitude. When a set of 11 fixes is averaged, very good results are obtained. When noise is applied to fan timing measurements, longer smoothing times are beneficial. Also, because of lower signal-to-noise ratios, the higher satellite fixes are less accurate than the lower for the same navigator site. It is found that a simple "time smoothing" technique is equivalent to smoothing fully calculated fixes. Finally, "operational" Navigational Satellite cases are run, in which satellite transmitter power, satellite antenna length and receiver antenna diameter are varied, as well as smoothing time, yielding a variation in the fix error of an order of magnitude.

1.3 NOTES

It will be noticed that the "case" numbers in the labelling of the graphical figures are not in a strictly ascending sequence thru the

report. This is because the order of presentation chosen differs from the order in which the computer runs were made. Also, some of the cases run have been omitted entirely to avoid repetition of nearly identical material.

Allusions to the references listed in Section 6 are made by means of brackets, [ ].

SECTION 2

SIMULATION MODEL

The simulation of the fan beam navigation concept, as implemented in the digital computer programs, will be described here in general terms. Full details of the procedures will be found in Section 3, supplemented by Section 5.

2.1 SATELLITE MODEL

A spinning satellite possessing an axis of inertial symmetry is assumed, and this axis forms one of the satellite coordinate axes. The angular momentum vector does not necessarily coincide with the axis of symmetry (although, of course, they do coincide in the ideal, or nominal, case). It is assumed that no torques are acting on the spinning body. These assumptions concerning the rotational dynamics are considered reasonable over the short time spans involved in the gathering of fan timing data for fix computations.

Two fan beam antennas are presumed mounted on the satellite structure, in the form of slotted planar, in-line, resonant arrays. In the nominal configuration, the two boom antennas are coplanar with the axis of symmetry and form an angle of 45 degrees and 135 degrees with that axis, respectively. Actually, preciseness in these mounting angles is not essential to the fix computations. In the more accurate of the computational procedures, what is needed by a navigator is accurate knowledge of the orientation in inertial space of the two booms at prescribed points in time--the times of the "reference pulses," discussed in Section 3.5. The effect of errors in this knowledge is one of the items considered in the computer simulation. It is realized, of course, that an actual boom antenna on a spinning satellite may undergo a deflection due to centrifugal force. Quantitative effects regarding this, and resultant effects upon the propagated antenna pattern, are discussed in Volume III of the study report. In practice, it would be the task of calibration stations to provide navigators with inertial reference vectors, at prescribed reference times, which are good estimates

for the actual antenna arrays on the satellite. One method of doing this is given in Section 5.3 (See also Section 3.7.1.)

At the start of the simulation, any set of initial conditions for the satellite may be assigned as regards position and translational velocity relative to the earth, initial attitude, and initial angular velocity vector. At any later time the true position and attitude of the satellite are obtained by an iterative solution of Kepler's equation (a conic orbit is assumed), and a closed-form solution of Euler's equations of motion for a torque-free spinning body with an axis of inertial symmetry.

2.2 NAVIGATOR MODEL

The navigator, at the start of the simulation, may be placed at any point relative to the satellite by prescribing a distance from the subsatellite point, an azimuth angle with respect to the orbit plane, and an altitude above the earth's surface. A velocity relative to the earth may be assigned in terms of a constant magnitude and initial azimuth with respect to north. At any subsequent time the true position of the navigator is computed on the assumption of a great circle course.

During an interval of time covering a set of satellite revolutions, the time points t_1 and t_2 at which the midplanes of the first and second fan beams pass the navigator are computed--a pair of such time points for each satellite revolution during the interval. Also, on each satellite revolution, a reference time t_o is computed to represent the times at which the spatial orientations of the satellite antenna booms are known (with some degree of accuracy), through the smoothing procedures of calibration stations.

In the simulation, the sets of ideal fan passage times t_1, t_2 may be perturbed in various ways by adding biases or noise to represent actual measurements of these quantities by the navigator. Also, a mathematical model of an actual fan beam pattern is available, so that threshold

detection of leading and trailing edges of the beam may be simulated. The times t_1 and t_2 for a particular satellite revolution are then estimated by averaging the threshold times, with or without addition of bias and noise.

The sets of time points t_o, t_1 and t_2 for one or more satellite revolutions are employed by the navigator to estimate his geographic position. There are several computational methods, varying in complexity and attainable accuracy of position fix. Where timing data from several satellite revolutions are employed, smoothing techniques are applied. These methods are discussed in Section 3.7.

2.3 ERROR SOURCES AND OPTIONS

The computer simulation includes means for evaluating the effects of numerous error sources, both dynamic and static. The dynamic sources (items A, B and C below) are operative during the time intervals separating the reference pulse, t_o, and the times, t_1 and t_2, for each fan beam detection by the navigator. If necessary, the position deviation resulting from these sources could presumably be calibrated out of the actual NavSat System. Section 5.1 contains a navigator fix computation method which includes the effects of items A and B. Indeed, control of the magnitude of the errors described in items D through J is also possible, depending upon the degree of sophistication of the calibration procedures.

In general, the major sources affecting the navigator's fix calculation are:

A. Earth rotation
B. Satellite orbital motion
C. Navigator motion relative to the earth (a great-circle, constant-speed path is assumed)
D. Errors in knowledge of satellite angular velocity vector misalignment with the axis of symmetry
E. Errors in knowledge of satellite angular velocity magnitude
F. Errors in knowledge of satellite antenna mounting angles

G. Errors in knowledge of satellite attitude
H. Errors in knowledge of satellite position and velocity
I. Antenna pattern characteristics
J. Bias in knowledge of the reference pulse time
K. Bias and noise in fan timing measurement.

In simulation, any one (or more) of the above error sources may be made operative, with the remaining sources assumed non-existent. For example, the effect of earth rotation or satellite orbital motion upon computation of the "fix" may be determined, with all other sources assumed zero. This may be done for a succession of assumed mavigator initial positions relative to the satellite. Also, program action may be caused to proceed through any prescribed number of satellite revolutions, with optional smoothing of fan beam detection times and position computations.

In another mode, the simulation programs may be made to cycle repeatedly with any of the error sources A through K in operation and with independent incrementation of as many as four chosen system parameters. Some examples of parameters which may be varied in this way are:

- Navigator azimuth from satellite orbit plane
- Navigator distance from subsatellite point
- Satellite latitude
- Satellite longitude
- Number of satellite antenna slots
- Receiver energy-detection threshold level.

The main usage of this facility is to study the effects of the error sources upon the navigator's fix computations, for various choices of navigator position relative to the satellite. The navigator positions are taken systematically as the intersection points in Figure 2-1.

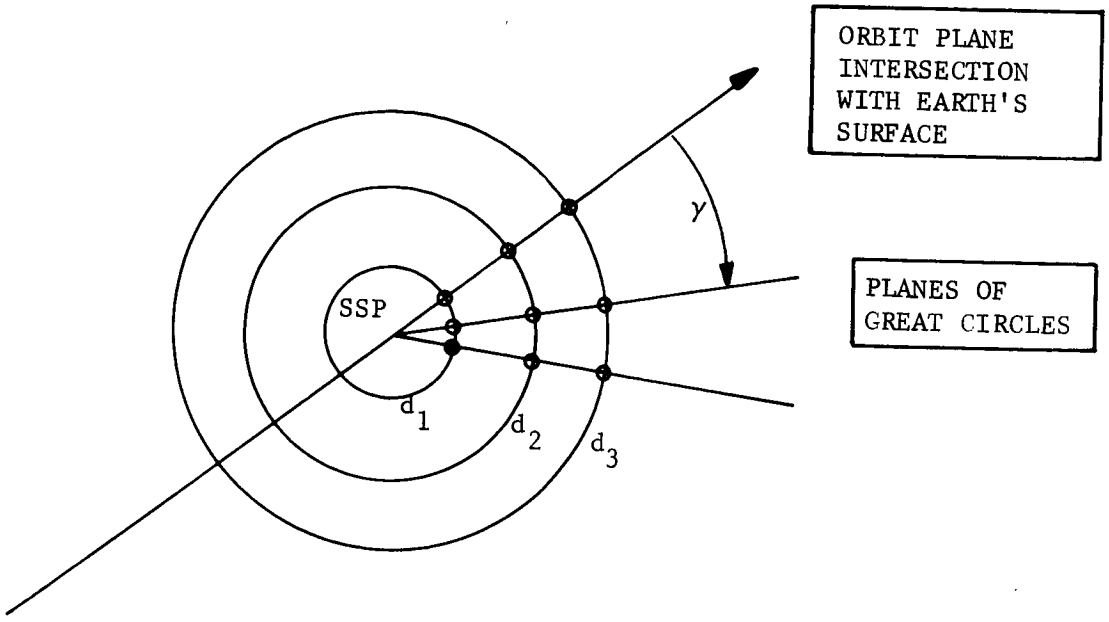

Figure 2-1 Navigator Positions

The circles d_i are circles of constant distance, measured along the curved surface of the earth, from the subsatellite point SSP. For each distance $d = d_i$, the azimuth angle γ is allowed to vary at equal increments over a given range. Various relationships from the simulation may then be plotted as functions of γ, with several curves per plot representing the values of d.

2.4 NAVSAT DIGITAL COMPUTER PROGRAMS

Four versions of the basic Fortran II digital computer program (differing only slightly) have evolved during the course of the NavSat simulation. Also, two additional programs were written to study alternative navigator methods in computing a fix.

A. Basic, single fix program

B. N-revolution program (N + 1 fixes) without smoothing of output. Plots from this program show the effects of precession upon the relative accuracies of successive fixes.

C. N-revolution program (N + 1 fixes), with or without noise and bias on timing measurements, with smoothing of the set of position calculations and smoothing of the sets of $t_1 - t_o$ and $t_2 - t_o$ values

D. N-revolution program (N + 1 fixes), with a 1σ error impressed upon the average $t_1 - t_o$ and average $t_2 - t_o$, where σ is a function of the fan beam and receiver properties as well as $\sqrt{N}$

E. Polynomial method for navigator computation of fix:

$$\text{latitude} = \sum_{j=0}^{n} \sum_{i=0}^{n} a_{ij}(t_2 + t_1)^i (t_2 - t_1)^j$$

$$\text{longitude} = \sum_{j=0}^{n} \sum_{i=0}^{n} b_{ij}(t_2 + t_1)^i (t_2 - t_1)^j \qquad (1)$$

where the a_{ij} and b_{ij} are computed by a least squares fitting procedure.

F. Differential method for navigator computation of fix:

$$d(\text{lat.}) = \frac{\partial(\text{lat.})}{\partial(t_2 + t_1)} \Delta(t_2 + t_1) + \frac{\partial(\text{lat.})}{\partial(t_2 - t_1)} \Delta(t_2 - t_1)$$

$$d(\text{lon.}) = \frac{\partial(\text{lon.})}{\partial(t_2 + t_1)} \Delta(t_2 + t_1) + \frac{\partial(\text{lon.})}{\partial(t_2 - t_1)} \Delta(t_2 - t_1). \qquad (2)$$

In addition to the construction of the above programs, an existing Plot Program was generalized to allow the flexibility needed for the present study. The graphical output is obtained from the Stromberg Carlson 4020 Cathode Ray Tube Microfilm Recorder and is of excellent quality.

SECTION 3

PROCEDURES AND EQUATIONS

The equations, transformations, iterations and other procedures which are used in the Navigational Satellite digital computer programs to perform the simulation described in Section 2 will now be given in detail.

3.1 NOTATION

Definitions will be given here for the several coordinate systems which are used, and also for most of the other quantities of importance.

$\hat{E}$-system: Earth-centered equatorial inertial system. $\hat{E}_3$ is directed toward the north pole, $\hat{E}_1$ is directed toward the vernal equinox and $\hat{E}_2$ completes a right-handed system.

$\hat{e}'$-system: Satellite-centered system. $\hat{e}'_1$ is directed along the satellite velocity vector, $\hat{e}'_3$ is in the orbit plane and directed perpendicularly to $\hat{e}'_1$ toward the earth. $\hat{e}_2$ completes a right-handed system.

$\hat{e}$-system: Satellite-centered system fixed in the body. $\hat{e}_2$ lies along the principal axis of inertial symmetry. The $\hat{e}$-system coincides with the $\hat{e}'$-system in the case of zero roll, pitch and yaw.

$\hat{f}$-system: Satellite-centered inertial system, coinciding with the $\hat{e}$-system as of time 0 (i.e. as of initial conditions).

$\hat{a}$-system: Coordinate system for fan beam No. 1. $\hat{a}_1$ lies along the antenna boom, $\hat{a}_2$ is in the direction of unity (maximum) gain and $\hat{a}_3$ completes a right-handed system. (See Section 3.2.)

$\hat{b}$-system: Coordinate system for fan beam No. 2, defined analogously to the $\hat{a}$-system.

M_{yx}: General notation for the orthogonal transformation from $\hat{x}$-coordinates to $\hat{y}$-coordinates.

A(t): Orthogonal (rotation) matrix used to obtain the $\hat{f}$-coordinates at time t of any vector fixed in the satellite. (See Section 3.7.2.)

$T_p^{\rightarrow}(\psi)$: Orthogonal (rotation) matrix for rotation of any vector $\vec{q}$ about an axis $\vec{p}$ thru the angle ψ. (See Section 3.2.)

$W_p^{\rightarrow}(\vec{q})$: An alternate (nonorthogonal) matrix for the same purpose as $T_p^{\rightarrow}(\psi)$.

$$\vec{q}(\varphi) = W_p^{\rightarrow}(\vec{q}) \begin{bmatrix} 1 \\ \cos\psi \\ \sin\psi \end{bmatrix} .$$

(See Section 3.2.)

L: Longitude.

λ: Latitude.

Az: Azimuth with respect to north.

GHA: Greenwich Hour Angle.

SSD: Distance of navigator from subsatellite point. (See Section 2.3.)

γ: Azimuth of the great-circle plane containing the navigator, measured from the satellite orbit plane. (See Section 2.3.)

$\hat{h}$(or $\hat{H}$): Satellite angular momentum unit vector (fixed in space).

$\hat{\omega}$: Satellite angular velocity unit vector (time varying).

α: Angle between $\hat{\omega}$ and $\hat{e}_2$ (constant).

β: Angle between $\hat{h}$ and $\hat{e}_2$ (constant).

ρ: Moment-of-inertia ratio.

Ω: Angular rate of rotation of the $(\hat{\omega}, \hat{e}_2)$-plane about $\hat{h}$ (relative to the $\hat{f}$-system).

C: Angular rate of rotation of $\hat{\omega}$ about $\hat{e}_2$ (relative to the $\hat{e}$-system; this is the "precession" of $\hat{\omega}$ in the body).

$\hat{n}_1$, $\hat{n}_2$: Body-fixed vectors representing the satellite antenna booms, i.e. normals to the mid-planes of the antenna patterns. Ordinarily, these vectors need be known (in $\hat{E}$-coordinates) only at the times $t_o(k)$.

$t_o(k)$: The time of the reference pulse during satellite revolution k.

$t_1(k)$, $t_2(k)$: The times of detection by navigator for fan beams No. 1 and No. 2 during satellite revolution k.

φ_1, φ_2, φ_3: Satellite roll, pitch and yaw angles as of time 0 (i.e., initially).

3.2 TRANSFORMATIONS

The initial position and velocity of the satellite are given in terms of latitude, longitude and azimuth (and, of course, altitude). Let $G = L + GHA$. The initial transformation from orbital to equatorial inertial coordinates is then

$$M_{Ee'} = \begin{bmatrix} -\cos G\sin\lambda & -\sin G & -\cos G\cos\lambda \\ -\sin G\sin\lambda & \cos G & -\sin G\cos\lambda \\ \cos\lambda & 0 & -\sin\lambda \end{bmatrix} \begin{bmatrix} \cos Az & -\sin Az & 0 \\ \sin Az & \cos Az & 0 \\ 0 & 0 & 1 \end{bmatrix}. \quad (3)$$

(The columns of the left matrix factor are the "north, east and down" vectors, respectively, at the satellite.)

The initial attitude of the satellite relative to the orbital system is given in terms of a roll, pitch and yaw. The initial transformation from body to orbital coordinates is

$$M_{e'e} = \begin{bmatrix} \cos\varphi_3 & -\sin\varphi_3 & 0 \\ \sin\varphi_3 & \cos\varphi_3 & 0 \\ 0 & 0 & 1 \end{bmatrix} \begin{bmatrix} \cos\varphi_2 & 0 & \sin\varphi_2 \\ 0 & 1 & 0 \\ -\sin\varphi_2 & 0 & \cos\varphi_2 \end{bmatrix} \begin{bmatrix} 1 & 0 & 0 \\ 0 & \cos\varphi_1 & -\sin\varphi_1 \\ 0 & \sin\varphi_1 & \cos\varphi_1 \end{bmatrix} \quad (4)$$

To obtain the initial transformation from body to equatorial inertial coordinates:

$$M_{Ee} = M_{Ee'}M_{e'e} \quad (5)$$

Two further transformations are needed in order to refer the satellite-to-navigator vector to the satellite antenna coordinate systems in gain calculations.

The axes in the coordinate system for antenna #1 are defined as follows. Let coordinates be referred to the body axes, and let the body vector $\hat{e}_3$ be

projected into the mid-plane of fan beam #1. This is assumed to give the nominal direction $\vec{m}_o$ of unity gain (maximum energy propagation):

$$\vec{m}_o = \hat{e}_3 - (\hat{n}_1 \cdot \hat{e}_3)\hat{n}_1 .$$

This vector is then rotated through a small given angle ψ_1 about $\hat{n}_1$ to simulate a twisted mounting of the slot array about its longitudinal axis. This new direction $\vec{m}$ is taken as the true direction of unity gain. Then, the antenna axes are:

$$\begin{aligned} \hat{a}_1 &= \hat{n}_1 \\ \hat{a}_2 &= \vec{m}/|\vec{m}| \\ \hat{a}_3 &= \hat{a}_1 \times \hat{a}_2 . \end{aligned} \tag{6}$$

Figure 3-2 in Section 3.6 shows these axes in relation to the antenna array. The transformation from body to antenna coordinates for antenna #1 is then written:

$$M_{ae} = \begin{bmatrix} \hat{a}_1 \\ \hat{a}_2 \\ \hat{a}_3 \end{bmatrix} . \tag{7}$$

The analogous transformation for antenna #2 is:

$$M_{be} = \begin{bmatrix} \hat{b}_1 \\ \hat{b}_2 \\ \hat{b}_3 \end{bmatrix} \tag{8}$$

An important transformation used in describing the rotational motion of the precessing satellite is the transformation which will rotate a vector $\vec{q}$ about an axis $\vec{p}$ through an angle ϕ. Let q' be the new coordinates after the rotation. Then,

$$\hat{p} = \vec{p}/|\vec{p}|$$
$$\hat{q} = \vec{q}/|\vec{q}| \qquad (9)$$
$$\hat{q}' = q'/|\vec{q}| \ .$$

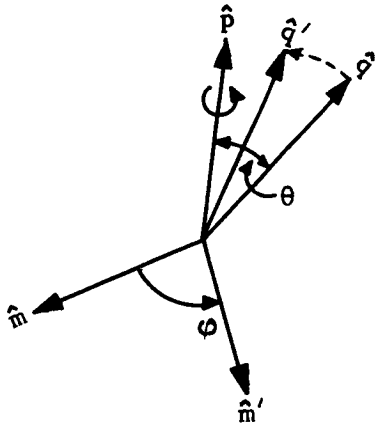

$$\cos\theta = \hat{p}\cdot\hat{q} = \hat{p}\cdot\hat{q}'$$
$$\hat{q} \times \hat{p} = \hat{m}\sin\theta \qquad (10)$$
$$\hat{q}' \times \hat{p} = \hat{m}'\sin\theta$$

$$\hat{m}\cdot\hat{m}' = \frac{1}{\sin^2\theta}(\hat{q}\times\hat{p})\cdot(\hat{q}'\times\hat{p})$$

$$= \frac{1}{\sin^2\theta}\left[(\hat{q}\cdot\hat{q}')(\hat{p}\cdot\hat{p}) - (\hat{p}\cdot\hat{q}')(\hat{q}\cdot\hat{p})\right]$$

$$= \frac{1}{\sin^2\theta}(\hat{q} - \hat{p}\cos\theta)\cdot\hat{q}' = \cos\varphi \qquad (11)$$

$$\hat{m}\times\hat{m}' = \frac{1}{\sin^2\theta}(\hat{q}\times\hat{p})\times(\hat{q}'\times\hat{p})$$

$$= \frac{1}{\sin^2\theta}\left\{-\hat{q}\left[(\hat{q}'\times\hat{p})\cdot\hat{p}\right] + \hat{p}\left[(\hat{q}'\times\hat{p})\cdot\hat{q}\right]\right\}$$

$$= \frac{1}{\sin^2\theta}\hat{p}\left[(\hat{p}\times\hat{q})\cdot\hat{q}'\right] = \hat{p}\sin\varphi \ . \qquad (12)$$

Equations (10), (11) and (12) may be arranged to yield the matrix equation (superscript ^{T} denotes a transpose):

$$\begin{bmatrix} \hat{p}^T \\ \hline \frac{1}{\sin\theta}(\hat{q} - \hat{p}\cos\theta)^T \\ \hline \frac{1}{\sin\theta}(\hat{p} \times \hat{q})^T \end{bmatrix} \begin{bmatrix} \\ \hat{q}' \\ \\ \end{bmatrix} = \begin{bmatrix} \cos\theta \\ \sin\theta\cos\varphi \\ \sin\theta\sin\varphi \end{bmatrix} .$$

It is easily verified that the 3 x 3 matrix is orthogonal. So,

$$\begin{bmatrix} \\ \hat{q}' \\ \\ \end{bmatrix} = \left[\begin{array}{c|c|c} \hat{p} & \frac{1}{\sin\theta}(\hat{q} - \hat{p}\cos\theta) & \frac{1}{\sin\theta}(\hat{p} \times \hat{q}) \end{array}\right] \begin{bmatrix} \cos\theta \\ \sin\theta\cos\varphi \\ \sin\theta\sin\varphi \end{bmatrix} .$$

It will be noticed that the $\sin\theta$ factors cancel out. Also, the $\cos\theta$ term in the vector on the right may be brought into the matrix. Then, multiplying through by $|\vec{q}|$,

$$\begin{bmatrix} \\ \vec{q}' \\ \\ \end{bmatrix} = |\vec{q}| \left[\begin{array}{c|c|c} \hat{p}\cos\theta & (\hat{q} - \hat{p}\cos\theta) & (\hat{p} \times \hat{q}) \end{array}\right] \begin{bmatrix} 1 \\ \cos\varphi \\ \sin\varphi \end{bmatrix} \qquad (13)$$

$$\vec{q}(\varphi) = \underbrace{\qquad\qquad}_{W_{\vec{p}}(\vec{q})} \vec{\tau}(\varphi) .$$

This, with equations (9) and (10), defines a nonorthogonal matrix $W_{\vec{p}}(\vec{q})$ and a vector $\vec{\tau}(\varphi)$, whose product yields the rotated vector $\vec{q}'$. This form of the transformation, in which the rotation angle φ is "factored out" in the form of a vector $\tau(\varphi)$, is sometimes useful. Two applications are given in Sections 3.7.2 and 5.3. Equation (13) will now be rearranged in the more

conventional form of an orthogonal transformation, operating upon the vector $\vec{q}$. Multiplying out Equation (13) (temporarily cancelling out the factor $|\vec{q}|$):

$$\hat{q}' = \hat{p}\cos\theta + (\hat{q} - \hat{p}\cos\theta)\cos\varphi + (\hat{p} \times \hat{q})\sin\varphi.$$

Then, since

$$\cos\theta = \hat{p} \cdot \hat{q} \equiv \hat{p}^T\hat{q}:$$

$$\hat{q}' = \hat{p}(\hat{p}^T\hat{q}) + \left[\hat{q} - \hat{p}(\hat{p}^T\hat{q})\right]\cos\varphi + (\hat{p} \times \hat{q})\sin\varphi.$$

But,

$$\hat{p} \times \hat{q} \equiv (\hat{p}\chi)\hat{q}$$

where, by definition:

$$(\hat{p}\chi) \equiv \begin{bmatrix} 0 & -p_3 & p_2 \\ p_3 & 0 & -p_1 \\ -p_2 & p_1 & 0 \end{bmatrix}. \tag{14}$$

Hence,

$$\hat{q}' = (\hat{p}\hat{p}^T)\hat{q} + \left[(I - \hat{p}\hat{p}^T)\cos\varphi\right]\hat{q} + \left[\sin\varphi(\hat{p}\chi)\right]\hat{q},$$

and multiplying through by $|\vec{q}|$:

$$\vec{q}' = T_{\vec{p}}(\varphi)\vec{q}$$

where

$$T_{\vec{p}}(\varphi) = \cos\varphi I + (1 - \cos\varphi)\hat{p}\hat{p}^T + \sin\varphi(\hat{p}\chi). \tag{15}$$

This is the orthogonal transformation sought. The proof of orthogonality is simple. By inspection of Equation (14),

$$(\hat{p}\chi)^T = -(\hat{p}\chi).$$

Also, obviously,

$$T_{\vec{p}}(-\varphi)\vec{q}' = \vec{q}, \text{ (i.e. } T_{\vec{p}}(-\varphi) = T_{\vec{p}}^{-1}(\varphi)).$$

Hence, using Equation (15),

$$T_{\vec{p}}^{T}(\varphi) = T_{\vec{p}}(-\varphi) = T_{\vec{p}}^{-1}(\varphi). \tag{16}$$

3.3 SATELLITE DYNAMICS

The satellite orbital motion is assumed to be elliptical. The initial position and velocity $\vec{r}_s(o)$ and $\vec{v}_s(o)$ are determined from input data. At any other time t, let the change in eccentric anomaly be $\Delta = E - E_o$. Also, denote the mean anomaly by n, and eccentricity by e. Kepler's equation is then

$$\begin{aligned} nt &= E - E_o - e\sin E + e\sin E_o \\ &= \Delta - e\sin(\Delta + E_o) + e\sin E_o \\ &= \Delta - e\sin\Delta\cos E_o - e\cos\Delta\sin E_o + e\sin E_o \\ &= F(\Delta). \end{aligned}$$

This equation is solved for Δ by Newton's method of iteration. Letting Δ_n be the n^{th} estimate of Δ, the next estimate is

$$\Delta_{n+1} = \Delta_n + \frac{nt - F(\Delta)}{F'(\Delta)}. \tag{17}$$

When the iteration has converged, the value of Δ is converted to an increment in true anomaly and the new position and velocity on the ellipse

are found using the theory of conical orbits [1].

The satellite attitude after time t is obtained in closed form, on the assumption of a torque-free spinning body with an axially symmetric momental ellipsoid. Figure 3-1 illustrates the geometry at time 0.

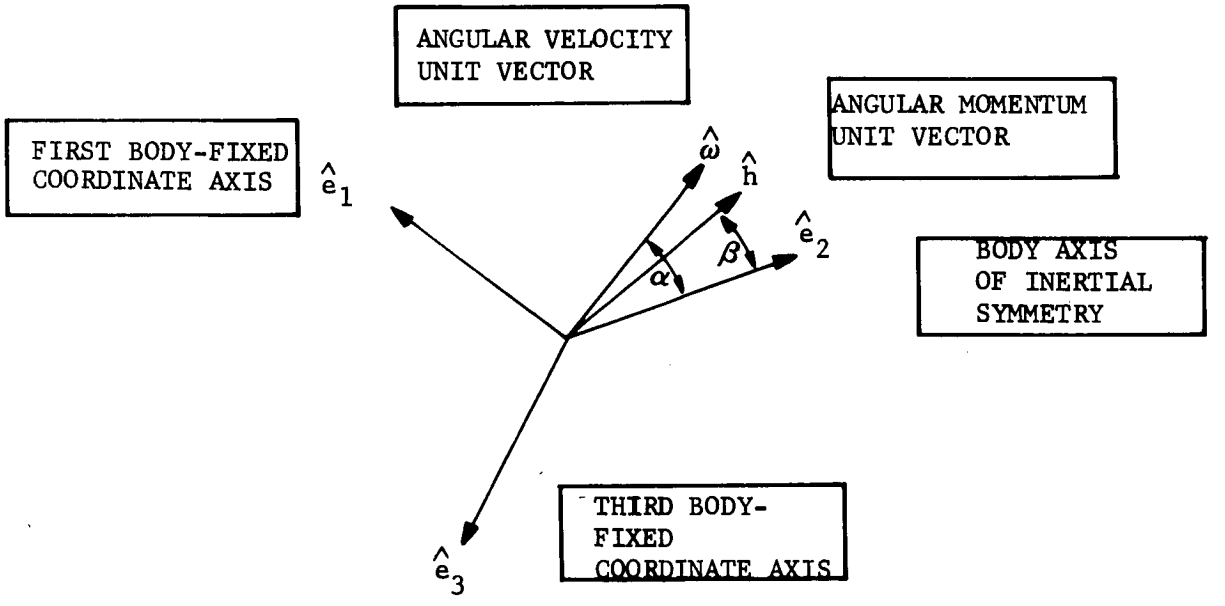

Figure 3-1 Initial Geometry

Let the initial directions of $\hat{e}_1$, $\hat{e}_2$ and $\hat{e}_3$ define an inertial coordinate system $\hat{f}_1$, $\hat{f}_2$ and $\hat{f}_3$ to be held fixed during the motion. The orthogonal transformation A(t) relating any body-fixed vector $\vec{v}_e$, at time t, to the $\hat{f}$-system is to be found. The equatorial inertial coordinates of $\vec{v}_e$, at time t, may then be found from

$$\vec{v}_E = M_{Ee}A(t)\vec{v}_e, \tag{18}$$

using Equation (5), (since the $\hat{f}$-system coincides with the initial $\hat{e}$-system).

Referring to Figure 3-1, the $(\hat{e}_2, \hat{\omega})$-plane rotates about $\hat{h}$ with a constant rate r, relative to the $\hat{f}$-frame, while $\hat{\omega}$ rotates about $\hat{e}_2$ with a constant rate C ("precession rate") relative to the $\hat{e}$-frame. The angles α and β remain constant. If ρ is the moment of inertia ratio,

$$\tan\beta = \frac{1}{\rho}\tan\alpha \tag{19}$$

$$\begin{aligned}\Omega &= \frac{\sin\alpha}{\sin\beta}\omega \\ &= \omega\sqrt{\sin^2\alpha + \rho^2\cos^2\alpha} \\ &= |\vec{h}|/J_{ns}.\end{aligned} \tag{20}$$

(J_{ns} is the moment of inertia about a principal axis perpendicular to the axis of inertial symmetry.)

$$C = (\rho - 1)\omega\cos\alpha. \tag{21}$$

Further discussion of the above motion may be found in References [2, 3].

The required transformation A(t) may be found in a manner analogous to the derivation of a roll-pitch-yaw transformation by successive rotations. In a time t, $\hat{\omega}$ rotates through an angle Ct about $\hat{e}_2$. Hence, if at time 0 the

body is rotated about $\hat{e}_2$ through an angle -Ct, then $\hat{\omega}$ will have the coordinates relative to the $\hat{e}$-frame that it would have in the actual motion at time t. This rotation does not disturb either $\hat{e}_2$ or $\hat{\omega}$, and is given by $T^{\wedge}_{f_2}(-Ct)$, defined by Equation (15). Next, holding $\hat{\omega}$ fixed in the body, the body is rotated about $\hat{h}$, through the angle Ωt (with $\hat{h}$ referred, of course, to the $\hat{f}$-frame). This rotation is given by $T^{\wedge}_{h}(\Omega t)$. The $(\hat{e}_2,\hat{\omega})$-plane will then be positioned relative to the $\hat{f}$-frame as it would be in the actual motion, at time t.

The two successive rotations performed upon the body result in precisely the attitude assumed by the body at time t in the actual motion. By simply multiplying (on the right) by the identity matrix the columns of the matrix

$$A(t) \equiv T^{\wedge}_{h}(\Omega t)\, T^{\wedge}_{f_2}(-Ct) \qquad (22)$$

are seen to be the vectors of direction cosines of $\hat{e}_1$, $\hat{e}_2$, and $\hat{e}_3$, referenced to the $\hat{f}$-frame. Hence, A(t) is the transformation from body coordinates to $\hat{f}$-coordinates, at time t.

3.4 NAVIGATOR DYNAMICS

Navigator motion (if any) relative to the earth is assumed to be of constant speed along a great circle path, defined by an initial azimuth relative to north. Input data for the initial position is in the form of an azimuth γ, from the orbit plane, and a distance d from the sub-satellite point, as illustrated in Section 2.3. These parameters are converted to an initial latitude and longitude. At any subsequent time t, a right-handed triad of unit vectors along the path, across path and "up" are computed (referenced to the equatorial inertial system $\hat{E}$) quite analogously to the construction of the M_{Ee}, matrix, Equation (3). This is done under the assumption of no navigator motion relative to the earth, but including the earth's rotation and GHA. Then the "up" vector is rotated about the across-path vector through an angle $\omega_N t$, where ω_N is the angular rate of the navigator

relative to the earth. Upon multiplication by earth radius plus navigator altitude, the navigator's inertial position at time t is obtained.

3.5 SIMULATION OF FAN BEAM TIMING

Within the limitations of the mathematical model as regards the motions of satellite, earth and navigator, the occurrences of the times t_o, t_1 and t_2 for a navigator are computed exactly (insofar as the 7094 single precision arithmetic will allow). The pure values may then be contaminated later in the simulation of the actual navigator detection process by adding biases or random noise. This will be discussed in Section 3.6. (Of course, even without any contamination, a navigator fix computation may be affected by errors in knowledge of the angular velocity vector of the satellite or other error sources listed in Section 2.3.)

Because of the nonlinear nature of the effects of the system motions on determination of t_o, t_1 and t_2, an iterative procedure is needed. Geometrical definitions of t_o, t_1 and t_2 as incorporated in the simulation are as follows:

- t_o is the time during a satellite revolution at which $\hat{n}_1 \times \hat{n}_2$ (i.e., the intersection of the mid-planes of the two fan beams) is perpendicular to the vector, fixed in space, having the direction of the initial satellite velocity. It is assumed that, through calibration, good estimates of the equatorial inertial orientation of $\hat{n}_1$ and $\hat{n}_2$ are known at time t_o. This is only one of many possible ways of defining such a time, but happens to be convenient in the computer program.

- t_1 is the time during a satellite revolution at which $\hat{n}_1$ is perpendicular to the instantaneous satellite-to-navigator vector (i.e., the time that the mid-plane of fan beam #1 passes the navigator).

- t_2 is defined for $\hat{n}_2$ and fan beam #2 as was t_1 for $\hat{n}_1$ and fan beam #1.

The iterative procedure used to compute t_o, t_1 and t_2 will be outlined here with omission of some of the details (which, however, are easily computed).

Let T_N be an initial approximation for t_o (or t_1 or t_2) at the N'th satellite revolution, N = 0, 1, . . . Each time that convergence of the iterations for a t_o is obtained, T_N for t_1 is taken as that value. Then the converged t_1 is taken as T_N for t_2. T_{N+1} for t_o is taken as $t_o(N) + 2\pi/\omega$. The whole thing is started by taking $t_o(0) = 0$.

Next, let $\hat{v}(T_N)$ represent $\hat{n}_1 \times \hat{n}_2/|\hat{n}_1 \times \hat{n}_2|$, (or $\hat{n}_1$ or $\hat{n}_2$) at time T_N. (All vectors are written in $\hat{E}$-coordinates.) Let $\hat{w}(T_N)$ represent the normalized <u>initial</u> satellite velocity vector (or the normalized satellite-to-navigator vector) at time T_N. Vectors $\hat{v}(T_N)$ and $\hat{w}(T_N)$ are obtained by updating the satellite position and attitude, and the navigator's position, to time T_N by the procedures of Sections 3.3 and 3.4.

A test is made for perpendicularity:

$$\hat{v}(T_N) \cdot \hat{w}(T_N) \stackrel{?}{=} 0. \tag{23}$$

If the test fails, an approximate correction ΔT_N for t_o(or t_1 or t_2) is computed by a simple rotation of $\hat{v}$ about $\hat{h}$, using the rate ω:

$$\hat{v}(T_N + \Delta T_N) \cong T_{\hat{h}}(\omega \Delta T_N)\hat{v}(T_N).$$

Invoking the perpendicularity condition,

$$\hat{w}^T(T_N)T_{\hat{h}}(\omega \Delta T_N)\hat{v}(T_N) = 0.$$

By observation of Equation (15), it is seen that this may be written in terms of three computable numbers c_1, c_2 and c_3:

$$c_1 \sin\omega\Delta T_N + c_2 \cos\omega\Delta T_N + c_3 = 0$$

$$(c_1^2 + c_2^2)\sin^2\omega\Delta T_N + 2c_1c_3\sin\omega\Delta T_N - c_2^2 = 0.$$

The two angles $\omega\Delta T_N$ which satisfy this are computed and the smaller in absolute value chosen. This determines ΔT_N.

Changing T_N to $T_N + \Delta T_N$, precise new vectors $\hat{v}(T_N + \Delta T_N)$ and $\hat{w}(T_N + \Delta T_N)$ are obtained by the full procedures of Sections 3.3 and 3.4.

The iterative process is continued until the perpendicularity test, Equation (23), is satisfied to a prescribed accuracy (the tolerance is $\pm$ .000001).

It will be noticed that, in the computations to determine t_o, t_1 and t_2, there is full provision for any and all system motions which may be assigned as operating.

3.6 SIMULATION OF FAN BEAM DETECTIONS BY NAVIGATOR

The analytical method of fix computation used in the simulation, to be described in Section 3.7.2, requires the notions of "normals to the planes of the fan beams." Since actual fan beams are not ideal planes, a mathematical model of a typical antenna pattern was constructed to simulate the fan beam detection process:

$$\text{GAIN} = F_A(\theta,\alpha)F_E(\theta,\alpha), \tag{24}$$

where the Array Factor is

$$F_A(\theta,\alpha) = \left| \frac{\sin(\frac{n\pi}{2}\cos\alpha\sin\theta)}{n\sin(\frac{\pi}{2}\cos\alpha\sin\theta)} \right| \tag{25}$$

and the Antenna Element Factor is

$$F_E(\theta,\alpha) = \tfrac{1}{2}(1 + \sin\theta\sin\alpha)\frac{\cos(\frac{\pi}{2}\cos\theta)}{\sin^2\theta} . \qquad (26)$$

These equations describe a Planar In-Line Resonant Array of n half-wave slots at half-wave spacings. The angles θ and α represent the direction of a navigator's receiver antenna, found by transforming the satellite-to-navigator vector from equatorial inertial coordinates to antenna coordinates, using the transformations for the two fan beams;

$$\begin{aligned} M_{aE} &= M_{ae}M_{Ee}^T \\ M_{bE} &= M_{be}M_{Ee}^T, \end{aligned} \qquad (27)$$

and finally transforming to the θ and α spherical coordinates. Figure 3-2 illustrates the geometry for fan beam #1.

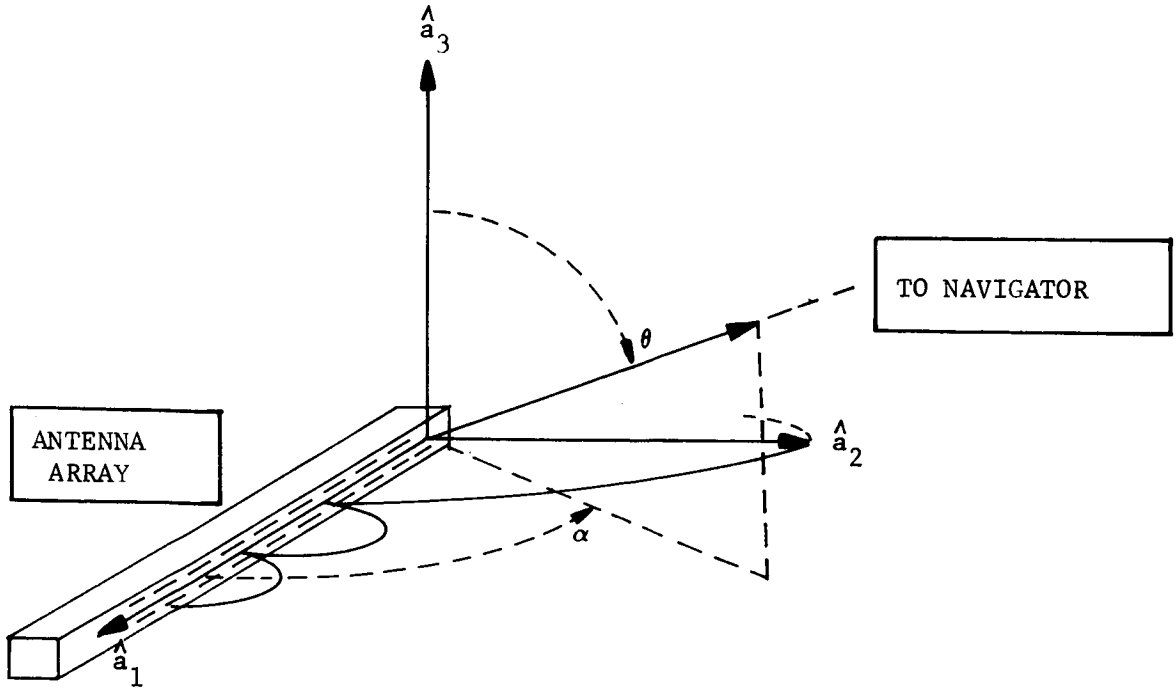

Figure 3-2 Antenna #1 Coordinate System

Figure 3-3 is a composite plot of the 60-slot pattern for θ = 60 degrees to θ = 90 degrees at intervals of 5 degrees.

The detection times t_1 and t_2 for the fan beams are defined as the averages of the two threshold times (the instants when GAIN = .6) for the respective fan beams. To find these threshold times, say for fan beam #1, the first step is to calculate t_1 on the assumption of an ideal planar beam by the method described in Section 3.5. Defining the function

$$F(t) \equiv G(t) - .6$$

where G(t) is the gain or intensity of the beam at the navigator given by Equations (24, 25, 26), a root-finding procedure is used to find the time points where F(t) = 0. The computer subrouting FINDV uses the calculated value of t_1 based on the assumption of an ideal planar beam as a starting value, and searches at small increments in time until the two threshold time points are localized. Then, employing a sequence of second degree polynomial approximations to F(t) in neighborhoods about the threshold points, the appropriate polynomial roots are caused to converge arbitrarily close to the desired zeros of F(t)--the threshold times. During the time variations in this iterative procedure, the full system model as regards earth, satellite and navigator motions is operative.

It turns out that when the two threshold times are averaged, the result is not in general equal to the value of t_1 originally computed for an ideal planar beam. This phenomenon is discussed further in Section 4.1.1.

Once the "pure" fan timing quantities t_o, t_1 and t_2 have been computed, either on the assumption of an ideal planar pattern or the more realistic pattern given by Equations (24, 25, 26) (requiring threshold averaging), it is possible to impress an assumed bias on any one or all three. Also, for studies of smoothing techniques applied to sets of t_o, t_1 and t_2 obtained over many satellite revolutions, random Gaussian noise may be applied to the t_1 and t_2 timing items. The smoothing techniques are discussed in Section 3.7.

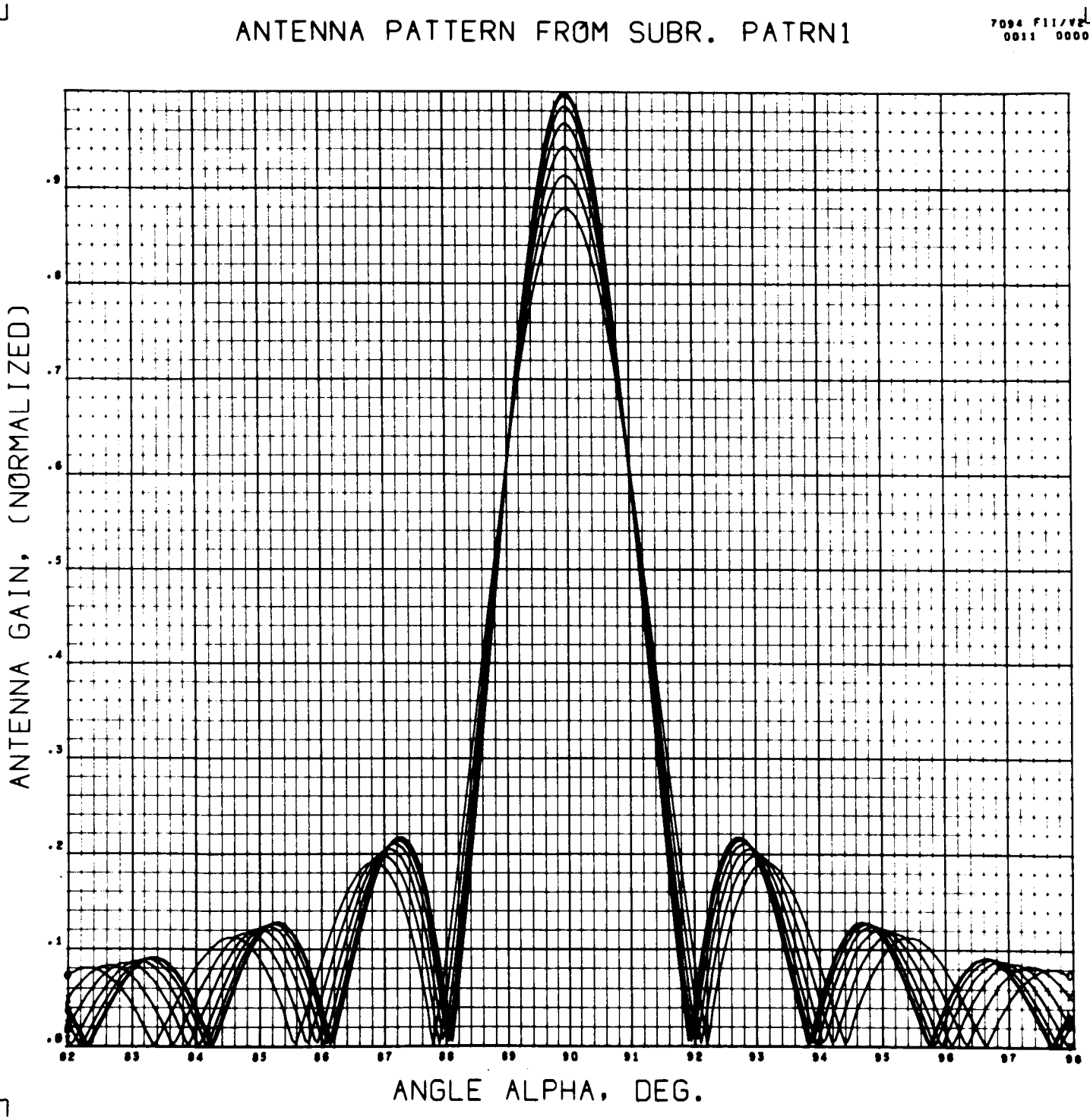
ANTENNA PATTERN FROM SUBR. PATRN1
7094 F11/V2
0011 0000
ANTENNA GAIN, (NORMALIZED)
.9
.8
.7
.6
.5
.4
.3
.2
.1
.0
82
83
84
85
86
87
88
89
90
91
92
93
94
95
96
97
98
ANGLE ALPHA, DEG.

Figure 3-3

3.7 NAVIGATOR COMPUTATION OF FIX

The basic quantities accessable to a navigator, using the fan beam concept, are the timing items t_o, t_1 and t_2. There are several different methods by which he might use these items to compute his position. In fact, there are methods (not investigated directly in this study) which do not require the t_o pulses--but which do require two satellites. The primary method of this study is known as the "analytical method of fix computation." Two other methods have had tentative trials in the study. In connection with the analytical method, techniques of smoothing data have been investigated.

For the analytical method of fix computation, the navigator needs good estimates in E-coordinates of $\hat{\omega}$, $\hat{n}$, and $\hat{n}_2$ at the time of the reference pulse t_o within the satellite revolution in which the fix computation is made. The next section contains some preliminary material to illustrate the type of problem this poses for calibration stations.

3.7.1 Reference Vectors as a Function of Revolution Number

There are essentially two levels of precision in which calibration stations might specify $\hat{\omega}(t_o)$, $\hat{n}_1(t_o)$ and $\hat{n}_2(t_o)$ where $t_o = t_o(k)$ with k representing the satellite revolution number:

A. Provide estimates for the inertial coordinates of $\hat{\omega}(t_o)$, $\hat{n}_1(t_o)$ and $\hat{n}_2(t_o)$ which actually vary with k and represent as accurately as possible the true vectors at times $t_o(k)$.

B. Provide estimates for the inertial coordinates of $\hat{\omega}(t_o)$, $\hat{n}_1(t_o)$ and $\hat{n}_2(t_o)$ which are fixed in inertial space (do not vary with k) but represent good average positions of the varying true vectors over some range of k.

For efficient employment of precision (A), the vectors would have to be transmitted very frequently along with the $t_o(k)$ pulses, (highest efficiency requiring the vector transmissions with every t_o pulse). With use of precision (B), the vectors need be transmitted only when they are updated (say after N satellite revolutions).

Which degree of precision is needed depends upon the accuracy of fix computation required by a navigator. For precision (A), the navigation hardware would inevitably need to be more sophisticated than that for precision (B), especially where smoothing techniques are used.

A worthwhile characterization of the positions of the reference vectors at the times $t_o(k)$ will be described. The following discussion, although couched in general terms, will be applied to the specific vectors $\hat{n}_1(t_o)$ and $\hat{n}_2(t_o)$.

As a preliminary, the following question is asked. Given any unit vector fixed in the satellite and its inertial coordinates at a time t_o, what are its coordinates at times $t_o + 2k_\pi/\omega$, where ω is the true angular velocity magnitude and $k = 1, 2, \ldots, N$? Since in the present application the angle between the $\hat{h}$ vector and axis of symmetry is presumed small, a simple answer is obtained using small angle assumptions.

Without loss of generality, t_o may be taken $t_o = 0$ and the inertial reference frame for present purposes may be chosen as follows:

- $\hat{f}_2$ along the axis of symmetry, $\hat{e}_2$, at time 0.
- $\hat{f}_3$ in the direction of $\hat{h} \times \hat{e}_2$ at time 0.
- $\hat{f}_1 = \hat{f}_2 \times \hat{f}_3$.

With this choice, the geometry is that of Figure 3-1 of Section 3.3, with the symbols $\hat{e}_i$ replaced by $\hat{f}_i$.

In the $\hat{f}$ system, referring to Figure 3-1:

$$\hat{h} = \begin{bmatrix} \sin\beta \\ \cos\beta \\ 0 \end{bmatrix} \cong \begin{bmatrix} \beta \\ 1 \\ 0 \end{bmatrix} . \tag{28}$$

Let $\hat{u}$ be the $\hat{f}$-coordinates at time 0 of any unit vector fixed in the satellite. Using the transformation A(t), Equation (22) of Section 3.3, the $\hat{f}$-coordinates of $\hat{u}$ at time t_k are

$$\hat{u}(t_k) = T_{\hat{h}}(\Omega t_k) T_{\hat{f}_2}(-Ct_k)\hat{u}, \tag{29}$$

where Ω and C are given by Equations (20) and (21) of Section 3.3.

Also, for any unit vector $\hat{a}$ and angle b:

$$T_{\hat{a}}(b) \equiv \cos b I + (1 - \cos b)\hat{a}\hat{a}^T + \sin b\,(a\chi) \tag{30}$$

where

$$(\hat{a}\chi) \equiv \begin{bmatrix} 0 & -a_3 & a_2 \\ a_3 & 0 & -a_1 \\ -a^2 & a_1 & 0 \end{bmatrix}$$

Under small angle assumptions, inspection of Equations (19), (20) and (21) shows that

$$\begin{aligned} \Omega &\cong \rho\omega \\ C &\cong (\rho - 1)\,\omega \end{aligned} \tag{31}$$

where ρ is the moment of inertia ratio.

Present interest is in the discrete time points $t_k = 2k_\pi/\omega$:

$$\begin{aligned}\Omega t_k &= 2k_\pi\rho \\ &= 2k_\pi(\rho - 1) + 2k_\pi \\ &= Ct_k + 2k_\pi.\end{aligned}$$

Hence, Ωt_k in Equation (29) may be replaced by Ct_k. Let $\varphi_t = Ct_k$. Then the first rotation in Equation (29) is

$$\hat{v} \equiv T_{\hat{f}_2}(-\varphi_k)\hat{u} = \begin{bmatrix} \cos\varphi_k & 0 & -\sin\varphi_k \\ 0 & 1 & 0 \\ \sin\varphi_k & 0 & \cos\varphi_k \end{bmatrix} \begin{bmatrix} u_1 \\ u_2 \\ u_3 \end{bmatrix}$$

or

$$\begin{bmatrix} v_1 \\ v_2 \\ v_3 \end{bmatrix} \equiv \begin{bmatrix} u_1\cos\varphi_k - u_3\sin\varphi_k \\ u_2 \\ u_1\sin\varphi_k + u_3\cos\varphi_k \end{bmatrix}. \tag{32}$$

From Equation (28):

$$\hbar\hbar^T \approx \begin{bmatrix} \beta^2 & \beta & 0 \\ \beta & 1 & 0 \\ 0 & 0 & 0 \end{bmatrix}$$

$$(\hbar\chi) \approx \begin{bmatrix} 0 & 0 & 1 \\ 0 & 0 & -\beta \\ -1 & \beta & 0 \end{bmatrix}$$

and, referring to Equation (30):

$$\hat{u}(t_k) \cong T_{\hat{h}}(Ct_k)\hat{v}$$

$$\cong \begin{bmatrix} v_1\cos\omega_k \\ v_2\cos\omega_k \\ v_3\cos\omega_k \end{bmatrix} + (1 - \cos\omega_k) \begin{bmatrix} \beta^2 v_1 + \beta v_2 \\ \beta v_1 + v_2 \\ 0 \end{bmatrix} + \sin\omega_k \begin{bmatrix} v_3 \\ -\beta v_3 \\ -v_1 + \beta v_2 \end{bmatrix}.$$

Combining terms, and using Equation (32):

$$\hat{u}(t_k) \cong \begin{bmatrix} u_1 \\ u_2 \\ u_3 \end{bmatrix} + \beta \begin{bmatrix} u_2(1 - \cos\omega_k) \\ u_3\sin\omega_k - u_1(1 - \cos\omega_k) \\ u_2\sin\omega_k \end{bmatrix} + \beta^2 \begin{bmatrix} v_1(1 - \cos\omega_k) \\ 0 \\ 0 \end{bmatrix}. \quad (33)$$

In terms of the small parameter β, Equation (33) shows how the arbitrary vector $\hat{u}$ is displaced, at the times $t_k = 2k\pi/\omega$, from its original position.

Suppose the vector $\hat{u}$ has $u_2 = 0$ (i.e., the vector is perpendicular to the axis of symmetry). Then, to first order in β, the vector returns to a fixed inertial plane after each time interval $2\pi/\omega$ (since u_1 and u_3 have the same values). The successive positions of the vector in the plane form a fan as in Figure 3-4. The apex angle of the fan is 2β.

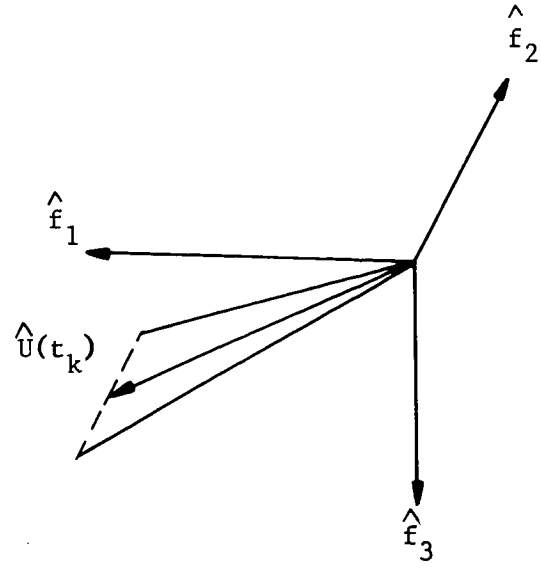

Figure 3-4 Planar Fan Locus

For other choices of the $\hat{u}$ vector, with $0 < |u_2| \leq 1$, the behavior is similar except that the fixed inertial plane is absent. The fan becomes a cone of elliptical cross-section, approaching circular as $|u_2| \rightarrow 1$(i.e., as $\hat{u}$ approaches the axis of symmetry). The choices of fan beam normals for $\hat{u}$ are plotted in Figure 3-5 .

For nominal fan beam normals, the intersection of the two fan beams is a $\hat{u}$ vector having $u_2 = 0$. Regardless of the choice of $t_o(0)$ on the real time scale, if reference pulses are issued at times

$$t_o(k) = t_o(0) + 2k\pi/\omega \qquad k = 0, 1, \ldots \qquad (34)$$

they will conform to the definition of the t_o times in Section 3.5, except that the fixed inertial vector will not in general be the initial satellite velocity vector (which is immaterial).

To illustrate the application of interest, Equation (33) is applied to nominal fan beam normals. Initial orientation is chosen so that the normals can be represented by the two vectors:

$$\begin{bmatrix} \frac{1}{2}\sqrt{2} \\ -\frac{1}{2}\sqrt{2} \\ 0 \end{bmatrix}, \begin{bmatrix} \frac{1}{2}\sqrt{2} \\ \frac{1}{2}\sqrt{2} \\ 0 \end{bmatrix} .$$

Using each of these in turn for $\hat{u}$, the successive position vectors $\hat{u}(t_k)$ are computed from Equation (33), (β = .0909 mrad, ω = 100 revs/min). For a moment of inertia ratio ρ = 1.1, the $\hat{u}(t_k)$ repeat for k = 1, 11, 21, . . ., 2, 12, 22, . . ., etc. Further, due to symmetries present, only k = 0, 1, 2, 3, 4, 5 need be employed. After converting the $\hat{u}(t_k)$ vectors to spherical coordinates, the following charts give the fan beam directions as functions of k. The units are degrees.

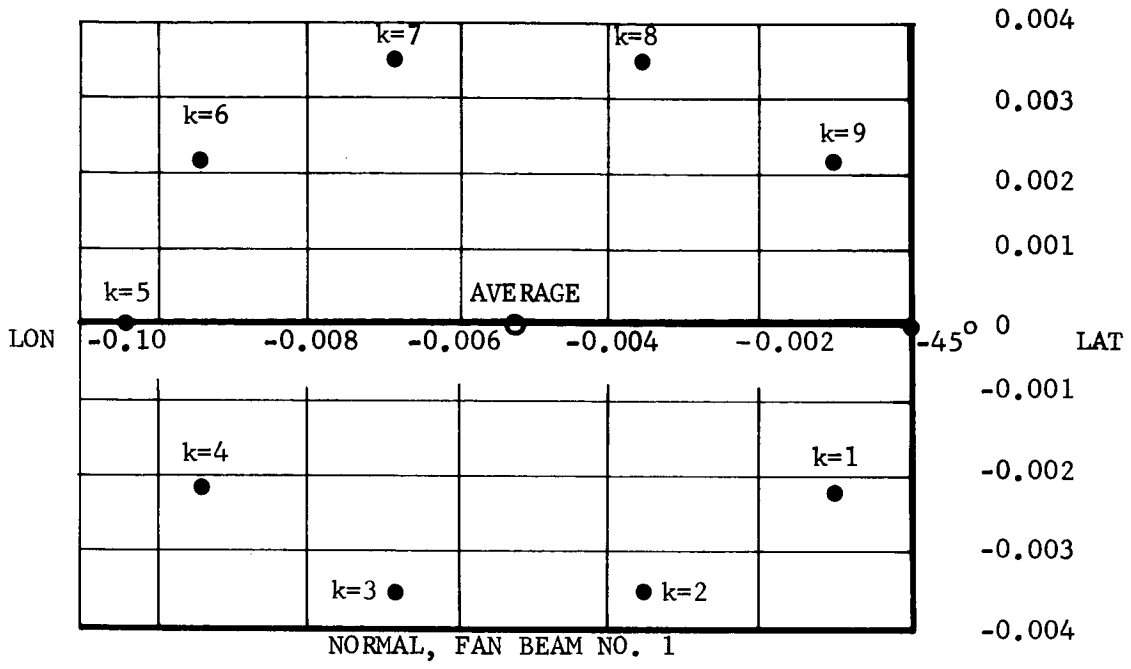

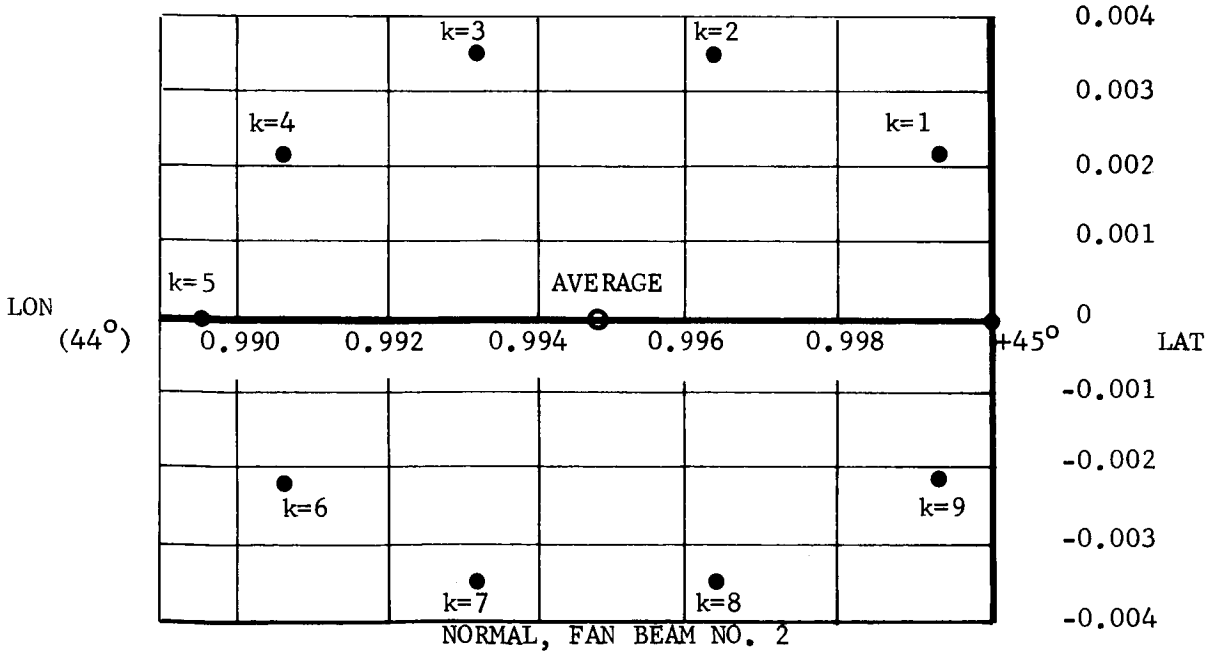

Figure 3-5 Positions of Fan Beam Normals

NORMAL, FAN BEAM #1

k	0	1	2	3	4	5
LAT	-45.00000	-45.00097	-45.00361	-45.00682	-45.00940	-45.01042
LON	0.00000	- 0.00219	- 0.00352	- 0.00352	- 0.00219	0.00000

NORMAL, FAN BEAM #2

k	0	1	2	3	4	5
LAT	45.00000	44.99903	44.99639	44.99318	44.99060	44.98958
LON	0.00000	0.00219	0.00352	0.00352	0.00219	0.00000

These cases were checked against computer output and complete agreement noted over 100 satellite revolutions. (The printing of the LAT and LON in the computer output contained only three decimal places.)

The above data are plotted in Figure 3-5. Of course, it is not meaningful to draw curves connecting the points since each point represents a complete satellite revolution.

Equation (34) shows that the reference pulses $t_o(k)$ occur periodically in time, with period $2\pi/\omega$. The reference vector $\hat{\omega}(t_o)$ as a function of k may now easily be visualized. Since $\hat{\omega}$ rotates about $\hat{h}$ with rate $\Omega \cong \rho\omega$, the angle thru which $\hat{\omega}$ has rotated at time $t_o(k)$, (relative to time $t_o(0)$), is

$$\Psi_k = \Omega \left[t_o(k) - t_o(0) \right] \cong 2k\pi\rho. \qquad (35)$$

In the present application $\rho = 1.1$, so

$$\Psi_k \cong 2k\pi + .1k(2\pi).$$

Thus, at the time of each reference pulse, $\hat{\omega}$ appears to have advanced 36° in its rotation about $\hat{h}$ while in fact it has advanced 396°.

For values of k = 10, 20, 30, . . ., the reference vectors $\hat{\omega}$, $\hat{n}_1$ and $\hat{n}_2$ (and indeed all vectors fixed in the satellite) occupy the same positions that they do for k = 0. In this report an interval of 10 satellite revolutions is called a "precession cycle." It should be cautioned, however, that the strict periodicity of 10 revolutions displayed in the present instance is due to the assumption that $\rho = 1.1$ exactly. For a value slightly different, the positions of $\hat{\omega}$, $\hat{n}_1$ and $\hat{n}_2$ at times $t_o(k)$ will be advanced or retarded from their positions for the case of $\rho = 1.1$. More on this in the discussion of the simulation results in Section 4.2.2.

It will be noticed that the derivation of Equation (33) did not depend upon any specific value of ρ. Hence, the periodic nature of the t_o pulses as expressed in Equation (34)is not affected by the above comments.

For calibration with precision (A), as previously defined, the procedures used must be capable of determining accurate estimates of the <u>true</u> orientations of $\hat{\omega}$, $\hat{n}_1$ and $\hat{n}_2$ at some base time $t_o(0)$, and be able to predict from them the positions $\hat{\omega}(t_o)$, $\hat{n}_1(t_o)$ and $\hat{n}_2(t_o)$ at subsequent times $t_o(k)$, as exemplified by Ψ_k in Equation (35) and the points for k = 0, 1, 2, ..., in Figure 3-5. For calibration with precision (B), the procedures used need only be capable of evaluating from observations good average positions of $\hat{\omega}$, $\hat{n}_1$ and $\hat{n}_2$ as exemplified by $\hat{h}$ and the points marked "average" in Figure 3-5.

The simulations performed in this study in some instances employ somewhat arbitrarily placed estimates for the reference vectors, especially in the earlier cases. In the later cases (simulation of an operational Navigational Satellite system), calibration with precision (B) is assumed.

Discussion of actual procedures designed to achieve calibration of the desired precision will be found in Section 5.3 of this report and in Volume V, Section 5.

3.7.2 Analytical Method of Fix Computation

Although the vector relationships to be described could be presented without reference to any coordinate system, it is more useful to view all vectors in relation to the $\hat{f}_i$ inertial coordinate system. This system has been defined as being coincident with the $\hat{e}_i$ (body) coordinate system as of the epoch of initial conditions (time = 0). These are the coordinates used for computation in the Navigational Satellite program. In the final stages of the fix computation, a transformation to the $\hat{E}_i$ equatorial inertial coordinate system is made, followed by transformation to spherical coordinates to obtain latitude and longitude.

The observations taken by a navigator using the fan beam satellite for a position fix are measurements of two time intervals. These intervals are the times (from a reference time) when the navigator's position is contained in the two signal transmission planes of the rotating satellite.

Figure 3-6 shows the satellite and the navigator at the instant that the navigator's position lies in one of the transmission planes of the fan beam satellite. The navigator's position vector relative to the satellite is denoted by $\vec{r}$ and the unit vector normal to the fan beam by $\hat{n}$.

The condition that $\vec{r}$ lies in the fan beam plane may be stated by saying that the component of $\vec{r}$ normal to the plane is zero. The mathematical formulation of this condition is

$$\vec{r} \cdot \hat{n} = 0$$

The vectors $\vec{r}$ and $\hat{n}$ vary with time: i.e., $\vec{r}$ varies with the orbital motion of the satellite and rotation of the earth, and $\hat{n}$ varies with rotation of the satellite. The time interval, t, at the end of which $\vec{r}$ lies in the fan beam plane, is a solution of $\vec{r}(t) \cdot \hat{n}(t) = 0$. The problem of determining t is not of primary importance here, however. Rather, we are concerned with determining $\vec{r}$ from

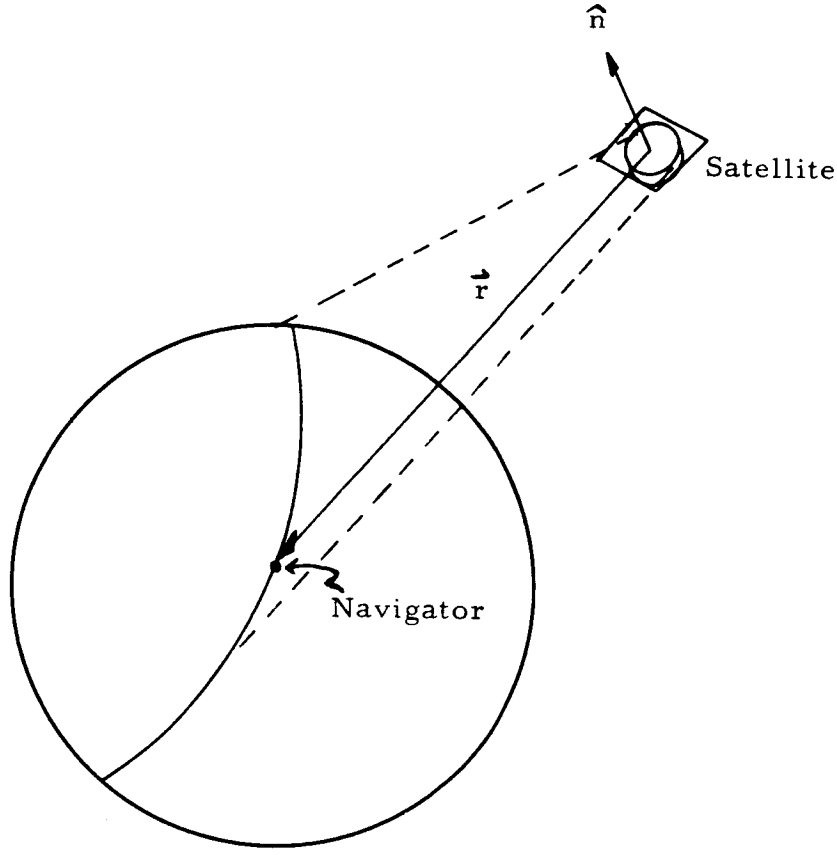

Figure 3-6 Fan Beam-Navigator Intercept

$$\vec{r}(t_1) \cdot \hat{n}_1(t_1) = 0$$

and (36)

$$\vec{r}(t_2) \cdot \hat{n}_2(t_2) = 0$$

where $\hat{n}_i(t_i)$ is the unit normal vector to the i^{th} $(i = 1,2)$ fan beam at time t_i. The navigation problem may be stated simply,

Given: $n_1(t_o)$, $n_2(t_o)$, t_1 and t_2 (and t_o)

Find: $\vec{r}(t_o)$ (or equivalently, $\vec{r}(t_1)$ or $\vec{r}(t_2)$)

The solution of Equations (36) for $\vec{r}$ may be approximated by assuming that $\vec{r}(t)$ is constant over the interval covering t_o, t_1 and t_2. Any vector parallel to

$$\hat{n}_1(t_1) \times \hat{n}_2(t_2)$$

satisfies Equations (36) when substituted for $\vec{r}$. Such a vector lies along the intersection of the planes defined by $\hat{n}_1(t_1)$ and $\hat{n}_2(t_2)$. Letting the magnitude of $\hat{n}_1(t_1) \times \hat{n}_2(t_2)$ be denoted by M, we may express a unit vector in the direction of $\vec{r}(t_o)$ approximately as

$$\hat{r}(t_o) = \frac{1}{M} \hat{n}_1(t_1) \times \hat{n}_2(t_2) \qquad (37)$$

Equation (37) requires a knowledge of $\hat{n}_1(t_1)$ and $\hat{n}_2(t_2)$, the unit normals to each fan beam at the time of contact with the navigator. Presuming that we know the direction of the fan beam normals, $\hat{n}_1(t_o)$ and $\hat{n}_2(t_o)$, at the reference time, the direction of each fan beam normal at a later time, t, may be written

$$\hat{n}(t) = A(t)\hat{n}(t_o) \qquad (38)$$

where A(t) is an appropriate 3 x 3 orthogonal (rotation) matrix which describes the angular motion of the satellite. Under an assumption of constant angular velocity, A(t) has the form

$$T_{\hat{\omega}}(\varphi) = \cos\varphi I + (1 - \cos\varphi)\hat{\omega}\hat{\omega}^T + \sin\varphi\,(\hat{\omega}X) \qquad (39)$$

where

φ is the angle $\omega(t-t_o)$

ω is the angular velocity magnitude,

$\hat{\omega}$ is the direction of the angular velocity

I is the identity matrix,

and $$\hat{\omega}\hat{\omega}^T = \begin{pmatrix} \omega_1\omega_1 & \omega_1\omega_2 & \omega_1\omega_3 \\ \omega_1\omega_2 & \omega_2\omega_2 & \omega_2\omega_3 \\ \omega_1\omega_3 & \omega_2\omega_3 & \omega_3\omega_3 \end{pmatrix}, \quad (\hat{\omega}X) = \begin{pmatrix} 0 & -\omega_3 & \omega_2 \\ \omega_3 & 0 & -\omega_1 \\ -\omega_2 & \omega_1 & 0 \end{pmatrix}$$

ω_1, ω_2 and ω_2 are the components of $\hat{\omega}$.

It may be shown that if the angular motion of the satellite is free precession of an axially symmetric rigid body, the matrix $A(t)$ in $\hat{n}(t) = A(t)\hat{n}(t_o)$ may be written as

$$A(t) = T_{\hat{H}}\left(\frac{H}{J_{ns}}t\right) T_{\hat{f}_2}(ct). \qquad (40)$$

(See Section 3.3.)

Each matrix in the product is of the form (39). H is the angular momentum magnitude while $\hat{H}$ is the direction of the angular momentum in $\hat{f}$ coordinates. J_{ns} is the moment of inertia for a non-symmetric principal axis and c is the precession rate of $\hat{\omega}$ in the body, or e-system:

$$c = \frac{(J_s - J_{ns})}{J_{ns}}\,\omega_2 \quad (\omega_2 \text{ is the } \hat{e}_2\text{-coordinate of } \hat{\omega})$$

In the fix computation, the simpler assumption of (39) is made to obtain A(t) for Equation (38). The navigator's direction from the satellite may thus be calculated approximately (assuming a constant satellite-to-navigator vector, $\vec{r}$, and a constant angular velocity vector, $\vec{\omega}$) from the time interval measurements by

$$
\begin{aligned}
&(1)\quad \varphi_i = \omega(t_i - t_o),\ (i = 1, 2)\\
&(2)\quad \hat{n}_1(t_1) = T_{\hat{\omega}}(\varphi_1)\hat{n}_1(t_o)\\
&(3)\quad \hat{n}_2(t_2) = T_{\hat{\omega}}(\varphi_2)\hat{n}_2(t_o)\\
&(4)\quad M = \left|\hat{n}_1(t_1) \times \hat{n}_2(t_2)\right|\\
&(5)\quad \hat{f} = \frac{1}{M}\,\hat{n}_1(t_1) \times \hat{n}_2(t_2)
\end{aligned}
\qquad (41)
$$

The navigator's position, $\vec{r}_n$, may be computed (see Figure 3-7) by the vector sum

$$\vec{r}_n = \vec{r}_s + \vec{r}$$

The magnitude, r, of $\vec{r}$ must satisfy

$$\vec{r}_n \cdot \vec{r}_n = (r_e + h)^2 = r_s^2 + r^2 + 2r\,\vec{r}_s \cdot \hat{f}\ .$$

That is,

$$r = -\vec{r}_s \cdot \hat{f} - \sqrt{(\vec{r}_s \cdot \hat{f})^2 - r_s^2 + (r_e + h)^2}$$

and $\vec{r} = r\hat{f}$, so that the navigator's position is

$$\vec{r}_n = \vec{r}_s + r\hat{f}\ . \qquad (42)$$

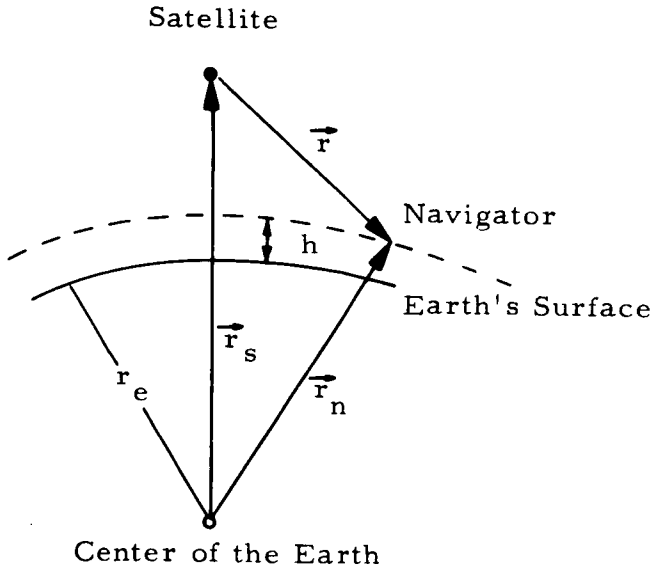

Figure 3-7 Satellite-Navigator Geometry

Vector $\vec{r}_n$ is now expressed in equatorial inertial coordinates

$$\vec{R} = M_{Ee}\,\vec{r}_n ,$$

(since $M_{Ef} = M_{Ee}$), and then transformed to spherical coordinates:

$$\begin{aligned} \cos\mu &= R_1 \cos GHA + R_2 \sin GHA \\ \sin\mu &= -R_1 \sin GHA + R_2 \cos GHA \\ \text{Latitude} &= \tan^{-1}\left(R_3/\sqrt{R_1^2 + \bar{R}_2^2}\right) \\ \text{Longitude} &= \tan^{-1}\left(\sin\mu/\cos\mu\right) . \end{aligned} \tag{43}$$

It turns out that, when consideration is given to the respective roles played by calibration stations and a navigator, an improvement from the navigator's standpoint is possible in accomplishing the calculations of Equations (41) . (The basic theory is, of course, unchanged.) Refer to Section 3.2, Equations (9) thru (13) for the derivation of matrix $W_{\hat{\omega}}(\hat{n})$ and its use.

The two alternative implementations of the analytical method of fix computation are outlined in the following chart.

It can be seen that considerable economy in navigator computation is obtained with the improved method in block Ⓒ of the chart. (Some improvement in the original method is obtained if the calibration station provides the $\hat{\omega}\hat{\omega}^T$ matrix.)

The analytical method as described (and incorporated in the Navigational Satellite programs) does not account for earth rotation and satellite orbital motion effects during the interval encompassing t_o, t_1 and t_2. In Section 5.1 an extension of the method is made, to include the effects of those motions.

Alternate Implementations of Analytical Method of Fix Computation

	Method of Equations (41)	Improved Method
(A) Provided by Calibration Station	t_o, ω, $\hat{\omega}$, $\hat{n}_1(t_o)$, $\hat{n}_2(t_o)$	t_o, ω, $W_{\hat{\omega}}\left[\hat{n}_1(t_o)\right]$, $W_{\hat{\omega}}\left[\hat{n}_2(t_o)\right]$
(B) Provided by Navigator	t_1, t_2	t_1, t_2
(C) Navigator Preliminary Computations	$\varphi_1 = \omega(t_1 - t_o)$, $\varphi_2 = \omega(t_2 - t_o)$ $T_{\hat{\omega}}(\varphi_1) = \cos\varphi_1\, I + \sin\varphi_1(\hat{\omega}\chi) + (1 - \cos\varphi_1)\hat{\omega}\hat{\omega}^T$ $T_{\hat{\omega}}(\varphi_2) = \cos\varphi_2 I + \sin\varphi_2(\hat{\omega}\chi) + (1 - \cos\varphi_2)\hat{\omega}\hat{\omega}^T$ where $\hat{\omega}\hat{\omega}^T = \begin{bmatrix} \omega_1\omega_1 & \omega_1\omega_2 & \omega_1\omega_3 \\ \omega_1\omega_2 & \omega_2\omega_2 & \omega_2\omega_3 \\ \omega_1\omega_3 & \omega_2\omega_3 & \omega_3\omega_3 \end{bmatrix}$ $(\hat{\omega}\chi) = \begin{bmatrix} 0 & -\omega_3 & \omega_2 \\ \omega_3 & 0 & -\omega_1 \\ -\omega_2 & \omega_1 & 0 \end{bmatrix}$	$\varphi_1 = \omega(t_1 - t_o)$, $\varphi_2 = \omega(t_2 - t_o)$ $\vec{\tau}_1 = \begin{bmatrix} 1 \\ \cos\varphi_1 \\ \sin\varphi_1 \end{bmatrix}$ $\vec{\tau}_2 = \begin{bmatrix} 1 \\ \cos\varphi_2 \\ \sin\varphi_2 \end{bmatrix}$
(D) Navigator Computation of Fix	$\hat{n}_1(t_1) = T_{\hat{\omega}}(\varphi_1)\hat{n}_1(t_o)$ $\hat{n}_2(t_2) = T_{\hat{\omega}}(\varphi_2)\hat{n}_2(t_o)$	$\hat{n}_1(t_1) = W_{\hat{\omega}}\left[\hat{n}_1(t_o)\right]\vec{\tau}_1$ $\hat{n}_2(t_2) = W_{\hat{\omega}}\left[\hat{n}_2(t_o)\right]\vec{\tau}_2$
	$\hat{r} = \hat{n}_1(t_1) \times \hat{n}_2(t_2) \Big/ \left\lvert \hat{n}_1(t_1) \times \hat{n}_2(t_2) \right\rvert$ $r = -\vec{r}_s \cdot \hat{r} - \sqrt{(\vec{r}_s \cdot \hat{r})^2 - \vec{r}_s \cdot \vec{r}_s + (r_e + h)^2}$ $\vec{r}_n = \vec{r}_s + r\hat{r}$.	

3.7.3 Smoothing

In connection with the analytical method of fix computation, to average out the effects of satellite precession and smooth the effects of noise in the fan beam transmissions, two techniques of smoothing are included in the Navigational Satellite programs for optional use. For both techniques, the result of smoothing over an even number N of satellite revolutions is a navigator position determination for the time of satellite revolution 1/2 N.

- Position smoothing consists simply of averaging the set of latitude and longitude fixes obtained over the N satellite revolutions. Then, the estimates are:

$$\text{Lat } (\tfrac{1}{2}\,N) = \frac{1}{N}\sum_{k=1}^{N} \text{lat } (k)$$

$$\text{Lon } (\tfrac{1}{2}\,N) = \frac{1}{N}\sum_{k=1}^{N} \text{lon } (k)\ . \qquad (44)$$

- Time smoothing is applied to the timing data t_1-t_o and t_2-t_o, obtained for each satellite revolution, for the N satellite revolutions. Let $\Delta_1(k) = t_1-t_o$ and $\Delta_2(k) = t_2-t_o$ be the data observed during satellite revolution k. Then, the estimates are:

$$t_1\,(\tfrac{1}{2}\,N) = \frac{1}{N}\sum_{k=1}^{N} \Delta_1(k) + t_o(\tfrac{1}{2}\,N)$$

$$t_2\,(\tfrac{1}{2}\,N) = \frac{1}{N}\sum_{k=1}^{N} \Delta_2(k) + t_o(\tfrac{1}{2}\,N), \qquad (45)$$

where $t_o(\frac{1}{2}\,N)$ is the time of the reference pulse during satellite revolution $\frac{1}{2}\,N$, assumed to be noise-free (but possibly containing a bias). These timing values are then employed to estimate Lat $(\frac{1}{2}\,N)$

and Lon ($\frac{1}{2}$ N). Thus, time smoothing requires only one fix computation in contrast to position smoothing which requires N fixes. It will be seen in Section 4.2.3 that the two smoothing techniques yield comparable accuracies in position estimation.

3.7.4 Polynomial Method of Fix Computation

The primary items used in the analytical method of fix computation are t_1-t_o and t_2-t_o (within a satellite revolution). Let S and d be defined by

$$S = t_2 + t_1 - 2t_o$$

$$d = t_2-t_1$$

Then,

$$t_1-t_o = \frac{1}{2} (S-d)$$

$$t_2-t_o = \frac{1}{2} (S + d)$$

This suggests that it may be possible to obtain satisfactory latitude and longitude estimates from two finite power series in S and d:

$$\text{Lat} = \sum_{j=0}^{n} \sum_{i=0}^{n} a_{ij} S^i d^j$$

$$\text{Lon} = \sum_{j=0}^{n} \sum_{i=0}^{n} b_{ij} S^i d^j \qquad (46)$$

when n is a convenient value. For each function there will be $(n + 1)^2$ coefficients to determine. They may be determined by the method of least squares, if the S and d corresponding to $(n + 1)^2$ or more different calibration station locations are available. Assume there are $m > (n + 1)^2$ stations. Consider the Lat function. The problem is to determine the

$(n + 1)^2$ coefficients a_{ij} so as to minimize Q, where

$$Q = \sum_{k=1}^{m} \left[Lat\ (k) - \sum_{j} \sum_{i} a_{ij}\ S^i(k)\ d^j(k) \right]^2 . \qquad (47)$$

Differentiating with respect to any coefficient a_{pq} and setting equal to zero:

$$-\frac{1}{2} \frac{\partial Q}{\partial a_{pq}} = \sum_{k} \left[Lat(k) - \sum_{j} \sum_{i} a_{ij}\ S^i(k)\ d^j(k) \right] S^p(k)\ d^q(k) = 0.$$

Rearranging,

$$\sum_{j} \sum_{i} \left[\sum_{k} S^{i+p}(k)\ d^{j+q}(k) \right] a_{ij} = \sum_{k} S^p(k)\ d^q(k)\ Lat\ (k) . \qquad (48)$$

As p and q range independently over the values 0, 1, ..., n this represents a set of $(n + 1)^2$ linear equations by which to determine the $(n + 1)^2$ coefficients a_{ij}.

Replacing the symbols a_{ij} by b_{ij} and the Lat(k) by Lon(k), the coefficients b_{ij} may also be found. The same matrix of order $(n + 1)^2$ is used -- it is only the "right-hand side" of Equations (48) which changes.

Once the a_{ij} and b_{ij} are evaluated by the calibration stations, the Formulas (46) could be used by any navigator located within the region covered by the set of calibration stations.

This method has had only brief trial during the study because of lack of time. The results were inconclusive.

There are several variations possible in the polynomial method. For example, with equatorial orbits it might be advantageous to express the latitude polynomial in terms of d only. (In Section 5.2 it is shown that the

component transverse to the orbit plane depends primarily on d.) For the same number of coefficients, relatively high powers of d would be employed. Another approach would be to formulate the polynomials in terms of the primary items (t_1-t_o) and (t_2-t_o) instead of s and d. Still another would be to fit to cross-range and down-range distances from subsatellite point instead of to latitude and longitude. As yet these variations have not been tried.

It should be noted that misalignment of the satellite angular velocity vector will have some (unknown) effect on the values of the a_{ij} and b_{ij} for successive satellite revolutions, due to variations in S and d. Also, of course, recalibration of the coefficients would be needed at intervals because of earth and satellite motions.

3.7.5 Differential Method of Fix Computation

In this section a method is given by which a navigator's position may be evaluated relative to a preassigned (Lat, Lon) base-point, for which the fan times t_1 and t_2 are assumed accurately known.

There are some minor notational deviations in the present section. To avoid confusion they are listed here, within this section only:

a. $S = \frac{1}{2}(t_2 + t_1)$

b. $d = \frac{1}{2}(t_2-t_1)$

c. $t_o = 0$

d. Lon is the longitude of the navigator referred to the $\hat{E}$-axis of the equatorial inertial system.

Where "equatorial" or "space" axes are mentioned, the $\hat{E}$-system is meant.

The mapping of sums and differences of fan beam intercept times into longitudes and latitudes of points on the earth is complicated. In the neighborhood of a pre-determined point, however, the mapping is simple.

$$\begin{pmatrix} \text{Lon} \\ \text{Lat} \end{pmatrix} = \begin{pmatrix} f(s,d) \\ g(s,d) \end{pmatrix} \quad \text{Complicated}$$

$$\begin{pmatrix} \delta\text{Lon} \\ \delta\text{Lat} \end{pmatrix} = \begin{pmatrix} \frac{\partial f}{\partial s} & \frac{\partial f}{\partial d} \\ \frac{\partial g}{\partial s} & \frac{\partial g}{\partial d} \end{pmatrix} \begin{pmatrix} \delta s \\ \delta d \end{pmatrix} \quad \text{Simple} \tag{49}$$

The neighborhood of satisfactory validity of the simple (linear) formulation is yet to be determined. What follows here is a derivation of the partial derivatives or gradient

$$G = \begin{pmatrix} \frac{\partial f}{\partial s} & \frac{\partial f}{\partial d} \\ \frac{\partial g}{\partial s} & \frac{\partial g}{\partial d} \end{pmatrix}$$

For purposes of this derivation, the observer is assumed situated on the surface of a stationary sphere (earth) and not to be moving on that sphere. The satellite is assumed to have a constant angular velocity (vector) and also not to be moving relative to the sphere.

The navigator's position, $\vec{R}_N$, is written in terms of the satellite's position, $\vec{R}_S$, and the satellite-to-navigator vector, $\vec{R}$, as

$$\vec{R}_N = \vec{R}_S + \vec{R}$$

The navigator's position, written in equatorial coordinates, is

$$\vec{R}_N = r_N \begin{pmatrix} \cos \text{Lat} \cos \text{Lon} \\ \cos \text{Lat} \sin \text{Lon} \\ \sin \text{Lat} \end{pmatrix}$$

The satellite's position, is

$$\vec{R}_S = r_s \begin{pmatrix} \cos \text{Lat}_s \cos \text{Lon}_s \\ \cos \text{Lat}_s \sin \text{Lon}_s \\ \sin \text{Lat}_s \end{pmatrix}$$

The satellite-to-navigator vector, $\vec{R}$, is given by

$$\vec{R} = r\, T_{B_o 2S}\, T_{\hat{\omega}}(\omega s) \left[T_{\hat{\omega}}(\omega d)\ \hat{n}_1(0) \right] x \left[T_{\hat{\omega}}(-\omega d)\ \hat{n}_2(0) \right]$$

since $\hat{n}_1(t_1) \times \hat{n}_2(t_2) = \left[T_{\hat{\omega}}(\omega t_1)\ \hat{n}_1(0) \right] x \left[T_{\hat{\omega}}(\omega t_2)\ \hat{n}_2(0) \right]$ and $t_1 = s + d$, $t_2 = s-d$. The quantity r is defined as the satellite-to-navigator distance divided by $|\hat{n}_1(t_1) \times \hat{n}_2(t_2)|$. $T_{B_o 2S} \equiv M_{E_e}$.

The longitude and latitude of the navigator are defined by

$$\tan \text{Lon} = \frac{\hat{2}'\vec{R}_N}{\hat{1}'\vec{R}_N} \quad \text{and} \quad \sin \text{Lat} = \frac{\hat{3}'\vec{R}_N}{r_N}$$

where

$$\hat{1}' = (1\ \ 0\ \ 0)$$

$$\hat{2}' = (0\ \ 1\ \ 0)$$

$$\hat{3}' = (0\ \ 0\ \ 1)$$

The (') symbol denotes the transpose of a column vector.

The partial derivatives of Lon and Lat with respect to sum and difference are, therefore

$$\frac{\partial Lon}{\partial(s,d)} = \frac{1}{\sec^2 Lon}\,\frac{\partial \tan Lon}{\partial(s,d)} = \cos^2 Lon\left(\frac{\hat{1}'\vec{R}_N\hat{2}' - \hat{2}'\vec{R}_N\hat{1}'}{(\hat{1}'\vec{R}_N)^2}\right)\frac{\partial \vec{R}_N}{\partial(s,d)}$$

$$= \frac{1}{r_N \cos Lat}\left[\cos Lon\ \hat{2}' - \sin Lon\ \hat{1}'\right]\frac{\partial \vec{R}_N}{\partial(s,d)}$$

$$\frac{\partial Lat}{\partial(s,d)} = \frac{1}{r_N \cos Lat}\,\frac{\partial \sin Lat}{\partial(s,d)} = \frac{1}{r_N \cos Lat}\left[\hat{3}'\right]\frac{\partial \vec{R}_N}{\partial(s,d)}$$

Since the satellite's position is not a function of sum or difference, we have

$$\frac{\partial \vec{R}_N}{\partial(s,d)} = \frac{\partial \vec{R}}{\partial(s,d)}$$

and

$$\frac{\partial}{\partial(s,d)}\begin{pmatrix} Lat \\ Lon \end{pmatrix} = \frac{1}{r_N \cos Lat}\begin{pmatrix} \cos Lon\ \hat{2}' - \sin Lon\ \hat{1}' \\ \hat{3}' \end{pmatrix}\frac{\partial \vec{R}}{\partial(s,d)}$$

The transformation from initial body axes to space axes is also not a function of sum or difference, so

$$\frac{\partial \vec{R}}{\partial(s,d)} = T_{B_o 2S}\,\frac{\partial}{\partial(s,d)}\left\{r\ T_{\hat{\omega}}(\omega s)\left[T_{\hat{\omega}}(\omega d)\ \hat{n}_1(o)\right] x \left[T_{\hat{\omega}}(-\omega d)\ \hat{n}_2(o)\right]\right\}$$

If we denote

$$T_{\hat{\omega}}(\omega s)\left[T_{\hat{\omega}}(\omega d)\hat{n}_1(o)\right] x \left[T_{\hat{\omega}}(-\omega d)\hat{n}_2(o)\right]$$

by $\vec{C}$, then

$$\frac{\partial \vec{R}}{\partial(s,d)} = T_{B_o 2S}\left[r \frac{\partial \vec{C}}{\partial(s,d)} + \vec{C} \frac{\partial r}{\partial(s,d)} \right],$$

$$\frac{\partial \vec{C}}{\partial s} = \hat{\omega} \times \vec{C}, \tag{50}$$

and

$$\frac{\partial \vec{C}}{\partial d} = T_{\hat{\omega}}(\omega s) \left\{ \left[\hat{\omega} \times T_{\hat{\omega}}(\omega d)\hat{n}_1(0) \right] \times \left[T_{\hat{\omega}}(-\omega d)\hat{n}_2(0) \right] \right.$$

$$\left. - \left[T_{\hat{\omega}}(\omega d)\hat{n}_1(0) \right] \times \left[\hat{\omega} \times T_{\hat{\omega}}(-\omega d)\hat{n}_2(0) \right] \right.$$

$$= (\hat{\omega} \times \vec{A}) \times \vec{B} - \vec{A} \times (\hat{\omega} \times \vec{B}) \tag{51}$$

where

$$\vec{A} = T_{\hat{\omega}}(\omega s)\ T_{\hat{\omega}}(\omega d)\hat{n}_1(0) = T_{\hat{\omega}}(\omega t_1)\hat{n}_1(0)$$

$$\vec{B} = T_{\hat{\omega}}(\omega s)\ T_{\hat{\omega}}(-\omega d)\hat{n}_2(0) = T_{\hat{\omega}}(\omega t_2)\hat{n}_2(0)$$

In order to compute $\frac{\partial r}{\partial(s,d)}$, we need an expression for r which shows its dependence on sum and difference. For this, we note that $r_N^2 = \vec{R}_N \cdot \vec{R}_N$ is a constant.

$$r_N^2 = \vec{R}_N \cdot \vec{R}_N = r_s^2 + 2\vec{R}_S \cdot \vec{R} + \vec{R} \cdot \vec{R}$$

$$= r_s^2 + 2r\ \vec{R}_S \cdot T_{B_o 2S}\vec{C} + r^2\ \vec{C} \cdot \vec{C} \tag{52}$$

Now we differentiate Equation (52) with respect to (s,d).

$$2r^2\vec{C} \cdot \frac{\partial \vec{C}}{\partial(s,d)} + 2r\ \vec{C} \cdot \vec{C} \frac{\partial r}{\partial(s,d)} + 2\vec{R}_S \cdot T_{B_o 2S}\ \vec{C} \frac{\partial r}{\partial(s,d)} + 2r\ \vec{R}_S \cdot T_{B_o 2S} \frac{\partial C}{\partial(s,d)} = 0 \tag{53}$$

Switching Equation (53) around, we have

$$\left[r\,\vec{C} \cdot \vec{C} + \vec{R}_S \cdot T_{B_o 2S}\,\vec{C} \right] \frac{\partial r}{\partial(s,d)} = -\left[r^2 \vec{C} \cdot \frac{\partial \vec{C}}{\partial(s,d)} + r\vec{R}_S \cdot T_{B_o 2S} \frac{\partial \vec{C}}{\partial(s,d)} \right] \quad (54)$$

The coefficient multiplying $\frac{\partial r}{\partial(s,d)}$ in Equation (54) is a scalar whose inverse is thus its reciprocal. The partial derivatives on the right-hand side of Equation (54) were expressed in Equations (50) and (51). In summary,

$$\underset{2x2}{G} = \frac{1}{r_n \cos \text{Lat}} \underset{2x3}{\begin{bmatrix} \cos \text{Lon}\ \hat{2}' - \sin \text{Lon}\ \hat{1}' \\ \hat{3}' \end{bmatrix}} T_{B_o 2S} \underset{3x3}{} \left[r \frac{\partial \vec{C}}{\partial(s,d)} + \vec{C} \frac{\partial r}{\partial(s,d)} \right]_{3x2} \quad (55)$$

where

$$\frac{\partial \vec{C}}{\partial(s,d)} = \left[\hat{\omega} \times \vec{C} \quad (\hat{\omega} \times \vec{A}) \times \vec{B} - \vec{A} \times (\hat{\omega} \times \vec{B}) \right]$$

$$\frac{\partial r}{\partial(s,d)} = -\frac{1}{\left[r\vec{C} \cdot \vec{C} + \vec{R}_S \cdot T_{B_o 2S} \right]} \left[r^2 \vec{C} \cdot \frac{\partial \vec{C}}{\partial(s,d)} + r\vec{R}_S \cdot T_{B_o 2S} \frac{\partial \vec{C}}{\partial(s,d)} \right]$$

$$\vec{A} = T_{\hat{\omega}}(\omega s)\ T_{\hat{\omega}}(\omega d)\hat{n}_1(o)$$

$$\vec{B} = T_{\hat{\omega}}(\omega s)\ T_{\hat{\omega}}(-\omega d)\hat{n}_2(o)$$

$$\vec{C} = \vec{A} \times \vec{B}$$

In use, the elements of matrix G are evaluated for the position of the preassigned base-point. The navigator computes the differences δs and δd between his observed s and d and the s and d for the base-point. Then, Equation (49) yields the increments δ Lon and δ Lat to apply to the Lon and Lat of the base-point to obtain his latitude and longitude. It will be necessary to subtract GHA from the longitude value to obtain his geographical longitude.

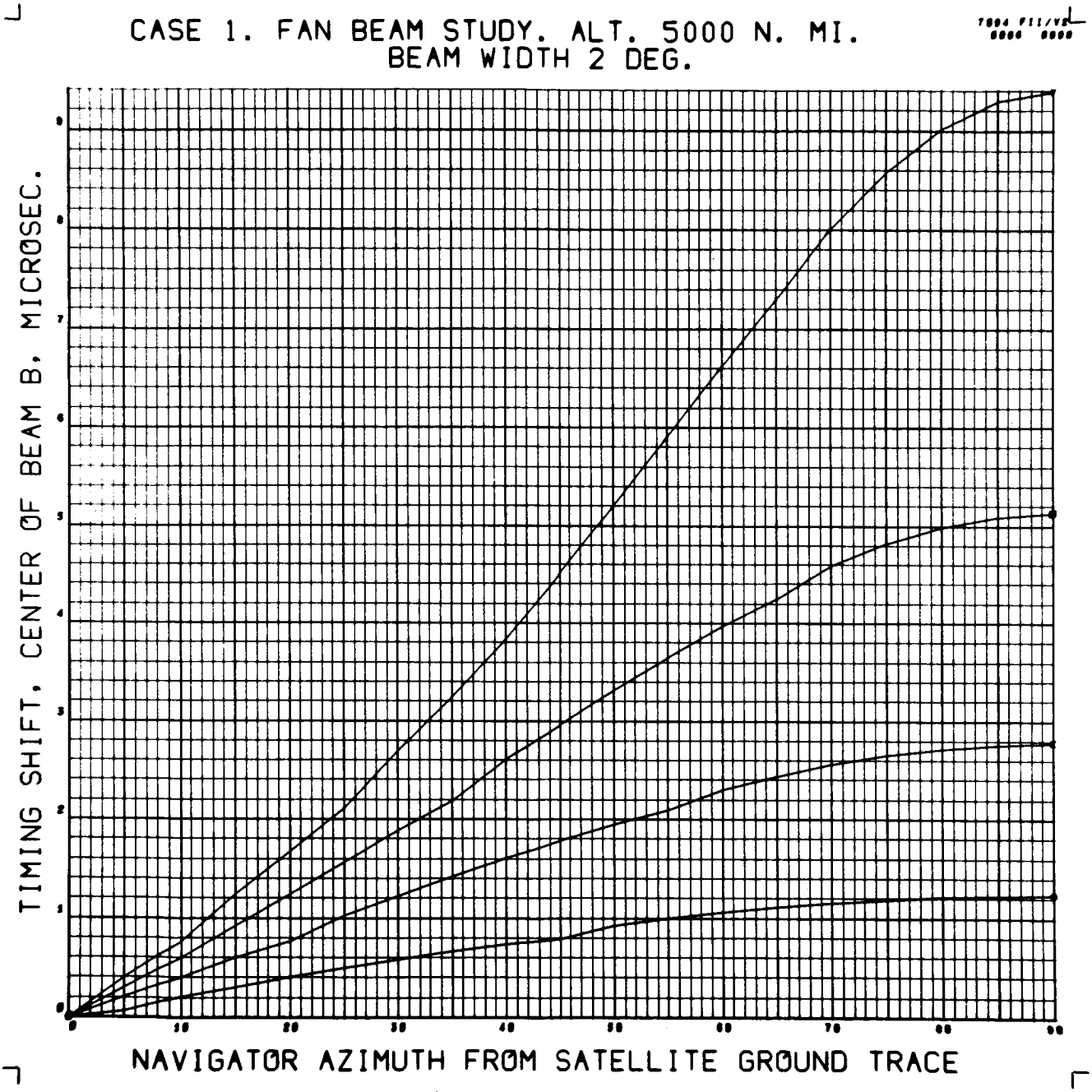
CASE 1. FAN BEAM STUDY. ALT. 5000 N. MI.
BEAM WIDTH 2 DEG.
TIMING SHIFT, CENTER OF BEAM B, MICROSEC.
NAVIGATOR AZIMUTH FROM SATELLITE GROUND TRACE

Figure 4-4

that at point a (threshold) to that at time T_m(maximum), is greater than the time interval ΔT_b required for the intensity to fall to that at point b (again, the threshold).

It will be observed that for the lower three curves the fix errors for both altitudes are nearly identical. For the fourth curve the high altitude case errors are considerably less than for the 5000 n.mi. case. This is due to earth curvature and the fact that, for a given subsatellite distance, the subtended angle at the satellite decreases with altitude. The latter feature results in a θ angle nearer 90^o in Figure 3-2 of Section 3.6 , and a smaller center shift error. Figures 4-4, 4-5 display the actual amounts of the center shift for the two altitudes. The total range in microseconds corresponds approximately to the range of the position error in nautical miles. (The slight irregularities in the center shift curves is due to round-off error. The computation of microsecond phenomena lies near the numerical precision limits.)

One further aspect of the center shift error is of interest. Figures 4-6 and 4-7 are plots of the center shift versus the difference of the two observed fan beam detection times. The curves for all distances of navigator from the subsatellite point are coincident (for the high altitude the plot is almost a straight line). This means that correction of the observed t_1 and t_2 for the center shift effect does not depend upon the particular navigator location, and hence the finite beam effects can be cancelled by calibration stations.

4.1.2 Effects of Earth and Satellite Motions

The computer runs made to assess effects of finite antenna patterns were repeated with earth rotation and satellite orbital motion operative. Figures 4-8 and 4-9 show the resulting fix errors. Comparing them with Figures 4-1 and 4-2, it is obvious that these motions have little effect on the fix computations except for the extreme subsatellite distance for the 5000 n.mi. altitude case, (for which the satellite elevation

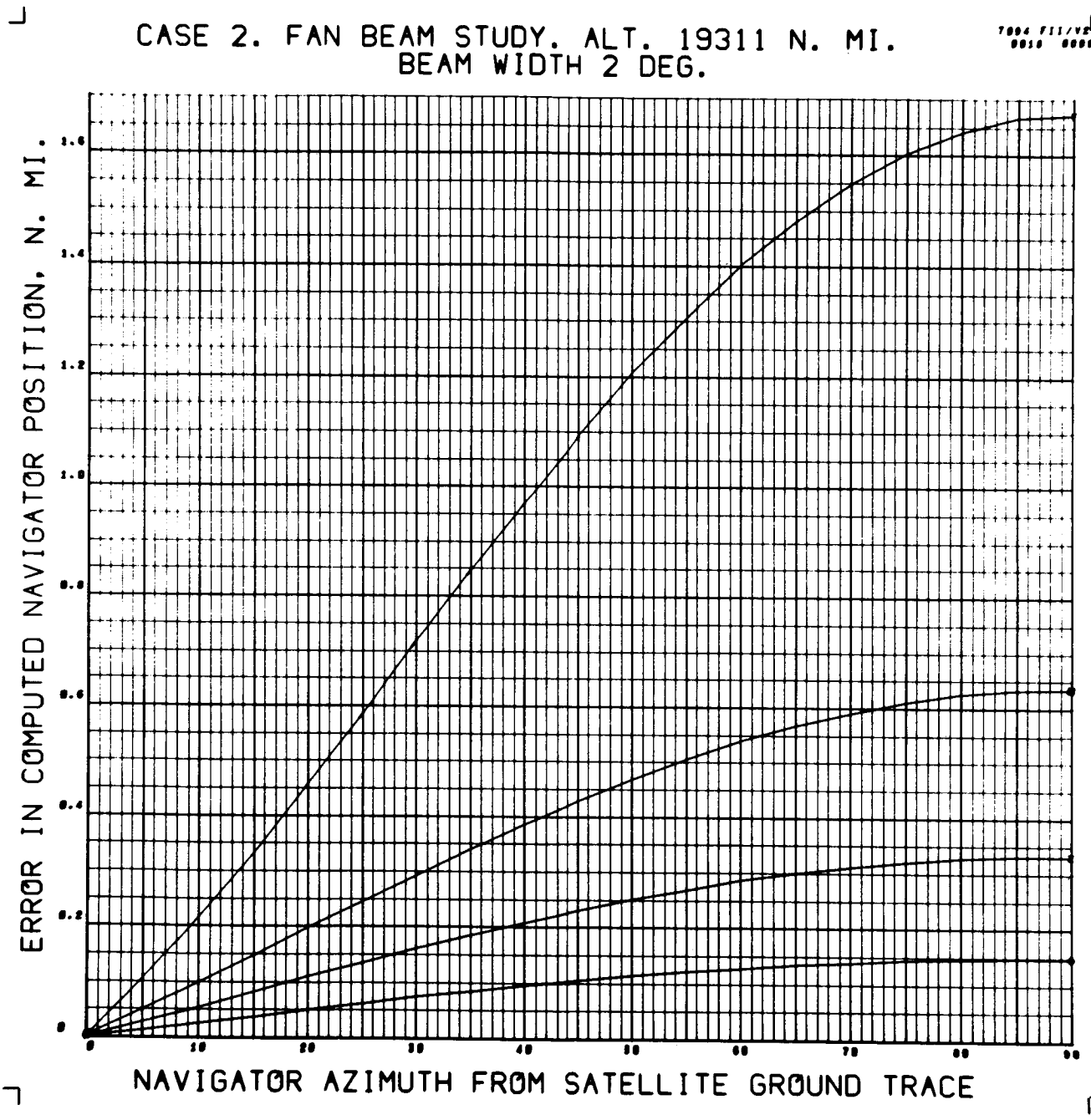
CASE 2. FAN BEAM STUDY. ALT. 19311 N. MI.
BEAM WIDTH 2 DEG.
ERROR IN COMPUTED NAVIGATOR POSITION, N. MI.
1.6
1.4
1.2
1.0
0.8
0.6
0.4
0.2
0
0
10
20
30
40
50
60
70
80
90
NAVIGATOR AZIMUTH FROM SATELLITE GROUND TRACE

Figure 4-2

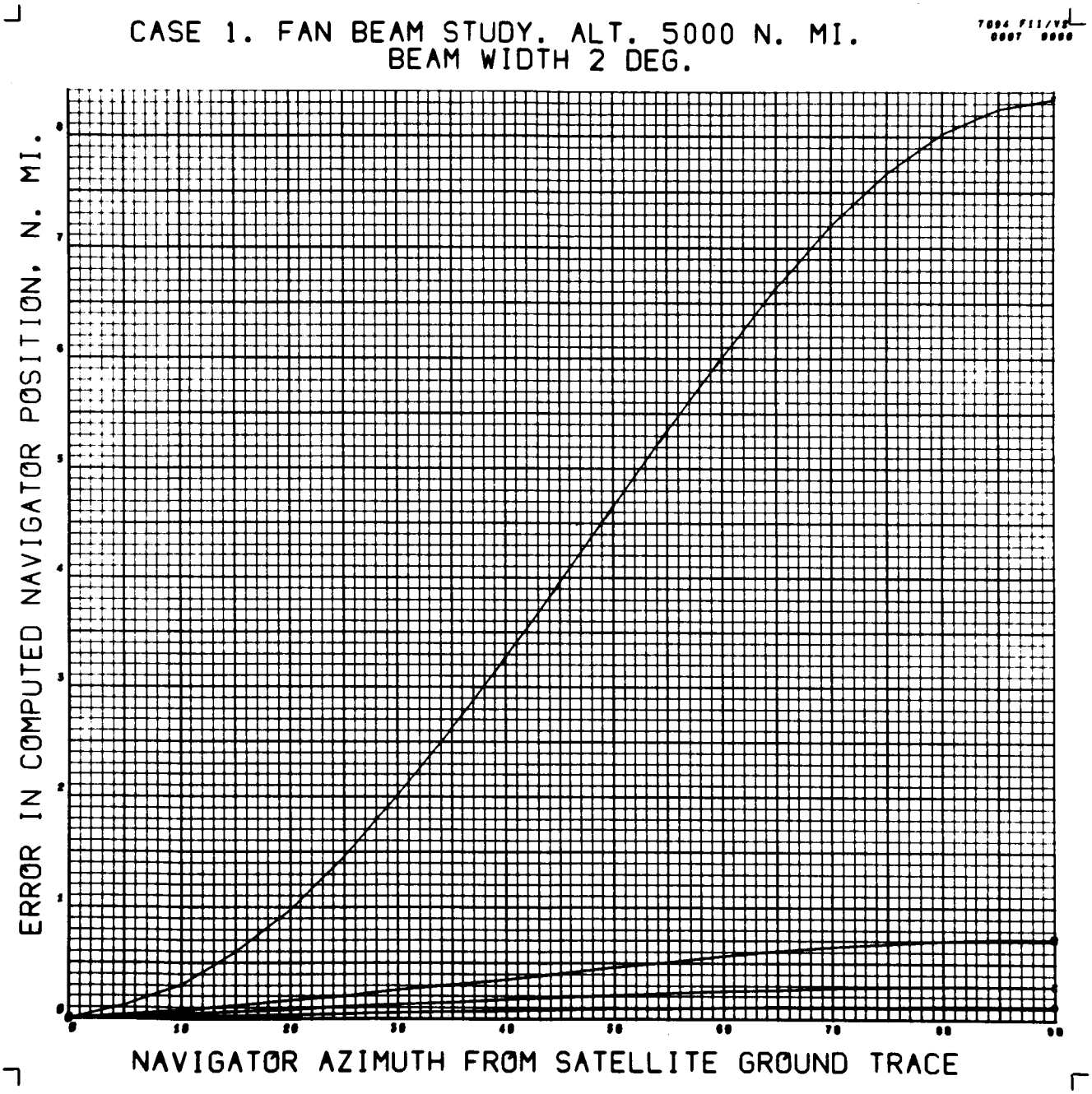
CASE 1. FAN BEAM STUDY. ALT. 5000 N. MI.
BEAM WIDTH 2 DEG.
ERROR IN COMPUTED NAVIGATOR POSITION, N. MI.
0
1
2
3
4
5
6
7
8
0
10
20
30
40
50
60
70
80
90
NAVIGATOR AZIMUTH FROM SATELLITE GROUND TRACE

Figure 4-1

in Section 3.6. A 60-slot antenna with 3 db beam-width of 2^{o} is assumed (an antenna length of five feet at 8 gHz).

In Figures 4-1 and 4-2 the only source of error in the fix computation is the finite fan beam width. A motionless earth and navigator and a satellite with no orbital motions are assumed. The four curves in the figures represent distances of the navigator from the subsatellite point of approximately 600, 1200, 2000 and 3600 nautical miles.

The fact that the threshold averaging for t_1 and t_2 gives rise to a fix error is a result of the angular manner in which the fan beams sweep past the navigator position. It is a purely geometrical effect, which causes the average of the threshold times to be unequal to the actual time of passage of the mid-plane of the beam. This will be called the "center shift" error. Figure 4-3 illustrates the situation for a navigator position with $\gamma = 90^{o}$.

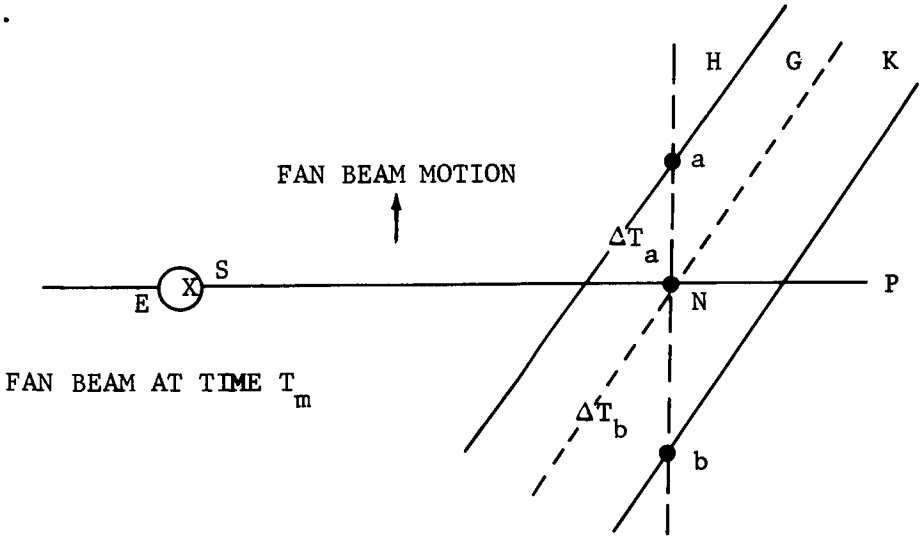

Figure 4-3. Center Shift Phenomenon.

Let P represent the edge view of the plane through the satellite S, Earth-Center E and navigator position N. Let G be the line through N along which the beam intensity is a maximum, at time T_m. Further, let H be the line through a and K be the line through b, where the line $\overline{a\ b}$ is perpendicular to P and passes through N. Finally, let $T_m - \Delta T_a$, and $T_m + \Delta T_b$ be chosen such that the beam intensities are equal when point a or b is at N (corresponding to the threshold value). The antenna pattern and geometry are such that the time interval ΔT_a, required for the beam intensity to increase from

The discussion of results is divided into five categories. Section 4.1 will consist mainly of comparative effects of various error sources, based upon a single fix computation. The actual numerical values of position error depend strongly upon the satellite attitude at reference pulse time. This will change from revolution to revolution, hence the computed position errors for a single fix calculation will depend upon the input initial conditions.

In Section 4.2 the variation of fix errors with satellite revolution number is shown. Also, the effects of smoothing upon position and fan timing values obtained over a set of satellite revolutions are discussed, with and without the assumption of the presence of noise.

Section 4.3 contains several cases constructed to approximate an operational fan beam navigation system. Typical errors are impressed upon most of the system parameters and the attainable accuracy in fix computation is displayed as a function of available satellite power and receiver antenna diameter as well as the smoothing time (in terms of satellite revolutions),

Section 4.4 gives some results from the differential fix computation method described in Section 3.7.5.

In Section 4.5 several other miscellaneous topics of interest are illustrated and discussed.

4.1 SINGLE FIX COMPARISONS

For the first presentation of results, it is assumed that the navigator's computation of position is based on fan beam timing detections t_1 and t_2 made on the first satellite revolution following time t = 0.

4.1.1 Effects of a Finite Antenna Pattern

An actual fan beam antenna pattern is only an approximation to the ideal planar fan. The pattern used in the NavSat programs has been described

Table 4-1 Simulation Input Summary

Case	Earth Rot.	Sat Mot.	Navigator Motion			Finite Beam	Spin Dir. Error	Spin Rate Error	Fan Normal Errors m rad.		Bias In Fan Timing		Noise In Fan Timing		Bias In t_o	Multiple Revs. No Smoothing		Smoothing			Navigator Location		Satellite Altitude	* Comments
		Azm. Deg.	Alt. n.mi.	Azm. Deg.	Vel. n.mi./Hr.		m rad.	μrad. sec.	Fan 1	Fan 2	Fan 1	Fan 2	σ μsec.	Noise Limit μsec.	μsec.	No. Revs.	True $\hat{n}_i(t_o)$	Delta Revs.	Max. Revs.	True $\hat{n}_i(t_o)$	γ Deg.	SSD n.mi.	n.mi.	
1						Yes															0(5)90	*	5000	180 rpm. ρ=1.4 SSD= 979,2061,3451,6615 km
2						Yes															0(5)90	*	19311	As in Case 1 SSD= 1262,2612,4198,6560 km
3	Yes	0				Yes															0(5)90	*	5000	As in Case 1.
4	Yes	0				Yes															0(5)90	*	1931	As in Case 1 SSD= 1262,2612,4198,6560 km
5							0.5 1.0														0(5)90	800 (800) 3200	5000	
6							0.5 1.0														0(5)90	800 (800) 4000	19311	
7							0.1														0(5)90	800 (800) 3200	5000	
8							0.1														0(5)90	800 (800) 3200	5000	Navigator uses $\hat{h}$ as estimate for $\hat{\omega}$
9							0.1														0(5)90	800 (800) 4000	19311	
10							0.1														0(5)90	800 (800) 4000	19311	Navigator uses $\hat{h}$ as estimate for $\hat{\omega}$
11							0.1									50	No				30 60	800 (800) 3200	5000	
12							0.1									50	No				30 60	800 (800) 3200	19311	
17									0.1	0.1											0(10)90	800 2400	5000	
18									0.5	0.5											0(10)90	800 2400	5000	
19									-1.0	1.0											0(10)90	800 2400	5000	
20									0.1	0.1											0(10)90	800 2400	19311	
21									0.5	0.5											0(10)90	800 2400	19311	
22									-1.0	1.0											0(10)90	800 2400	19311	
23	Yes	90	6	-90	600		0.1											10	50	NO	30 60	800 2400	5000	
24	Yes	90	6	-90	600		0.1											10	50	No	30 60	800 2400	19311	
25	Yes	90	6	-90	600		0.1						7.9	23.7				10	50	No	30 60	800 2400	5000	
29	Yes	90	6	-90	600		0.1						30.3	90.9	1			20	100	No	30 60	800 2400	19311	
42	Yes	90	6	-90	600		0.1	50			1 σ error applied. $\sigma=\sigma_\tau / \sqrt{N}$, both fans. See Section (4.3) for dependence of σ_τ on power and antennas.				.5			10	50	No *	60	2400	19311	Power 50 watts. Navigator uses calibrated $\hat{n}_i$ and $\hat{\omega}$.
43	Yes	90	6	-90	600		0.1	50							.5			10	50	No *	60	2400	19311	Power 100 watts. Navigator uses calibrated $\hat{n}_i$ and $\hat{\omega}$.
44	Yes	90	6	-90	600		0.1	50							.5			10	50	No *	60	2400	19311	Power 150 watts. Navigator uses calibrated $\hat{n}_i$ and $\hat{\omega}$.
45	Yes	90	6	-90	600		0.1	50							.5			10	50	No *	60	2400	19311	Power 200 watts. Navigator uses calibrated $\hat{n}_i$ and $\hat{\omega}$.

The computer runs were categorized by Case Number according to the types of input data being varied. Usually, each case resulted in several plots (Figures) of functional relationships. The inputs associated with any figure may be determined from the Case Number given at the top of the figure, by inspection of this chart. A tabular correlation of Case Number – Figures is given in the List of Illustrations, pages iv-viii.

Asterisks (*) in the chart refer to material in the "Comments" column.

SECTION 4
RESULTS OF SIMULATION

Forty-five computer runs, involving about five hours of IBM 7094 time, have been made to study the effects of the error sources listed in Section 2.3. Two satellite altitudes were studied, 5000 nautical miles and synchronous. Navigator positions were taken at increments in distance, d, from the subsatellite point of 800 nautical miles, (except for Section 4.1.1 where these distances are slightly different), and at varying directions given by increments in azimuth, γ, relative to the orbit plane as illustrated in Section 2.3. Where graphical output was desired plotted against γ, $\Delta\gamma$ was taken five or 10 degrees. Table 4-1 displays in chart form the major input characteristics for the 45 cases. Except where noted in this chart, other quantities required were set as follows:

Initial Time	0 seconds
Initial Satellite Latitude	0^o
Initial Satellite Longitude	0^o
Satellite Orbit Eccentricity	0^o
Navigator Altitude	0 n.mi.
Initial Roll, Pitch, Yaw	0^o
Satellite Angular Velocity Rate	100 rpm
Satellite Angular Velocity Direction	Normal to Orbit Plane
Fan Beam Normals	45^o and 135^o from satellite symmetry axis $\hat{e}_2$, coplanar with $\hat{e}_1$ and $\hat{e}_2$
Satellite Moment of Inertia Ratio	1.1

Characteristics of the fan beam antennas and beam propagation parameters will be given in connection with the relevant cases below (Sections 4.1.1 and 4.3).

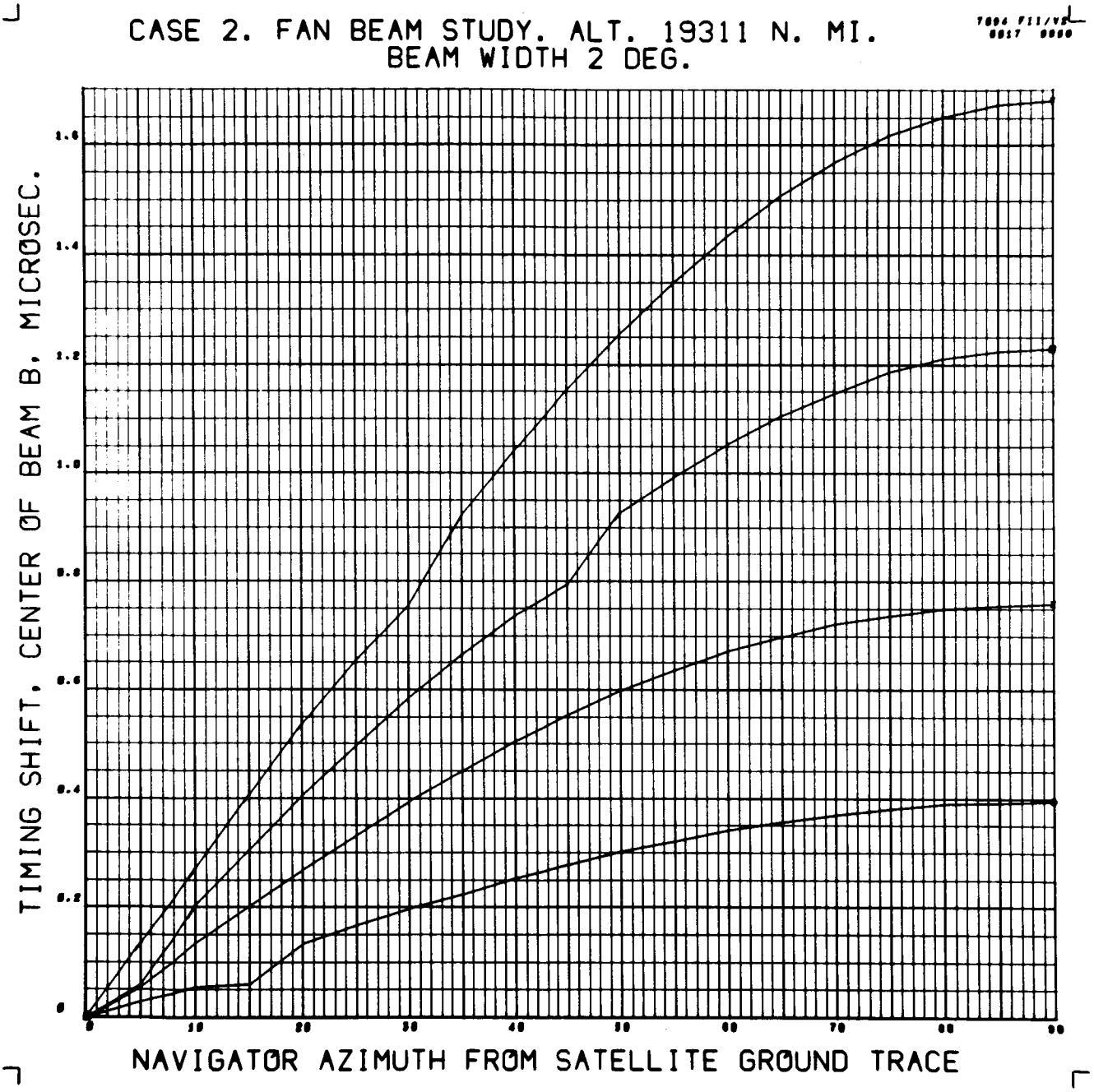
CASE 2. FAN BEAM STUDY. ALT. 19311 N. MI.
BEAM WIDTH 2 DEG.
TIMING SHIFT, CENTER OF BEAM B, MICROSEC.
1.6
1.4
1.2
1.0
0.8
0.6
0.4
0.2
0
10
20
30
40
50
60
70
80
90
NAVIGATOR AZIMUTH FROM SATELLITE GROUND TRACE

Figure 4-5

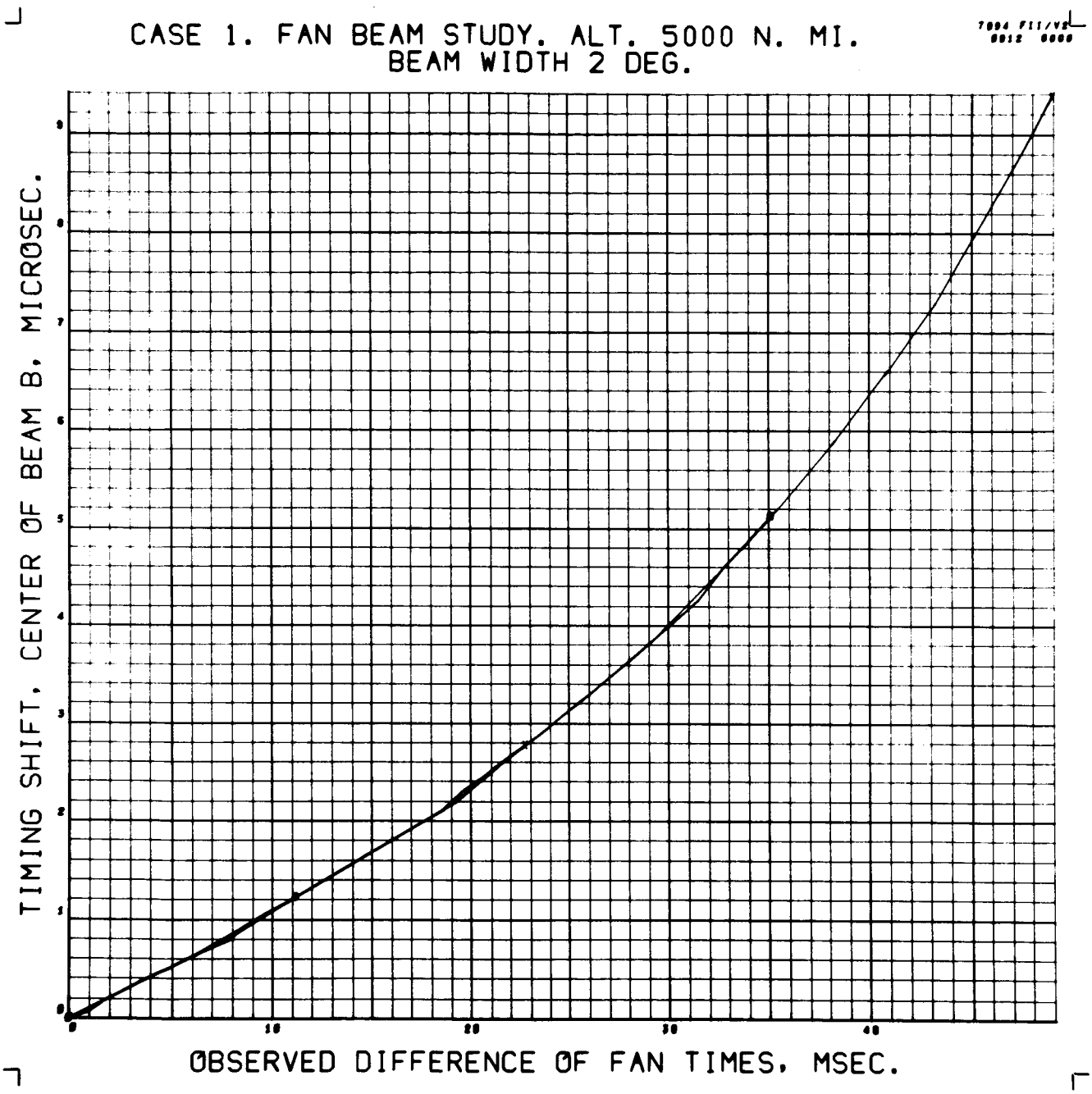
CASE 1. FAN BEAM STUDY. ALT. 5000 N. MI.
BEAM WIDTH 2 DEG.
TIMING SHIFT, CENTER OF BEAM B, MICROSEC.
0
1
2
3
4
5
6
7
8
9
0
10
20
30
40
OBSERVED DIFFERENCE OF FAN TIMES, MSEC.

Figure 4-6

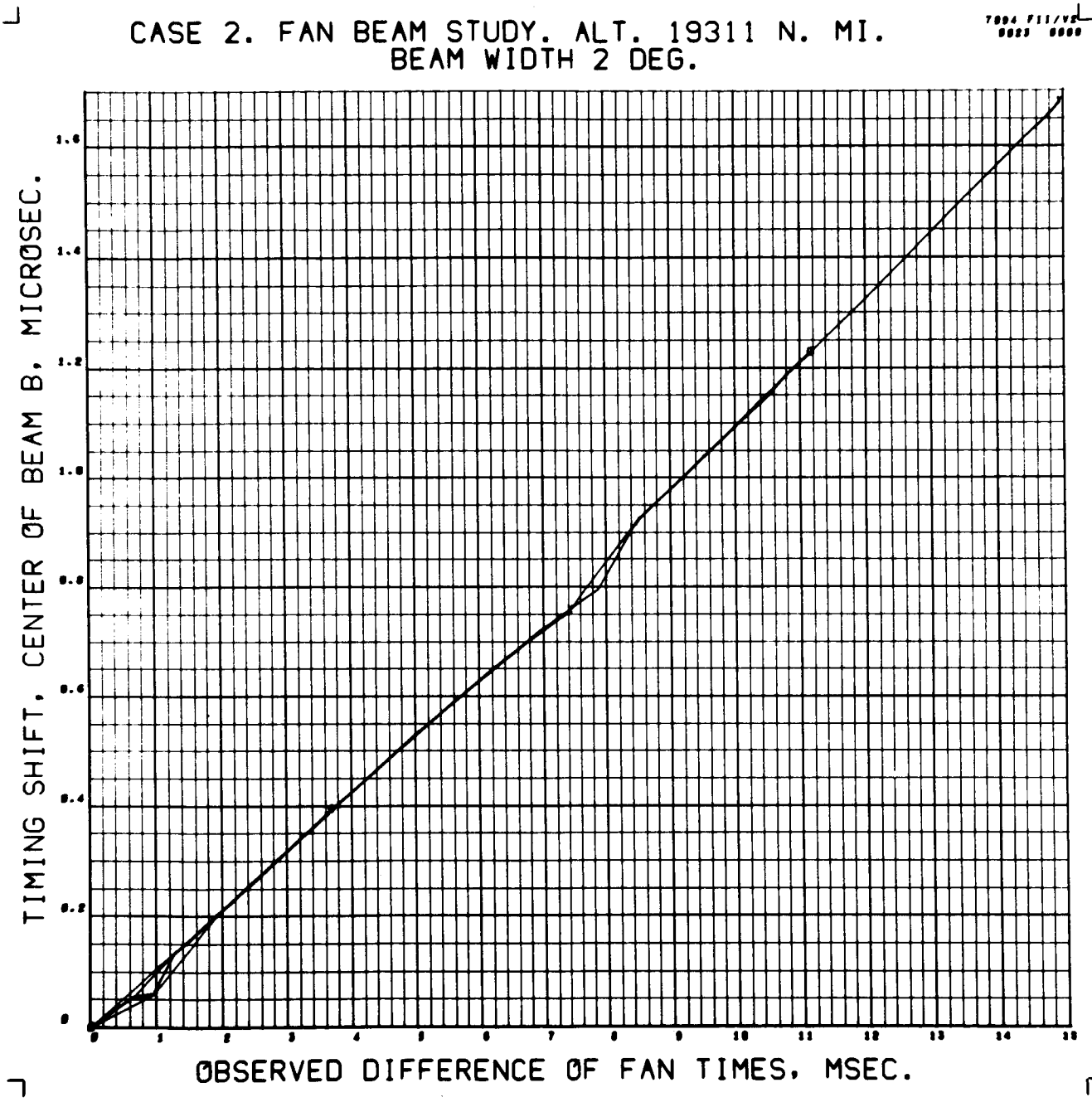
CASE 2. FAN BEAM STUDY. ALT. 19311 N. MI.
BEAM WIDTH 2 DEG.
TIMING SHIFT, CENTER OF BEAM B, MICROSEC.
OBSERVED DIFFERENCE OF FAN TIMES, MSEC.

Figure 4-7

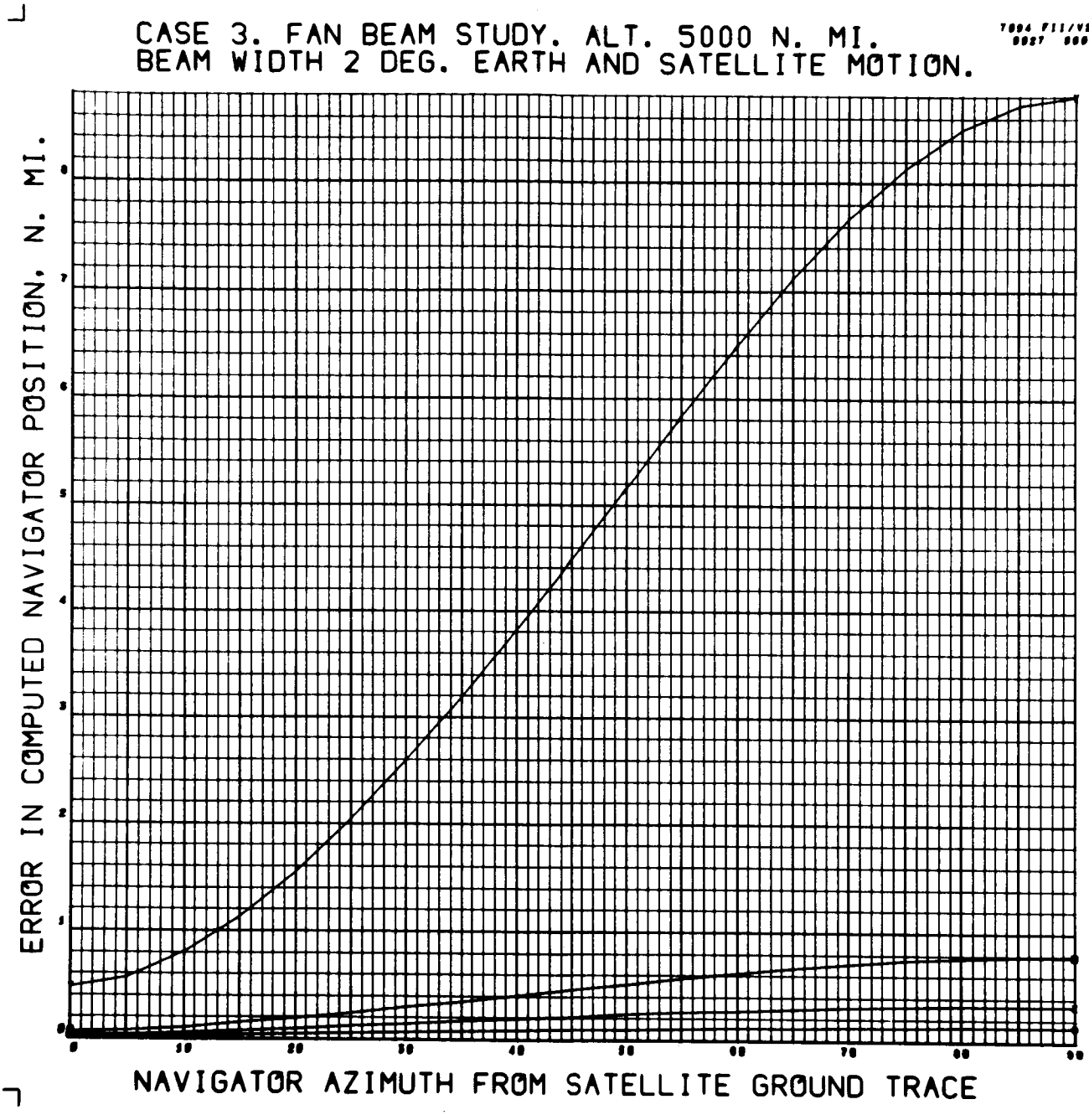
CASE 3. FAN BEAM STUDY. ALT. 5000 N. MI.
BEAM WIDTH 2 DEG. EARTH AND SATELLITE MOTION.
ERROR IN COMPUTED NAVIGATOR POSITION, N. MI.
NAVIGATOR AZIMUTH FROM SATELLITE GROUND TRACE

Figure 4-8

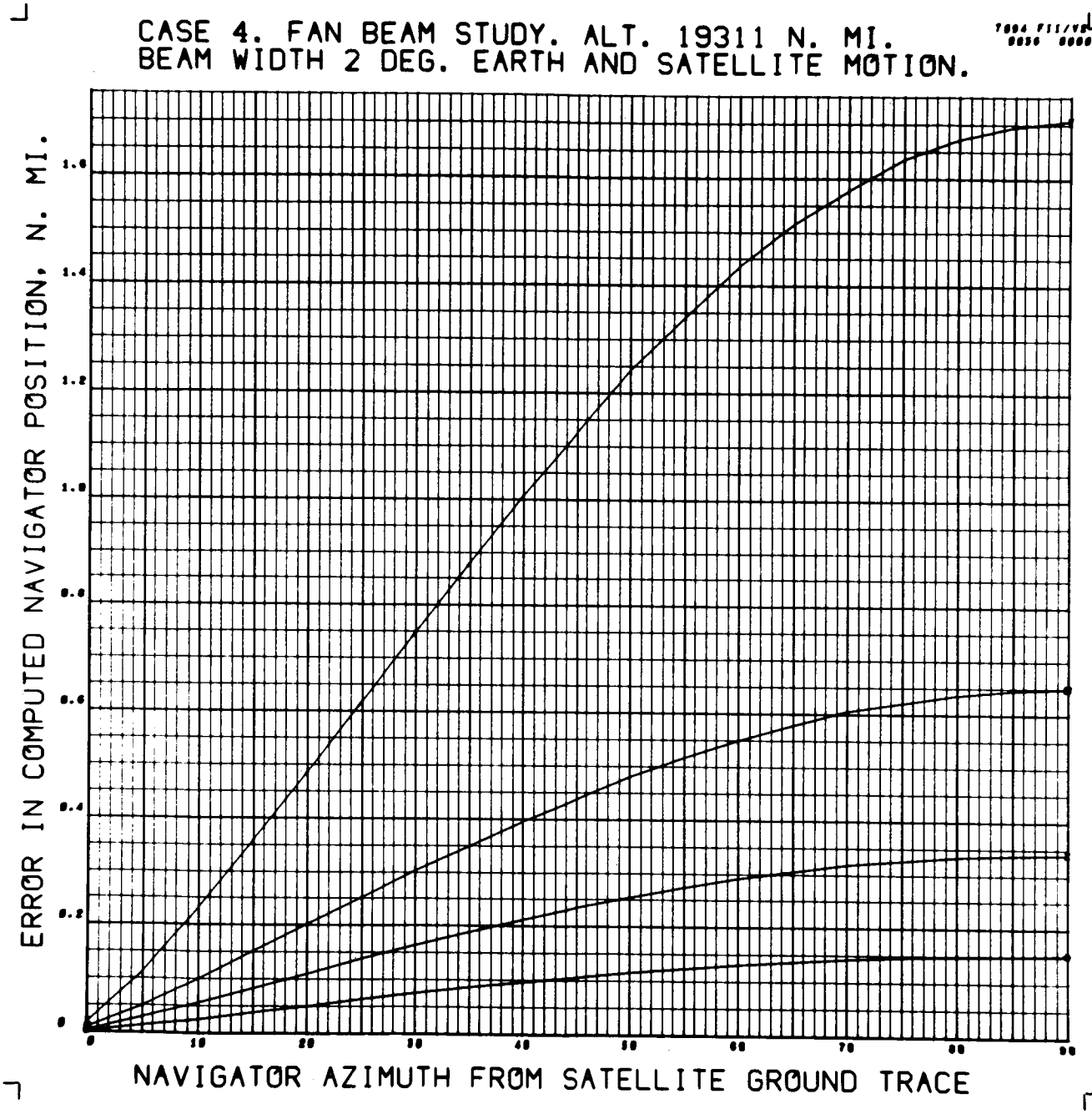
CASE 4. FAN BEAM STUDY. ALT. 19311 N. MI.
BEAM WIDTH 2 DEG. EARTH AND SATELLITE MOTION.
ERROR IN COMPUTED NAVIGATOR POSITION, N. MI.
NAVIGATOR AZIMUTH FROM SATELLITE GROUND TRACE

Figure 4-9

angle is only about 6^{o}). To obtain the effects of satellite altitude on these cases, polar orbits were assumed for both altitudes. Obviously, for the synchronous altitude with an equatorial (eastward) orbit, there would be no interaction effects between earth and satellite orbital motion, although there would be a small variation in the direction of the satellite-to-navigator vector in the $\hat{E}$-frame of coordinates during the passing of the two fan beams. The following brief table affords a comparison between the motion and no-motion cases.

Satellite Altitude (n.mi.)	Distance From Subsatellite Point (n.mi.)	Error in Computed Position (n.mi.)					
		$\gamma = 0$		$\gamma = 45^{o}$		$\gamma = 90^{o}$	
		No Motions	Motions	No Motions	Motions	No Motions	Motions
5000	600	0	.01	.08	.08	.12	.13
	1200	0	.03	.20	.21	.30	.33
	2000	0	.07	.41	.46	.72	.80
	3600	0	.48	3.96	4.48	8.33	8.80
19311	600	0	.001	.105	.105	.150	.150
	1200	0	.006	.230	.235	.328	.340
	2000	0	.013	.425	.435	.632	.650
	3600	0	.025	1.090	1.125	1.672	1.710

Comparison computer runs have also been made with the same inputs except that an ideal planar fan beam is assumed. The fix errors are reduced by an order of magnitude. This further suggests that the remaining sources of error (earth and satellite motion) contribute much less to the error in fix than does the finite fan beam width.

Unless the ultimate in accuracy of position determination is required, the navigator should not need to correct for earth rotation and satellite orbital motion.

4.1.3 Effects of Misalignment of Angular Velocity Vector

In the analytical method of fix computation, a navigator requires knowledge of the inertial components of the satellite angular velocity vector $\vec{\omega}$ at the time of the reference pulse t_o. Since it is not possible to obtain perfect alignment of $\vec{\omega}$ with the axis of inertial symmetry $\hat{e}_2$ there will in general be a precessive motion. Calibration stations must then determine $\vec{\omega}(t_o)$ at the times $t_o(k)$ of each satellite revolution, k, to the degree of accuracy necessary for use by navigators. This subject is discussed in Sections 3.7.1 and 5.3. In Figures 4-10 through 4-13, it is assumed that the navigator employs the initial $\hat{e}_2$ vector as the angular velocity vector direction $\hat{\omega}(t_o)$ in his fix computation (see Figure 3-1, Section 3.3). The figures display the fix error incurred for actual deviations, α, of $\hat{\omega}(t_o)$ from $\hat{e}_2$ of .1 and .5 milliradian for the two satellite altitudes of interest. The curves on each plate represent subsatellite distances of 800, 1600, 2400, and 3200 nautical miles, with one extra curve at 4000 for the high altitude. No other of the error sources of Section 2.3 are presumed operative.

It is seen that the fix errors for the .5 milliradian cases are almost precisely five times those for the .1 milliradian cases. For the same subsatellite distances, the fix errors for the high altitude are smaller than for the medium altitude. This is due to the smaller subtended angles at the satellite and the resulting smaller elapsed times between the two fan beam passings at the navigator sites.

It should be emphasized that the $\hat{\omega}$ deviations considered here represent errors in knowledge of the true vector $\vec{\omega}(t_o)$. It is not simply a misalignment of $\vec{\omega}$ with $\hat{e}_2$ which causes the fix errors. Vector $\vec{\omega}$ may be

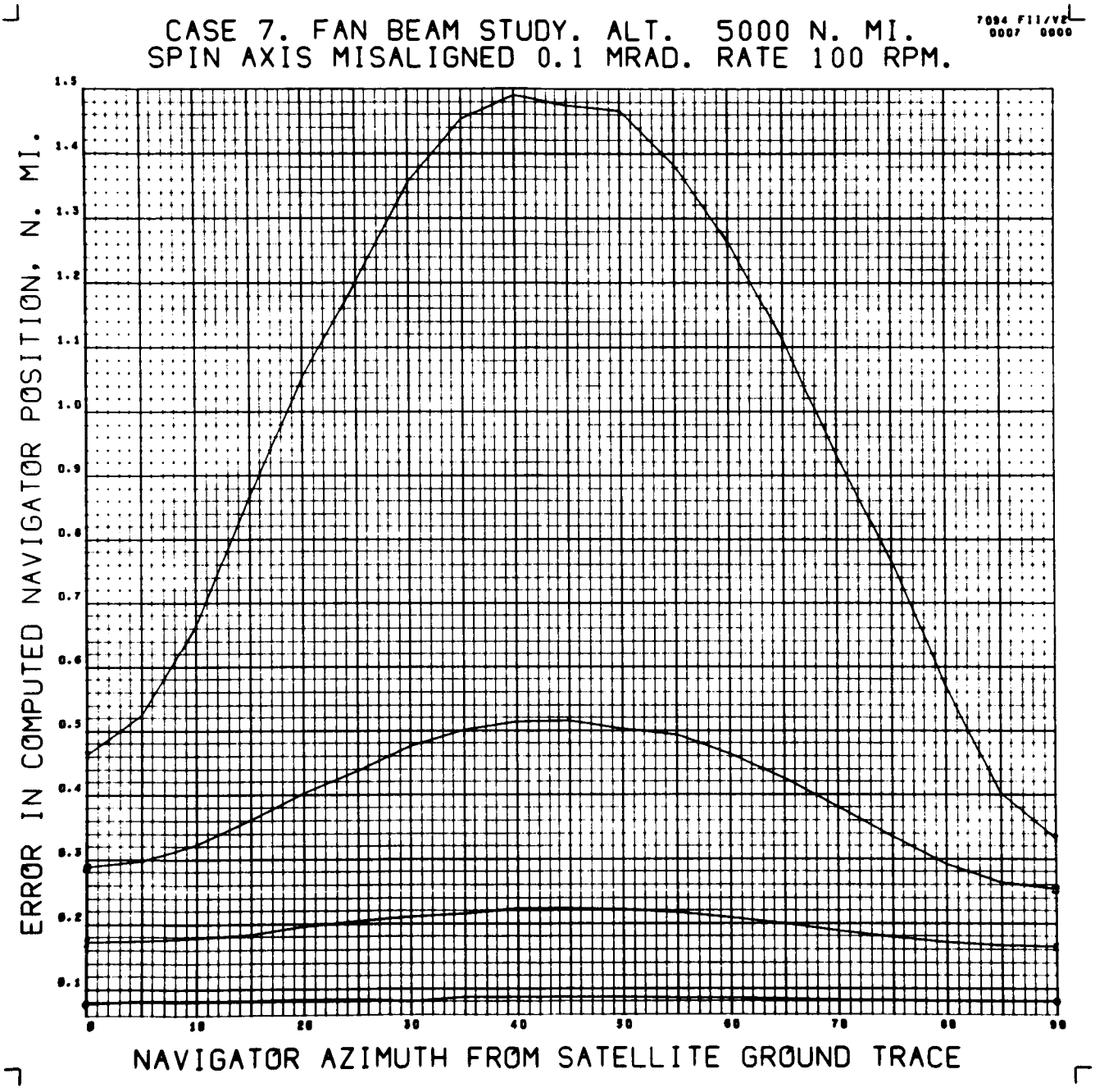
CASE 7. FAN BEAM STUDY. ALT. 5000 N. MI.
SPIN AXIS MISALIGNED 0.1 MRAD. RATE 100 RPM.
7094 F11/VS
0007 0000
ERROR IN COMPUTED NAVIGATOR POSITION, N. MI.
1.5
1.4
1.3
1.2
1.1
1.0
0.9
0.8
0.7
0.6
0.5
0.4
0.3
0.2
0.1
0
10
20
30
40
50
60
70
80
90
NAVIGATOR AZIMUTH FROM SATELLITE GROUND TRACE

Figure 4-10

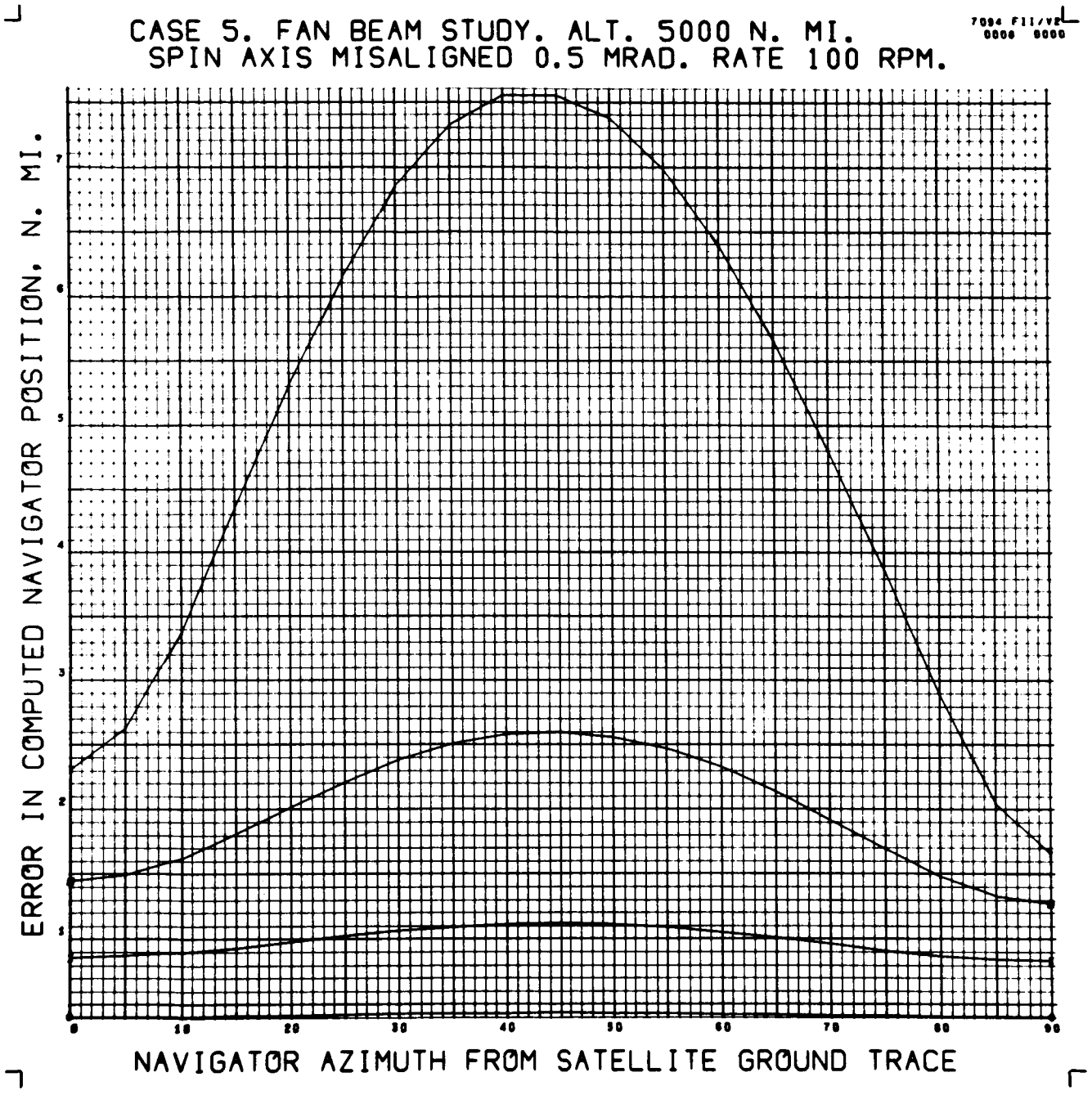
CASE 5. FAN BEAM STUDY. ALT. 5000 N. MI.
SPIN AXIS MISALIGNED 0.5 MRAD. RATE 100 RPM.
ERROR IN COMPUTED NAVIGATOR POSITION, N. MI.
NAVIGATOR AZIMUTH FROM SATELLITE GROUND TRACE

Figure 4-11

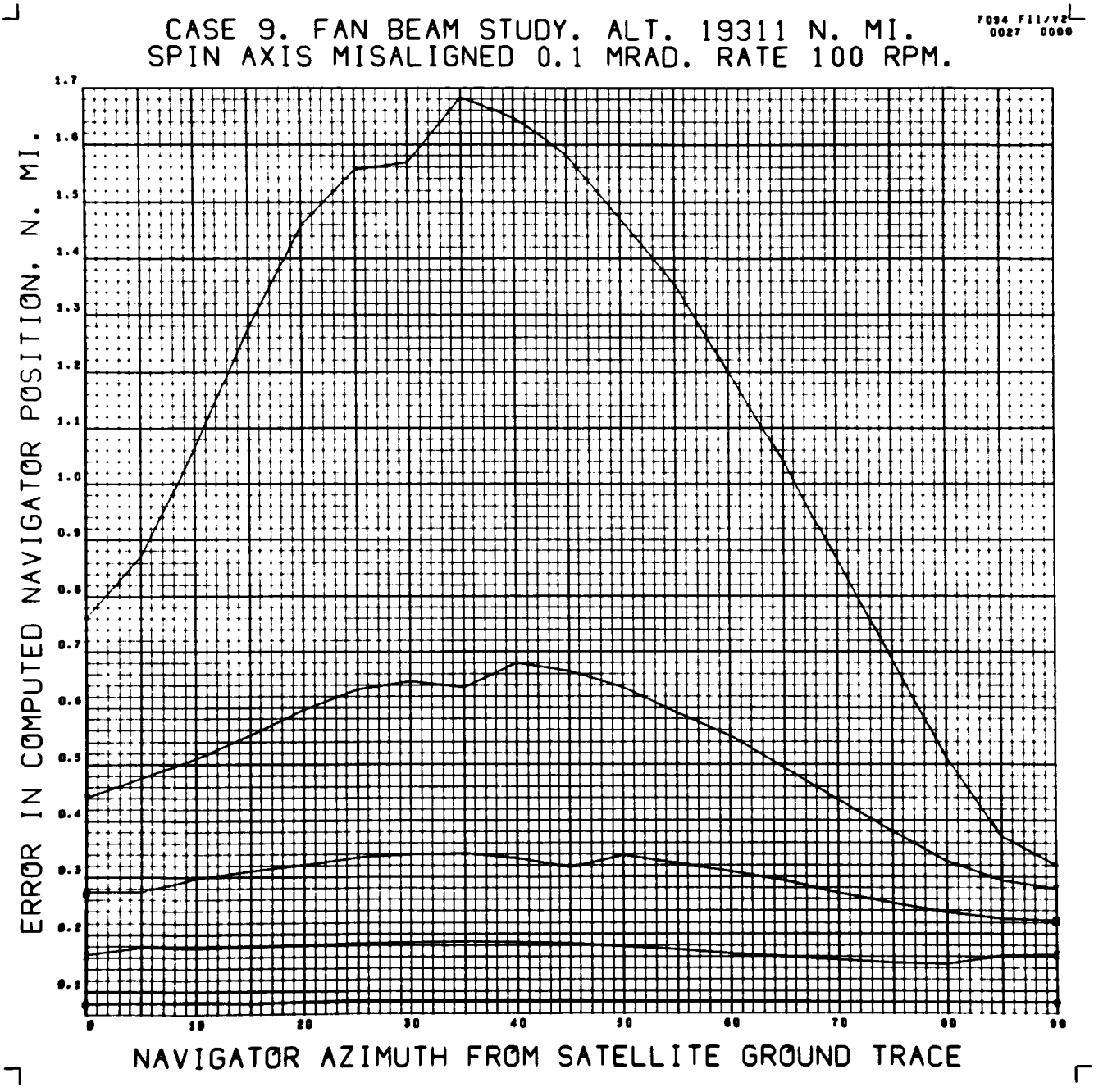
CASE 9. FAN BEAM STUDY. ALT. 19311 N. MI.
SPIN AXIS MISALIGNED 0.1 MRAD. RATE 100 RPM.
7094 F11/V2
0027 0000
ERROR IN COMPUTED NAVIGATOR POSITION, N. MI.
1.7
1.6
1.5
1.4
1.3
1.2
1.1
1.0
0.9
0.8
0.7
0.6
0.5
0.4
0.3
0.2
0.1
0
10
20
30
40
50
60
70
80
90
NAVIGATOR AZIMUTH FROM SATELLITE GROUND TRACE

Figure 4-12

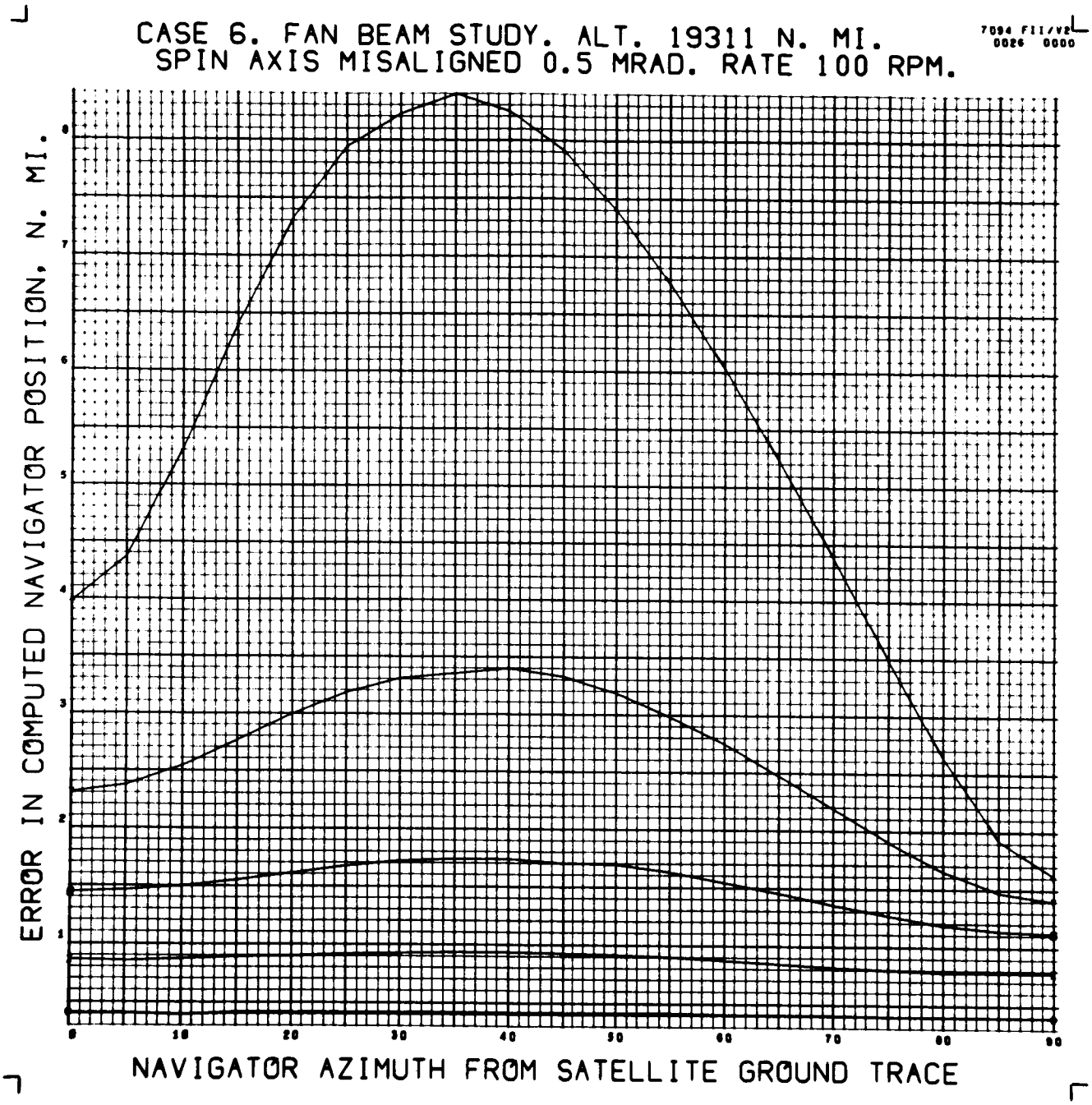
CASE 6. FAN BEAM STUDY. ALT. 19311 N. MI.
SPIN AXIS MISALIGNED 0.5 MRAD. RATE 100 RPM.
7094 FII/VS
0026 0000
ERROR IN COMPUTED NAVIGATOR POSITION, N. MI.
0
1
2
3
4
5
6
7
8
0
10
20
30
40
50
60
70
80
90
NAVIGATOR AZIMUTH FROM SATELLITE GROUND TRACE

Figure 4-13

misaligned with $\hat{e}_2$ so long as a sufficiently accurate estimate of the true $\vec{\omega}$ is available at the time of the reference t_o pulse. As discussed in Section 5.3, relatively simple calibration procedures should allow estimation of $\hat{\omega}(t_o)$ with an angular deviation of about $(\rho-1)$ times the actual angular misalignment of $\hat{\omega}$ with $\hat{e}_2$. This would be done by obtaining an estimate for the spatially fixed $\hat{h}$ vector. Figures 4-14 and 4-15 display the fix errors resulting for the cases of Figures 4-10 and 4-12 when $\hat{h}$ is used as an estimate for $\hat{\omega}(t_o)$. Since $\rho = 1.1$, the angle between $\hat{h}$ and $\hat{\omega}$ is less than one-tenth of the angle between $\hat{e}_2$ and $\hat{\omega}$. Comparing Figures 4-14 and 4-15 with Figures 4-10 and 4-12 it is seen that the fix errors are now less than one-tenth of their previous values. Roundoff error (i.e., truncation error in the IBM 7094) accounts for the rather rough appearance of the curves but the relationships are clear.

The linearity previously noted with respect to the fix errors for .5 and .1 milliradian $\hat{\omega}$ misalignments indicates that, by using $\hat{h}$ to approximate $\hat{\omega}$, the maximum fix errors for the .5 milliradian case would be about .5 nautical mile, over a large range of possible navigator placements. Of course, through use of calibration procedures which can predict $\hat{\omega}$ almost exactly (perhaps by means of a satellite-mounted star detector, as described in Section 5.2 of Volume V of this study), fix errors due to $\hat{\omega}$ misalignment may be practically eliminated.

Some further discussion of the use of $\hat{h}$ to approximate $\hat{\omega}$ will be found in Section 4.3, in connection with multiple fix calculations and smoothing.

4.1.4 Effects of Errors in Fan Beam Reference Normals

As has been mentioned in Sections 2.1 and 3.7.1, at the time of a reference t_o pulse, the navigator requires good estimates of the orientation in inertial space of the two boom antenna arrays on the satellite, as well as the estimate for $\vec{\omega}$. In this simulation, the required orientations are represented by vectors $\hat{n}_1(t_o)$ and $\hat{n}_2(t_o)$, normal respectively to the

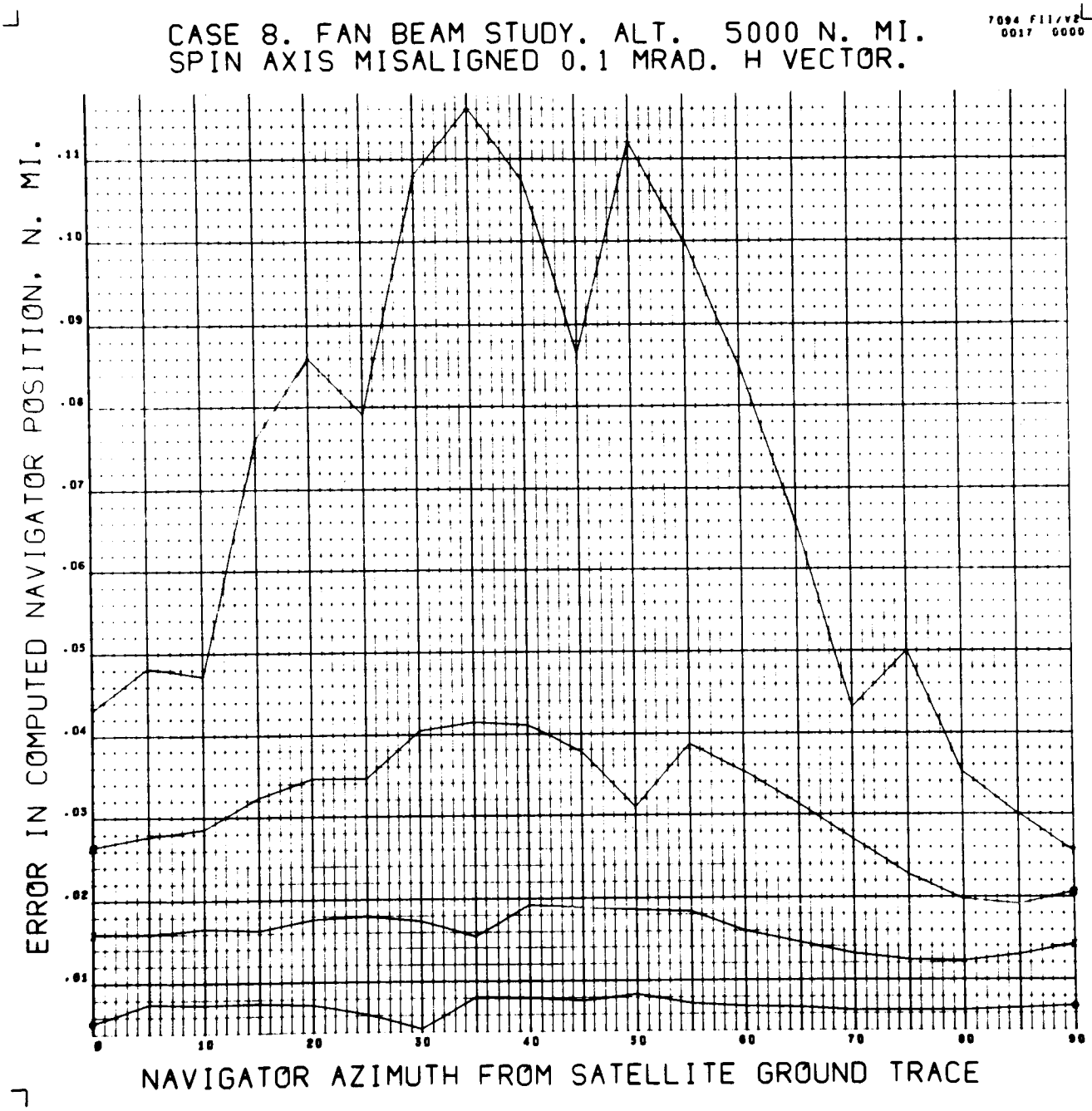
CASE 8. FAN BEAM STUDY. ALT. 5000 N. MI.
SPIN AXIS MISALIGNED 0.1 MRAD. H VECTOR.
7094 F11/V2
0017 0000
ERROR IN COMPUTED NAVIGATOR POSITION, N. MI.
.11
.10
.09
.08
.07
.06
.05
.04
.03
.02
.01
0
10
20
30
40
50
60
70
80
90
NAVIGATOR AZIMUTH FROM SATELLITE GROUND TRACE

Figure 4-14

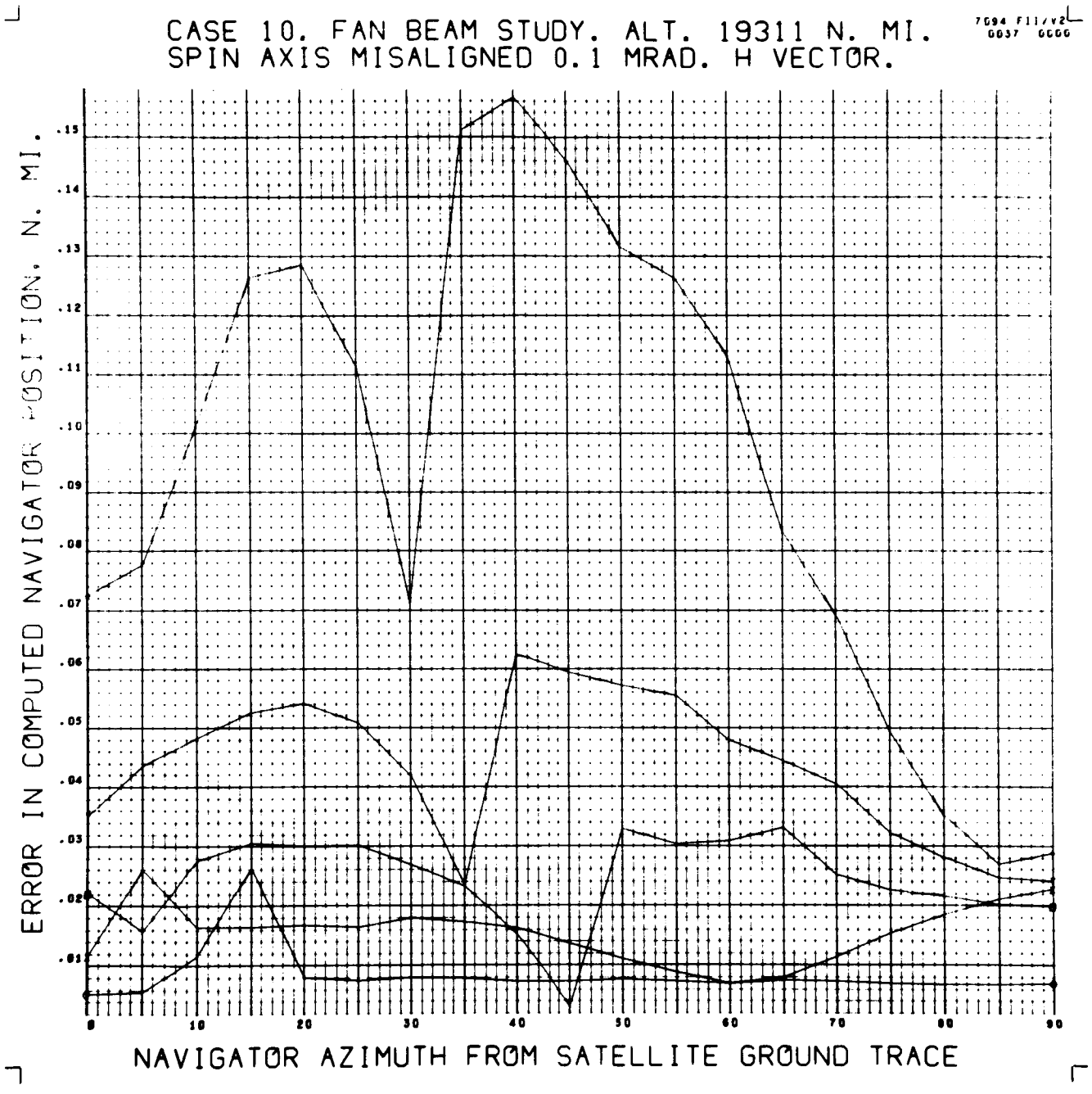
CASE 10. FAN BEAM STUDY. ALT. 19311 N. MI.
SPIN AXIS MISALIGNED 0.1 MRAD. H VECTOR.
7094 F11/V2
0037 0000
ERROR IN COMPUTED NAVIGATOR POSITION, N. MI.
.15
.14
.13
.12
.11
.10
.09
.08
.07
.06
.05
.04
.03
.02
.01
0
10
20
30
40
50
60
70
80
90
NAVIGATOR AZIMUTH FROM SATELLITE GROUND TRACE

Figure 4-15

mid-planes of fan beams Nos. 1 and 2. Estimates of the $\hat{E}$-components of these vectors must be determined by calibration stations along with the estimation of $\vec{\omega}(t_o)$. Figures 4-17 through 4-20 display the amounts of fix error resulting from miscalibration of $\hat{n}_1(t_o)$ and $\hat{n}_2(t_o)$ directions by .1 and .5 milliradian for the two satellite altitudes of interest. The two curves per frame correspond to distances of the navigator from the subsatellite point of 800 and 2400 nautical miles. The reference normal errors are the only sources of Section 2.3 presumed to be contributing to the fix computation errors. Figure 4-16 illustrates the type of miscalibration assumed. (Note that no knowledge of $\hat{e}_1(t_o)$ or $\hat{e}_2(t_o)$ is needed by the navigator.)

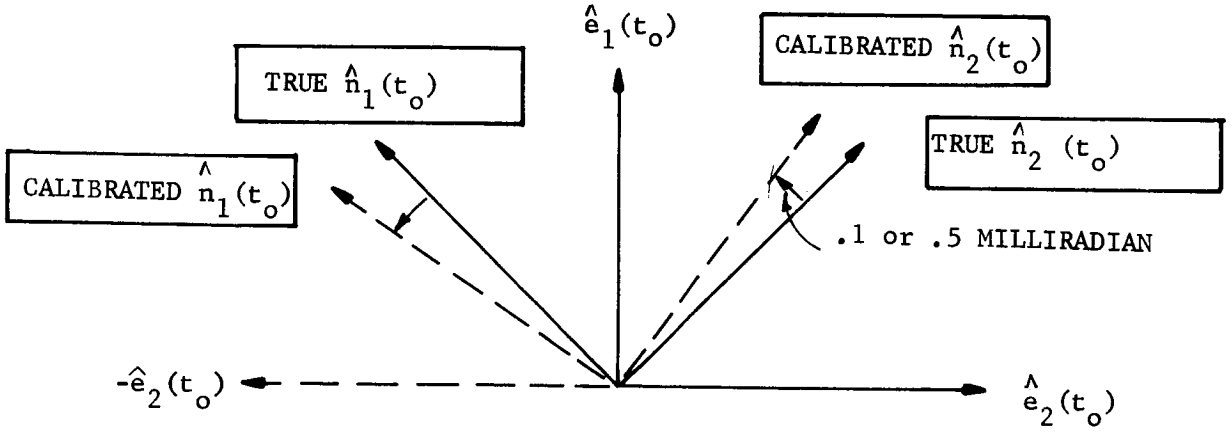

Figure 4-16. Miscalibrated Reference Normals

As was the case for $\hat{\omega}$ errors, the curves for .5 milliradian show fix errors almost exactly five times those for .1 milliradian. Also, the same beneficial effects of the higher altitude are present, for the same reasons. The shapes of these curves differ from the curves for the $\hat{\omega}$ errors in that the symmetry with respect to an azimuth, γ, of 35 or 45 degrees is absent, the fix errors near γ = 90 degrees tending to be the largest.

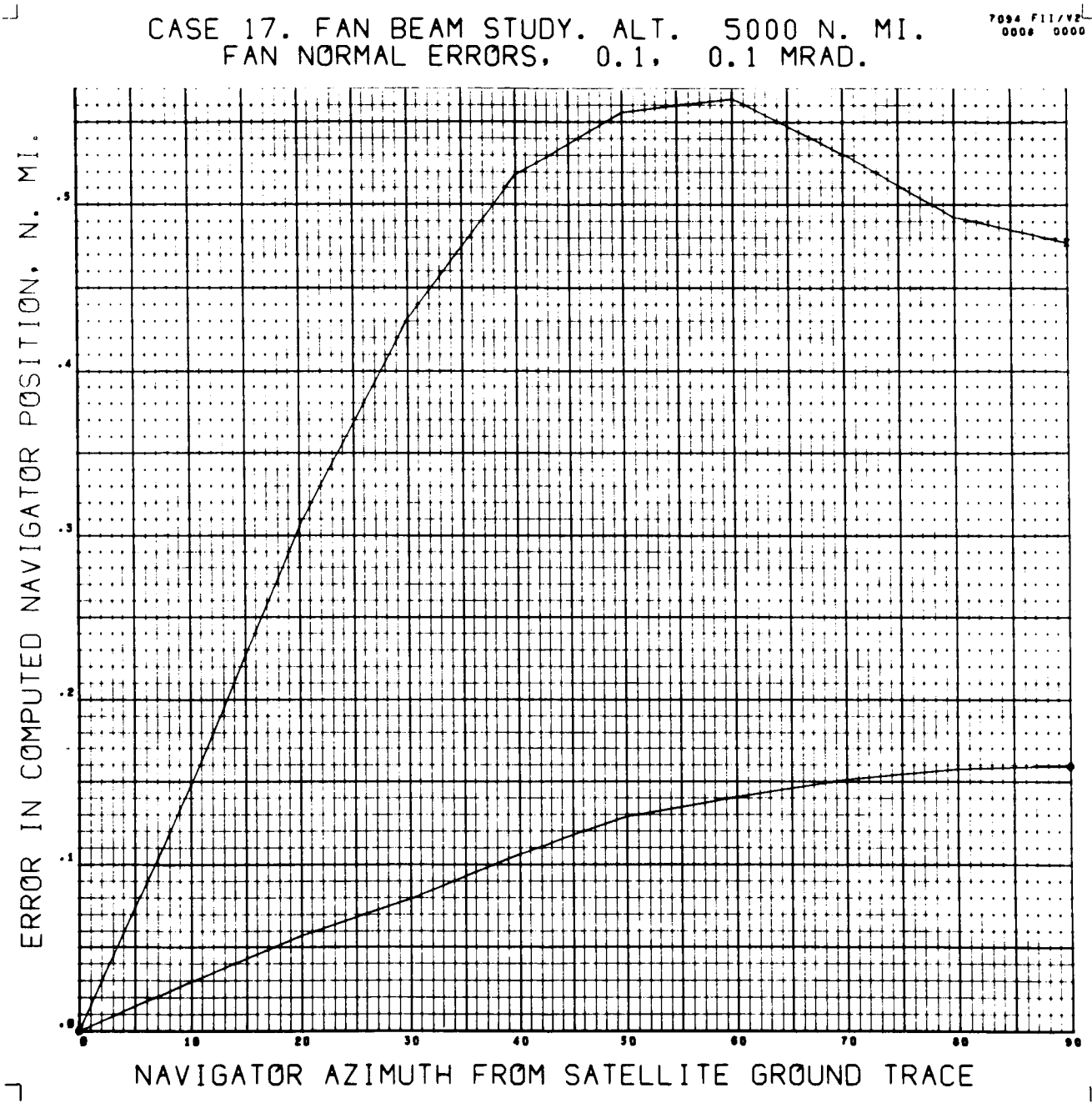
CASE 17. FAN BEAM STUDY. ALT. 5000 N. MI.
FAN NORMAL ERRORS, 0.1, 0.1 MRAD.
ERROR IN COMPUTED NAVIGATOR POSITION, N. MI.
.5
.4
.3
.2
.1
0
0
10
20
30
40
50
60
70
80
90
NAVIGATOR AZIMUTH FROM SATELLITE GROUND TRACE

Figure 4-17

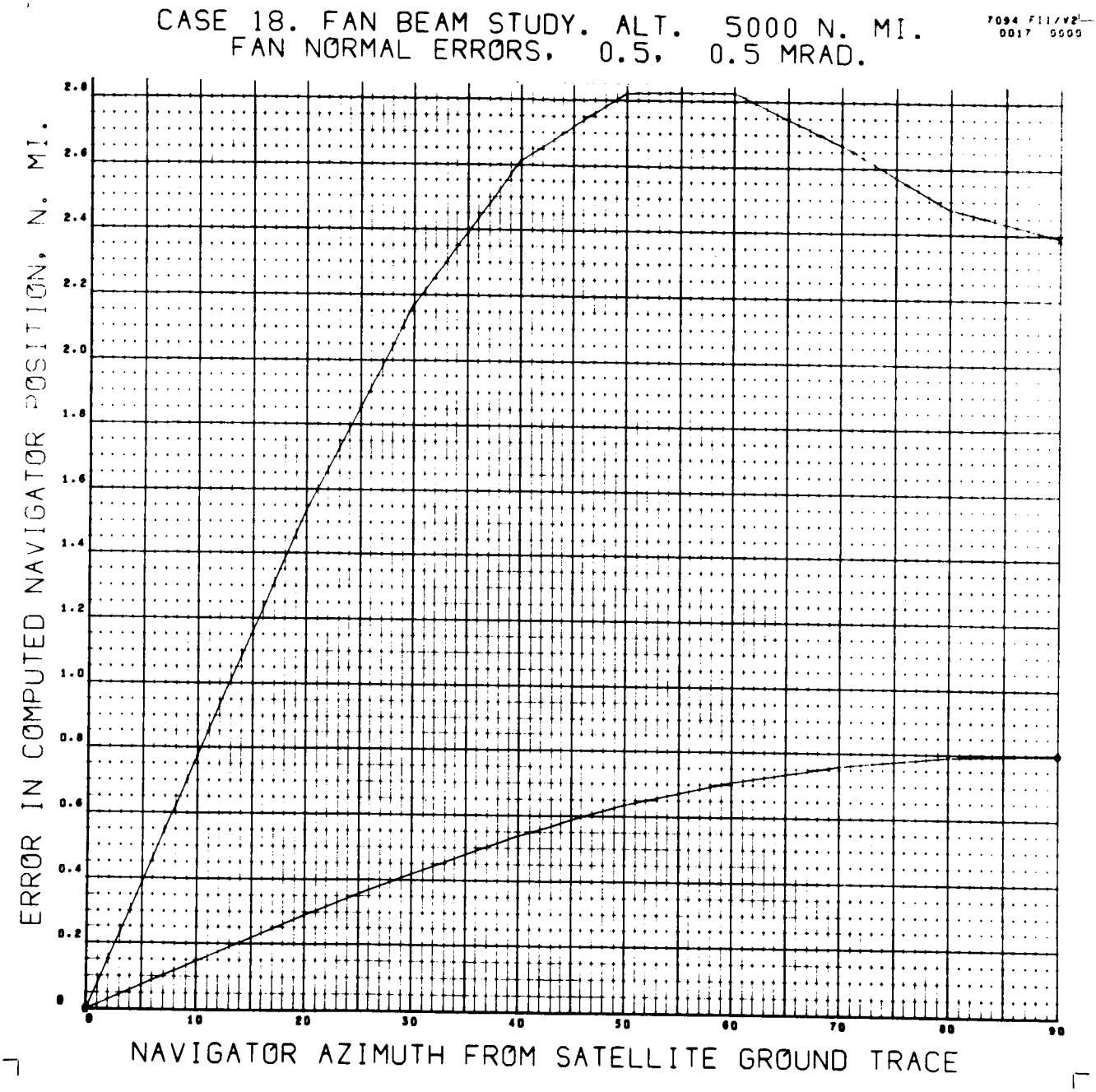
CASE 18. FAN BEAM STUDY. ALT. 5000 N. MI.
FAN NORMAL ERRORS, 0.5, 0.5 MRAD.
ERROR IN COMPUTED NAVIGATOR POSITION, N. MI.
NAVIGATOR AZIMUTH FROM SATELLITE GROUND TRACE
0
0.2
0.4
0.6
0.8
1.0
1.2
1.4
1.6
1.8
2.0
2.2
2.4
2.6
2.8
10
20
30
40
50
60
70
80
90

Figure 4-18

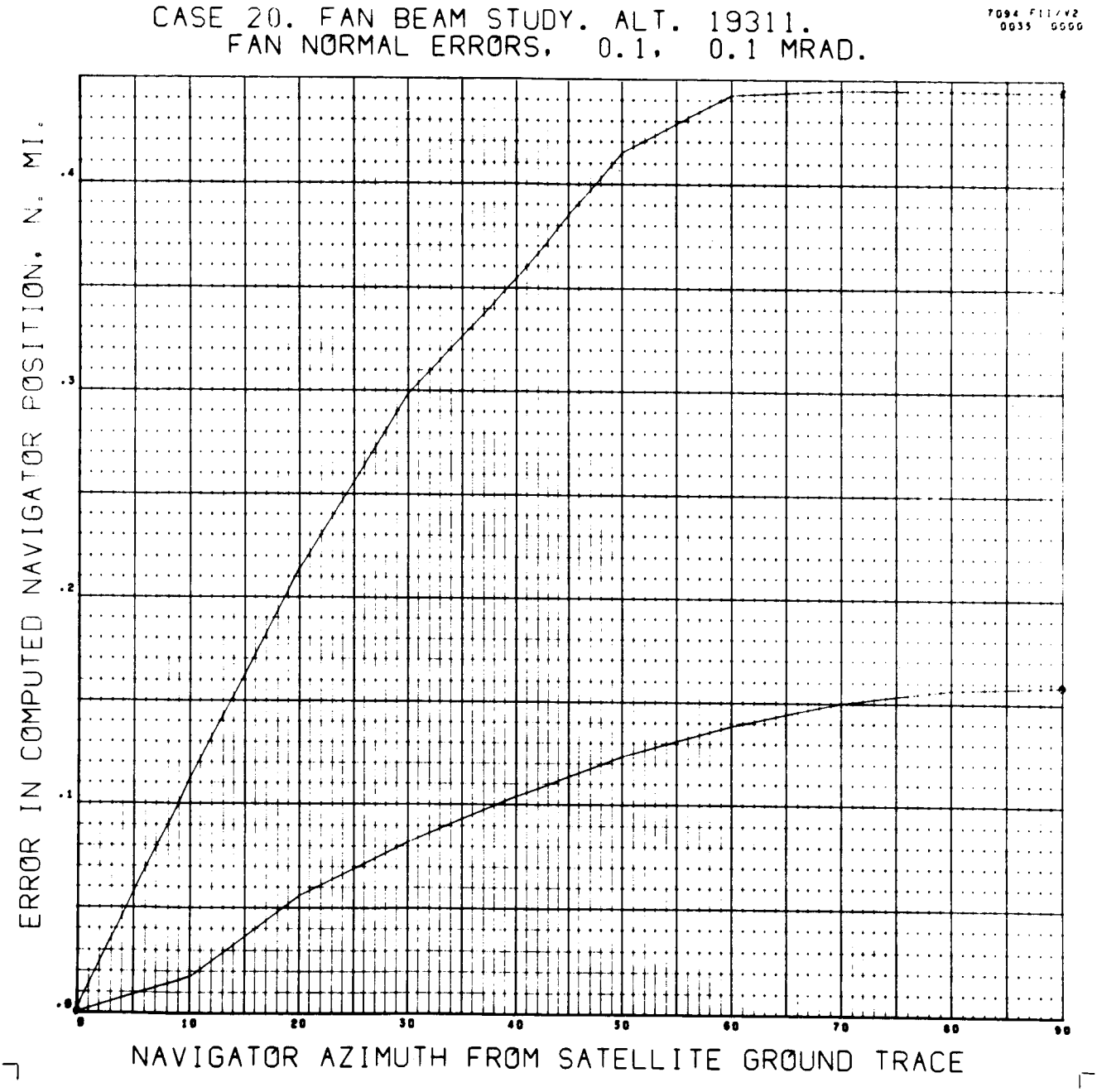
CASE 20. FAN BEAM STUDY. ALT. 19311.
FAN NORMAL ERRORS, 0.1, 0.1 MRAD.
ERROR IN COMPUTED NAVIGATOR POSITION, N. MI.
.4
.3
.2
.1
0
0
10
20
30
40
50
60
70
80
90
NAVIGATOR AZIMUTH FROM SATELLITE GROUND TRACE

Figure 4-19

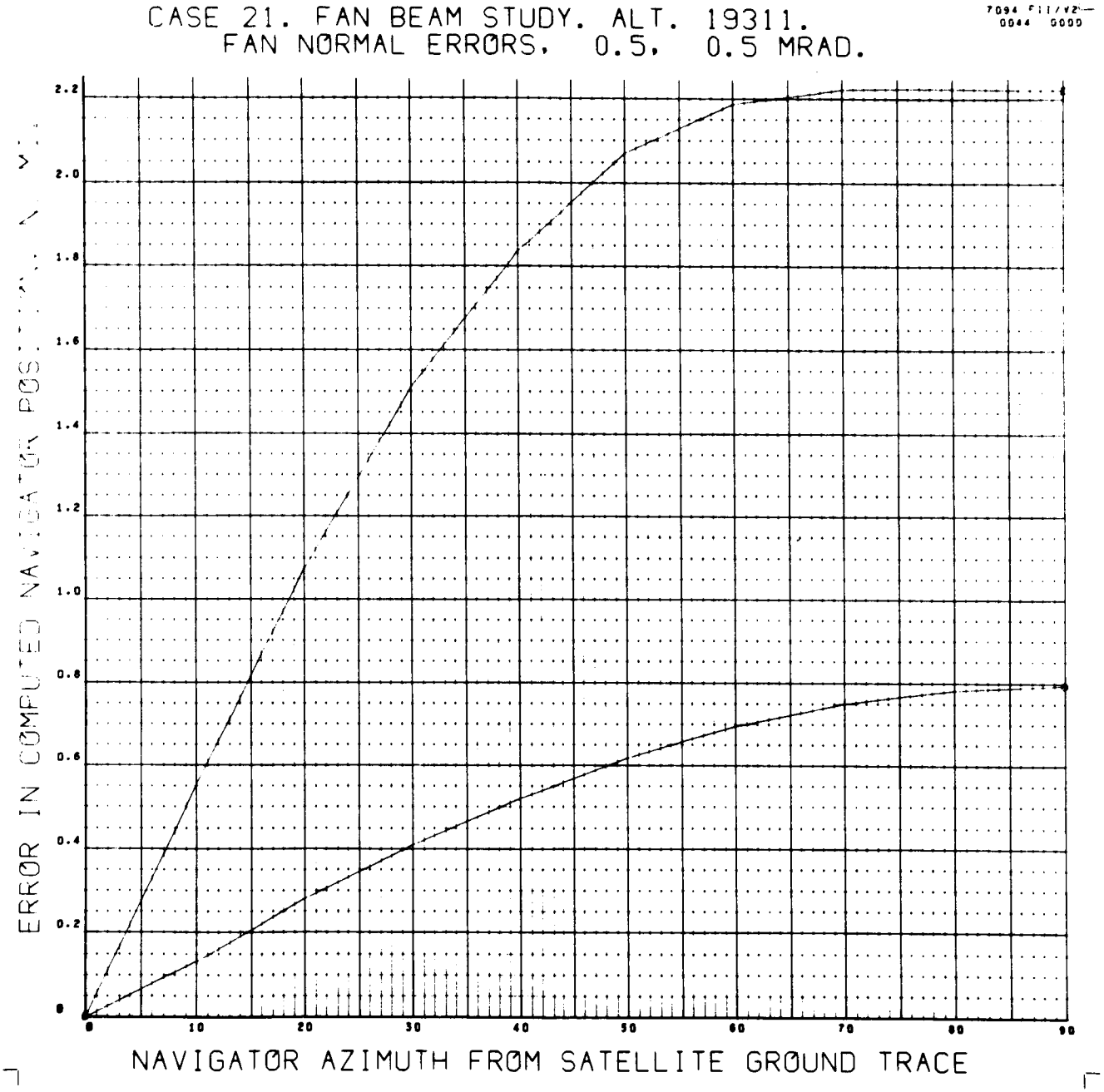
CASE 21. FAN BEAM STUDY. ALT. 19311.
FAN NORMAL ERRORS. 0.5. 0.5 MRAD.
ERROR IN COMPUTED NAVIGATOR POSITION, N.M.
2.2
2.0
1.8
1.6
1.4
1.2
1.0
0.8
0.6
0.4
0.2
0
0
10
20
30
40
50
60
70
80
90
NAVIGATOR AZIMUTH FROM SATELLITE GROUND TRACE

Figure 4-20

In comparison, for both altitudes and for the same error magnitudes (.1 or .5 milliradian), $\hat{\omega}$ miscalibration causes a larger fix error for γ up to 30 or 40 degrees depending upon subsatellite distance. Then, for γ on up to 90 degrees, $\hat{n}_i$ miscalibration causes a larger fix error.

Figures 4-21 and 4-22 show the fix error relationships when the miscalibrations of $\hat{n}_i(t_o)$ are of opposite sign. Although the assumed deviations are -1 and 1 milliradian, assuming the previously observed linearity of the error propagation,these curves may be compared with Figures 4-10 and 4-12 where the deviations were of same sign and magnitude .1 milliradian. From γ = 15 to 90 degrees the opposite-sign case displays the larger fix errors, the difference increasing with subsatellite distance.

The same comments as made in Section 4.1.2 for $\hat{\omega}$ apply here for $\hat{n}_i$. Fix determination does not depend on precision of attainment of the nominal 45^o mounting angles for the boom antennas, but upon accuracy of knowledge of $\hat{n}_1(t_o)$ and $\hat{n}_2(t_o)$ in $\hat{E}$-coordinates. Two levels of sophistication in estimating these reference normals were discussed in Section 3.7.1 .

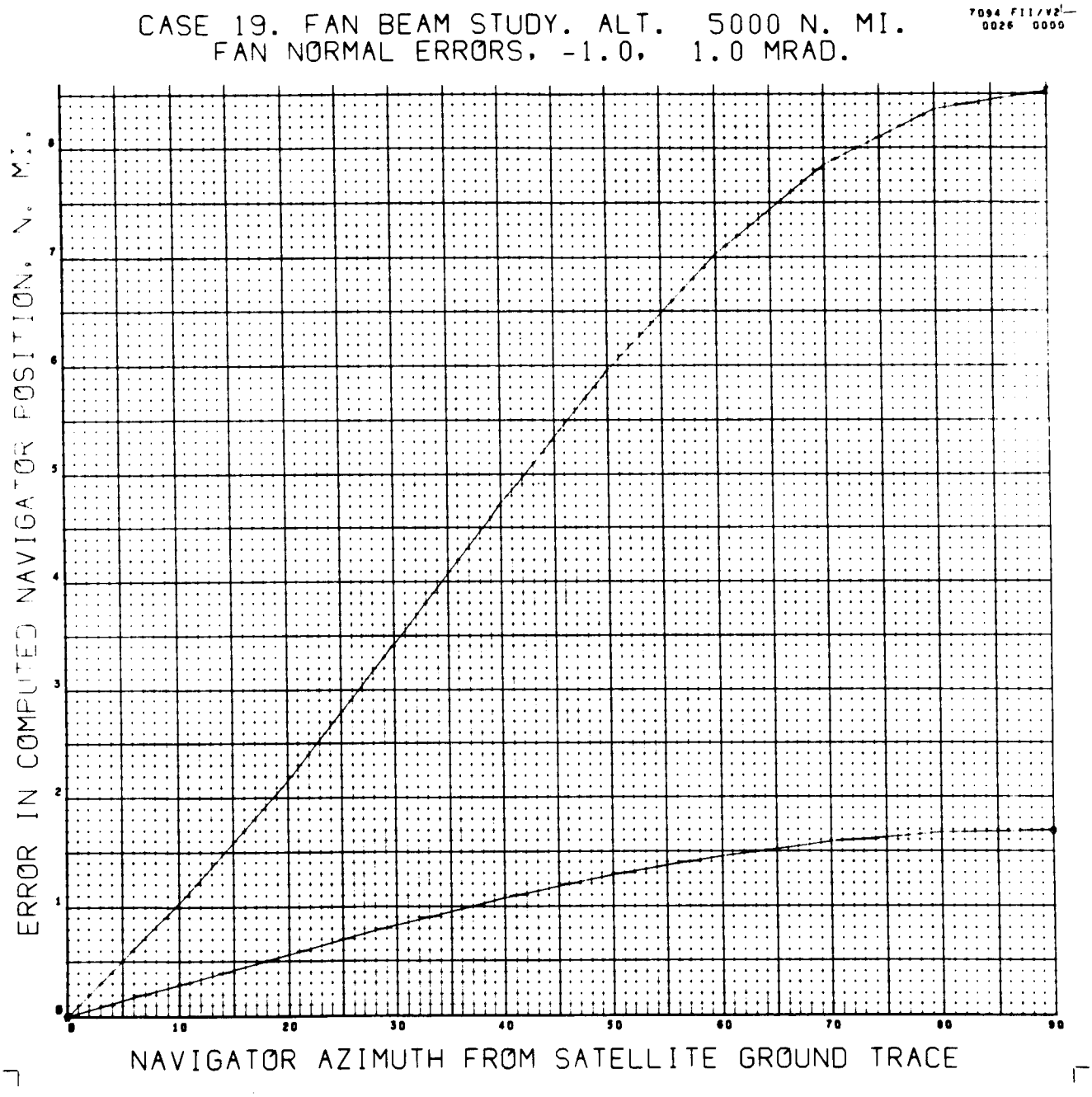
CASE 19. FAN BEAM STUDY. ALT. 5000 N. MI.
FAN NORMAL ERRORS, -1.0, 1.0 MRAD.
7094 F11/V2
0026 0000
ERROR IN COMPUTED NAVIGATOR POSITION, N. M.
0
1
2
3
4
5
6
7
8
0
10
20
30
40
50
60
70
80
90
NAVIGATOR AZIMUTH FROM SATELLITE GROUND TRACE

Figure 4-21

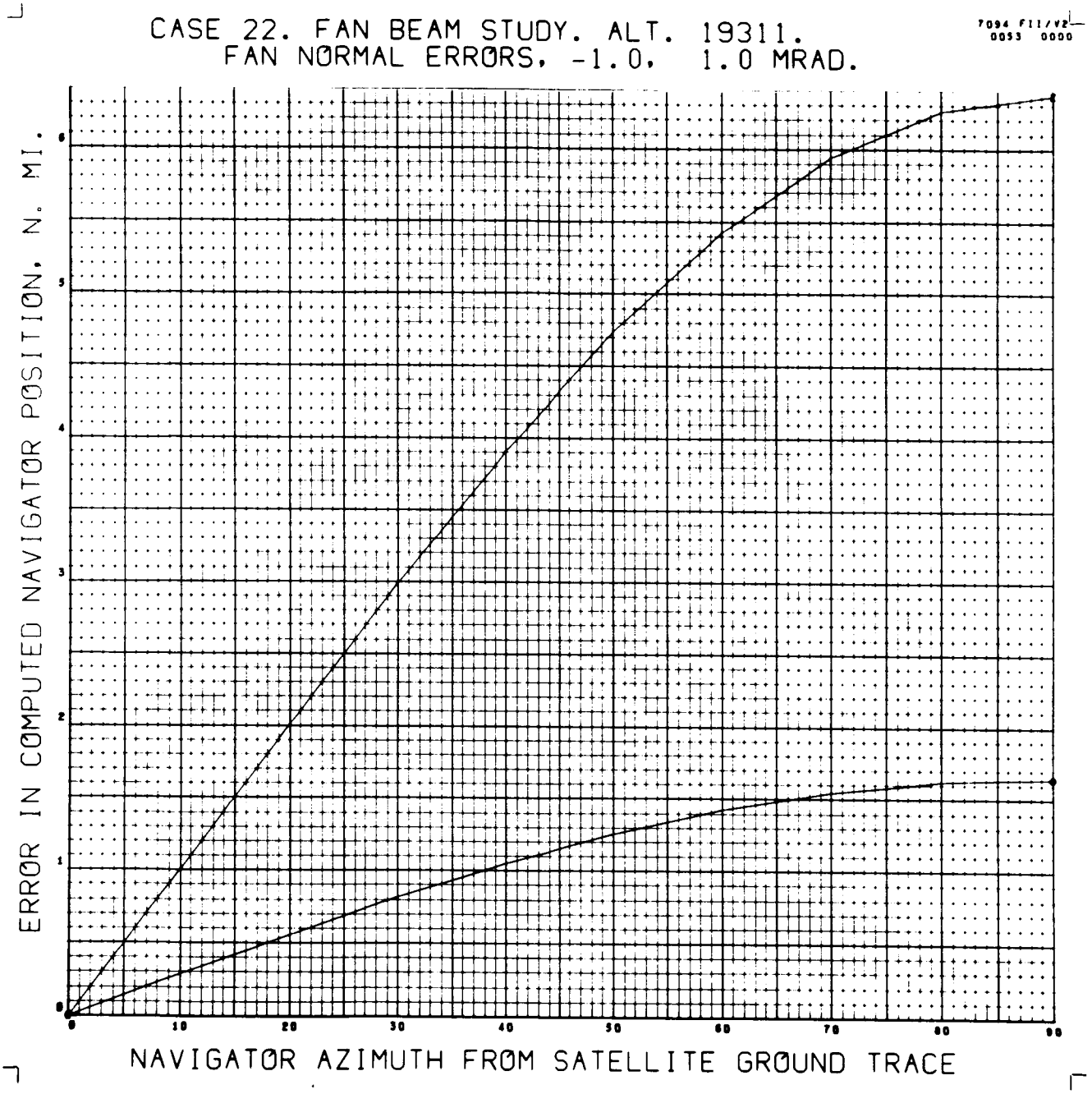
CASE 22. FAN BEAM STUDY. ALT. 19311.
FAN NORMAL ERRORS, -1.0, 1.0 MRAD.
7094 F11/V2
0053 0000
ERROR IN COMPUTED NAVIGATOR POSITION, N. MI.
0
1
2
3
4
5
6
0
10
20
30
40
50
60
70
80
90
NAVIGATOR AZIMUTH FROM SATELLITE GROUND TRACE

Figure 4-22

4.2 MULTIPLE FIX ANALYSIS

In Section 4.1 the fix errors were computed on the assumption of a single fix computation made during the first satellite revolution after the epoch defined by initial conditions. It will now be assumed that fan timing measurements are taken each revolution of the satellite, over N revolutions.

4.2.1 Effect of Revolution Number on Single Fix

Figures 4-23 through 4-28 display the magnitude of fix error experienced when a single fix computation is made during satellite revolution k + 1, for a range of k from 0 to 49. The only source of error operating during the first revolution, of those listed in Section 2.3, is a miscalibration of $\hat{\omega}(t_o)$. On subsequent revolutions, however, there will be a miscalibration of $\hat{n}_1(t_o)$ and $\hat{n}_2(t_o)$, do to the precessive motion of $\hat{n}_1$ and $\hat{n}_2$ described in Section 3.7.1. For the first fix computation the navigator has the correct $\hat{n}_1(t_o)$ and $\hat{n}_2(t_o)$ in inertial coordinates. Since no updating of these vectors (nor of $\hat{\omega}(t_o)$) from a calibration station is assumed, the same inertially oriented vectors will be used in the fix computation for every satellite revolution. The true $\hat{n}_1$ and $\hat{n}_2$ positions in an inertial frame at the times $t_o(k)$ are shown in Figure 3-5, where the positions at $\underline{k = 0}$ are the $\hat{n}_1$ and $\hat{n}_2$ assumed by the navigator for every satellite revolution. The $\hat{n}_1$ and $\hat{n}_2$ miscalibration thus varies between 0 and about 2(.0909) or .1818 milliradian over each ten satellite revolutions. (The value of β in Section 3.7.1 is .0909).

The vector $\hat{\omega}$ at each $t_o(k)$ is assumed by the navigator to be the initial $\hat{e}_2$ as in Section 4.1.3, (i.e. $\hat{f}_2$). Thus it is miscalibrated, even for k = 0. On succeeding satellite revolutions, k = 1, ..., 49, the magnitude of the miscalibration of direction varies from the initial .1 milliradian to a minimum of about .082 milliradian as the true $\hat{\omega}$ revolves about $\hat{h}$, (see Figure 3-1 in Section 3.3, $\alpha - \beta = .0091$).

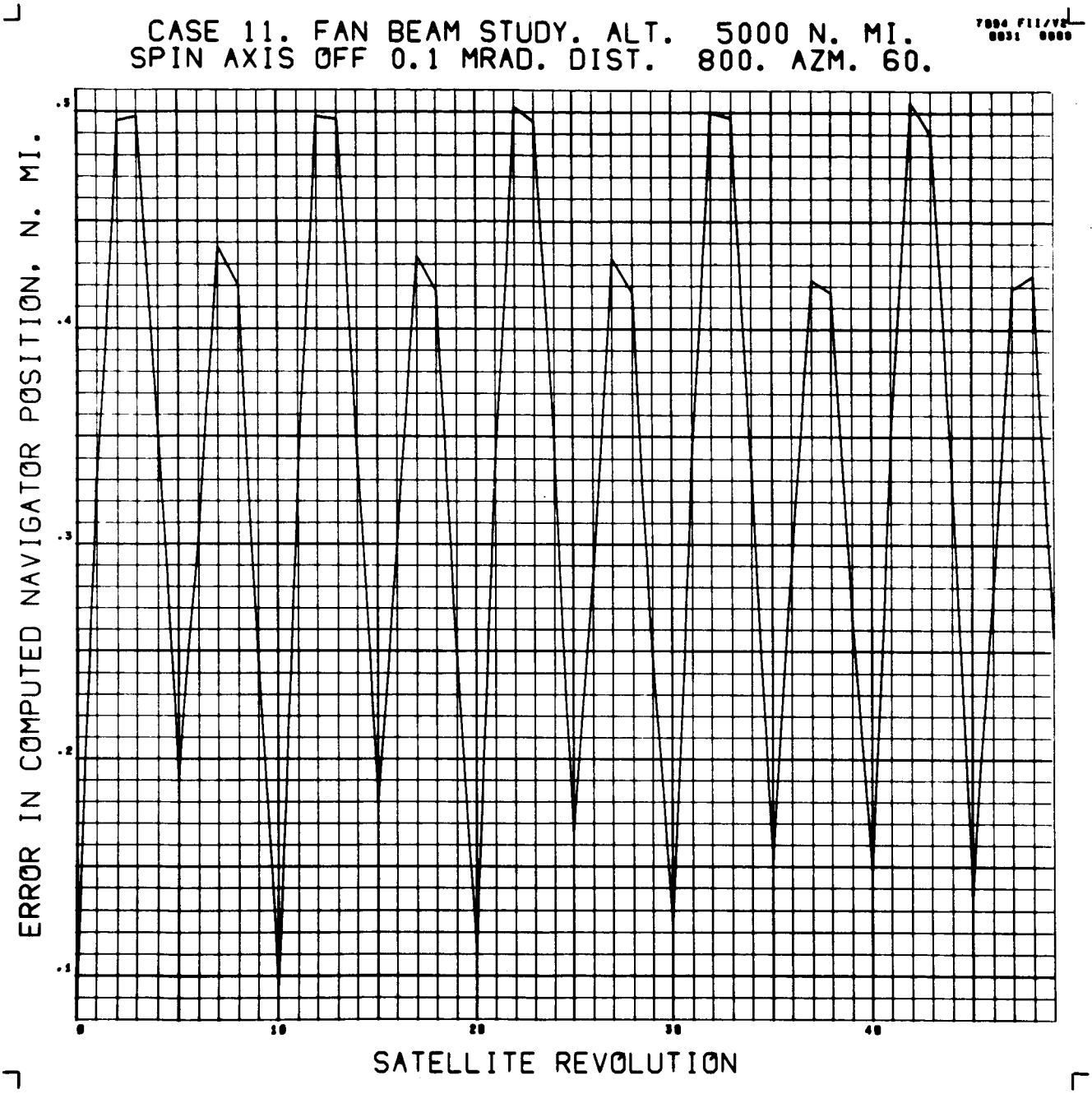
CASE 11. FAN BEAM STUDY. ALT. 5000 N. MI.
SPIN AXIS OFF 0.1 MRAD. DIST. 800. AZM. 60.
ERROR IN COMPUTED NAVIGATOR POSITION, N. MI.
.5
.4
.3
.2
.1
0
10
20
30
40
SATELLITE REVOLUTION

Figure 4-23

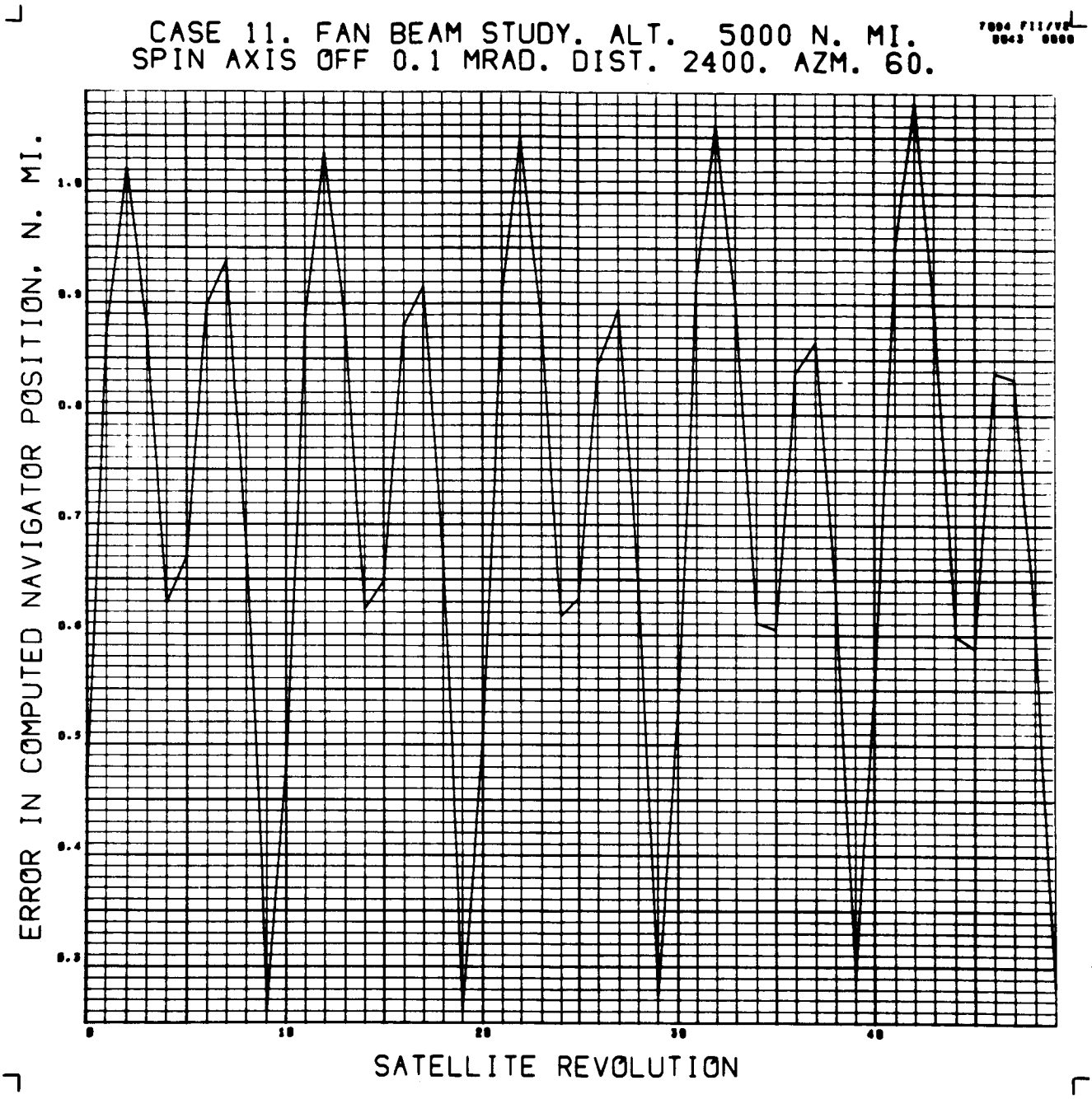
CASE 11. FAN BEAM STUDY. ALT. 5000 N. MI.
SPIN AXIS OFF 0.1 MRAD. DIST. 2400. AZM. 60.
ERROR IN COMPUTED NAVIGATOR POSITION, N. MI.
1.0
0.9
0.8
0.7
0.6
0.5
0.4
0.3
0
10
20
30
40
SATELLITE REVOLUTION

Figure 4-24

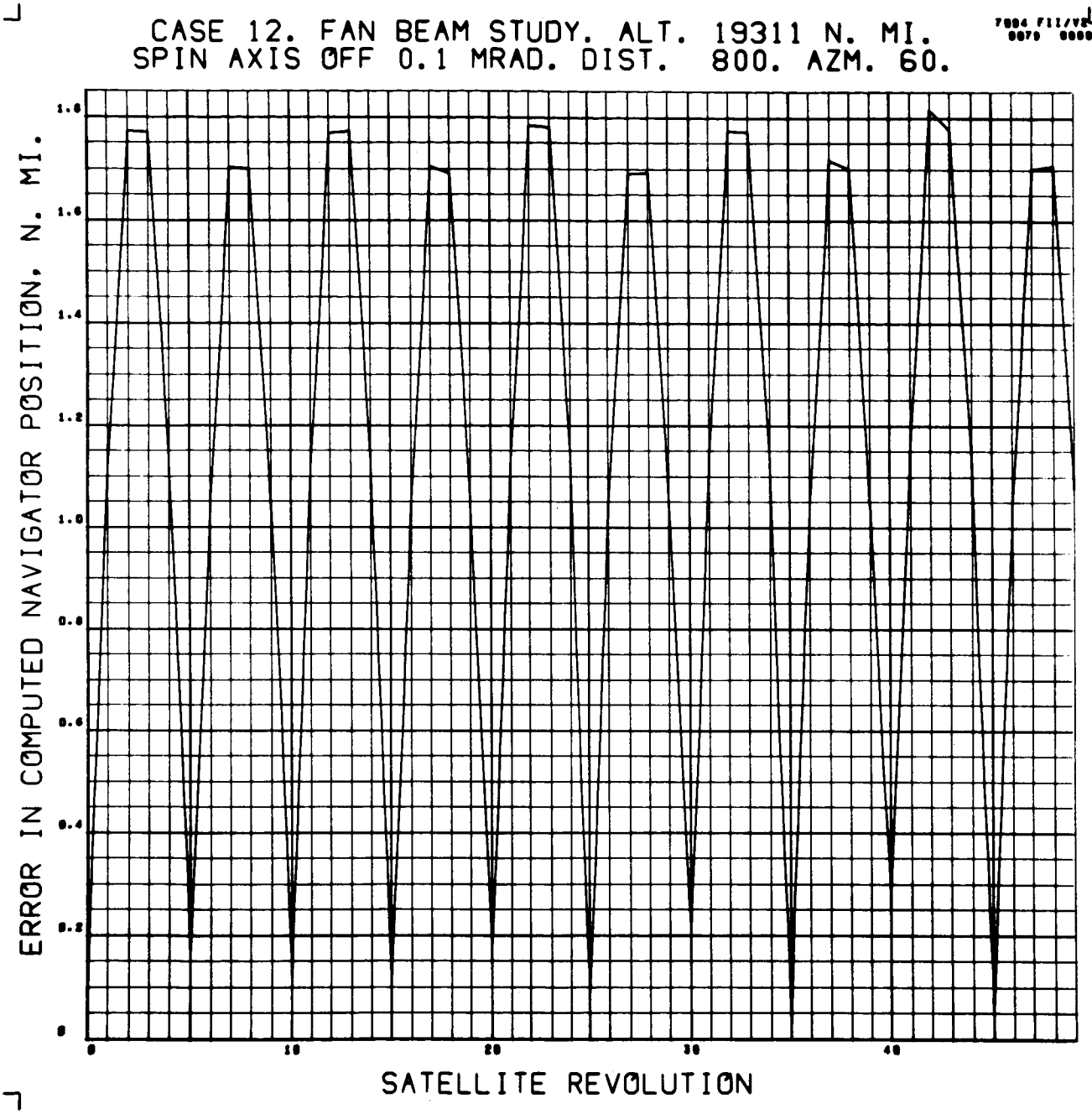
CASE 12. FAN BEAM STUDY. ALT. 19311 N. MI.
SPIN AXIS OFF 0.1 MRAD. DIST. 800. AZM. 60.
ERROR IN COMPUTED NAVIGATOR POSITION, N. MI.
1.8
1.6
1.4
1.2
1.0
0.8
0.6
0.4
0.2
0
0
10
20
30
40
SATELLITE REVOLUTION

Figure 4-25

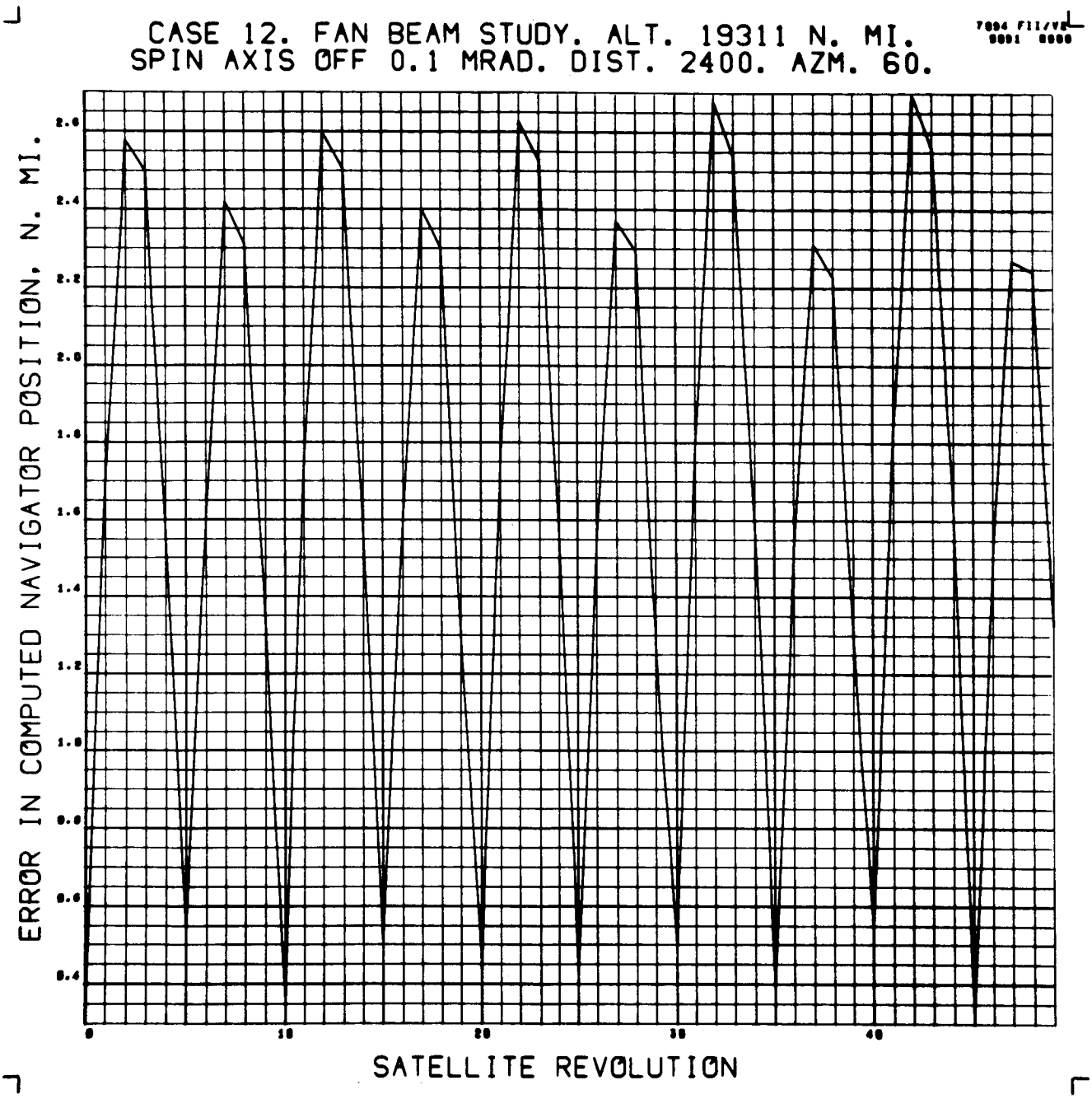
CASE 12. FAN BEAM STUDY. ALT. 19311 N. MI.
SPIN AXIS OFF 0.1 MRAD. DIST. 2400. AZM. 60.
ERROR IN COMPUTED NAVIGATOR POSITION, N. MI.
2.6
2.4
2.2
2.0
1.8
1.6
1.4
1.2
1.0
0.8
0.6
0.4
0
10
20
30
40
SATELLITE REVOLUTION

Figure 4-26

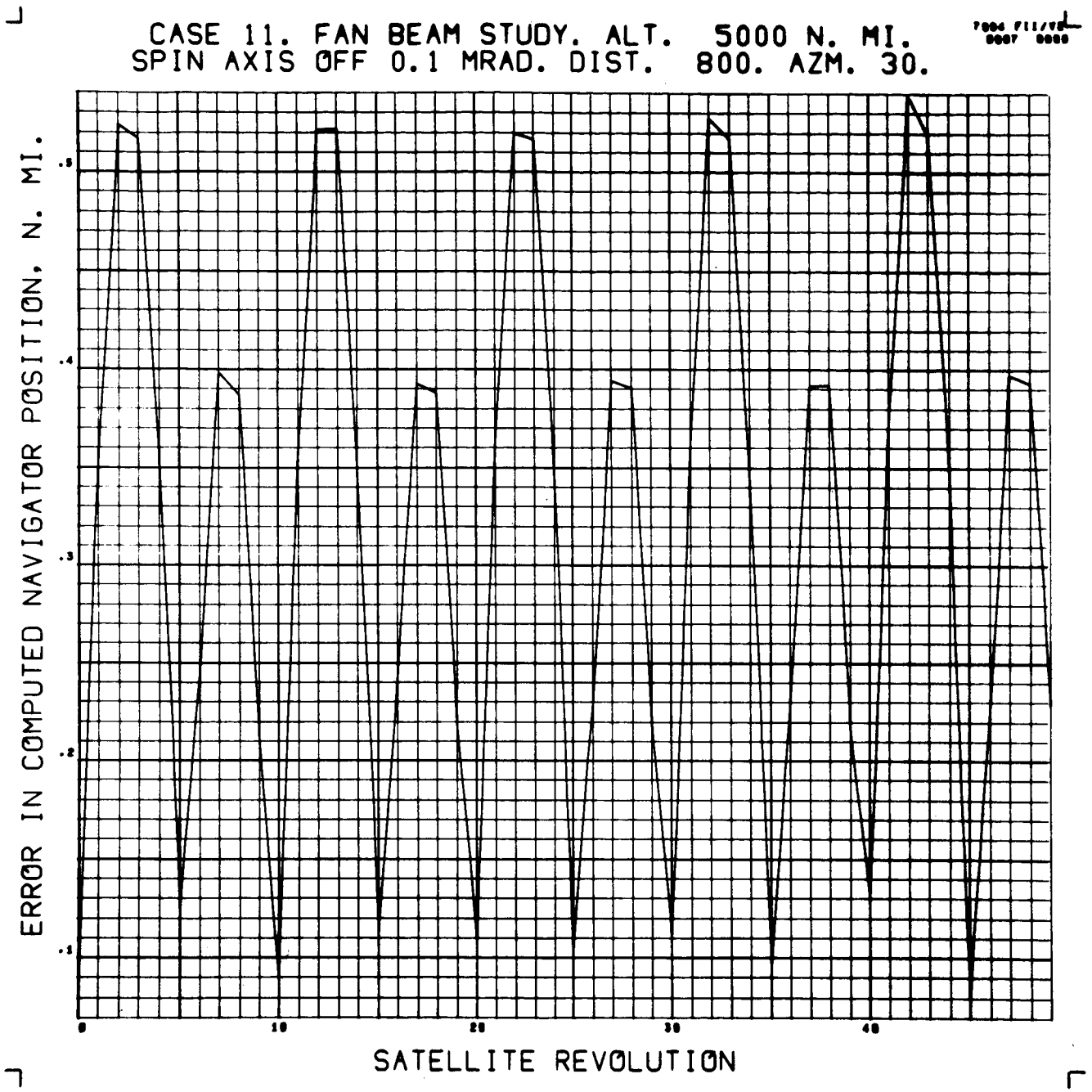
CASE 11. FAN BEAM STUDY. ALT. 5000 N. MI.
SPIN AXIS OFF 0.1 MRAD. DIST. 800. AZM. 30.
ERROR IN COMPUTED NAVIGATOR POSITION, N. MI.
.5
.4
.3
.2
.1
0
10
20
30
40
SATELLITE REVOLUTION

Figure 4-27

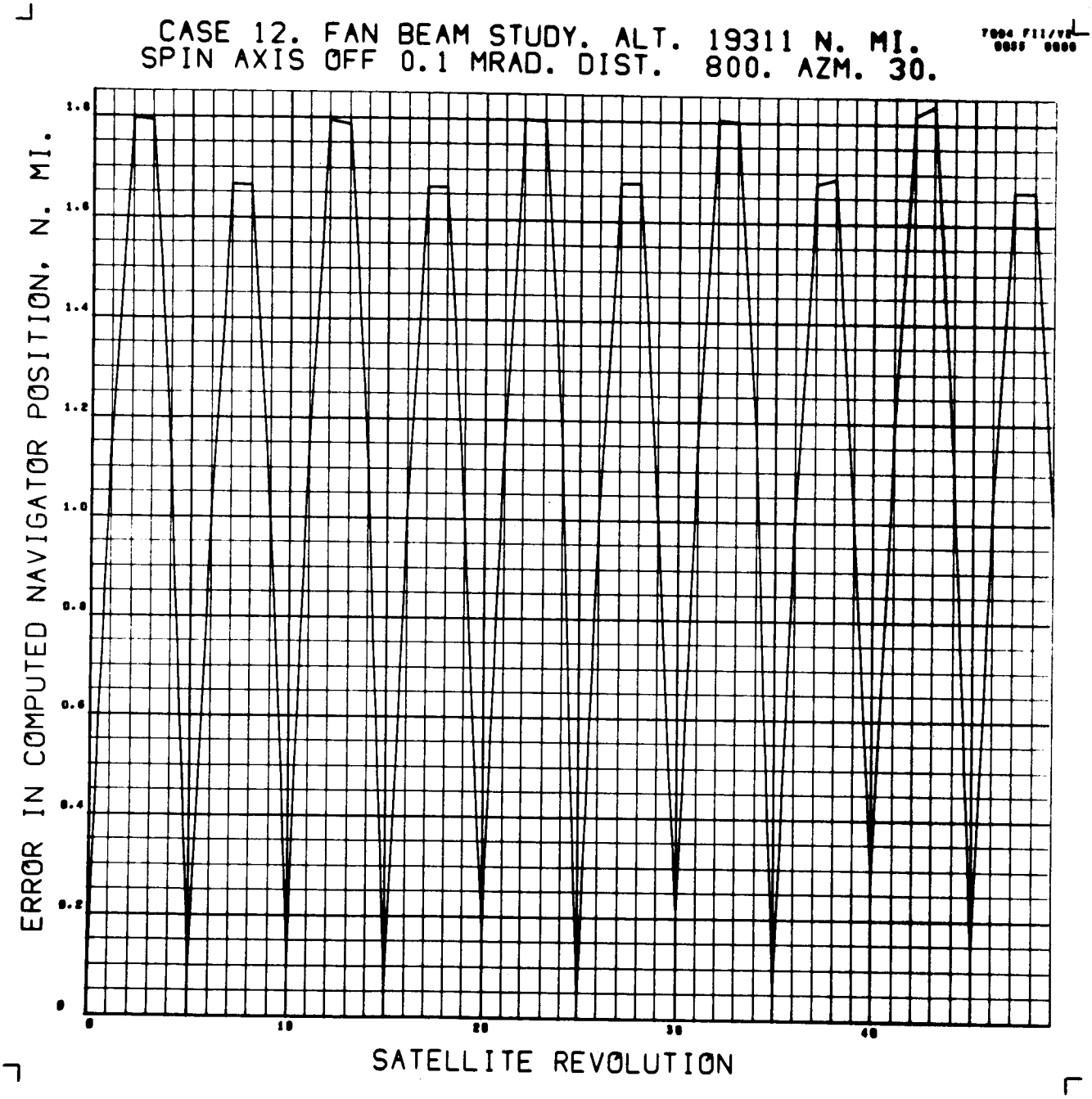
CASE 12. FAN BEAM STUDY. ALT. 19311 N. MI.
SPIN AXIS OFF 0.1 MRAD. DIST. 800. AZM. 30.
ERROR IN COMPUTED NAVIGATOR POSITION, N. MI.
1.8
1.6
1.4
1.2
1.0
0.8
0.6
0.4
0.2
0
0
10
20
30
40
SATELLITE REVOLUTION

Figure 4-28

Figures 4-23 thru 4-26 illustrate the cases of navigator subsatellite distances of 800 and 2400 nautical miles at an azimuth of 60 degrees from the orbit plane, for the two satellite altitudes of interest. Figures 4-27 and 4-28 are also included to show the increased oscillation of the peaks of the curves for an azimuth of 30 degrees (compared with Figures 4-23 and 4-25).

The curves exhibit what might be an expected appearance of "almost" periodic motion effects, over any ten satellite revolutions. Within a 10-revolution interval there are two unequal peaks in fix error due to the interaction between the satellite precession and the direction of the satellite-to-navigator vector. It will be noticed that the maximum fix errors occur during the third and eighth satellite revolution (k = 2 and 7, respectively).

In examining the figures, it is also seen that the "upper" peaks of the oscillations themselves gradually increase in amplitude, while the "lower" peaks decrease in amplitude, and is especially noticeable for the more extreme satellite-to-navigator orientations, as in Figures 4-24 and 4-26. This is due to basic dynamical relationships, and is an illustration of second-order effects in this study. The explanation will be given in the following section when the individual errors in computed latitude and longitude, which are the components of the position error, are inspected.

The figures show that fix errors can be rather large when only a single computation is made. Accuracy depends upon the satellite being in a favorable inertial orientation (at t_o of the satellite revolution in which the fix computation is made) relative to the navigator's last updating for the $\hat{\omega}$, $\hat{n}_1$ and $\hat{n}_2$ estimates. It turns out, however, that when the results of sets of fix computations are averaged, reductions occur in the error of position determination of an order of magnitude or more, as will be seen in the next section.

4.2.2 Effect of Smoothing in the Absence of Noise

The single-fix computational error as a function of satellite revolution number, described in the preceding section, is due to errors in the computed latitude and longitude. For the same cases as in that section, Figures 4-29 thru 4-40 display these latitude and longitude errors as a function of satellite revolution number.

It is seen that the latitude error curves oscillate about an inclined line. This is the source of the error-peak variation discussed in Section 4.2.1, and is a result of the fact that the satellite attitude motion is not precisely periodic, as will be shown below. The 10-revolution period displayed by the example in Section 3.7.1 is due to an assumed value of $\rho = 1.1$ exactly, (along with small angle assumptions). The satellite attitude in inertial space is then precisely the same after every ten revolutions and the observed error-peak variation would be absent in such a case.

A quantitative evaluation of the lack of periodicity in the actual motion may be had by considering only the rotation of the $(\hat{e}_2, \hat{\Omega})$-plane about $\hat{h}$. From Section 3.3, the angular rate (inertially) is

$$\Omega = \frac{\sin \alpha}{\sin \beta} \omega$$

Since $\rho = \tan \alpha / \tan \beta$ and angles α and β are small, it is possible to write

$$\Omega = (\rho + \Delta\rho)\omega$$

where $\Delta\rho$ will be small. Since interest is in satellite attitude at the reference pulse times, $t_o(k)$ corresponding to 0, 10, 20, ... satellite revolutions, recalling the results of Section 3.7.1, Equation (34), define

$$t_k = 20\, k\, \pi/\omega \qquad k = 0, 1, 2, \ldots$$

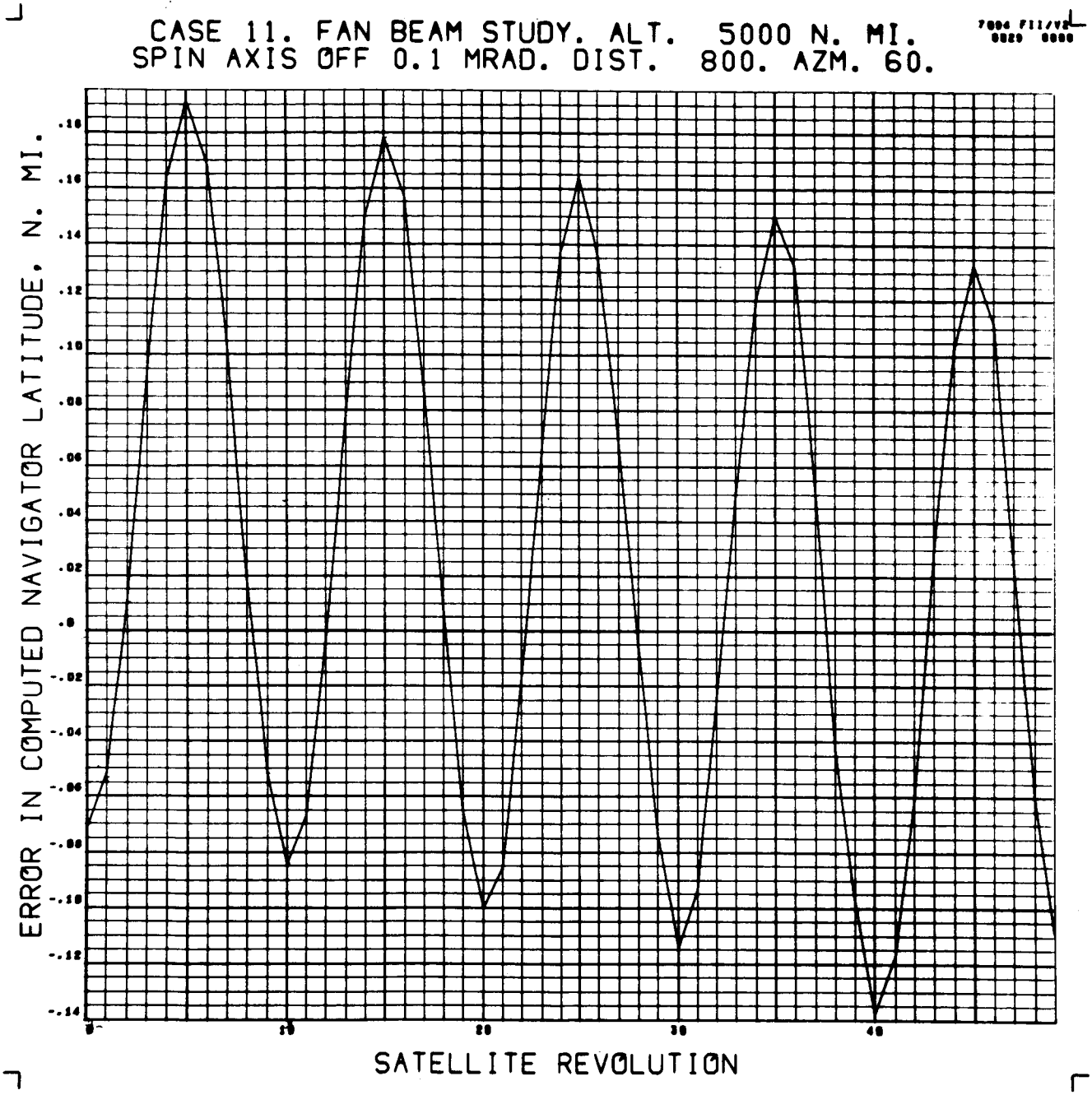
CASE 11. FAN BEAM STUDY. ALT. 5000 N. MI.
SPIN AXIS OFF 0.1 MRAD. DIST. 800. AZM. 60.
ERROR IN COMPUTED NAVIGATOR LATITUDE, N. MI.
.18
.16
.14
.12
.10
.08
.06
.04
.02
.0
-.02
-.04
-.06
-.08
-.10
-.12
-.14
0
10
20
30
40
SATELLITE REVOLUTION

Figure 4-29

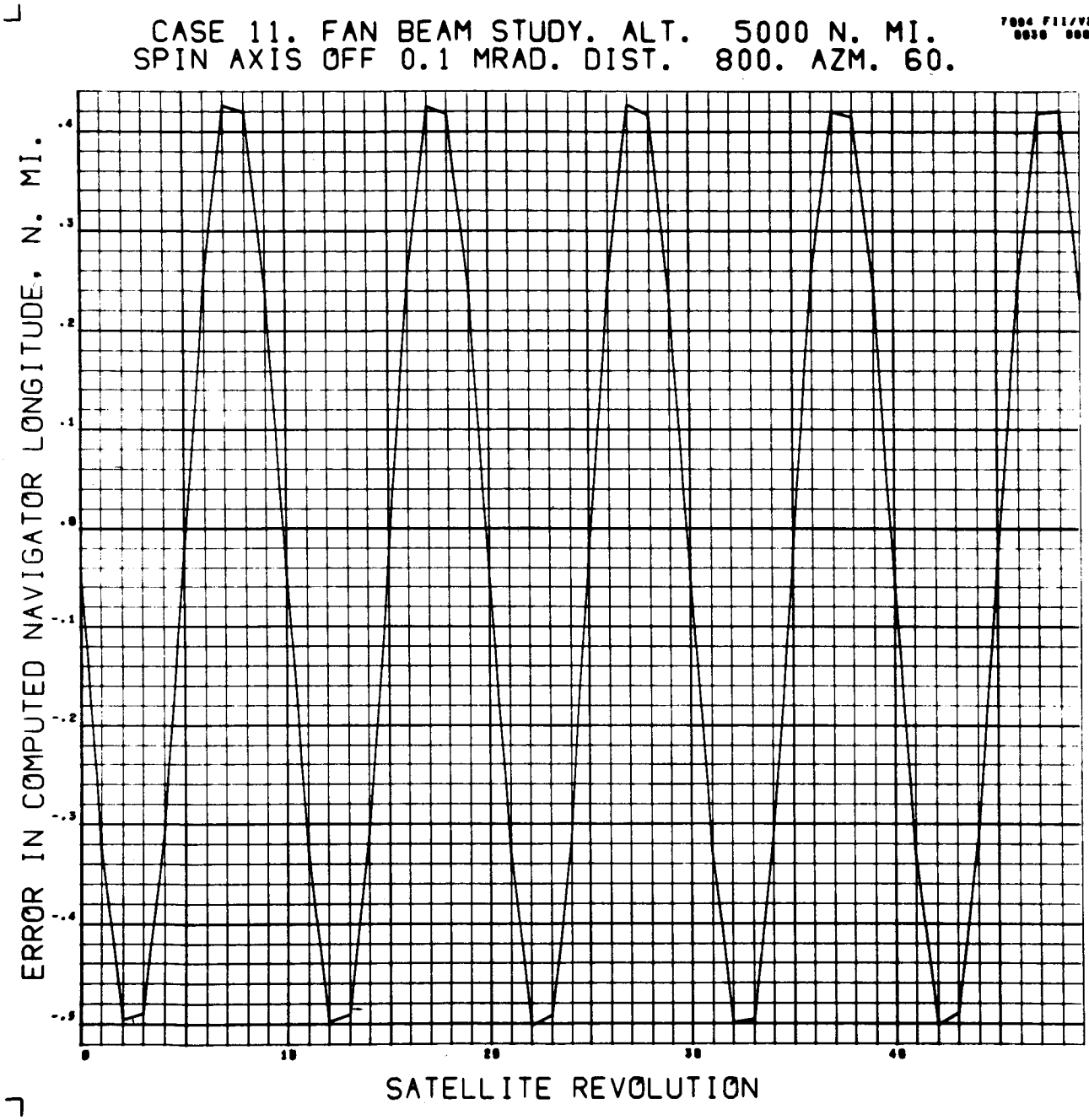
CASE 11. FAN BEAM STUDY. ALT. 5000 N. MI.
SPIN AXIS OFF 0.1 MRAD. DIST. 800. AZM. 60.
ERROR IN COMPUTED NAVIGATOR LONGITUDE, N. MI.
.4
.3
.2
.1
0
-.1
-.2
-.3
-.4
-.5
0
10
20
30
40
SATELLITE REVOLUTION

Figure 4-30

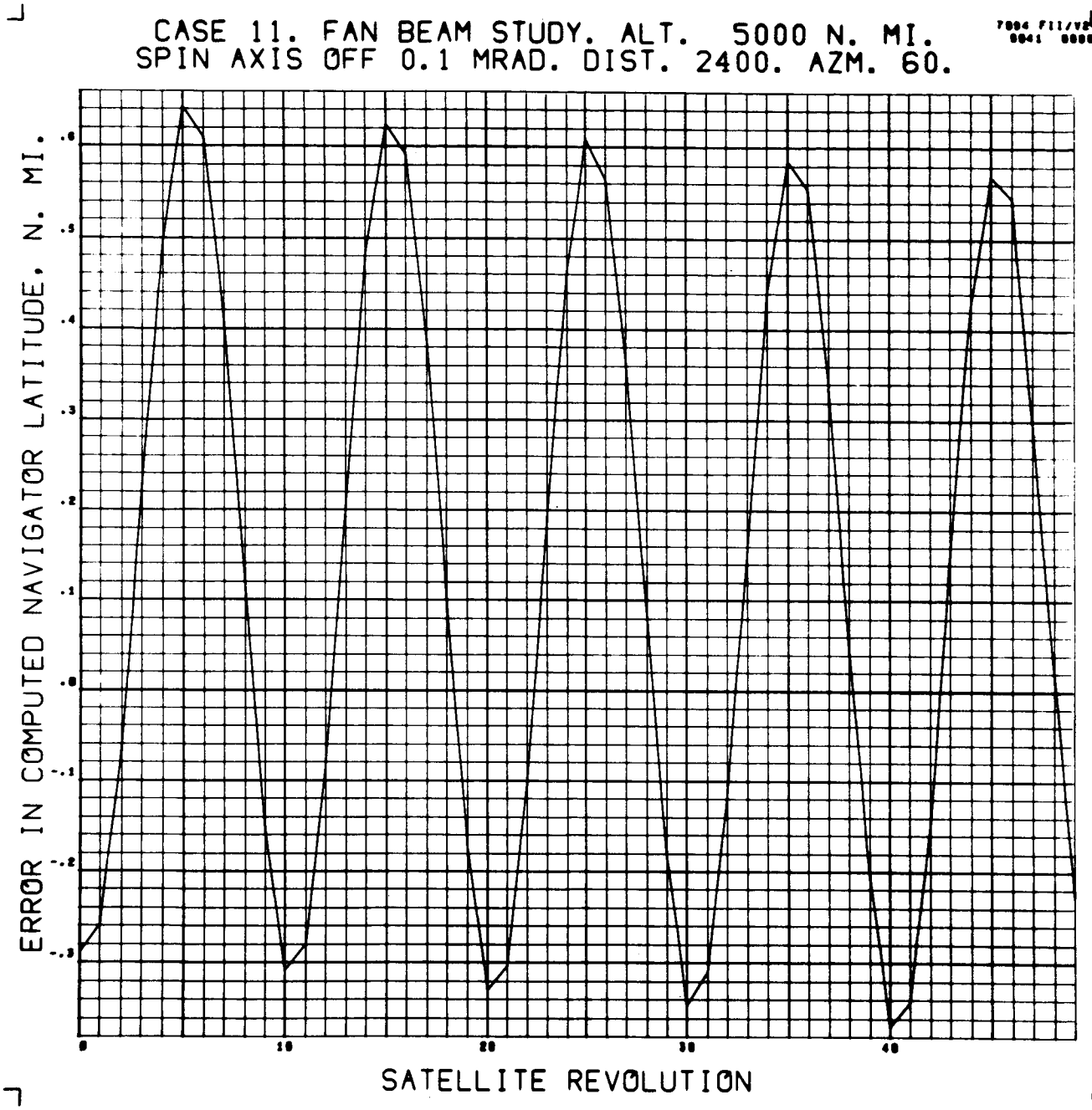
CASE 11. FAN BEAM STUDY. ALT. 5000 N. MI.
SPIN AXIS OFF 0.1 MRAD. DIST. 2400. AZM. 60.
ERROR IN COMPUTED NAVIGATOR LATITUDE, N. MI.
.6
.5
.4
.3
.2
.1
.0
-.1
-.2
-.3
0
10
20
30
40
SATELLITE REVOLUTION

Figure 4-31

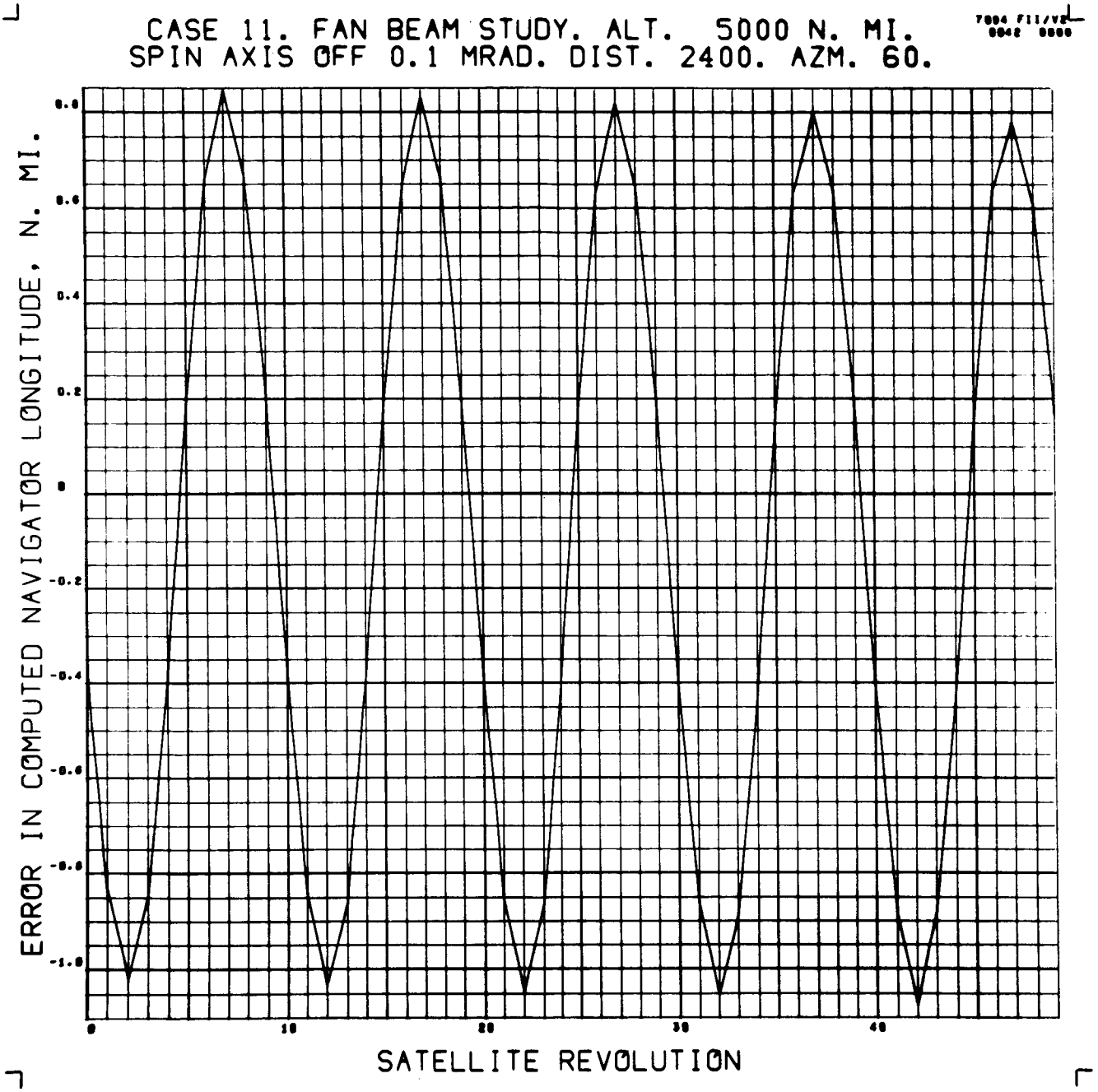
CASE 11. FAN BEAM STUDY. ALT. 5000 N. MI.
SPIN AXIS OFF 0.1 MRAD. DIST. 2400. AZM. 60.
ERROR IN COMPUTED NAVIGATOR LONGITUDE, N. MI.
0.8
0.6
0.4
0.2
0
-0.2
-0.4
-0.6
-0.8
-1.0
0
10
20
30
40
SATELLITE REVOLUTION

Figure 4-32

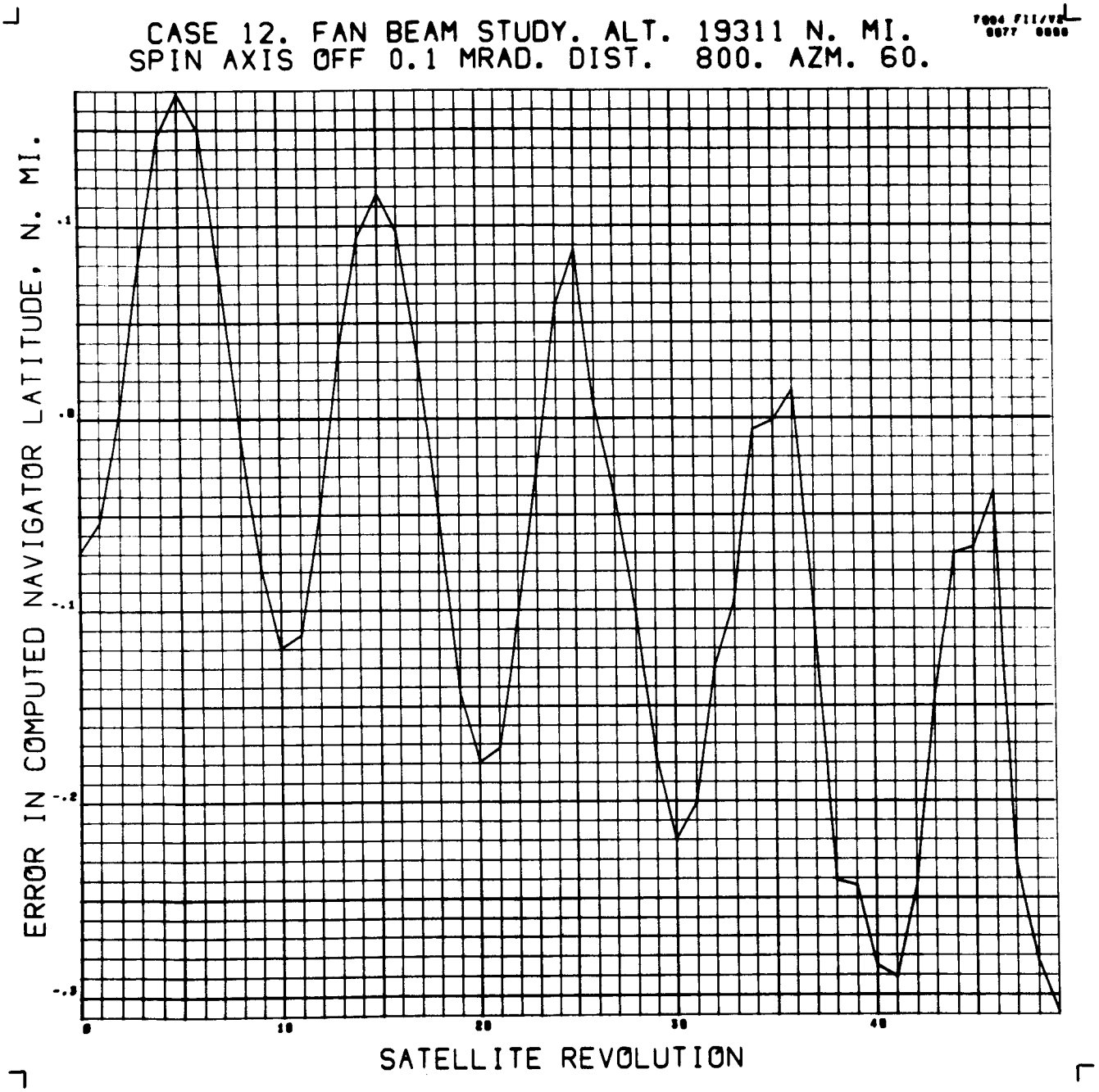
CASE 12. FAN BEAM STUDY. ALT. 19311 N. MI.
SPIN AXIS OFF 0.1 MRAD. DIST. 800. AZM. 60.
ERROR IN COMPUTED NAVIGATOR LATITUDE, N. MI.
.1
0
-.1
-.2
-.3
0
10
20
30
40
SATELLITE REVOLUTION

Figure 4-33

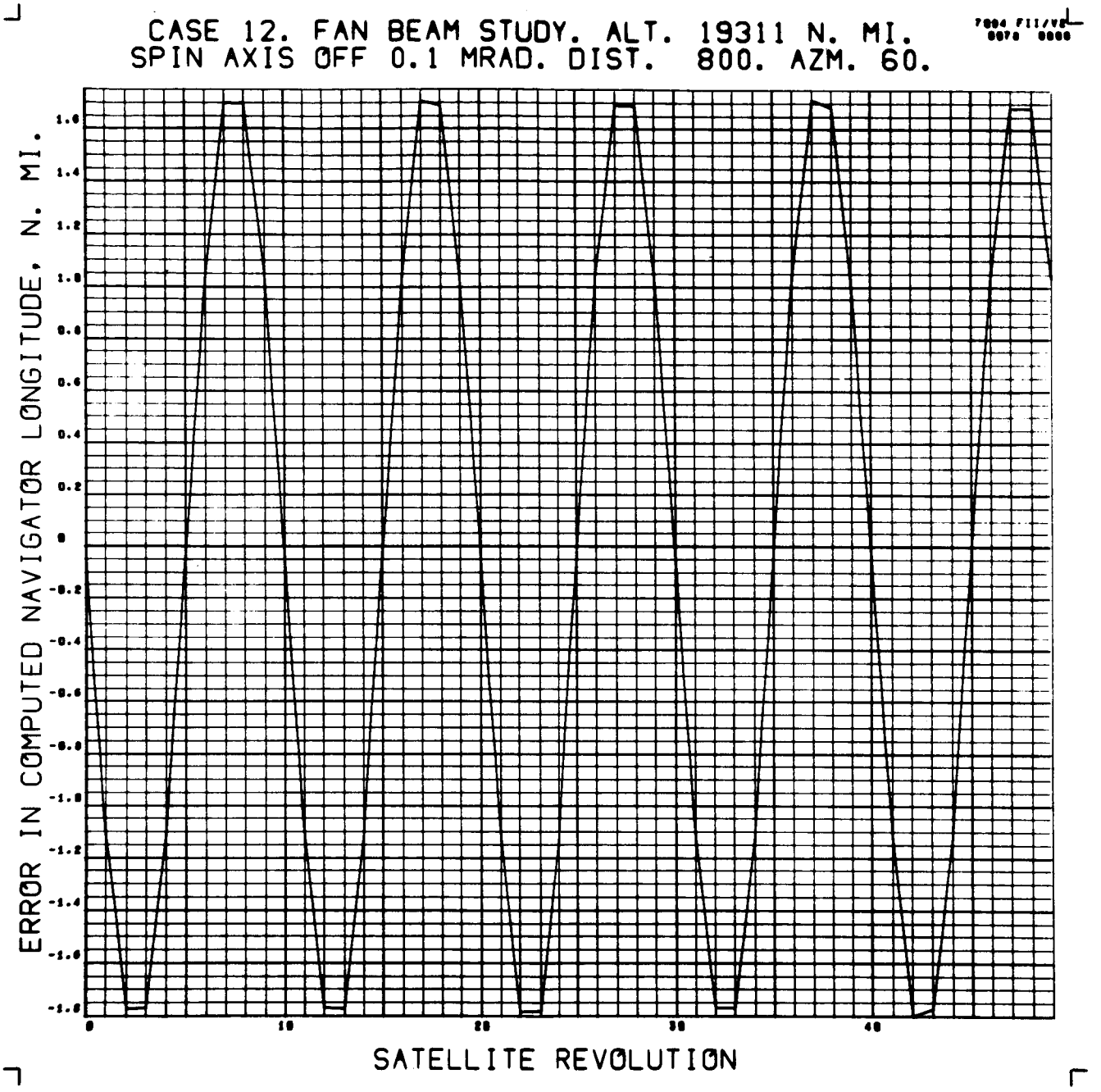
CASE 12. FAN BEAM STUDY. ALT. 19311 N. MI.
SPIN AXIS OFF 0.1 MRAD. DIST. 800. AZM. 60.
ERROR IN COMPUTED NAVIGATOR LONGITUDE, N. MI.
1.6
1.4
1.2
1.0
0.8
0.6
0.4
0.2
0
-0.2
-0.4
-0.6
-0.8
-1.0
-1.2
-1.4
-1.6
-1.8
0
10
20
30
40
SATELLITE REVOLUTION

Figure 4-34

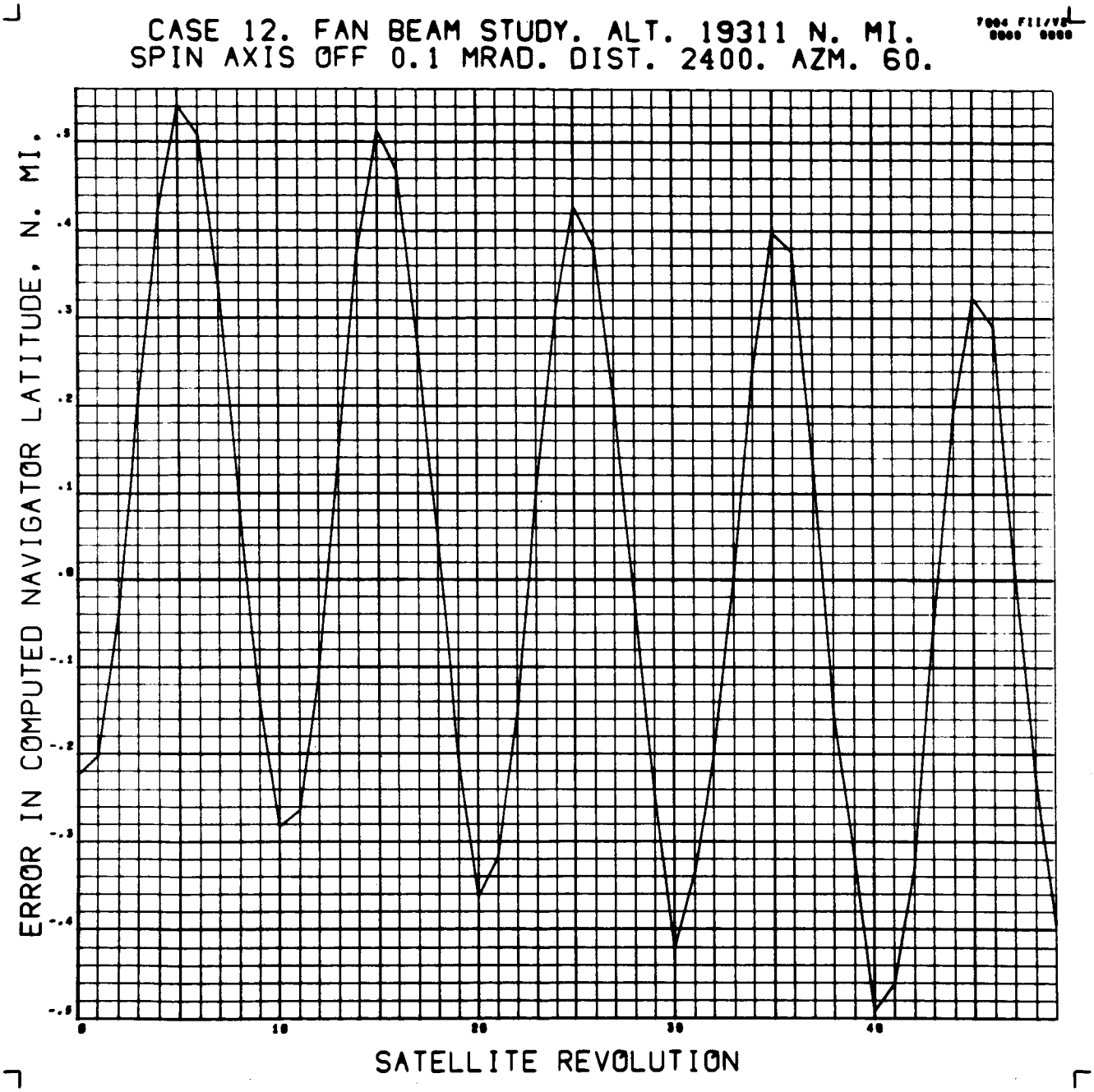
CASE 12. FAN BEAM STUDY. ALT. 19311 N. MI.
SPIN AXIS OFF 0.1 MRAD. DIST. 2400. AZM. 60.
ERROR IN COMPUTED NAVIGATOR LATITUDE, N. MI.
.5
.4
.3
.2
.1
0
-.1
-.2
-.3
-.4
-.5
0
10
20
30
40
SATELLITE REVOLUTION

Figure 4-35

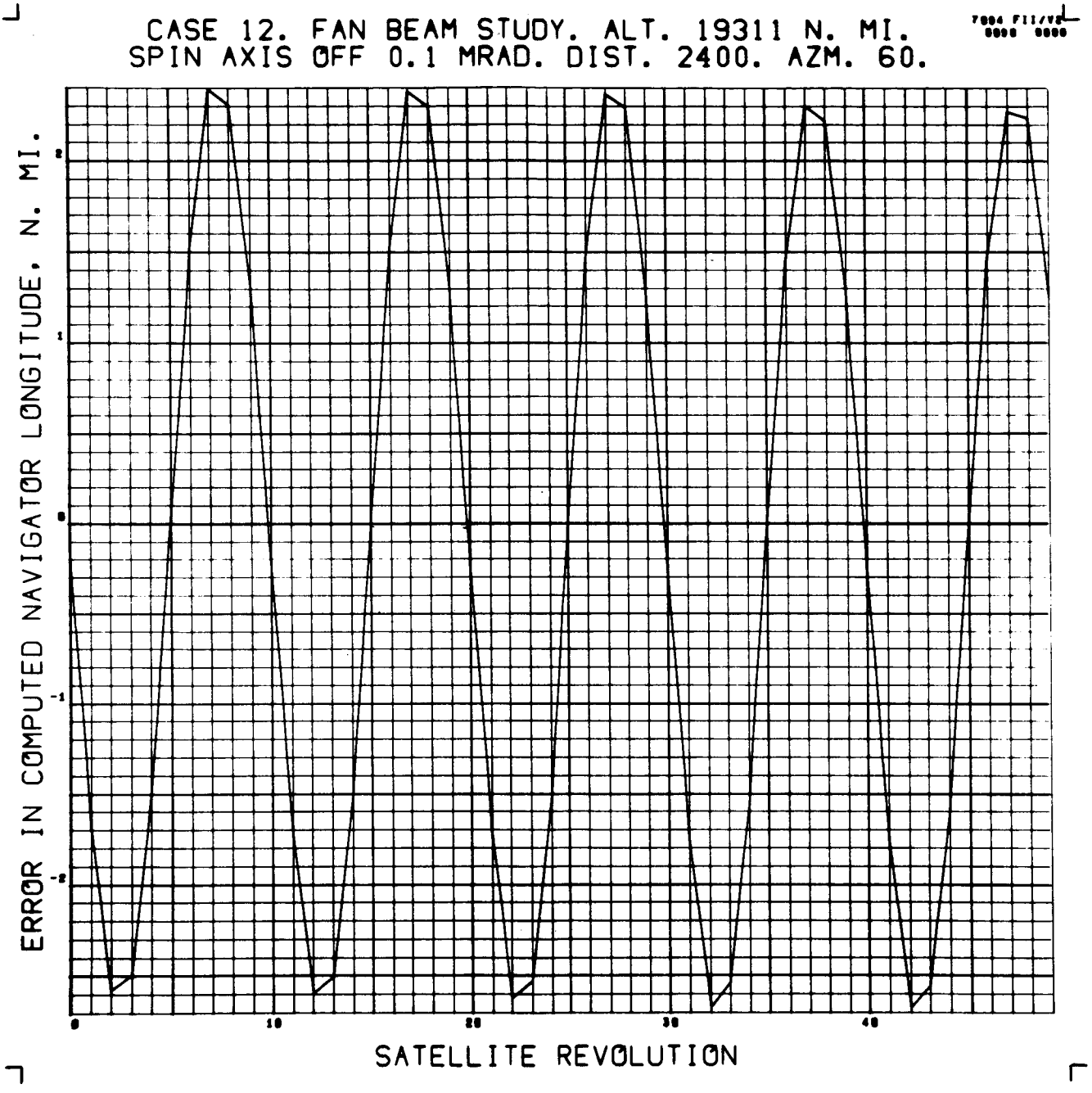
CASE 12. FAN BEAM STUDY. ALT. 19311 N. MI.
SPIN AXIS OFF 0.1 MRAD. DIST. 2400. AZM. 60.
ERROR IN COMPUTED NAVIGATOR LONGITUDE, N. MI.
SATELLITE REVOLUTION

Figure 4-36

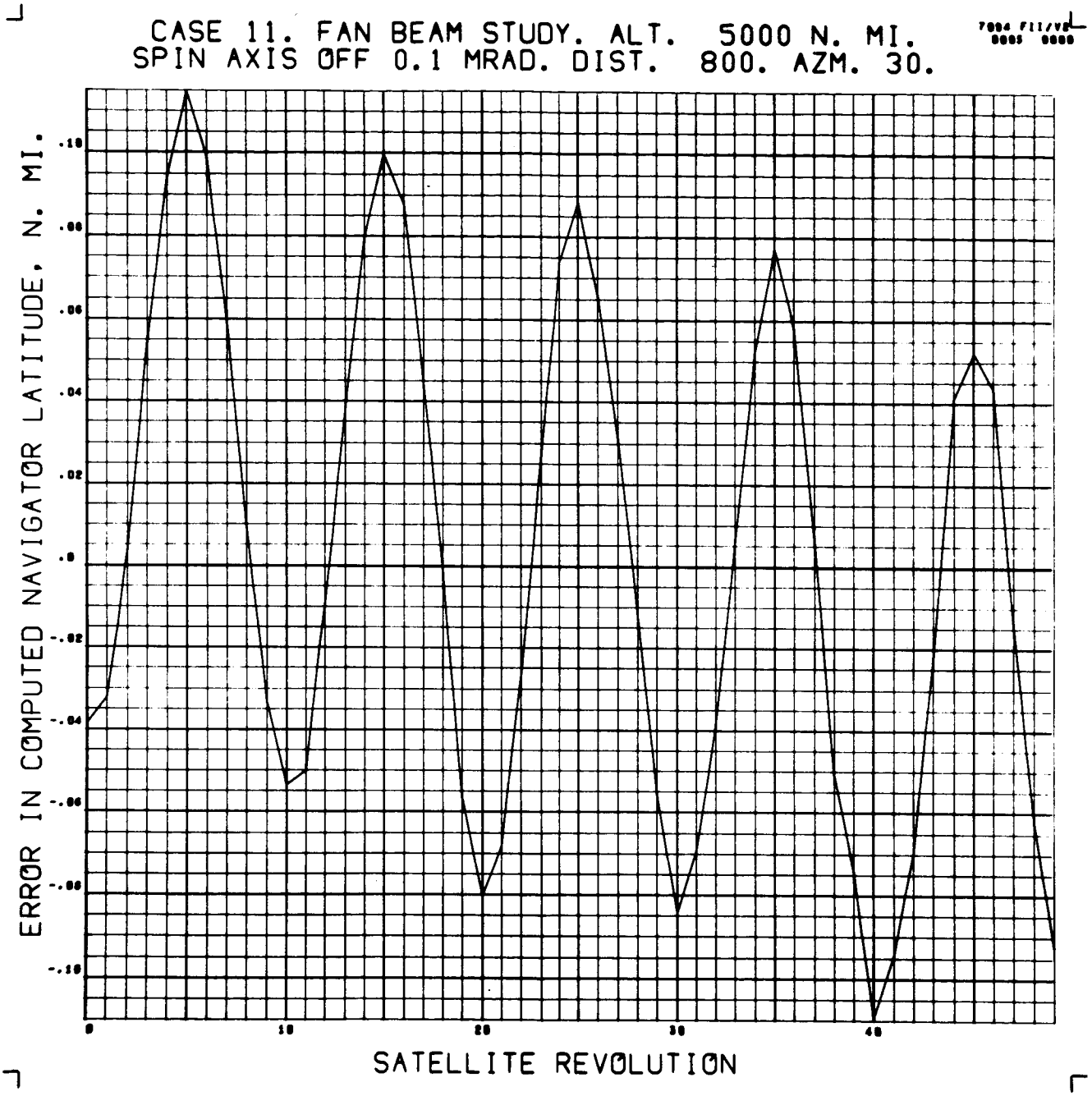
CASE 11. FAN BEAM STUDY. ALT. 5000 N. MI.
SPIN AXIS OFF 0.1 MRAD. DIST. 800. AZM. 30.
ERROR IN COMPUTED NAVIGATOR LATITUDE, N. MI.
.10
.08
.06
.04
.02
0
-.02
-.04
-.06
-.08
-.10
0
10
20
30
40
SATELLITE REVOLUTION

Figure 4-37

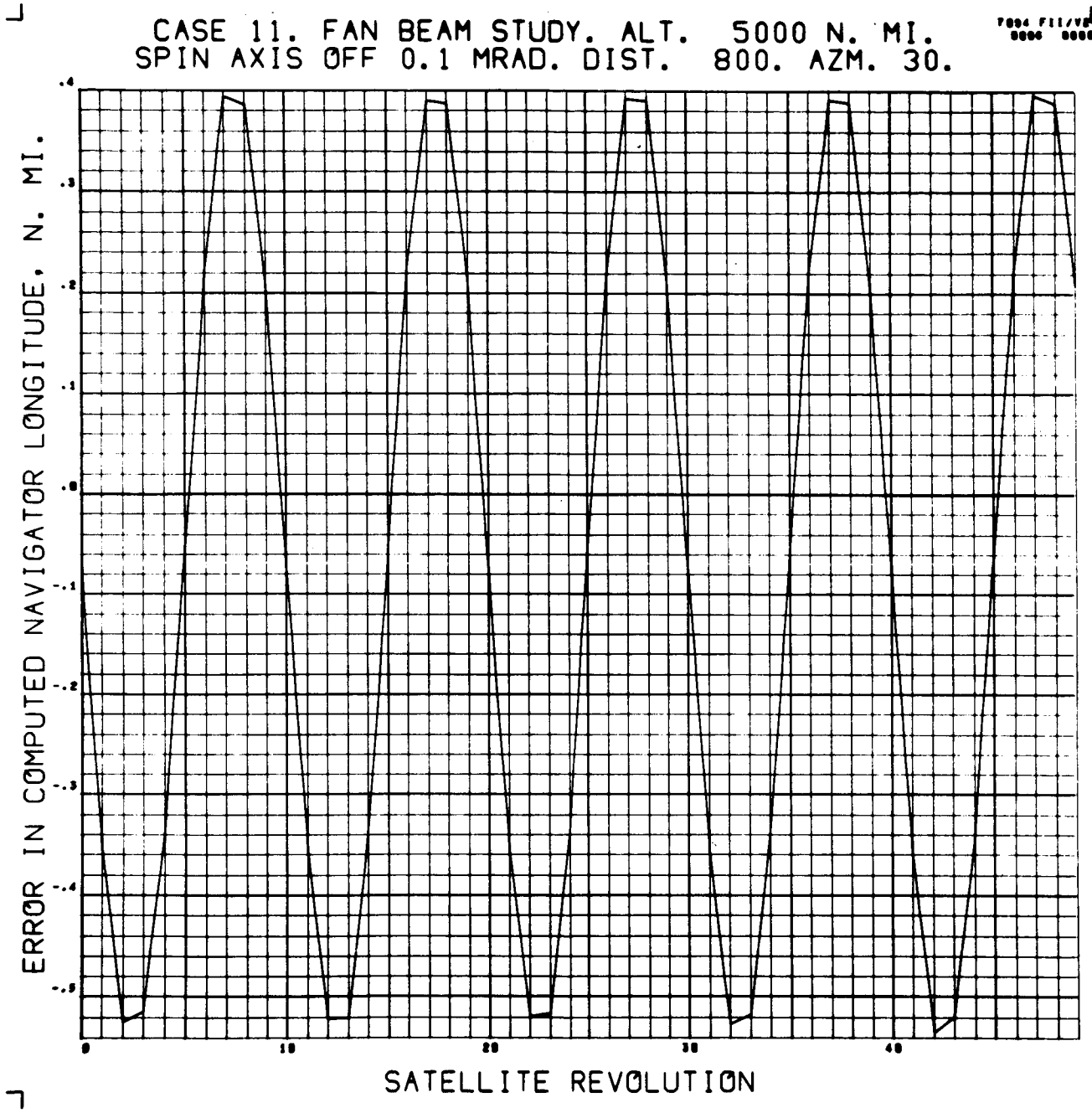
CASE 11. FAN BEAM STUDY. ALT. 5000 N. MI.
SPIN AXIS OFF 0.1 MRAD. DIST. 800. AZM. 30.
ERROR IN COMPUTED NAVIGATOR LONGITUDE, N. MI.
.4
.3
.2
.1
0
-.1
-.2
-.3
-.4
-.5
0
10
20
30
40
SATELLITE REVOLUTION

Figure 4-38

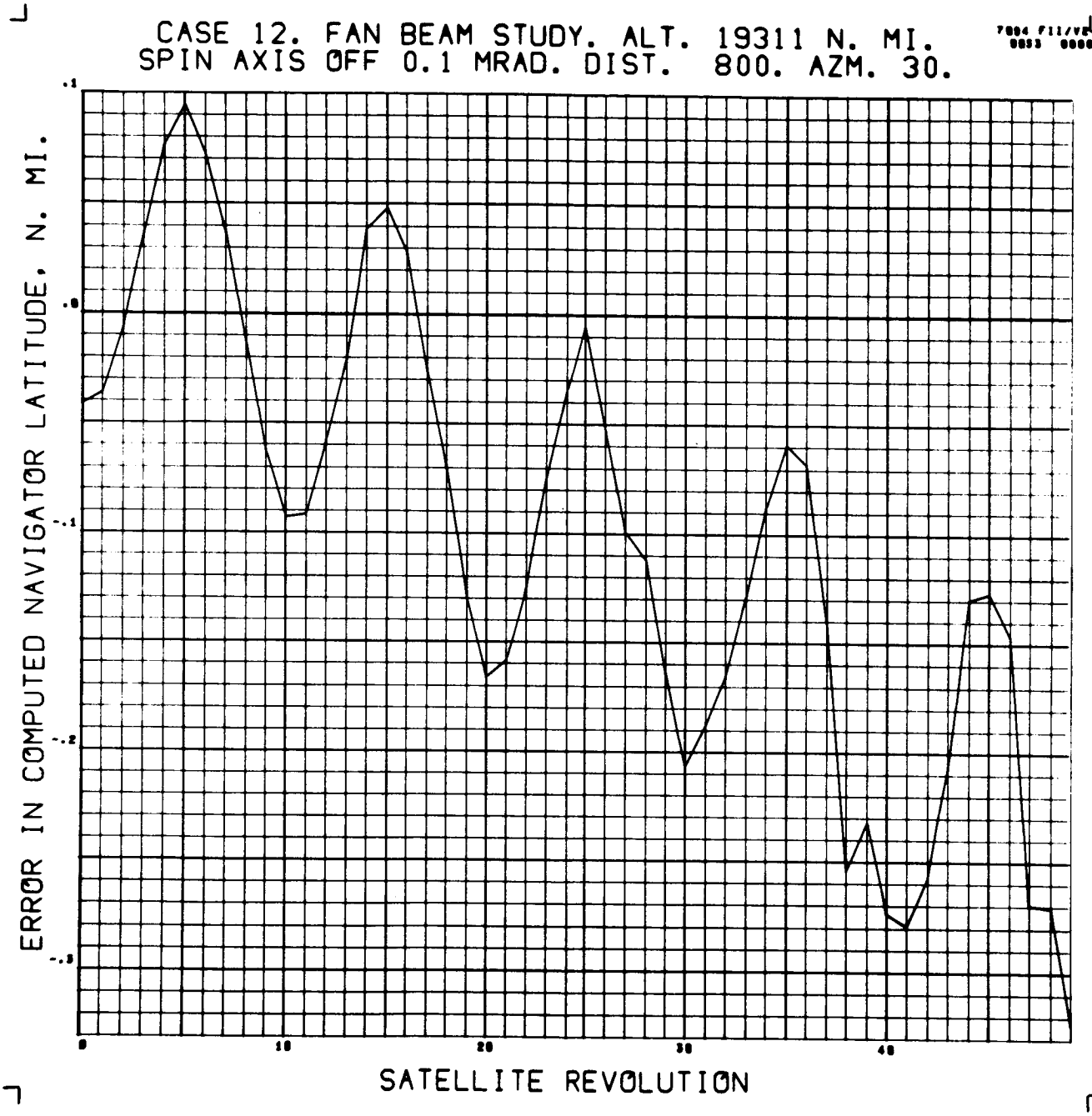
CASE 12. FAN BEAM STUDY. ALT. 19311 N. MI.
SPIN AXIS OFF 0.1 MRAD. DIST. 800. AZM. 30.
ERROR IN COMPUTED NAVIGATOR LATITUDE, N. MI.
.1
0
-.1
-.2
-.3
0
10
20
30
40
SATELLITE REVOLUTION

Figure 4-39

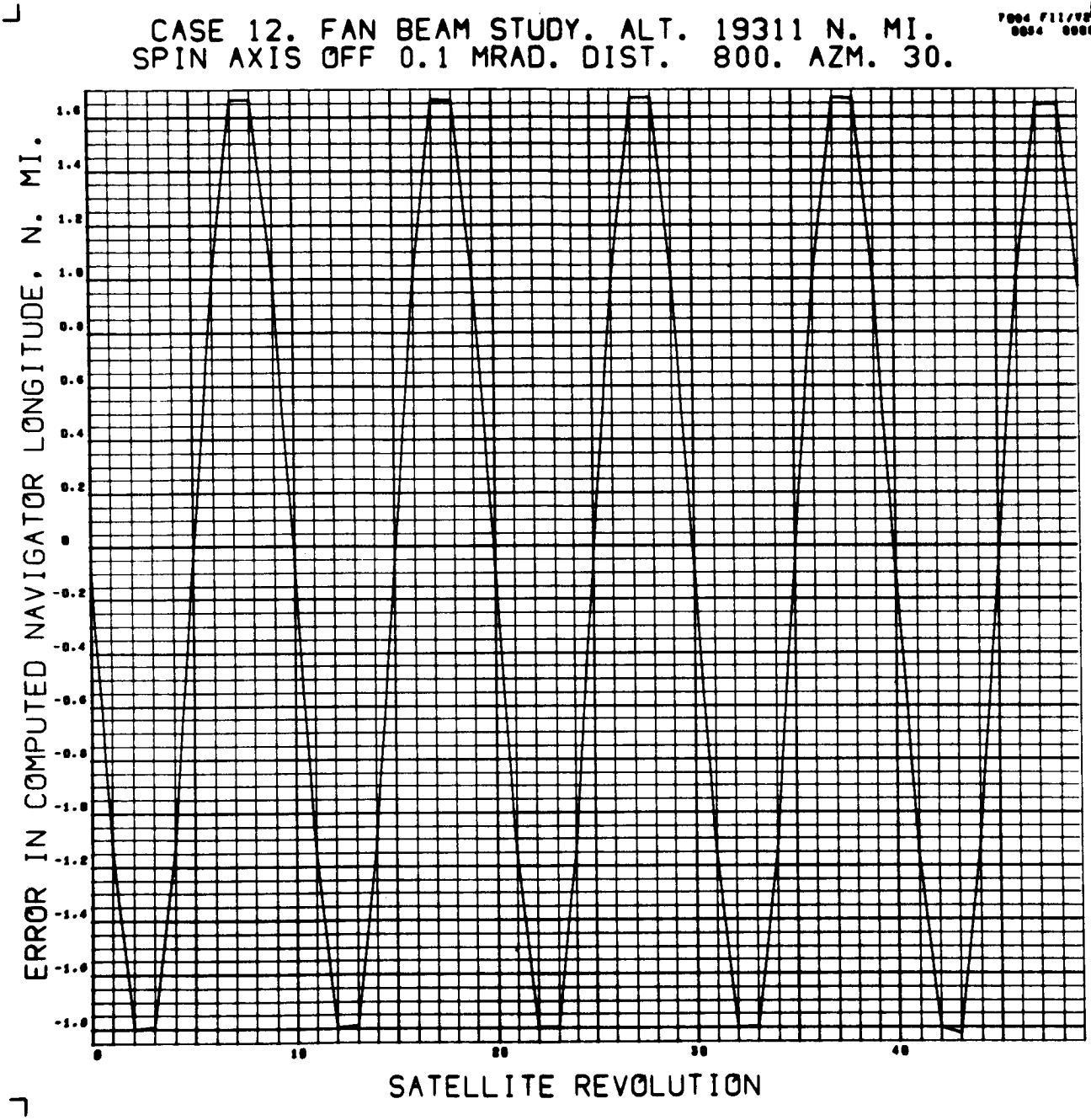
CASE 12. FAN BEAM STUDY. ALT. 19311 N. MI.
SPIN AXIS OFF 0.1 MRAD. DIST. 800. AZM. 30.
ERROR IN COMPUTED NAVIGATOR LONGITUDE, N. MI.
1.6
1.4
1.2
1.0
0.8
0.6
0.4
0.2
0
-0.2
-0.4
-0.6
-0.8
-1.0
-1.2
-1.4
-1.6
-1.8
0
10
20
30
40
SATELLITE REVOLUTION

Figure 4-40

Then, the angle of rotation of the $(\hat{e}_2, \hat{\omega})$-plane is

$$\Psi_k = \Omega t_k = 20\ k\ \pi\ (\rho + \Delta\rho)$$

In the simulation, $\rho = 1.1$. So

$$\Psi_k = 11\ k\ (2\ \pi) + 20\ k\ \pi\ \Delta\rho$$

The $(\hat{e}_2, \hat{\omega})$-plane will deviate from its original inertial orientation at $k = 0$ by the angle

$$\Delta\Psi_k = 20\ k\ \pi\ \Delta\rho, \qquad (56)$$

which is linear with k.

To compute the approximate $\Delta\rho$ which is present in the digital computations, the latitude error curves for the high altitude are inspected. The slope of the line about which the curves oscillate is estimated at about .05 n. miles per 10 revolutions. It is noted that, for the system being simulated, latitude measurements correspond to a position component parallel to the orbit plane. Hence, an estimate for $\Delta\Psi_k$ is

$$\Delta\Psi_k \cong \frac{.050}{19311} = .00000258 \text{ rad.}$$

Inserting this in Equation (56), with $k = 1$,

$$\Delta\rho \cong \frac{.00000258}{62.8} = .0000000412$$

This value of $\Delta\rho$ is seen to be in the region of round-off error compared to $\rho = 1.1$, (for the IBM 7094 computer). Round-off error in the input conversion of 1.1, which is not commensurate with the binary system, would be enough to explain the ramp in the latitude error curves. The vectors $\hat{\omega}$, $\hat{n}_1$ and $\hat{n}_2$ all will have inertial orientations on successive satellite revolutions which differ slightly from the idealized locations of the

example of Figure 3-5. These angular deviations are practically linear with k. As no updating for the navigator's available estimates for $\hat{\omega}$, $\hat{n}$ and $\hat{n}_2$ are assumed, there will be a steadily varying deviation of these inertially fixed estimates from the true vectors at the reference pulse times $t_o(10k + j)$, $k = 0, 1, 2, \ldots$, for fixed values of $j = 0, 1, 2, \ldots, 9$.

The reason why practically no ramp is seen in the longitude error curves may be explained as follows. As will be shown in Section 5.2, (Equation 110)). the component of the satellite-to-navigator vector transverse to the orbit plane (i.e., longitude) depends mainly upon (t_2-t_1), during each satellite revolution. This will obviously be little affected by the aperiodicity which has been described.

It should be emphasized that, although the source of the phenomenon in the simulation was round-off error, aperiodicity is the rule in actual satellite attitude motion. Hence, ramps similar to those seen in the latitude error curves are to be expected. This suggests the importance of the navigator's having good estimates of "average" positions for $\hat{\omega}$, $\hat{n}_1$ and $\hat{n}_2$ if his estimates are to be held fixed over a set of satellite revolutions. As defined in Section 3.7.1, these average positions represent the axes of the cones which are the loci of the true vectors and should remain good estimates, regardless of the precise positions of the true vectors on the cones over any particular 10 t_o pulses. This will minimize ramp phenomena. In the cases discussed so far for multiple fixes, the navigator's estimated $\hat{n}_1$ and $\hat{n}_2$ have been taken on the surface of their respective cones while the estimated $\hat{\omega}$ has been even more poorly placed (the $\hat{f}_2$ vector). The effect of ramps when smoothing is applied to multiple fixes will be discussed below.

The method of position smoothing described in Section 3.7.3 was applied to Figures 4-29 thru 4-40, the error curves for latitude and longitude, over ten satellite revolutions (11 fixes). The average errors were estimated directly from the curves. Table 4-2 shows the resulting fix errors and compares them with the fix error experienced from

Table 4-2 Benefits from Smoothing 11 Fixes

Satellite Altitude (n. mi.)	Subsatellite Distance (n. mi.)	Azimuth (Degrees)	Ave. Error δ Lat (n. mi.)	Ave. Error δ Lon (n. mi.)	$\delta P = \sqrt{\delta \text{ Lat}^2 + \delta \text{ Lon}^2}$ (n. mi.)	δ P Single Fix, Third Rev.
5000	800	60	.047	-.032	.057	.498
	2400	60	.150	-.070	.165	1.200
19311	800	60	.002	-.040	.040	1.770
	2400	60	.112	.090	.143	2.575
5000	800	30	.023	-.070	.073	.523
19311	800	30	-.010	-.060	.061	1.800

a single-fix computation made during the third satellite revolution (taken from the curves of Section 4.2.1).

The smoothing done here has been applied to a set of 11 position fixes, with a complete fix calculation for each satellite revolution. Upon inspection of the latitude error curves for the medium altitude cases, it may be seen that due to the ramp, if the smoothing were performed over all 50 satellite revolutions, the position error δP would be even further reduced, since the average δ Lat would be smaller, with little change in the average δ Lon. This is also true for the high altitude case for subsatellite distance 2400 nautical miles. However, in the other high altitude cases, the severe latitude error ramp limits the usefulness of the total range of fixes available. In the following examples, curves illustrating this will be shown.

Figures 4-41 and 4-46 show the effects of smoothing position computations for a system very similar to that which has been described, except that more of the perturbative sources listed in Section 2.3 are presumed operating, namely: satellite orbital motion, earth rotation and navigator motion relative to the earth. See Table 4-1 for details (Cases 23 and 24).

The abscissa for the curves is the mid-revolution number for the smoothing interval. Effects of smoothing are shown for smoothing intervals of 0, 10, 20, 30, 40 and 50 satellite revolutions, which yield estimates of the position of the moving navigator at the times corresponding to the t_o pulse after 0, 5, 10, 15, 20 and 25 satellite revolutions.

It will be noticed that the position error for 0 revolutions is sometimes better and sometimes worse than for abscissa 5. This is due entirely to the relative "goodness" of the initial satellite attitude for computation of a single fix -- something a navigator could not know in practice. Hence, little if any significance should be given to the points for 0 revolutions.

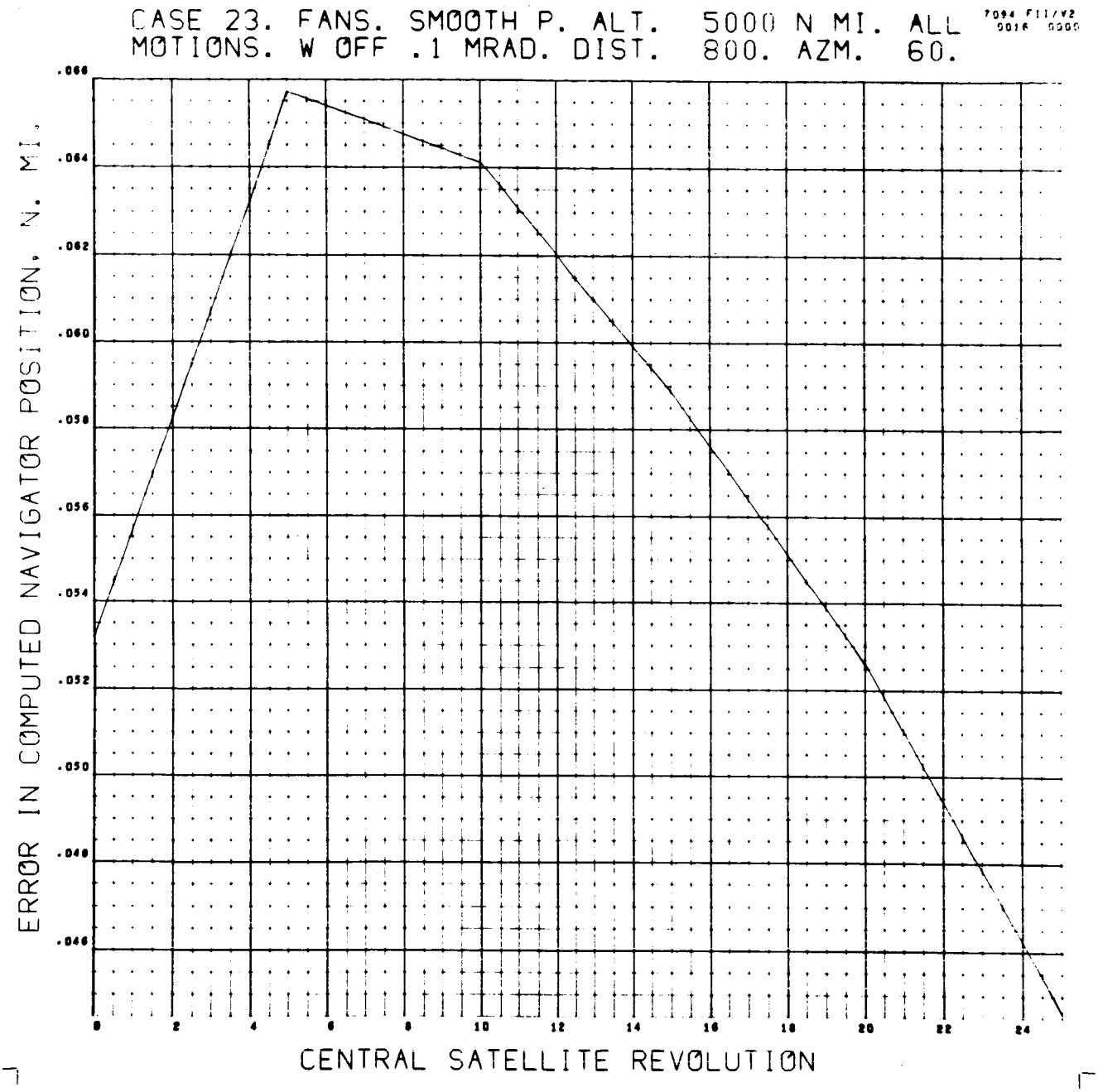
CASE 23. FANS. SMOOTH P. ALT. 5000 N MI. ALL MOTIONS. W OFF .1 MRAD. DIST. 800. AZM. 60.
7094 FII/V2
ERROR IN COMPUTED NAVIGATOR POSITION, N. MI.
.066
.064
.062
.060
.058
.056
.054
.052
.050
.048
.046
0
2
4
6
8
10
12
14
16
18
20
22
24
CENTRAL SATELLITE REVOLUTION

Figure 4-41

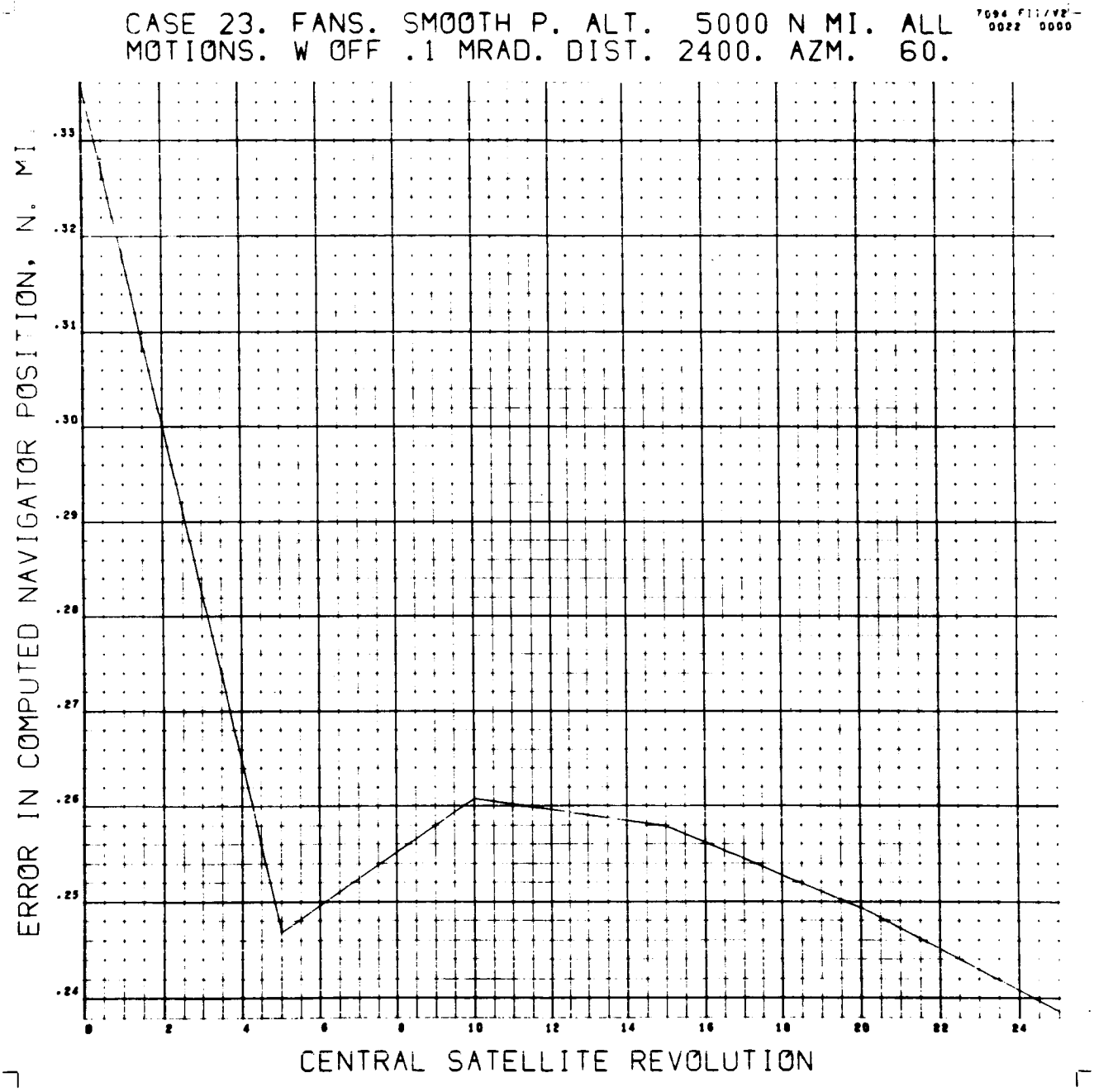
CASE 23. FANS. SMOOTH P. ALT. 5000 N MI. ALL MOTIONS. W OFF .1 MRAD. DIST. 2400. AZM. 60.
7094 FII/V2 0022 0000
ERROR IN COMPUTED NAVIGATOR POSITION, N. MI.
.33
.32
.31
.30
.29
.28
.27
.26
.25
.24
0
2
4
6
8
10
12
14
16
18
20
22
24
CENTRAL SATELLITE REVOLUTION

Figure 4-42

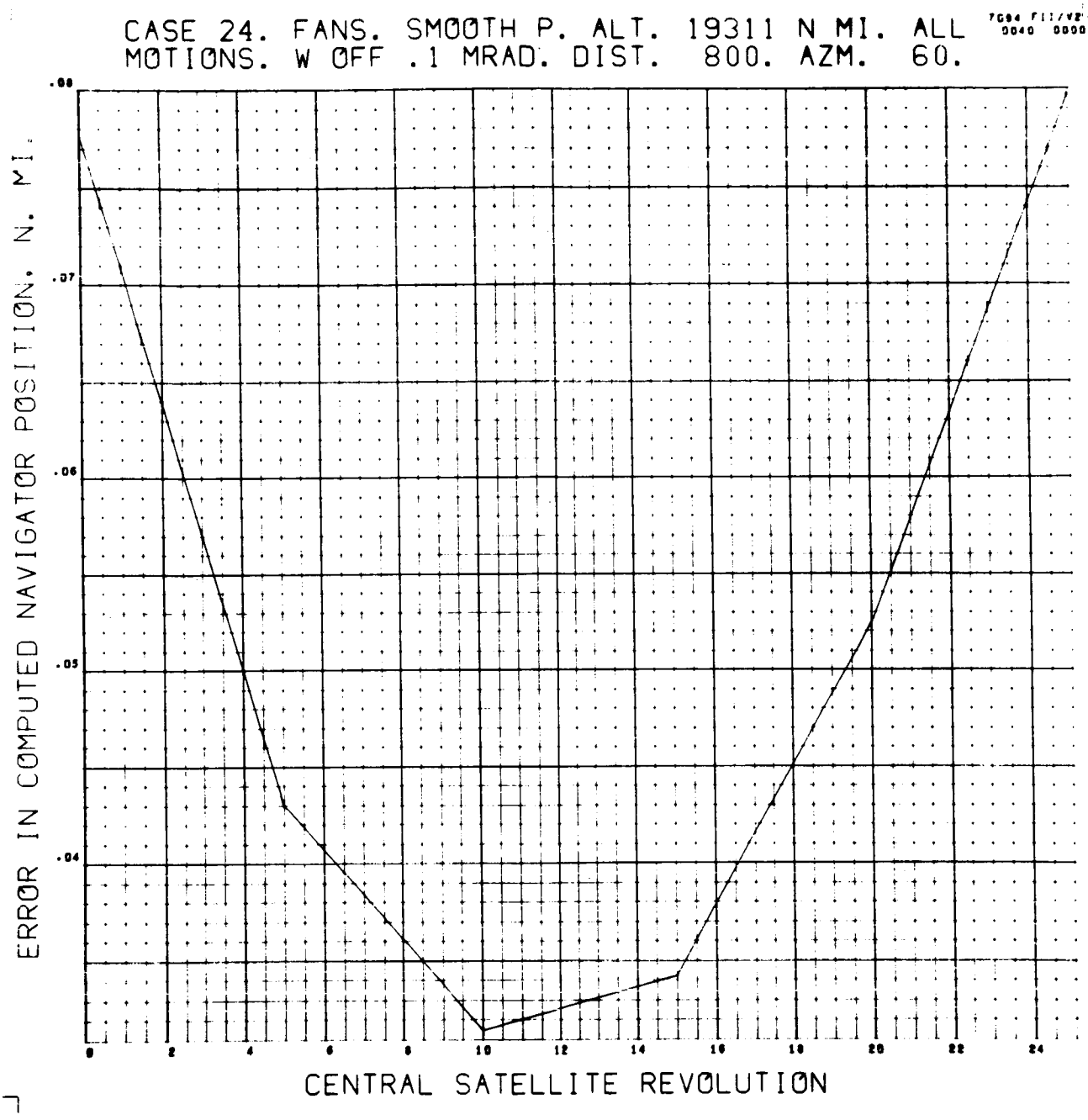
CASE 24. FANS. SMOOTH P. ALT. 19311 N MI. ALL MOTIONS. W OFF .1 MRAD. DIST. 800. AZM. 60.
ERROR IN COMPUTED NAVIGATOR POSITION, N. MI.
.08
.07
.06
.05
.04
0
2
4
6
8
10
12
14
16
18
20
22
24
CENTRAL SATELLITE REVOLUTION

Figure 4-43

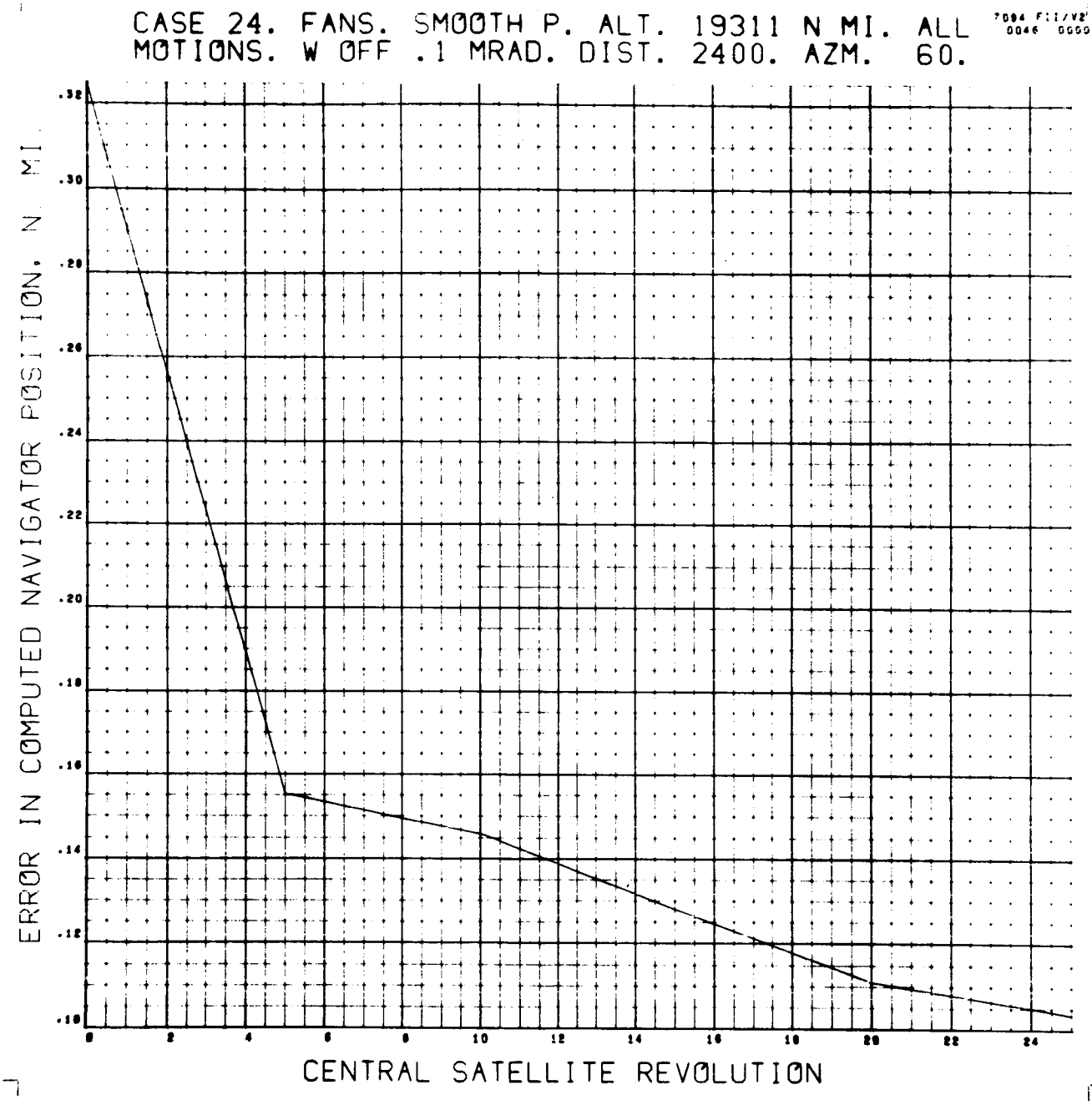
CASE 24. FANS. SMOOTH P. ALT. 19311 N MI. ALL MOTIONS. W OFF .1 MRAD. DIST. 2400. AZM. 60.
ERROR IN COMPUTED NAVIGATOR POSITION, N MI
.32
.30
.28
.26
.24
.22
.20
.18
.16
.14
.12
.10
0
2
4
6
8
10
12
14
16
18
20
22
24
CENTRAL SATELLITE REVOLUTION

Figure 4-44

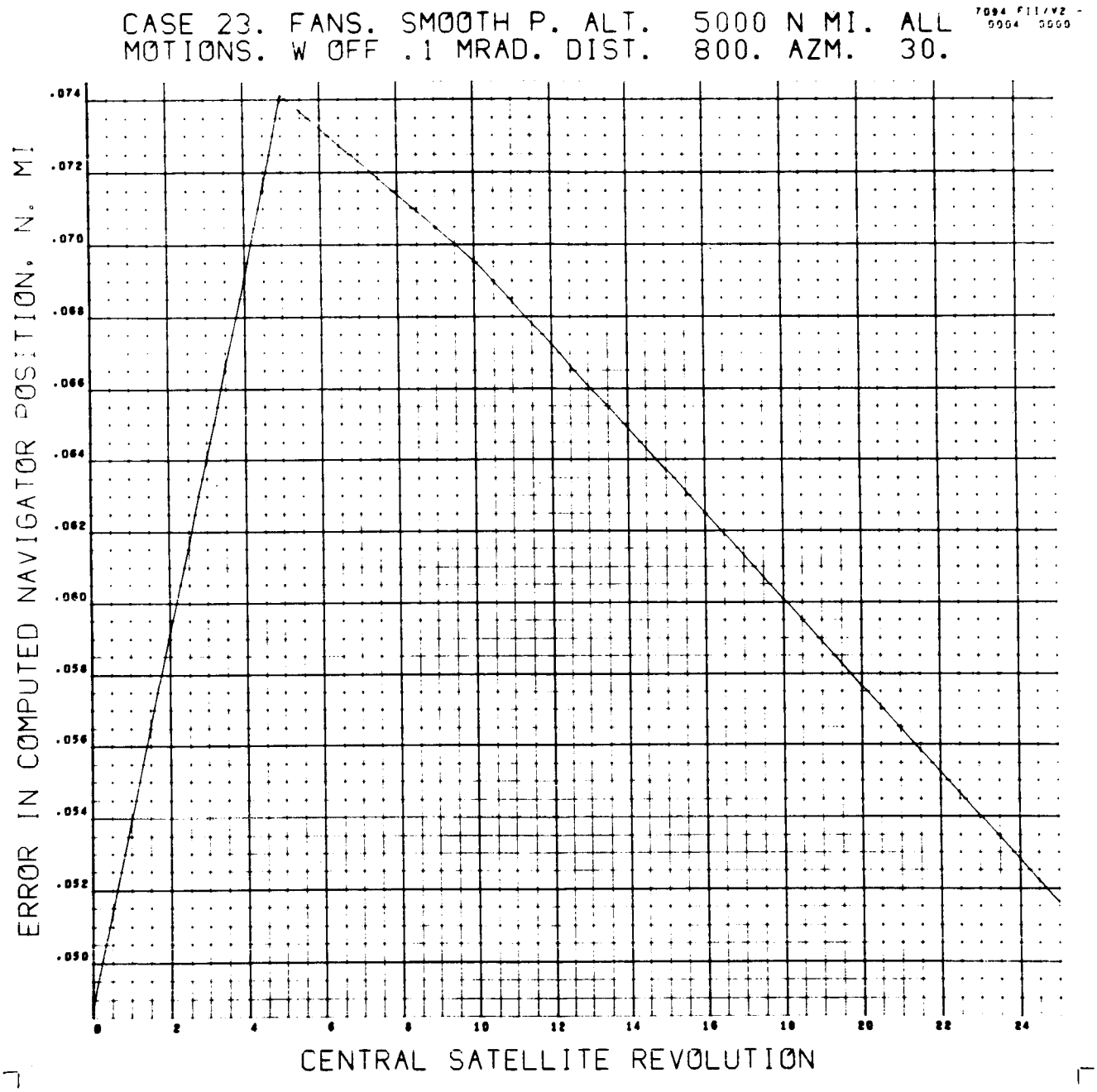
CASE 23. FANS. SMOOTH P. ALT. 5000 N MI. ALL MOTIONS. W OFF .1 MRAD. DIST. 800. AZM. 30.
7094 FII/VZ - 9004 3000
ERROR IN COMPUTED NAVIGATOR POSITION, N. MI
.074
.072
.070
.068
.066
.064
.062
.060
.058
.056
.054
.052
.050
0
2
4
6
8
10
12
14
16
18
20
22
24
CENTRAL SATELLITE REVOLUTION

Figure 4-45

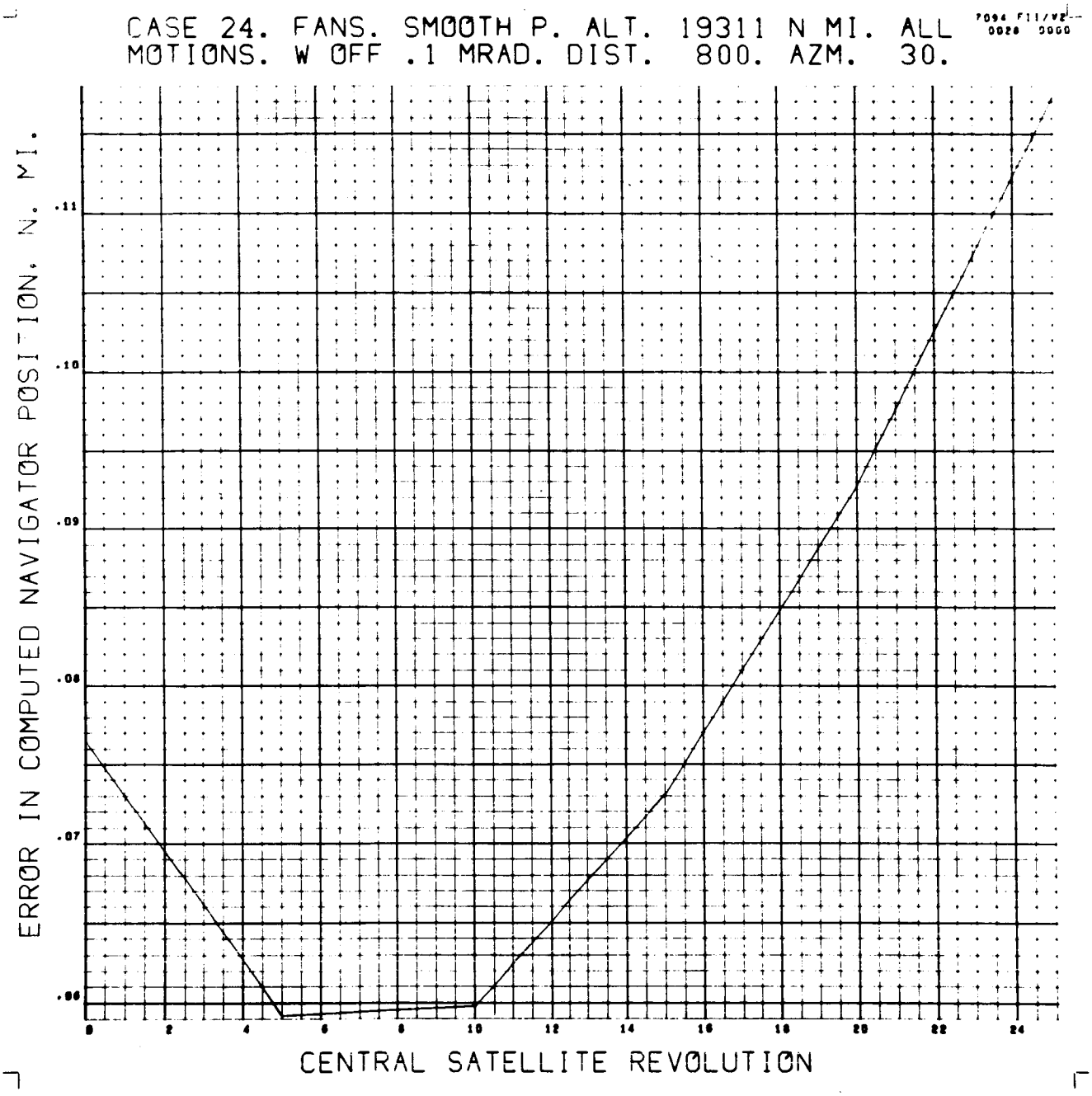
CASE 24. FANS. SMOOTH P. ALT. 19311 N MI. ALL MOTIONS. W OFF .1 MRAD. DIST. 800. AZM. 30.
ERROR IN COMPUTED NAVIGATOR POSITION, N. MI.
.11
.10
.09
.08
.07
.06
0
2
4
6
8
10
12
14
16
18
20
22
24
CENTRAL SATELLITE REVOLUTION

Figure 4-46

The curves show that position averaging over 10 satellite revolutions yields a position computation, for the time of the t_o pulse after 5 revolutions, of accuracy better than .25 nautical mile for all curves. For most of the curves the accuracy is better than .1 nautical mile.

Inspecting the position errors obtained by averaging over longer intervals, it is seen that for some system configurations the error decreases monotonically with length of smoothing time. However, the high altitude cases for subsatellite distances of 800 nautical miles present the smallest fix error after smoothing over 10 or 20 satellite revolutions (mid-revolution 5 or 10), and then the error increases, for longer smoothing intervals. This is due to the previously discussed aperiodicity of the satellite attitude motion. The bias in the average error for the position component parallel to the orbit plane causes an increase in total position error if the averaging is carried beyond 10 or 20 satellite revolutions.

The discussion in this section has been concerned with the employment of multiple fix computations under the assumption of the absence of noise on the timing data. It is not entirely accurate to use the term "smoothing" for such data, "averaging" is a better word. Also, as might be expected, averaging over one or two "processioncycles" of the satellite (10 or 20 revolutions for the cases being studies) produces practically all of the error reduction obtainable. The aperiodicity effect is sometimes beneficial and sometimes detrimental if longer averaging times are used.

The next section contains a preliminary consideration of statistical noise impressed on the fan timing data, to be followed in Section 4.3 by a further discussion based upon satellite transmitter power and antenna properties along with receiver antenna diameters.

4.2.3 Smoothing of Position and Time Data in the Presence of Noise

The cases in which satellite orbital motion, earth rotation and navigation motion relative to the earth are presumed operating, discussed in the

preceding section, are now considered anew with the assumption that the fan beam timing values t_1 and t_2 for each satellite revolution contain random noise. For the high altitude cases, the navigator is assumed to employ $\hat{h}$ as his estimate for $\hat{\omega}$, and to have for his estimates of $\hat{n}_1$ and $\hat{n}_2$ good average values as defined in Section 3.7.1. However, there is an assumed bias error of 1 μ sec in each reference pulse, $t_o(k)$.

A computer subroutine which provides random noise from a normal distribution with zero mean is used to impress noise upon the pure timing data t_1 and t_2. The standard deviations σ chosen are a function of satellite altitude and various assumptions regarding the satellite-to-navigator energy propagation, taken from the example in Volume IV, Section 4 of this study. For the medium altitude cases σ = 7.9 μ sec while for the high altitude cases σ = 30.3 μ sec. A limit of 3σ was placed upon the random values generated by the noise subroutine, any value exceeding this limit being rejected with another call upon the subroutine.

As the latitude and longitude computed values are summed for successive satellite revolutions, k, the noisy $(t_1-t_o)_k$ and $(t_2-t_o)_k$ data are also summed. Smoothed values of t_1 and t_2 are thus obtained as described in Section 3.7.3, to apply at the time of the satellite revolution halfway thru the number of revolutions smoothed.

The position error curves of Figures 4-47 thru 4-54 will be seen to occur in pairs. The first of a pair represents smoothing of complete computations of latitude and longitude for each satellite revolution. The second of the pair represents a complete computation of latitude and longitude only at the "mid-revolution" of the smoothing interval, using the smoothed values of t_1 and t_2 (and the t_o for that particular time). The plate titles contain the words "smooth P" and "smooth T" to distinguish type. When the two curves of a pair are compared, it will be seen that there is very little difference. This is of considerable practical value since, in an operational navigator installation, it would be much simpler to average only the timing quantities with a final single-fix computation than to compute a complete fix for every satellite revolution and then average them.

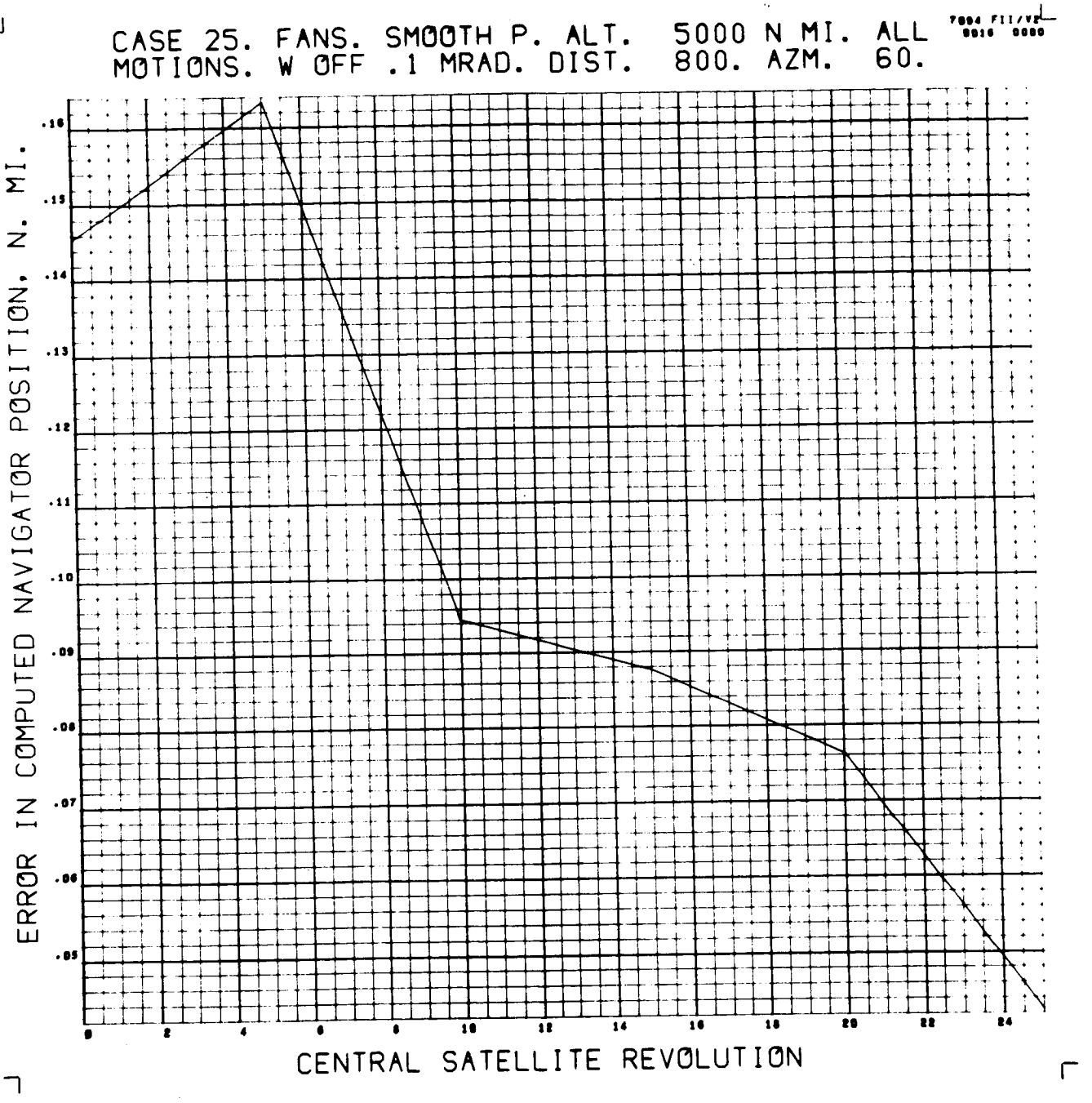
CASE 25. FANS. SMOOTH P. ALT. 5000 N MI. ALL
MOTIONS. W OFF .1 MRAD. DIST. 800. AZM. 60.
ERROR IN COMPUTED NAVIGATOR POSITION, N. MI.
.16
.15
.14
.13
.12
.11
.10
.09
.08
.07
.06
.05
0
2
4
6
8
10
12
14
16
18
20
22
24
CENTRAL SATELLITE REVOLUTION

Figure 4-47

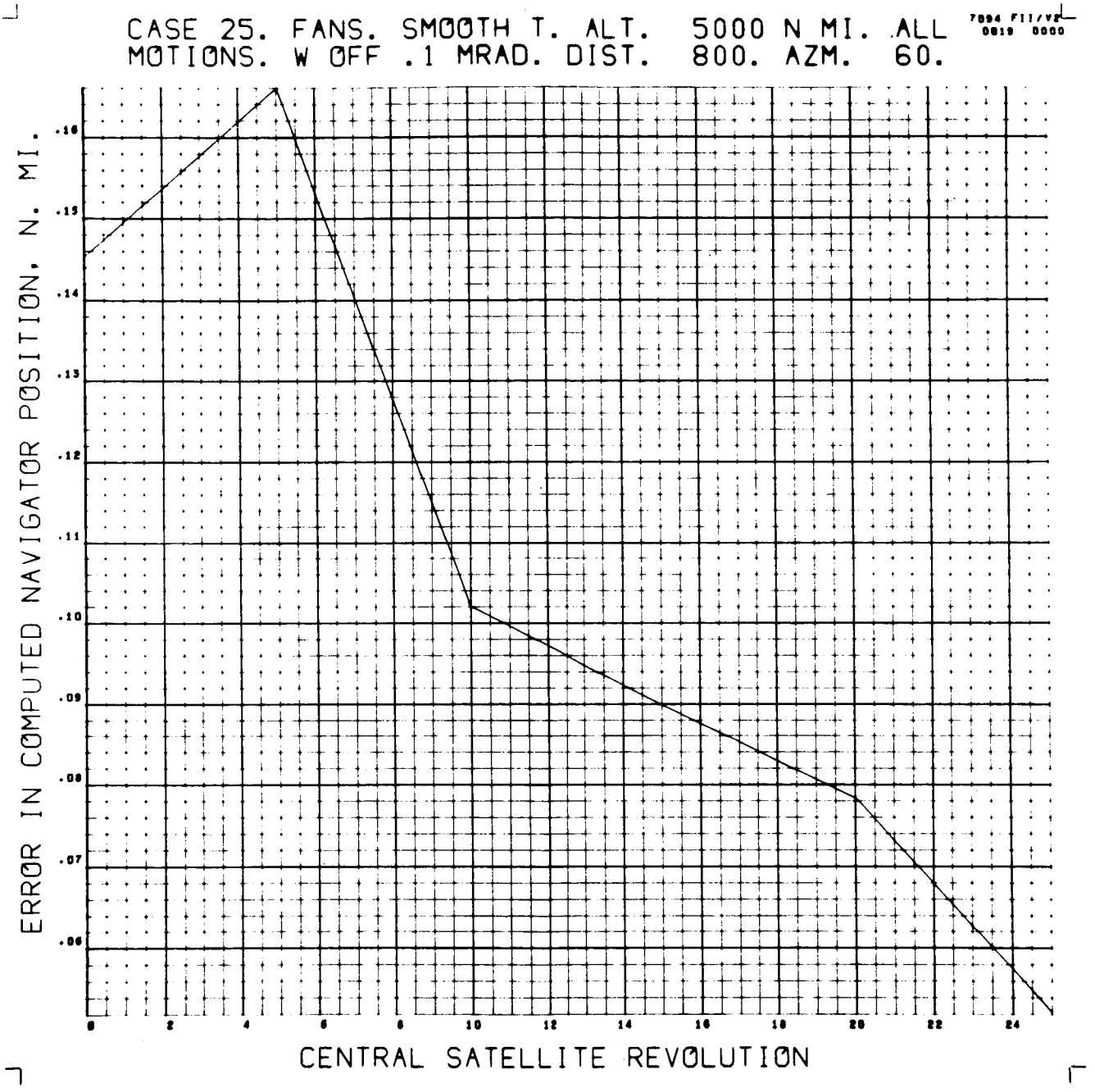
CASE 25. FANS. SMOOTH T. ALT. 5000 N MI. ALL MOTIONS. W OFF .1 MRAD. DIST. 800. AZM. 60.
7894 F11/V2 0819 0000
ERROR IN COMPUTED NAVIGATOR POSITION, N. MI.
.16
.15
.14
.13
.12
.11
.10
.09
.08
.07
.06
0
2
4
6
8
10
12
14
16
18
20
22
24
CENTRAL SATELLITE REVOLUTION

Figure 4-48

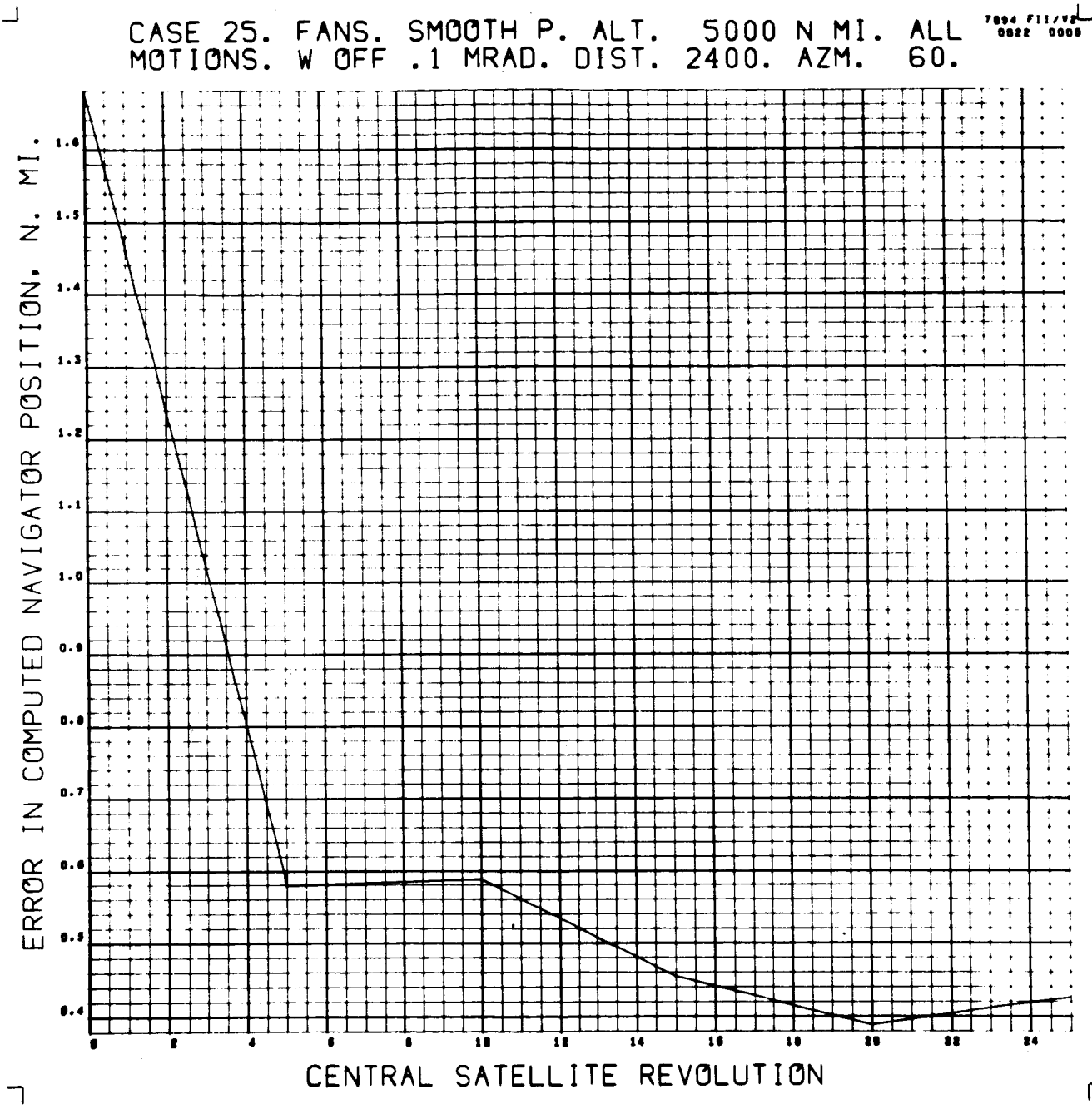
CASE 25. FANS. SMOOTH P. ALT. 5000 N MI. ALL MOTIONS. W OFF .1 MRAD. DIST. 2400. AZM. 60.
7894 F11/V2 0022 0000
ERROR IN COMPUTED NAVIGATOR POSITION, N. MI.
1.6
1.5
1.4
1.3
1.2
1.1
1.0
0.9
0.8
0.7
0.6
0.5
0.4
0
2
4
6
8
10
12
14
16
18
20
22
24
CENTRAL SATELLITE REVOLUTION

Figure 4-49

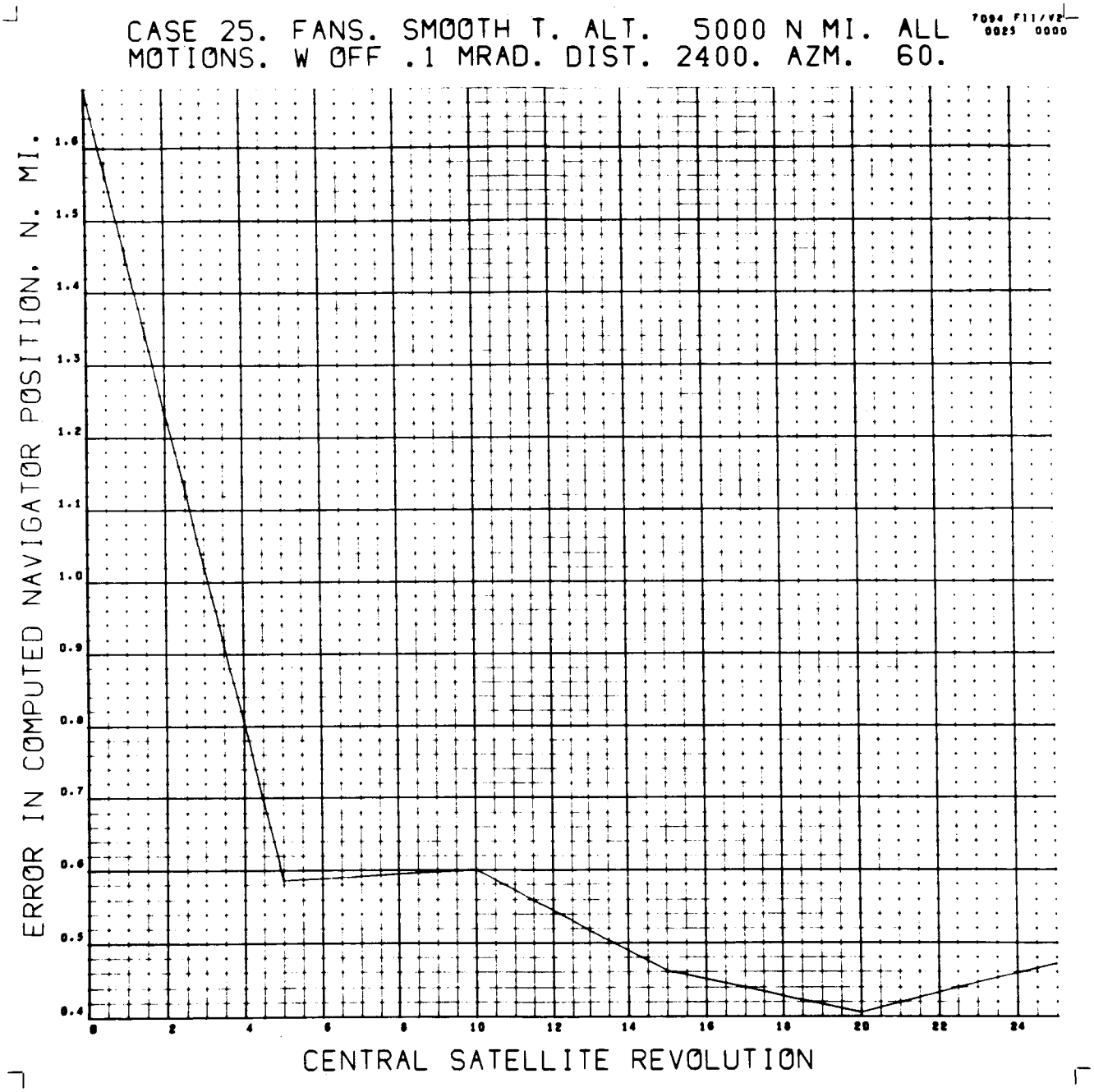
CASE 25. FANS. SMOOTH T. ALT. 5000 N MI. ALL MOTIONS. W OFF .1 MRAD. DIST. 2400. AZM. 60.
7094 F11/V2 0025 0000
ERROR IN COMPUTED NAVIGATOR POSITION, N. MI.
1.6
1.5
1.4
1.3
1.2
1.1
1.0
0.9
0.8
0.7
0.6
0.5
0.4
0
2
4
6
8
10
12
14
16
18
20
22
24
CENTRAL SATELLITE REVOLUTION

Figure 4-50

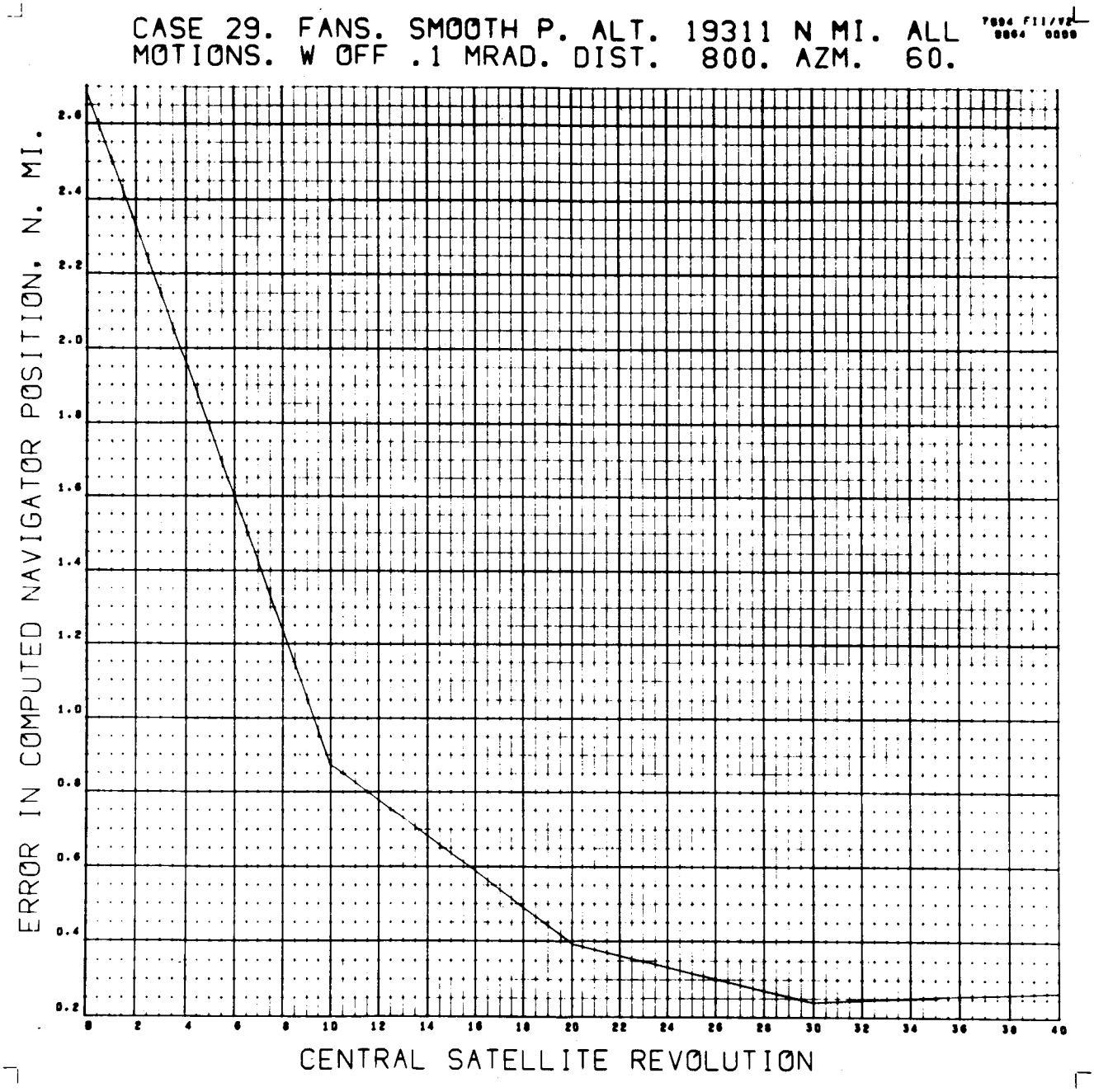
CASE 29. FANS. SMOOTH P. ALT. 19311 N MI. ALL MOTIONS. W OFF .1 MRAD. DIST. 800. AZM. 60.
ERROR IN COMPUTED NAVIGATOR POSITION, N. MI.
2.6
2.4
2.2
2.0
1.8
1.6
1.4
1.2
1.0
0.8
0.6
0.4
0.2
0 2 4 6 8 10 12 14 16 18 20 22 24 26 28 30 32 34 36 38 40
CENTRAL SATELLITE REVOLUTION

Figure 4-51

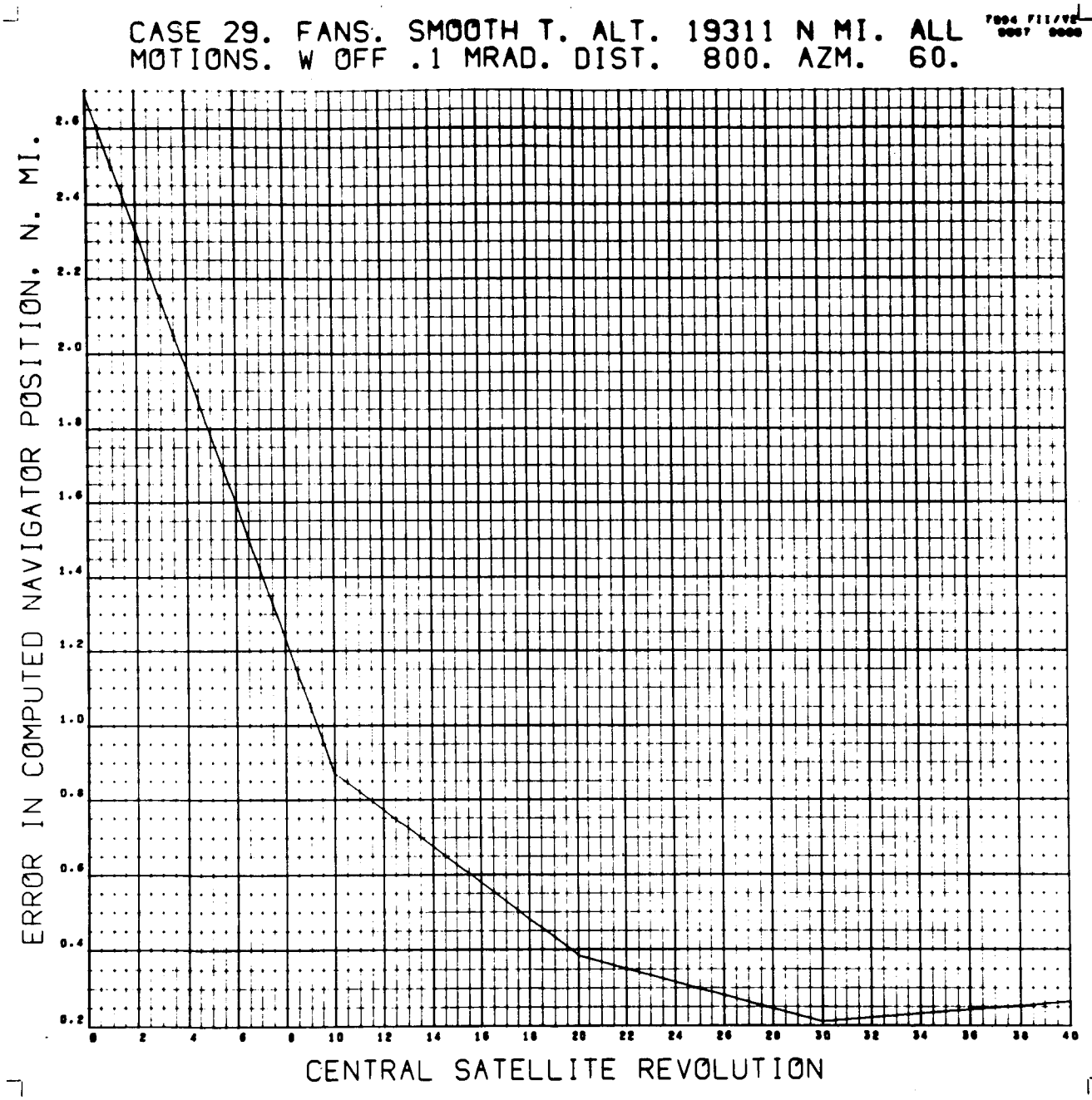
CASE 29. FANS. SMOOTH T. ALT. 19311 N MI. ALL MOTIONS. W OFF .1 MRAD. DIST. 800. AZM. 60.
ERROR IN COMPUTED NAVIGATOR POSITION. N. MI.
2.6
2.4
2.2
2.0
1.8
1.6
1.4
1.2
1.0
0.8
0.6
0.4
0.2
0
2
4
6
8
10
12
14
16
18
20
22
24
26
28
30
32
34
36
38
40
CENTRAL SATELLITE REVOLUTION

Figure 4-52

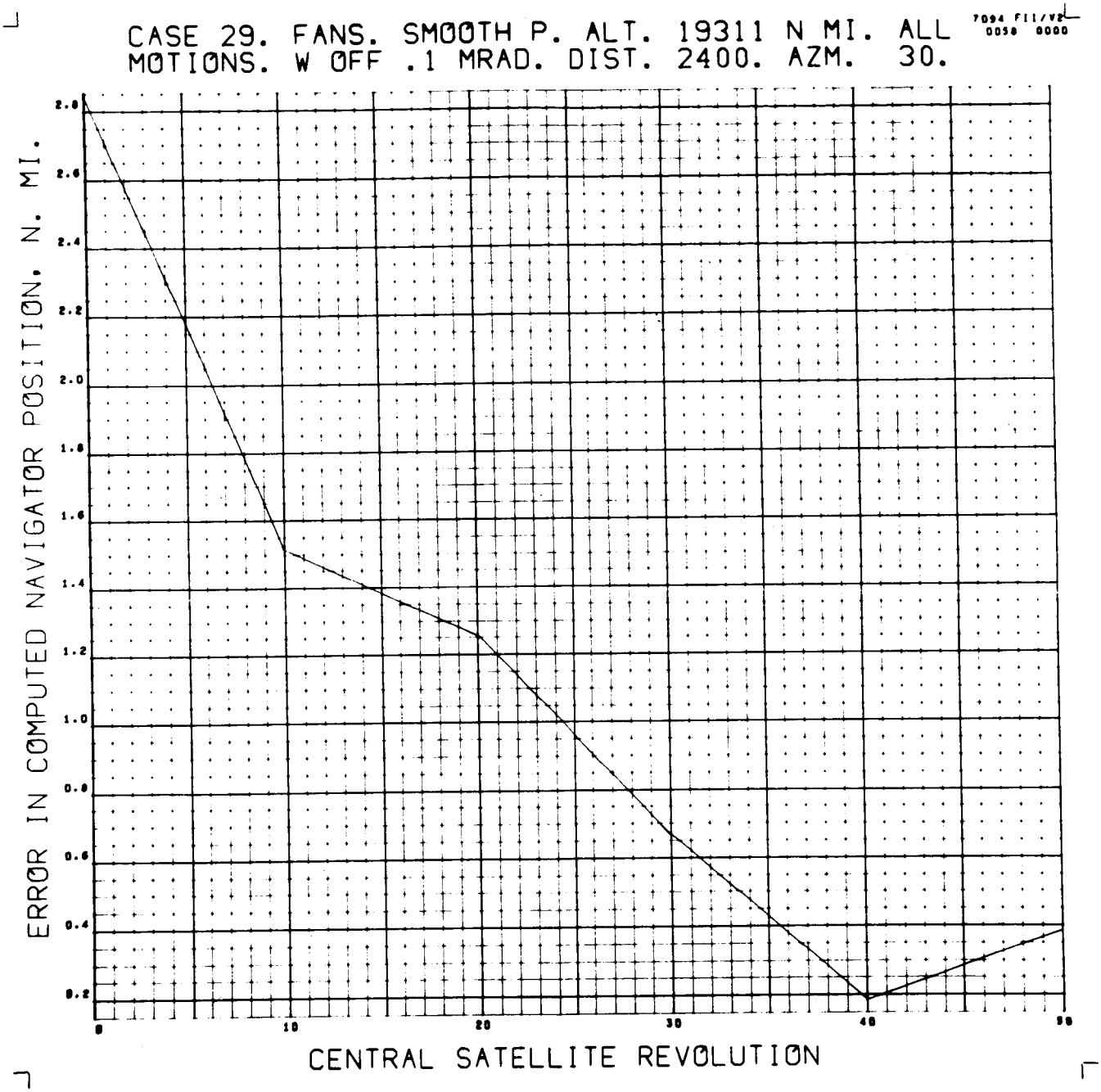
CASE 29. FANS. SMOOTH P. ALT. 19311 N MI. ALL MOTIONS. W OFF .1 MRAD. DIST. 2400. AZM. 30.
7094 FII/VS 0058 0000
ERROR IN COMPUTED NAVIGATOR POSITION, N. MI.
2.8
2.6
2.4
2.2
2.0
1.8
1.6
1.4
1.2
1.0
0.8
0.6
0.4
0.2
0
10
20
30
40
50
CENTRAL SATELLITE REVOLUTION

Figure 4-53

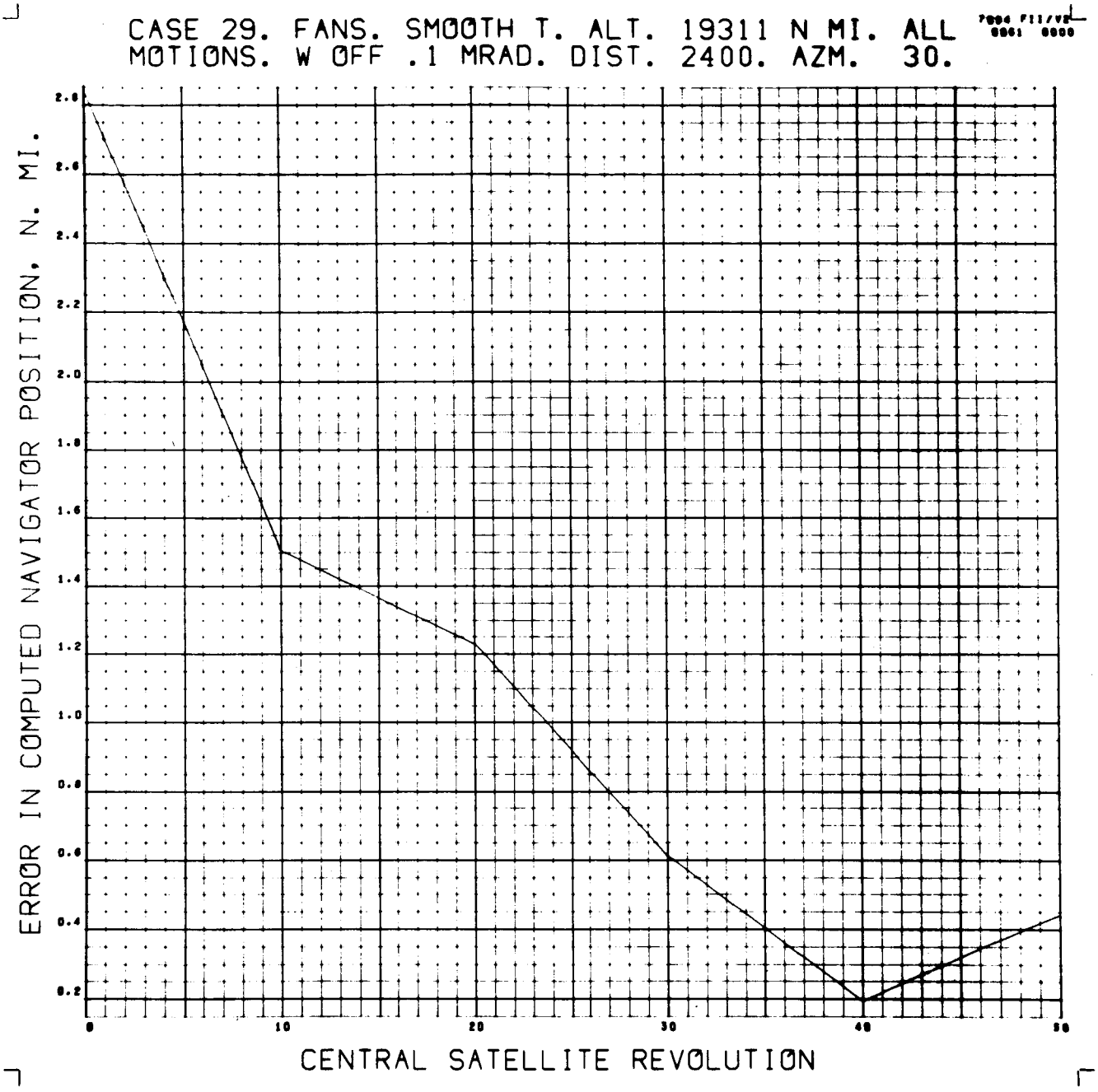
CASE 29. FANS. SMOOTH T. ALT. 19311 N MI. ALL MOTIONS. W OFF .1 MRAD. DIST. 2400. AZM. 30.
ERROR IN COMPUTED NAVIGATOR POSITION, N. MI.
2.8
2.6
2.4
2.2
2.0
1.8
1.6
1.4
1.2
1.0
0.8
0.6
0.4
0.2
0
10
20
30
40
50
CENTRAL SATELLITE REVOLUTION

Figure 4-54

For these cases there is a general reduction in position error as data from larger numbers of satellite revolutions are smoothed. However, there are instances where a slightly rising arc may be seen. This is a reasonable consequence of the fact that 10 to 100 satellite revolutions do not constitute very large samplings of the timing noise. Moreover, the random noise samples, of the order of magnitude of microseconds, are added to the pure t_1 and t_2 values very nearly in the region of round-off error for the IBM 7094, especially after 10 or 20 satellite revolutions have occurred. This results in partially destroying the Gaussian nature of the noise distribution. In the next section an alternate approach is taken in the simulation of noisy data.

4.3 OPERATIONAL NAVIGATIONAL SATELLITE SIMULATION

Having observed the effects of various error sources singly and in combination upon the navigator fix computation, a final set of computer runs was made, to simulate as closely as possible the satellite-navigator interplay in an operational system. Besides the various system motions and the $\hat{\omega}$ misalignment, as assumed in the preceding section, effects of satellite altitude, transmitter power and antenna length as well as receiver antenna diameter are introduced. In Volume IV (Section 4) of this study it is shown how these latter factors influence the signal-to-noise ratio at the receiver. An expression is then derived for the standard deviation σ_τ of the fan beam timing noise to be expected, (for a single detection). For ease of reference this expression is given here.

$$\sigma_\tau \triangleq 1.5 \sqrt{\frac{K\, T_e\, \delta_e}{\omega_s\, P_t\, G_r\, L}} \left(\frac{R}{D}\right) \tag{57}$$

where σ_τ will be in seconds if:

K = Boltzman's constant, 1.38×10^{-23} joules/°K.

T_e = system effective noise temperature, °K.

P_t = transmitter power output, watts

G_r = receiver antenna power gain

L = total link loss factor

δ_e = antenna beamwidth, transverse to the narrow fan beam

ω_s = satellite rotation rate

} in compatible units

R = range

D = antenna array length

} in the same units

The receiver gain G_r may be expressed in terms of the signal wave-length λ, receiver antenna diameter d, and a proportionality factor η as:

$$G_R = \eta \left(\frac{\pi d}{\lambda}\right)^2 \tag{58}$$

(a well-known formula in antenna design).

Along with the noise present in the detection of the t_1 and t_2 pulses there will be the systematic bias error sources discussed in the earlier sections. Note that a spin-rate error also is assumed. For completeness these sources will be summarized here.

a. Earth rotation
b. Satellite orbital motion (synchronous equatorial orbit)
c. Navigator motion (westward, altitude 6 n. miles, speed 600 n. mi./hr.
d. Satellite angular velocity vector misaligned .1 milliradian with principal axis (of symmetry).
e. Satellite angular velocity magnitude miscalibrated by 50 microradian/sec.
f. Reference pulse bias error .5 microsecond.

The initial position of the navigator was set at 2400 n. miles from the initial subsatellite point at an initial azimuth of 60 degrees from the orbit plane.

It is assumed that the navigator has for his use estimates of $\hat{\omega}$, $\hat{n}_1$ and $\hat{n}_2$, at the reference pulses times $t_o(k)$ (k being the satellite revolution number), which are the result of calibration of precision (B) as described in Sections 3.7.1 and 5.3 It should be pointed out that in a sense, these estimates represent miscalibrations of the true vectors (which vary with k), since they are held fixed over a set of N satellite revolutions. Moreover, they lie along the axes of the cones which are the loci of the true vectors, and hence cannot coincide with the true vectors at any time. It might be said that these estimates constitute the "best kind of miscalibration" in that they are the best "average vectors" to use in averaging out periodic errors due to precession. Reference to Section 3.7.1, Figure 3-5, shows that the actual angular deviation of the average $\hat{n}_1$ (or $\hat{n}_2$) from the true $\hat{n}_1$ (t_o) (or $\hat{n}_2(t_o)$) varies from about .066 to .091 milliradian over a complete precession cycle. Of course, the average $\hat{\omega}$ (being $\hat{h}$) makes a constant angle of about .0091 milliradian with the varying true $\hat{\omega}(t_o)$, (as was shown in Section 4.2.1). The values given are based on the value of moment of inertia ratio used, $\rho = 1.1$.

In an actual operational system, the calibration stations would inevitably not be able to specify even the average $\hat{\omega}$, $\hat{n}_1$ and $\hat{n}_2$ (defined as the respective cone axes) with zero errors. No attempt is made here to consider deviations of the calibrated vectors from the desired average vectors. Reference vectors other than the average vectors were employed in Section 4.2.1.

Under the governing assumptions described above, the results of the present computer runs illustrate the reduction of fix error attainable thru use of "time" smoothing (see Section 3.7.3), as a function of satellite transmitter power and antenna length, and receiver antenna diameter. The noise is assumed to be Gaussian. It is known that the sample mean, based on samples of order N from a normal distribution with standard deviation σ_τ, is normally distributed and has standard deviation $\sigma_\tau/\sqrt{N}$. Hence, when N = 10, 20, ..., 50 sets of timing data are smoothed, 1σ estimates of the residual timing errors are $\sigma_\tau/\sqrt{N}$. After time averaging, as described in Section 3.7.3, has been applied to the "pure" t_1 and t_2 values over N = 10, 20, ..., 50 satellite revolutions to average out periodic bias errors, a 1σ error as described above is impressed upon t_1 and t_2 to represent the effect of noise. The fix and fix error are then computed for the time of satellite revolution N/2, and are plotted in Figures 4-55 thru 4-58 for five assumed receiver antenna diameters, d = .4, .8, 1.6, 3.2 and 6.4 feet (highest curve to lowest).

Except for the patterns of values used for P_t, D and d, to be described in the next paragraph, the following values are assumed for the quantities in Equations (57) and (58):

$K = 1.38 \times 10^{-23}$ joule/deg.K.

T_e = 1000 deg. K.

$L = .5$

δ_e = 102 deg.

ω_s = 100 revs./min.
600 degs./sec.

R = synchronous altitude, ft.

$\eta = .5$

λ = 8 GHz

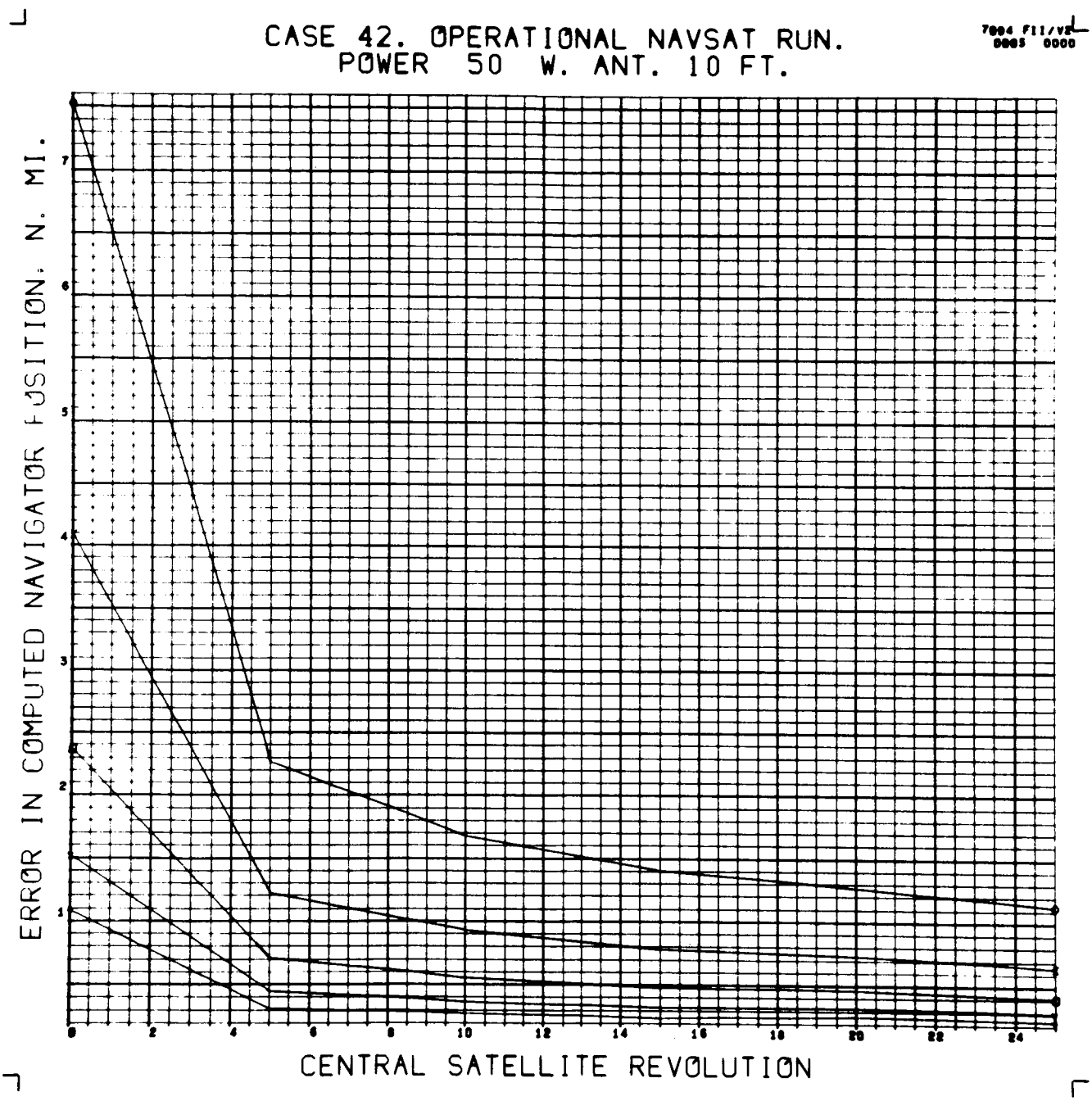
CASE 42. OPERATIONAL NAVSAT RUN.
POWER 50 W. ANT. 10 FT.
7004 F11/V2
0005 0000
ERROR IN COMPUTED NAVIGATOR POSITION, N. MI.
1
2
3
4
5
6
7
0
2
4
6
8
10
12
14
16
18
20
22
24
CENTRAL SATELLITE REVOLUTION

Figure 4-55

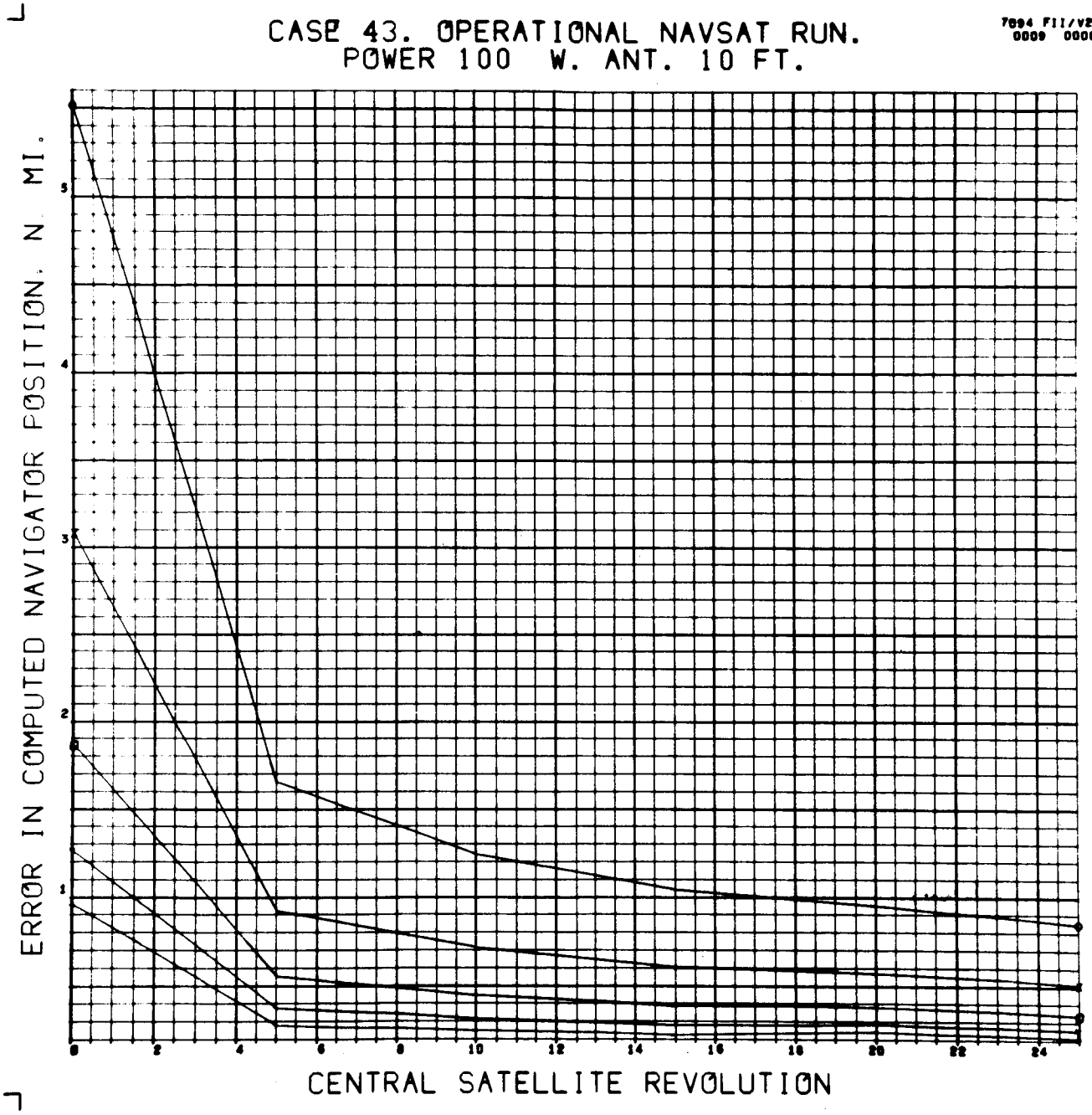
CASE 43. OPERATIONAL NAVSAT RUN.
POWER 100 W. ANT. 10 FT.
7094 FII/V2
0009 0000
ERROR IN COMPUTED NAVIGATOR POSITION. N MI.
1
2
3
4
5
0
2
4
6
8
10
12
14
16
18
20
22
24
CENTRAL SATELLITE REVOLUTION

Figure 4-56

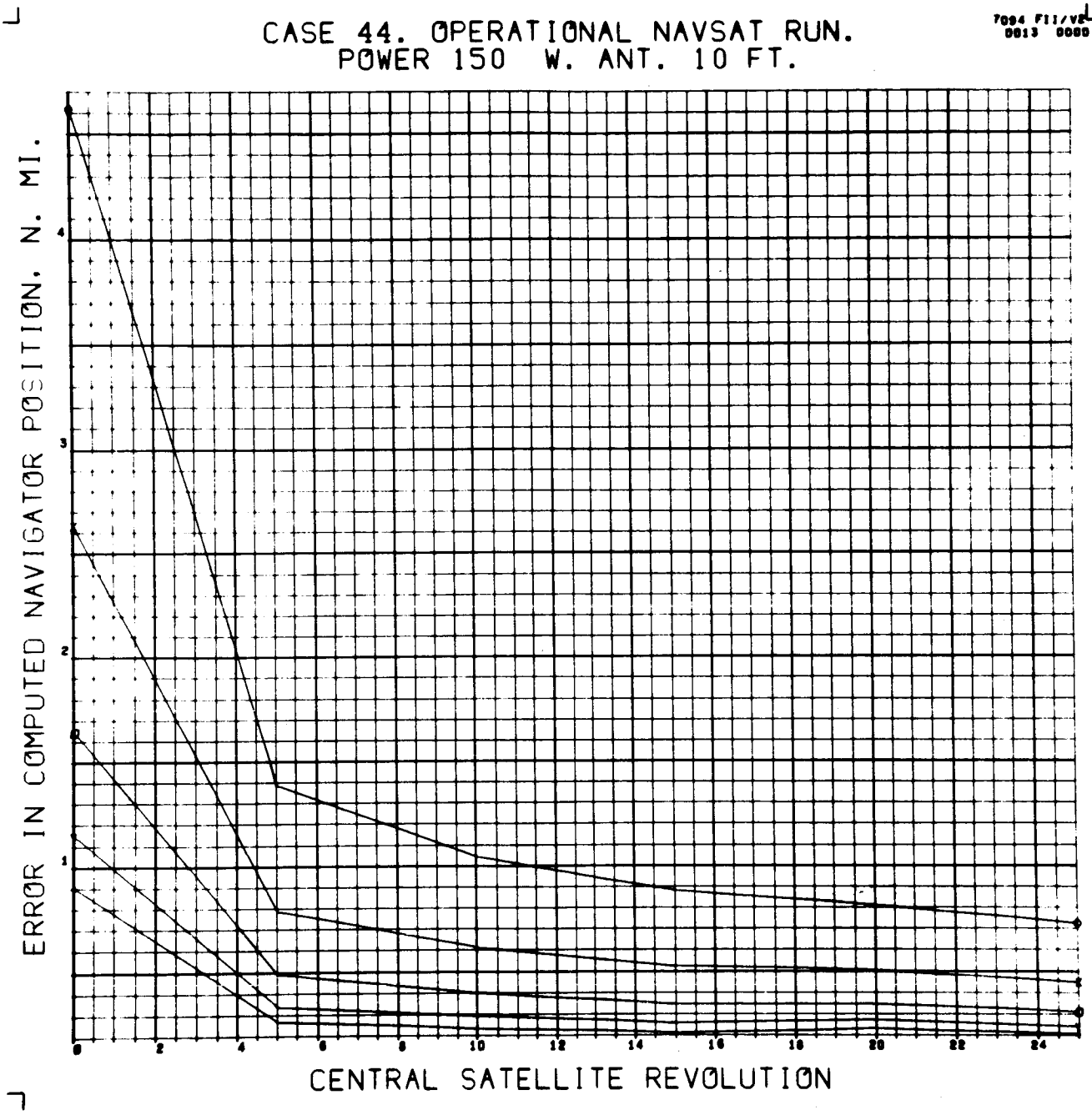
CASE 44. OPERATIONAL NAVSAT RUN.
POWER 150 W. ANT. 10 FT.
7094 F11/V2
0013 0000
ERROR IN COMPUTED NAVIGATOR POSITION, N. MI.
CENTRAL SATELLITE REVOLUTION
0
2
4
6
8
10
12
14
16
18
20
22
24
1
2
3
4

Figure 4-57

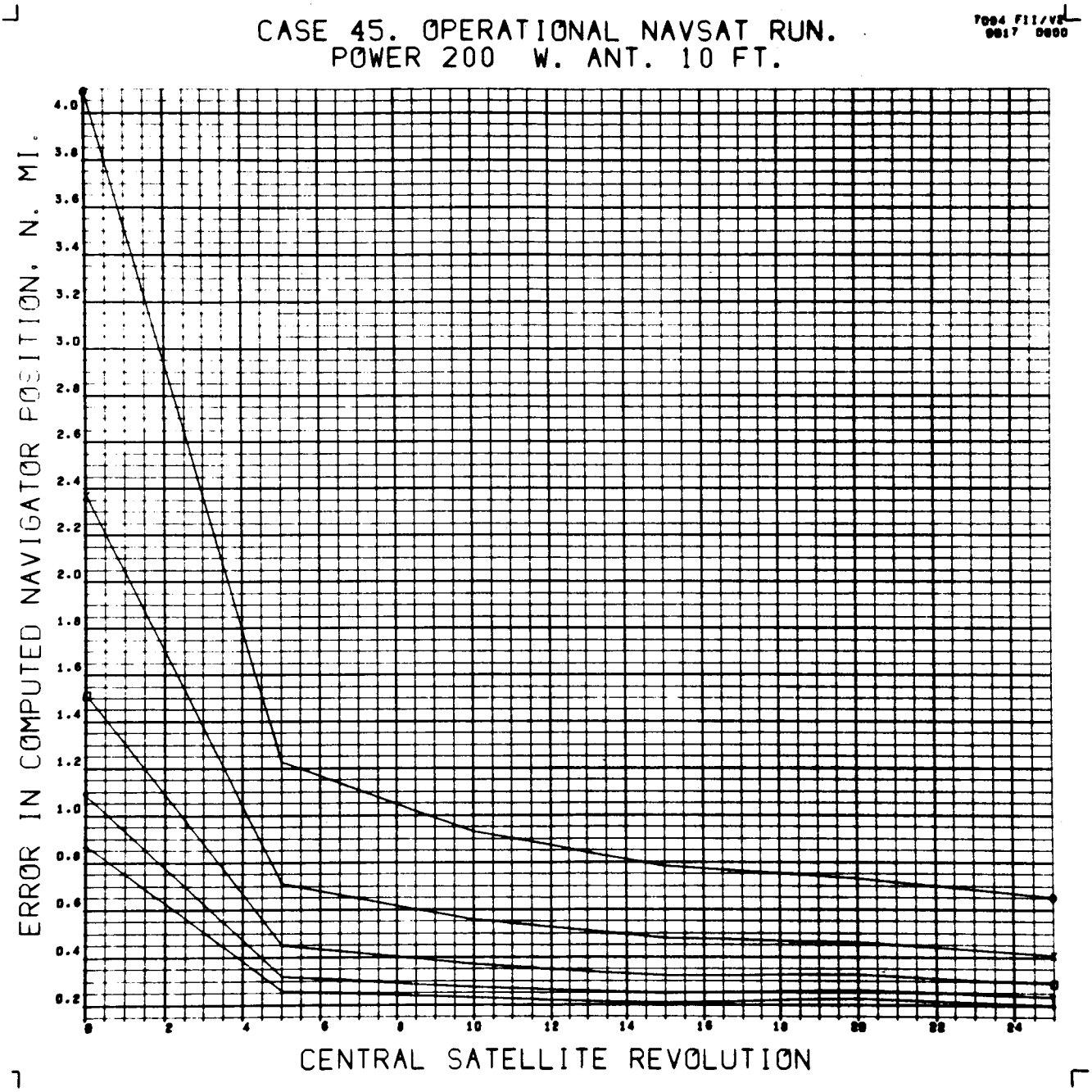
CASE 45. OPERATIONAL NAVSAT RUN.
POWER 200 W. ANT. 10 FT.
ERROR IN COMPUTED NAVIGATOR POSITION, N. MI.
4.0
3.8
3.6
3.4
3.2
3.0
2.8
2.6
2.4
2.2
2.0
1.8
1.6
1.4
1.2
1.0
0.8
0.6
0.4
0.2
0
2
4
6
8
10
12
14
16
18
20
22
24
CENTRAL SATELLITE REVOLUTION

Figure 4-58

Referring to Equations (57) and (58) it will be seen that σ_τ may be considered as a function of $(P_t D^2)$ when other quantities are held fixed. This means that computer results obtained for one pair of values $\bar{P}_t$ and $\bar{D}$ will equally well represent any other pair of value P_t and D so long as:

$$P_t D^2 = \bar{P}_t \bar{D}^2 \tag{59}$$

Accordingly, four computer runs were made with a fixed value $D = \bar{D} = 10$ feet and with values of $P_t = \bar{P}_t = 50$, 100, 150 and 200 watts respectively.

Figure 4-59 contains plots of the curves $\bar{P}_t \bar{D}^2 = 5000$, 10,000, 15,000 and 20,000. They may be used to apply Figures 4-55 thru 4-58 to other combinations of P_t and D. For example, consider a power value of $P_t = 125$. The vertical line for this value of P_t intersects the 5000, 10,000 and 15,000 curves at values for D of 6.3, 8.9, and 11 feet respectively. For this transmitter power and these antenna array lengths, Figures 4-55, 4-56 and 4-57, respectively apply. Alternatively, for a particular array length of interest, a horizontal line may be drawn to intersect the curves. This determines one or more power levels and the appropriate figures to consult for the error curves.

The fix errors for these operational Navigational Satellite runs extend over a considerable range depending upon the receiver antenna diameter and the number of satellite revolutions in the smoothing interval, as well as upon the satellite transmitter power and antenna array length. The overall range is from about 2.3 n. miles down to about .2 n. miles, or approximately an order of magnitude.

4.4 APPLICATION OF DIFFERENTIAL COMPUTATION METHOD

To show the potential capability of the differential position computation scheme (see Section 3.7.5), a sample set of latitude-longitude grid sizes were evaluated. The schematic below indicates the geometry of the sample case.

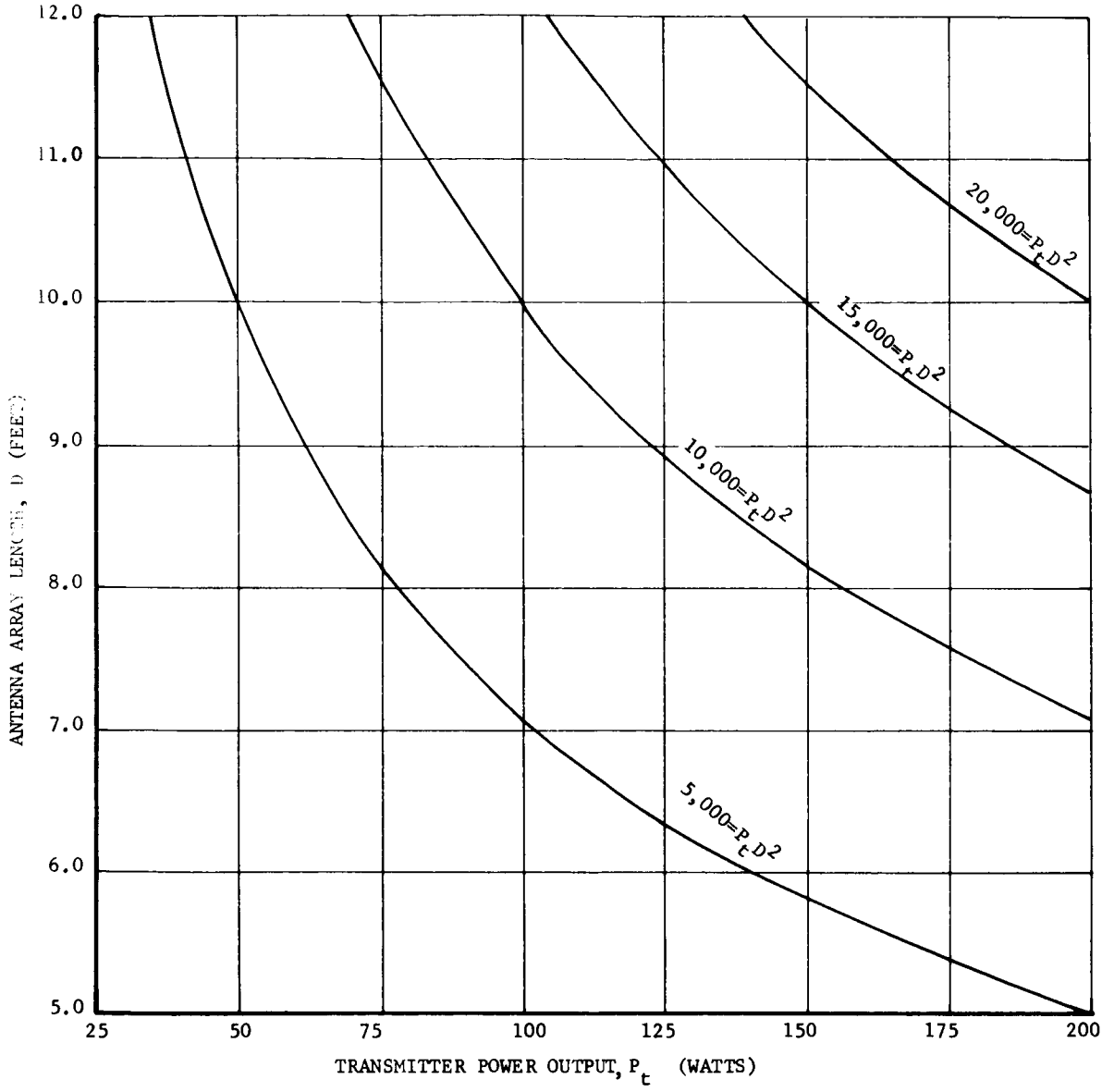

Figure 4-59 Antenna Array Length Vs Transmitter Power Output

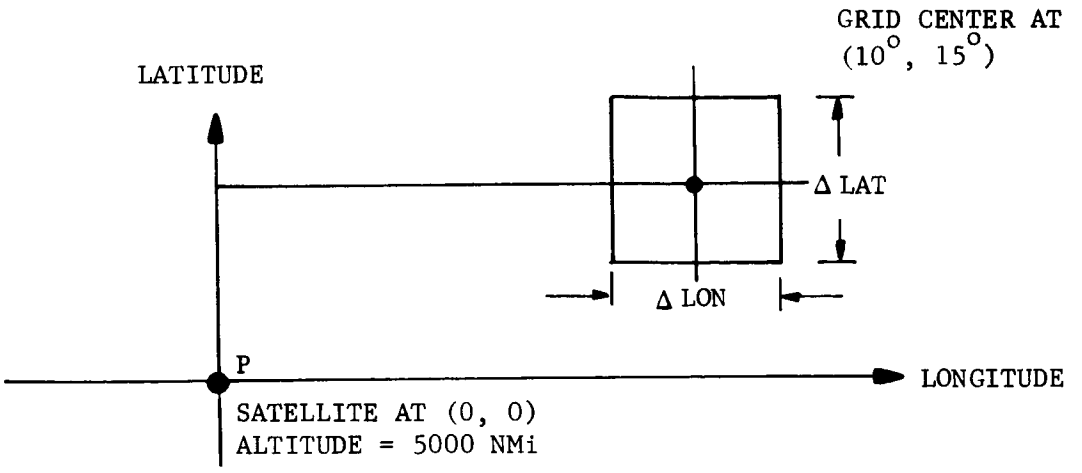

Consider a navigator located anywhere in the shaded area relative to a satellite located at point (P). In Table 4-3 are shown typical errors in latitude and longitude due to the first order approximation assured. The results of the example may be stated as follows:

a. For a realistic grid size (Δ lat = Δ lon = 60 n. mi.). The first order computational error is approximately 1 n. mi. in both co-ordinates.

b. The computation required by the navigator for this type of accuracy is extremely simple (four additions and four multiplications).

c. The accuracy of this method should improve with increasing altitude of the satellite.

d. For navigators located a considerable distance from the sub-satellite point, a navigator-altitude correction would most likely have to be factored into the computation.

In conclusion it is felt that a computation scheme of the type described offers the best accuracy for least amount of navigator computation. The accuracy of this method can be easily improved by either reducing grid size or carrying higher order terms. Both of these improvements still allow the simple first order computational method to be contained within the frame work of the more complex higher order computational scheme.

Table 4-3. Tabulated Differential Position Computation Data

Size of Navigation Grid				Position Error Due to 1st Order Differential Assumption		Time Measurement Error Due to 1st Order Differential Assumption	
Δ Lat		Δ Lon		ε Lat	ε Lon	εS	εD
Degr.	Ft & n.m.	Degr.	Ft & n.m.	Ft & n.m.	Ft & n.m.	μsec	μsec
.001	360	.001	360	.12	.04	1.05 μs	-1.02 μs
. 01	3600	. 01	3600	4	4	10.5 μs	-10.2 μs
. 05	3 nm	. 05	3 nm	18	15	52.3 μs	-50.9 μs
. 1	12 nm	. 1	12 nm	165	92	99.5 μs	-218 μs
. 5	30 nm	. 5	30 nm	.3 nm	.25 nm	.518 ms	-.504 ms
1.0	60 nm	1.0	60 nm	1.3 nm	1 nm	1.03 ms	-.997 ms
5.0	300 nm	5.0	300 nm	33 nm	26.5 nm	4.7 ms	-4.5 ms

4.5 MISCELLANEOUS

A few items not previously discussed will be presented here. They may be of interest for special purposes. See Table 4-1 for the conditions governing the cases.

Figures 4-60 thru 4-63 are plots of actual $(t_2 + t_1 - 2t_o)$ and $(t_2 - t_1)$ for the first satellite revolution following time = 0, for the two altitudes of interest (actually $t_o = 0$ also). Considerable symmetry will be noticed between the sum and difference plots. Especially for the high altitude case, for any azimuth Az, sum (Az) = difference (90-Az) very nearly.

In Figures 4-64 thru 4-67 correlation curves are displayed for the relationships between $(t_2 + t_1 - 2t_o)$ and the navigator position component parallel to the orbit plane (in this case latitude), and between $(t_2 - t_1)$ and the component transverse to the orbit plane (i.e. longitude).

Possibly of interest are the satellite elevation angles for the various distances from the subsatellite point as employed in this study:

Subsatellite Distance (n. mi.)	Satellite Altitude (n. mi.)	
	5000	19,311
800	67.8	74.3
1600	47.2	58.9
2400	29.1	43.8
3200	13.2	29.1
4000		15.0

Table 4-4 Satellite Elevation Angles

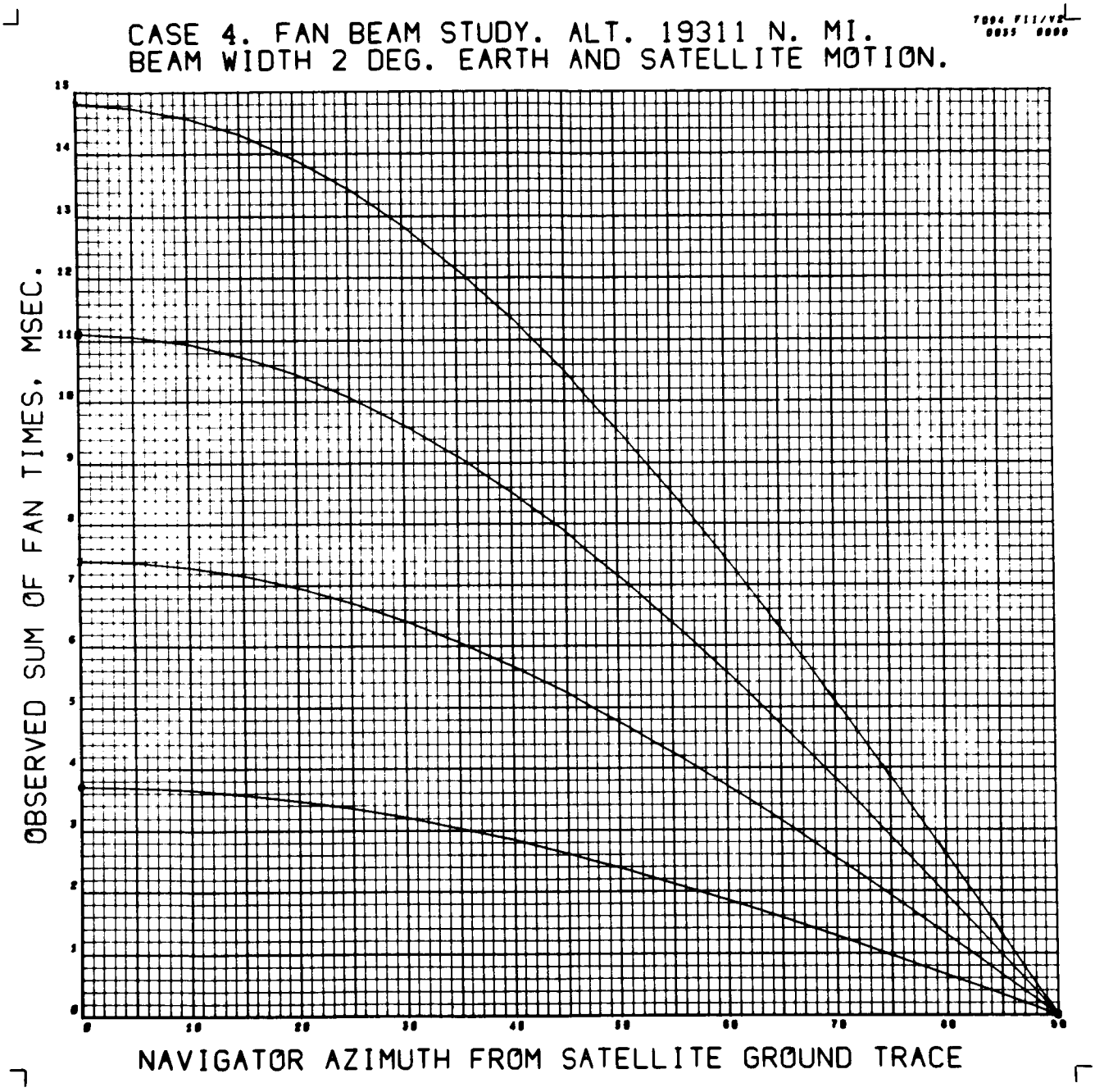
CASE 4. FAN BEAM STUDY. ALT. 19311 N. MI.
BEAM WIDTH 2 DEG. EARTH AND SATELLITE MOTION.
OBSERVED SUM OF FAN TIMES, MSEC.
NAVIGATOR AZIMUTH FROM SATELLITE GROUND TRACE

Figure 4-60

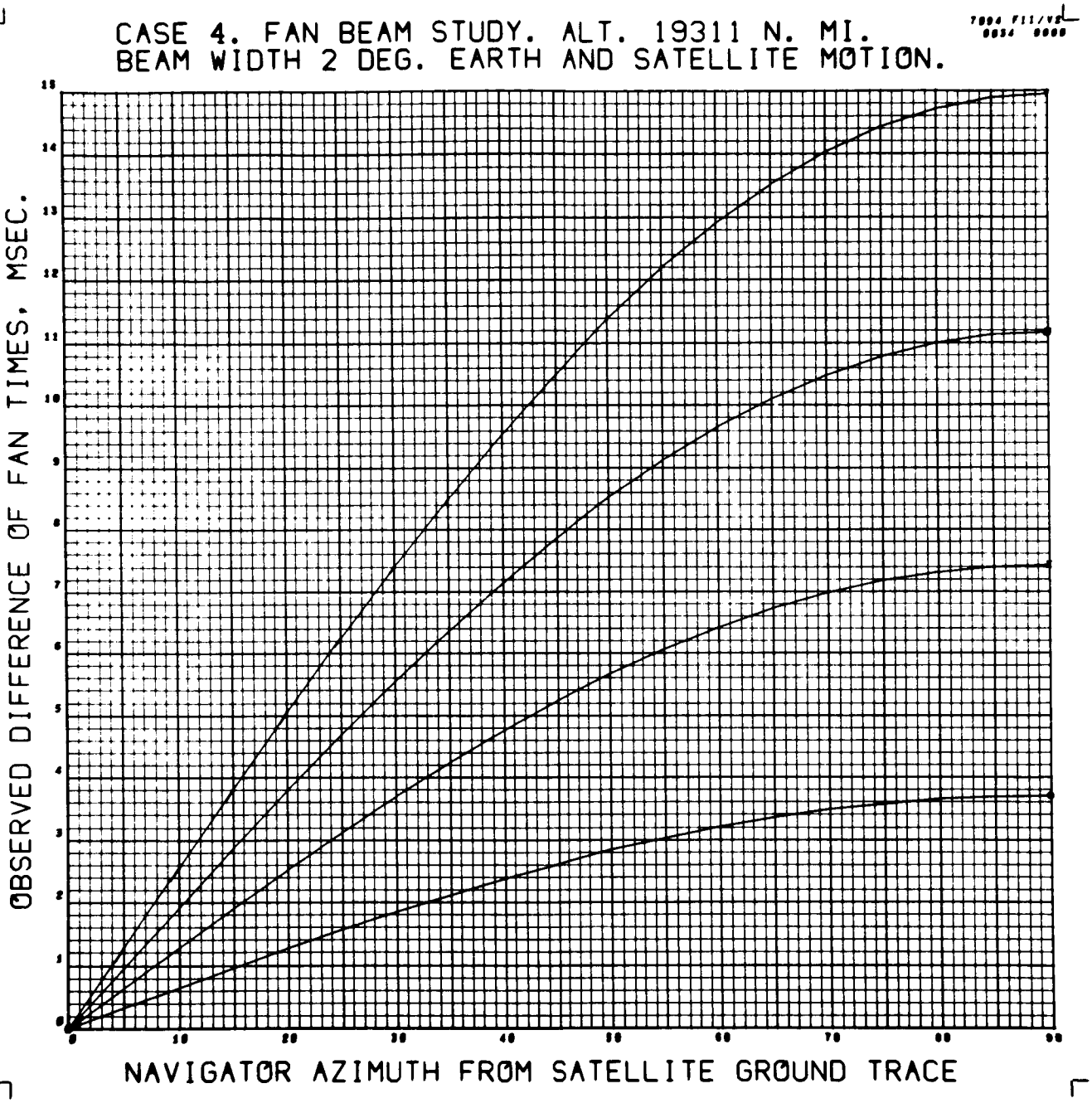
CASE 4. FAN BEAM STUDY. ALT. 19311 N. MI.
BEAM WIDTH 2 DEG. EARTH AND SATELLITE MOTION.
OBSERVED DIFFERENCE OF FAN TIMES, MSEC.
NAVIGATOR AZIMUTH FROM SATELLITE GROUND TRACE

Figure 4-61

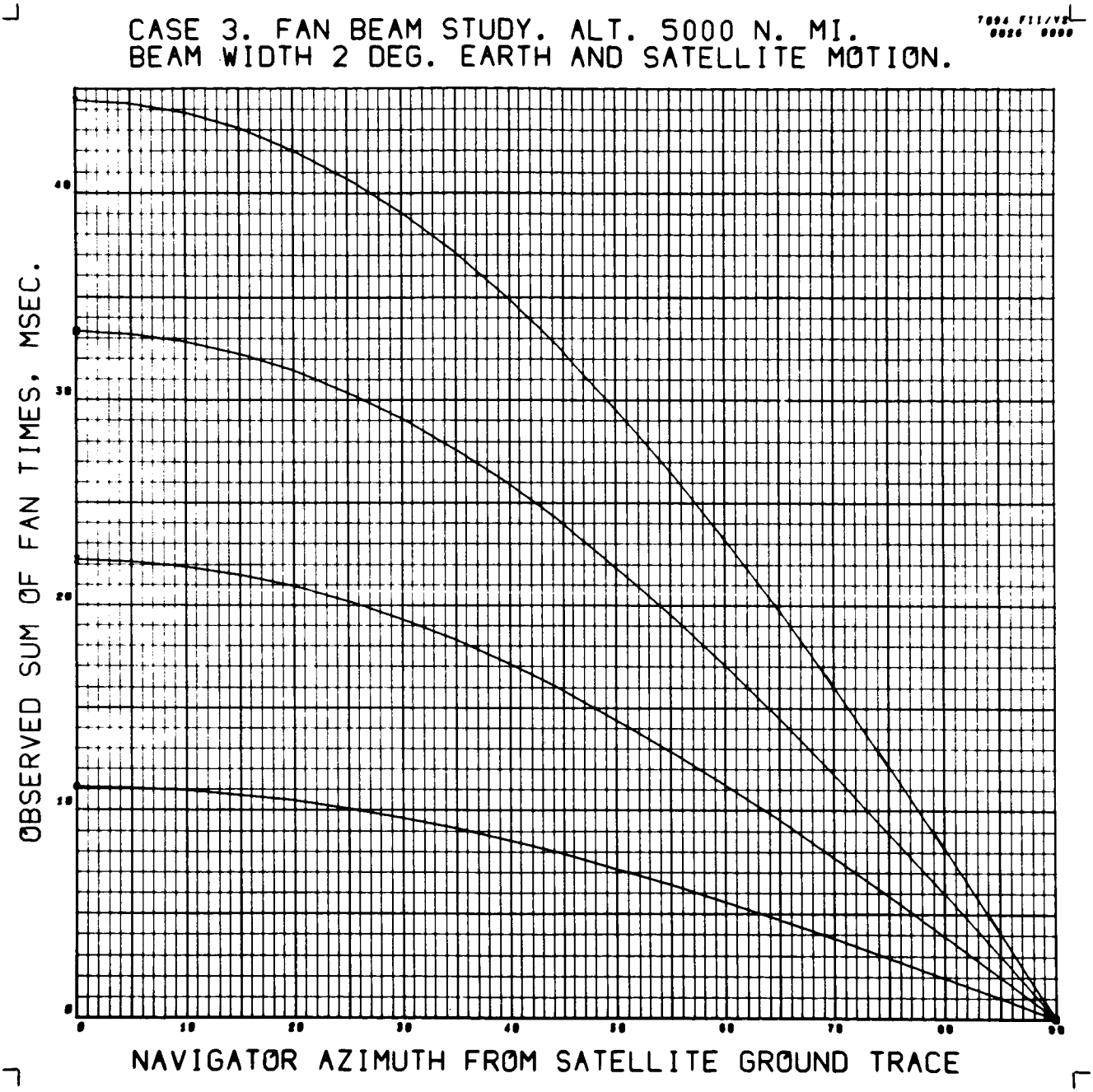
CASE 3. FAN BEAM STUDY. ALT. 5000 N. MI.
BEAM WIDTH 2 DEG. EARTH AND SATELLITE MOTION.
OBSERVED SUM OF FAN TIMES, MSEC.
NAVIGATOR AZIMUTH FROM SATELLITE GROUND TRACE

Figure 4-62

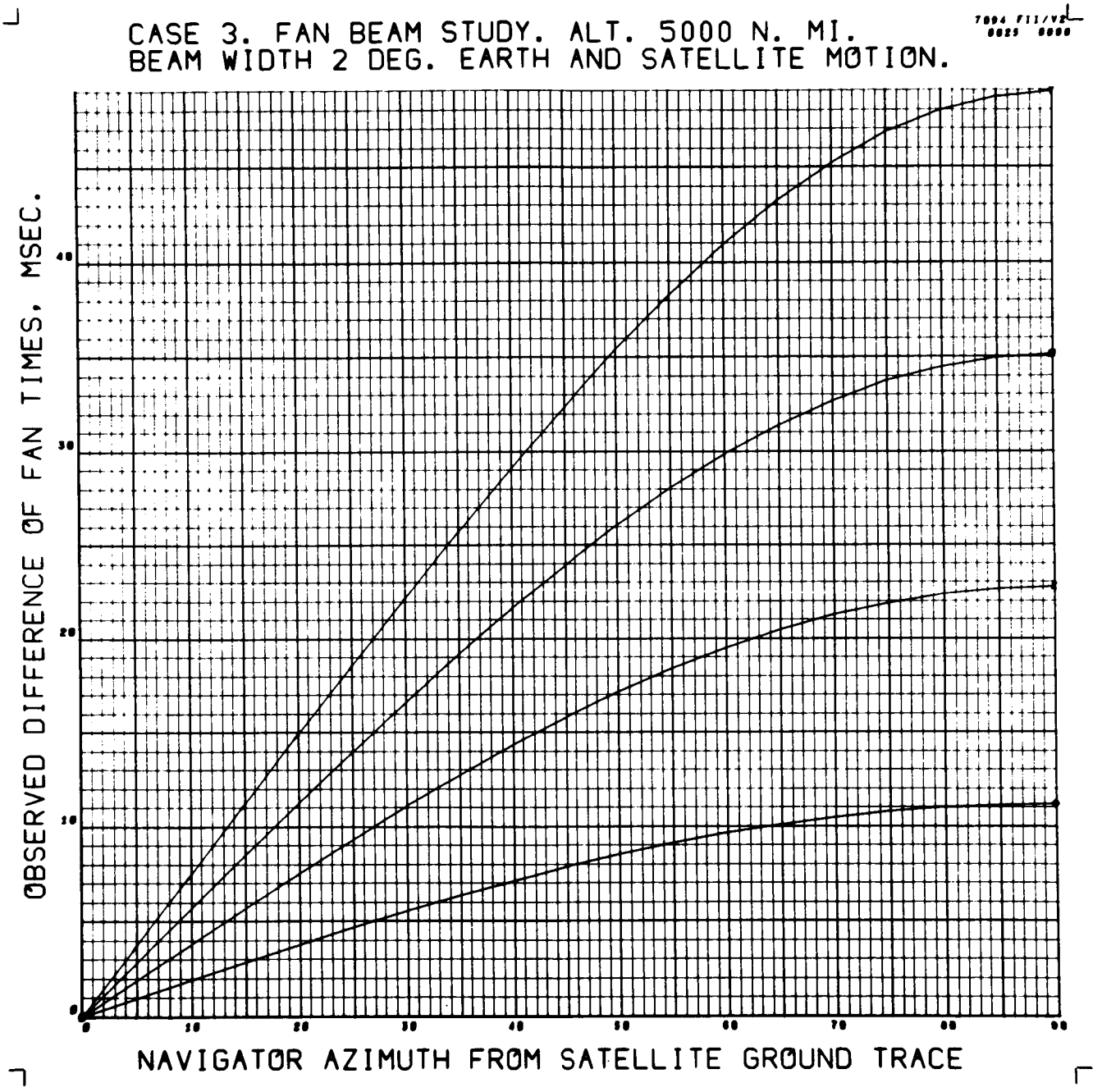
CASE 3. FAN BEAM STUDY. ALT. 5000 N. MI.
BEAM WIDTH 2 DEG. EARTH AND SATELLITE MOTION.
OBSERVED DIFFERENCE OF FAN TIMES, MSEC.
NAVIGATOR AZIMUTH FROM SATELLITE GROUND TRACE

Figure 4-63

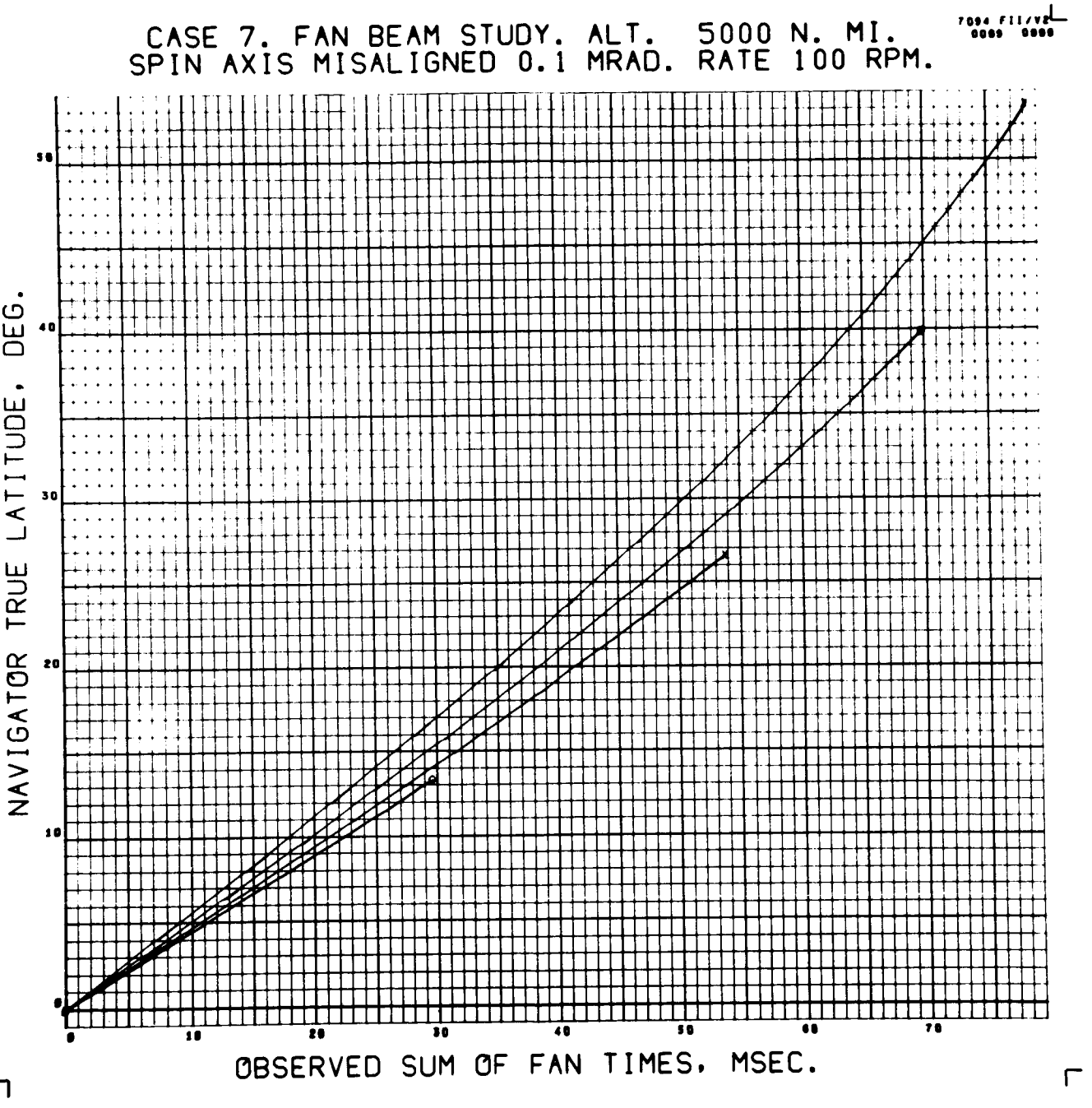
CASE 7. FAN BEAM STUDY. ALT. 5000 N. MI.
SPIN AXIS MISALIGNED 0.1 MRAD. RATE 100 RPM.
NAVIGATOR TRUE LATITUDE, DEG.
0
10
20
30
40
50
0
10
20
30
40
50
60
70
OBSERVED SUM OF FAN TIMES, MSEC.

Figure 4-64

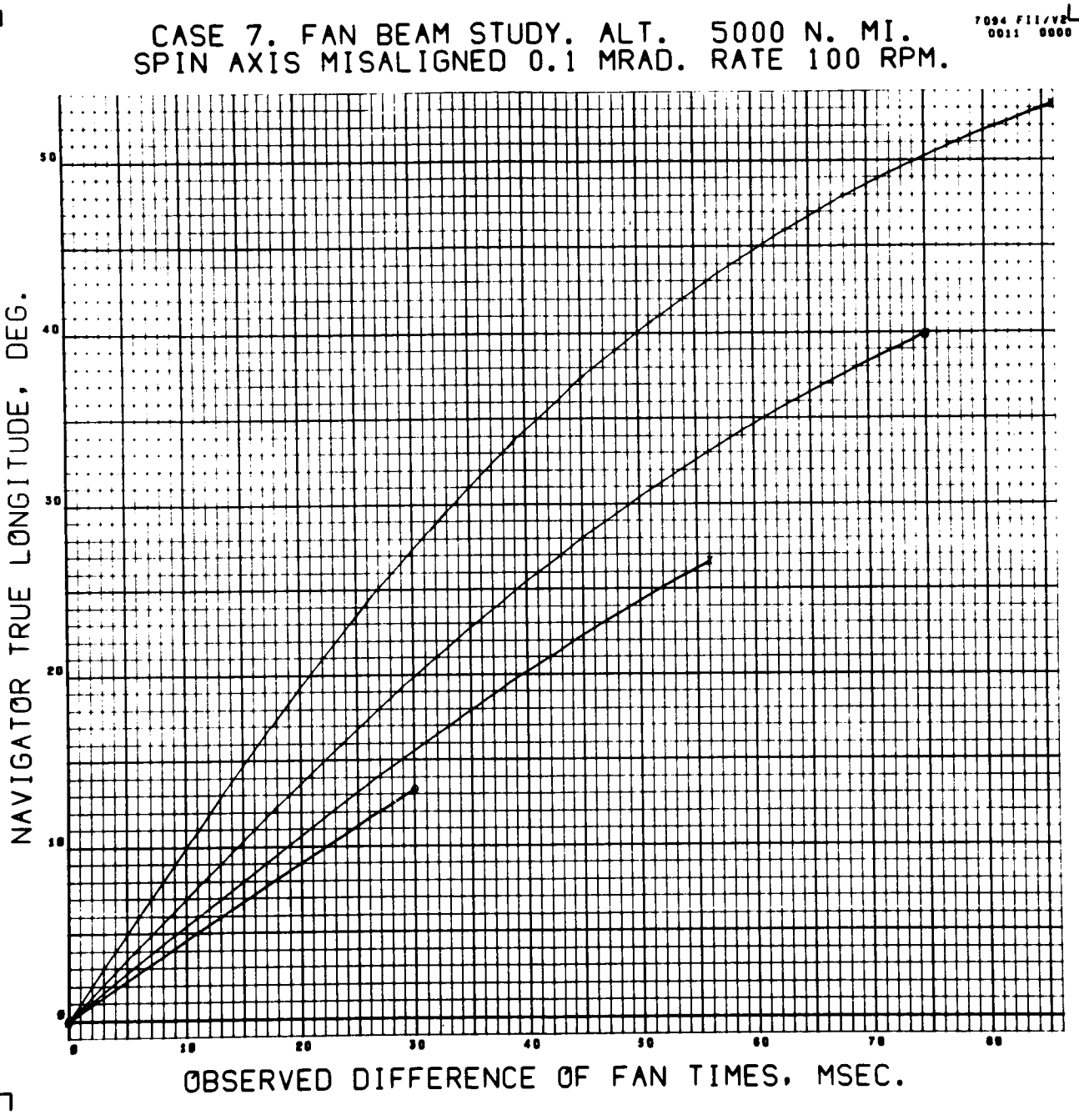
CASE 7. FAN BEAM STUDY. ALT. 5000 N. MI.
SPIN AXIS MISALIGNED 0.1 MRAD. RATE 100 RPM.
7094 FII/VS
0011 0000
NAVIGATOR TRUE LONGITUDE, DEG.
0
10
20
30
40
50
0
10
20
30
40
50
60
70
80
OBSERVED DIFFERENCE OF FAN TIMES, MSEC.

Figure 4-65

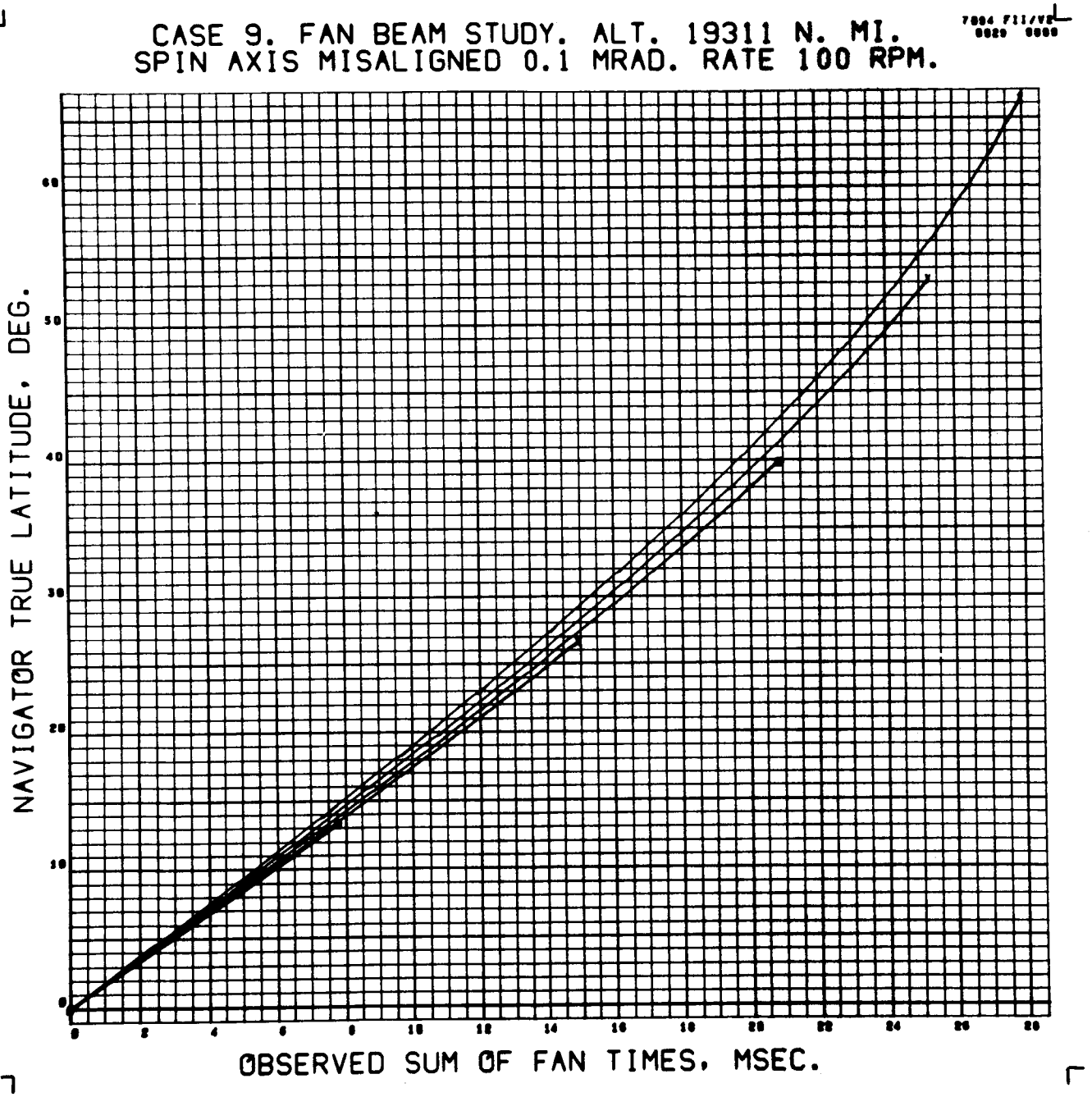
CASE 9. FAN BEAM STUDY. ALT. 19311 N. MI.
SPIN AXIS MISALIGNED 0.1 MRAD. RATE 100 RPM.
NAVIGATOR TRUE LATITUDE, DEG.
OBSERVED SUM OF FAN TIMES, MSEC.

Figure 4-66

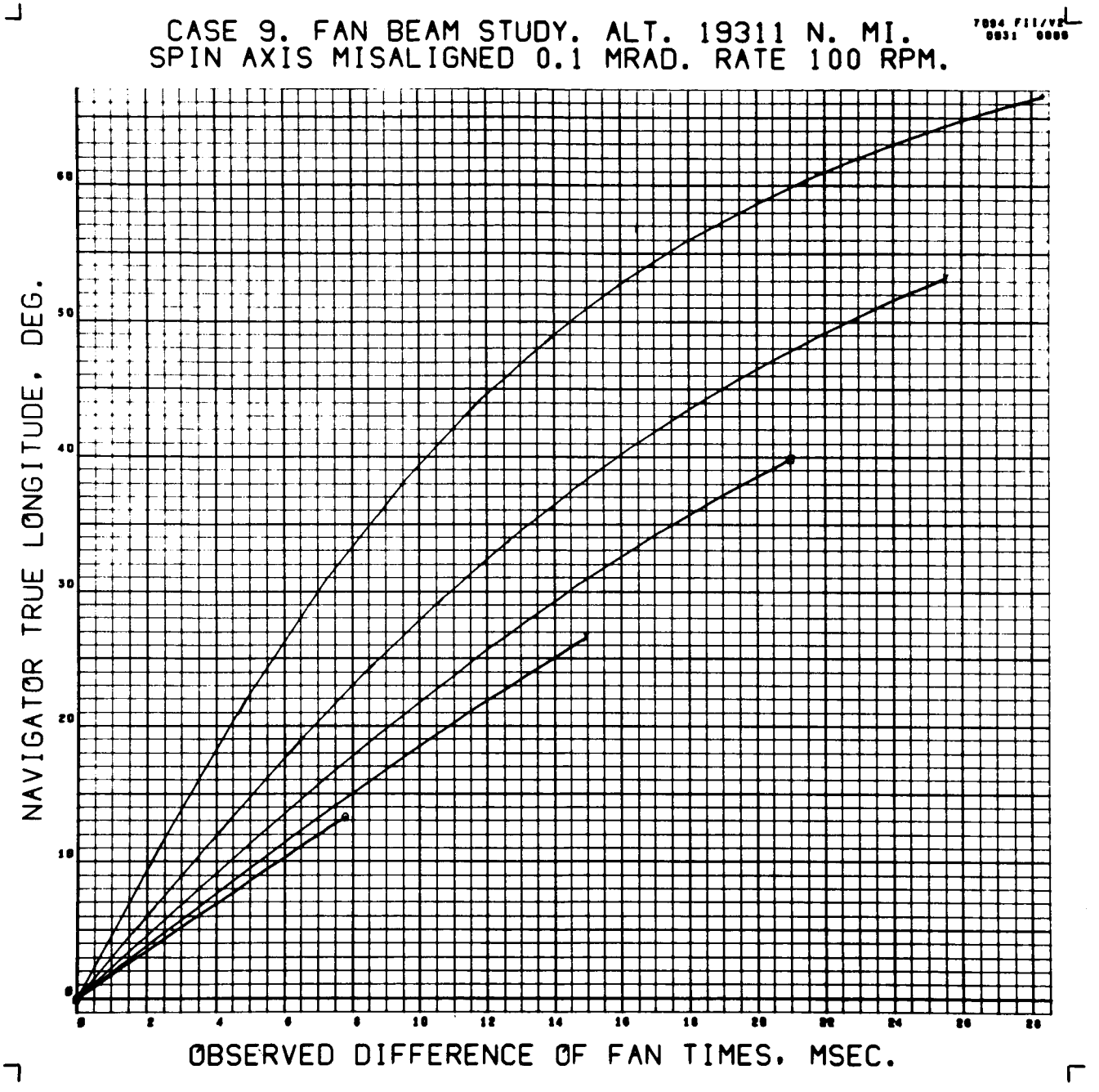
CASE 9. FAN BEAM STUDY. ALT. 19311 N. MI.
SPIN AXIS MISALIGNED 0.1 MRAD. RATE 100 RPM.
NAVIGATOR TRUE LONGITUDE, DEG.
OBSERVED DIFFERENCE OF FAN TIMES, MSEC.

Figure 4-67

SECTION 5

SUPPLEMENTAL ANALYTICAL RESULTS

Three reports which were generated during the course of the Navigation Satellite study are gathered together here. They pertain to: refinements in the navigator's fix determination methods, geometrical relationships existing between satellite rotations and navigator direction, and methods of calibration for estimation of necessary reference vectors. Some differential error analyses partially supplementing the computer results will be found in Section 5.2.

5.1 A NAVIGATOR "FIX" WHICH INCLUDES SATELLITE MOTION AND THE NAVIGATOR'S EARTH ROTATION

The earlier "fix" solutions assumed that the vector from the satellite to the navigator was fixed in direction during the interval which includes the reference pulse and the two intercept times. This new solution lets the satellite move in its orbit and lets the navigator rotate with the earth, including these effects in the solution.

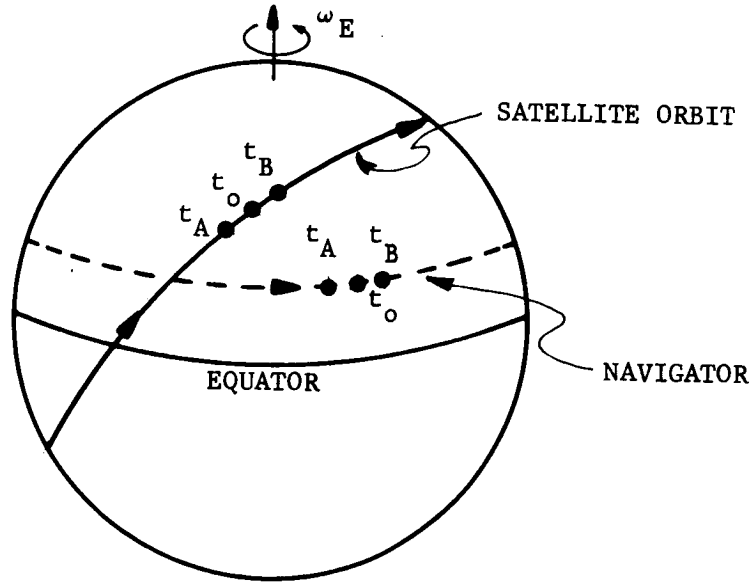

Notation:

t_o	=	time of the reference pulse
t_A	=	intercept time of fan beam A
t_B	=	intercept time of fan beam B
$R_S(t)$	=	satellite position vector at t
$R_N(t)$	=	navigator's position vector at t (to be determined)
$R(t)$	=	satellite-to-navigator vector at t
$\hat{a}$	=	unit normal to fan beam A at t_A
$\hat{b}$	=	unit normal to fan beam B at t_B
r_N	=	navigator's distance from the earth's center
ω_E	=	earth's rate
$T_3(\theta)$	=	rotation through θ about the 3-axis (a 3 x 3 matrix)

The satellite-to-navigator vector at t is identically

$$R(t) = R_N(t) - R_S(t) \tag{60}$$

and the "fix" equations are

$$\begin{aligned} \hat{a} \cdot R(t_A) &= 0 \\ \hat{b} \cdot R(t_B) &= 0 \\ R_N(t) \cdot R_N(t) &= r_N^2, \text{ a constant} \end{aligned} \tag{61}$$

Another form for the first two fix equations is

$$\begin{aligned} \hat{a} \cdot \left[R_N(t_A) - R_S(t_A)\right] &= 0 \\ \hat{b} \cdot \left[R_N(t_B) - R_S(t_B)\right] &= 0 \end{aligned}$$

or

$$\begin{aligned} \hat{a} \cdot R_N(t_A) = \hat{a} \cdot R_S(t_A) &= K_A \\ \hat{b} \cdot R_N(t_B) = \hat{b} \cdot R_S(t_B) &= K_B \end{aligned} \tag{62}$$

The right sides of the last two equations are known since $R_S(t)$ is the satellite's position vector at any time, t, and since $\hat{a}$ and $\hat{b}$ are the known directions of the fan beam normals at t_A and t_B, respectively. The left sides of these equations may be reduced by using the relationship

$$R_N(t) = T_3\left[\omega_E(t - t_o)\right] R_N(t_o) \tag{63}$$

which holds for a stationary (relative to the earth) navigator if inertial coordinates with the first two axes lying in the equatorial plane are used (e.g., equator and equinox of date).

Thus, if we let

$$\begin{aligned} \alpha_A &= \omega_E(t_A - t_o) \\ \alpha_B &= \omega_E(t_B - t_o), \end{aligned} \tag{64}$$

the fix equations become

$$\begin{aligned} \hat{a} \cdot T_3(\alpha_A)R_N(t_o) &= K_A \\ \hat{b} \cdot T_3(\alpha_B)R_N(t_o) &= K_B \\ R_N(t_o) \cdot R_N(t_o) &= r_N^2 \end{aligned} \tag{65}$$

The unknown in these equations is $R_N(t_o)$ which represents the navigator's position vector at the time of the reference pulse. Therefore, if we make the substitutions

$$\begin{aligned} \hat{a}' &= T_3^T(\alpha_A)\hat{a} \\ \hat{b}' &= T_3^T(\alpha_B)\hat{b} \\ X &= R_N(t_o) \end{aligned} \tag{66}$$

the fix equations have the simple-looking form

$$\begin{aligned} \hat{a}' \cdot X &= K_A \\ \hat{b}' \cdot X &= K_B \\ X \cdot X &= r_N^2 \end{aligned} \tag{67}$$

Solution

If $\hat{a}'$ and $\hat{b}'$ are not parallel, we can form a coordinate system whose basis vectors are

$$\begin{aligned} \hat{e}_1 &= \hat{a}' \\ \hat{e}_3 &= \frac{\hat{a}' \times \hat{b}'}{|\hat{a}' \times \hat{b}'|} \\ \hat{e}_2 &= \hat{e}_3 \times \hat{e}_1 \end{aligned} \tag{68}$$

The unknown, X, may be expressed as

$$X = (X\cdot\hat{e}_1)\hat{e}_1 + (X\cdot\hat{e}_2)\hat{e}_2 + (X\cdot\hat{e}_3)\hat{e}_3 \tag{69}$$

where the coefficients, $X\cdot\hat{e}_1$, $X\cdot\hat{e}_2$ and $X\cdot\hat{e}_3$, are to be determined. The first of these coefficients, $X\cdot\hat{e}_1$), is easily determined.

$$X\cdot\hat{e}_1 = X\cdot\hat{a}' = K_A \tag{70}$$

The second coefficient is

$$\begin{aligned} X\cdot\hat{e}_2 &= X \cdot \left\{ \frac{(\hat{a}' \times \hat{b}')}{|\hat{a}' \times \hat{b}'|} \times \hat{a}' \right\} \\ &= X \cdot \left\{ \frac{\hat{b}'(\hat{a}'\cdot\hat{a}') - \hat{a}'(\hat{a}'\cdot\hat{b}')}{|\hat{a}' \times \hat{b}'|} \right\} \\ &= \frac{K_B}{|\hat{a}' \times \hat{b}'|} - \frac{K_A(\hat{a}'\cdot\hat{b}')}{|\hat{a}' \times \hat{b}'|} \end{aligned} \tag{71}$$

The third coefficient is found from equation (67) and equation (71).

$$r_N^2 = (X\cdot\hat{e}_1)^2 + (X\cdot\hat{e}_2)^2 + (X\cdot\hat{e}_3)^2$$

$$r_N^2 = K_A^2 + \left(\frac{K_B - K_A(\hat{a}'\cdot\hat{b}')}{|\hat{a}' \times \hat{b}'|} \right)^2 + (X\cdot\hat{e}_3)^2$$

When the substitution, $|\hat{a}' \times \hat{b}'|^2 + (\hat{a}'\cdot\hat{b}')^2 = 1$, is used we have

$$(X\cdot\hat{e}_3)^2 = r_N^2 - \frac{\left[K_A^2 + K_B^2 - 2K_AK_B(\hat{a}'\cdot\hat{b}')\right]}{|\hat{a}' \times \hat{b}'|^2} \qquad (72)$$

which may be solved for $(X\cdot\hat{e}_3)$ with a sign ambiguity. The choice of sign should be such that

$$R_N(t_o)\cdot R_S(t_o) < |R_S(t_o)|^2$$

or that the navigator is below the satellite.

Equation (69) is the solution for the navigator's position at the time of the reference pulse. In summary:

$$K_A = \hat{a}\cdot R_S(t_A)$$

$$K_B = \hat{b}\cdot R_S(t_B)$$

$$\alpha_A = \omega_E(t_A - t_o)$$

$$\alpha_B = \omega_E(t_B - t_o)$$

$$\left.\begin{aligned}\hat{a}' &= T_3^T(\alpha_A)\,\hat{a}\\ \hat{b}' &= T_3^T(\alpha_B)\,\hat{b}\end{aligned}\right\}\ \text{where } \hat{a} \text{ and } \hat{b} \text{ are expressed in equatorial inertial coordinates}$$

$$\hat{e}_1 = \hat{a}'$$

$$\hat{e}_2 = \frac{\hat{a}' \times \hat{b}'}{|\hat{a}' \times \hat{b}'|} \times \hat{a}'$$

$$\hat{e}_3 = \frac{\hat{a}' \times \hat{b}'}{|\hat{a}' \times \hat{b}'|}$$

$$R_N(t_o) = K_A\hat{e}_1 + \frac{\left[K_B - K_A(\hat{a}' \cdot \hat{b}')\right]\hat{e}_2}{|\hat{a}' \times \hat{b}'|} \pm \sqrt{r_N^2 - \frac{\left[K_A^2 + K_B^2 - 2K_A K_B(\hat{a}' \cdot \hat{b}')\right]}{|\hat{a}' \times \hat{b}'|^2}}\,\hat{e}_3$$

and the sign is chosen to make

$$R_N(t_o) \cdot R_S(t_o) < R_S(t_o) \cdot R_S(t_o)$$

An alternative formation for $R_N(t_o)$ is

$$R_N(t_o) = \frac{1}{|\hat{a}' \times \hat{b}'|^2}\left\{\left[K_A - K_B(\hat{a}' \cdot \hat{b}')\right]\hat{a}' + \left[K_B - K_A(\hat{a}' \cdot \hat{b}')\right]\hat{b}' \pm \sqrt{r_N^2|\hat{a}' \times \hat{b}'|^2 - \left[K_A^2 + K_B^2 - 2K_A K_B(\hat{a}' \cdot \hat{b}')\right]}\,\hat{a}' \times \hat{b}'\right\}$$

5.2 SATELLITE ROTATIONS--SOME GEOMETRICAL RELATIONSHIPS

5.2.1 Introduction

Given a pair of angles describing the direction of a navigator's position relative to a satellite, expressions are derived for the satellite rotations required to bring each of two fan beams to that position. For any prescribed permissible error in fix determination (in nautical miles), the allowable errors in fan beam timing may be calculated from these expressions.

Error-free conditions in satellite antenna mounting and satellite spin are assumed since the objective is only to determine allowable fan beam timing errors as functions of tolerances in fix determination. This is essentially the inverse calculation to that performed by the NavSat Program.

A case from NavSat output is computed "in reverse," using the inverse calculations, and very close agreement is observed. This affords a useful check on the operation of NavSat, as well as upon the inverse calculation equations.

Finally, expressions are given for the direct relationship (given the satellite rotation angles, find the navigator's direction). Some numerical results based on these expressions are also obtained.

5.2.2 Satellite Rotations as Functions of Satellite to Navigator Direction

For present purposes, a single coordinate system suffices--the orbital coordinate system.

Case A. Both Fan Beams Propagated from the Same Side of the Satellite

This is the case currently being simulated by NavSat. The important unit vectors are shown in Figure 5-1.

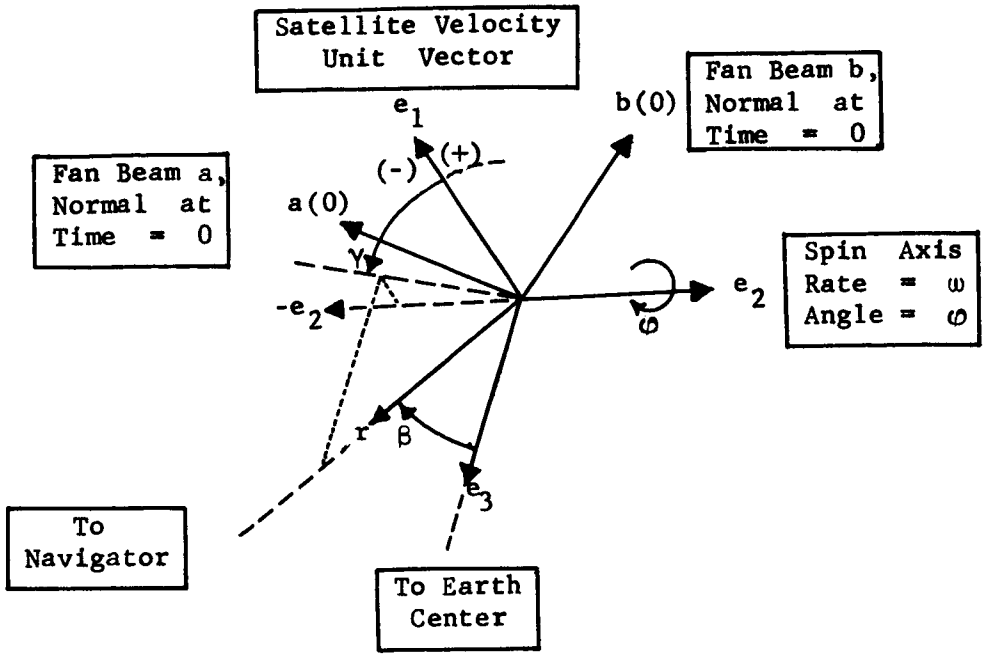

Figure 5-1 Unit Vectors of Interest

Vectors e_1, e_2, e_3 are the orbital system. For simplicity, the fan beam normals a and b are taken in the plane of e_1 and e_2 at time t = 0, with the two fan beams directed downward. The navigator's direction is described by a "co-depression" angle β and an azimuth γ.

Let $k^2 = 1/2$, and t_1, t_2 be the times of maximum energy received by the navigator for fan beams a and b, respectively. The corresponding satellite rotations are

$$\begin{aligned} \varphi_1 &= \omega t_1 \\ \varphi_2 &= \omega t_2, \end{aligned} \tag{73}$$

and the fan beam normals are:

$$\begin{aligned} a(t_1) &= (k\cos\varphi_1,\ -k,\ -k\sin\varphi_1) \\ b(t_2) &= (k\cos\varphi_2,\ k,\ -k\sin\varphi_2). \end{aligned} \tag{74}$$

The direction of the navigator is:

$$\begin{aligned} r &= (\sin\beta\cos\gamma,\ \sin\beta\sin\gamma,\ \cos\beta) \\ &\equiv (\ r_1\ ,\ r_2\ ,\ r_3). \end{aligned} \tag{75}$$

Then

$$\begin{aligned} r\cdot a(t_1) &= kr_1\cos\varphi_1 - kr_2 - kr_3\sin\varphi_1 = 0, \\ r_1\cos\varphi_1 &- r_3\sin\varphi_1 = r_2. \end{aligned} \tag{76}$$

Let $\rho = \sqrt{r_1^2 + r_3^2} \equiv \sqrt{1 - r_2^2}$. For all practical cases,

$r_3 \equiv \cos\beta \neq 0$. Then,

$$\frac{r_1}{\rho}\cos\varphi_1 - \frac{r_3}{\rho}\sin\varphi_1 = \frac{r_2}{\rho}. \tag{77}$$

Let $r_1/\rho \equiv \cos\Psi$, $r_3/\rho \equiv \sin\Psi$, which defines

$$\Psi \equiv \cot^{-1}\left(\frac{r_1}{r_3}\right), \quad 0 \leq \Psi \leq \pi, \tag{78}$$

(since $0 \leq \beta < \pi/2$ and $-\pi \leq \gamma \leq \pi$). Now, from Equation (77)

$$\cos(\varphi_1 + \Psi) = \frac{r_2}{\rho}, \tag{79}$$

whence,

$$\varphi_1 = \cos^{-1}\left(\frac{r_2}{\sqrt{1 - r_2^2}}\right) - \Psi. \tag{80}$$

Entirely similarly, from $r\cdot b(t_2) = 0$ is obtained

$$\varphi_2 = \cos^{-1}\left(\frac{-r_2}{\sqrt{1 - r_2^2}}\right) - \Psi,$$

or

$$\varphi_2 = \pi - \cos^{-1}\left(\frac{r_2}{\sqrt{1 - r_2^2}}\right) - \Psi. \qquad (81)$$

Also,

$$\varphi_1 + \varphi_2 = \pi - 2\Psi. \qquad (82)$$

The inverse cosines could conceivably be taken as positive or negative angles. But, since $0 \leq \Psi \leq \pi$, they should be taken as principal values in $(0, \pi)$ to obtain φ_1 and φ_2 as the <u>closest</u> alignment positions relative to time = 0.

The angle $-\Psi$ in Equations (80) and (81) represents a rotation to bring the two fan beam normals into the plane of r and e_2 in Figure 5-1. The inverse cosines then represent additional rotations to bring the normals into perpendicularity with r.

It may be noticed from Equations (80) and (81) that $|\varphi_2 - \varphi_1| \leq \pi$, or $|t_2 - t_1| \leq \pi/\omega$.

The above derivations suggest an alternate formulation in terms of the sum and difference of the rotation angles, which may be more efficient for computation than use of Equations (78), (80) and (81). This is especially true since in some aspects of the NavSat study, the sum and difference of the fan beam detection times at the navigator position are of interest. These quantities may be expressed in terms of β and γ.

From Equations (82), (78) and (75):

$$\cos(\omega_2 + \omega_1) = \cos(\pi - 2\Psi) = -\cos 2\Psi = 2\sin^2\Psi - 1$$

$$= \frac{2}{\cot^2\Psi + 1} - 1$$

$$= \frac{2r_3^2}{r_1^2 + r_3^2} - 1$$

$$= \frac{r_3^2 - r_1^2}{r_3^2 + r_1^2} .$$

Hence,

$$s = t_2 + t_1 = \pm \frac{1}{\omega} \cos^{-1}\left(\frac{\cos^2\beta - \sin^2\beta\cos^2\gamma}{\cos^2\beta + \sin^2\beta\cos^2\gamma}\right) . \qquad (83)$$

Inspection of Equations (82), (78) and (75) shows that the (+) sign should be used if $\cos\gamma \geq 0$, i.e., if $|\gamma| \leq \pi/2$. Otherwise, the (-) sign is used.

From Equations (80) and (81)

$$\omega_2 - \omega_1 = \pi - 2\cos^{-1}\left(\frac{r_2}{\sqrt{1 - r_2^2}}\right) . \qquad (84)$$

Using the identity $\cos 2x = 1 - 2\sin^2 x$,

$$\cos(\omega_2 - \omega_1) = 2\left(1 - \frac{r_2^2}{1 - r_2^2}\right) - 1$$

$$= 1 - \frac{2r_2^2}{1 - r_2^2} = \frac{1 - 3r_2^2}{1 - r_2^2}$$

$$= \frac{1 - 3(1 - r_3^2 - r_1^2)}{r_3^2 + r_1^2}$$

$$= 3 - \frac{2}{r_3^2 + r_1^2} .$$

Then,

$$d = t_2 - t_1 = \pm \frac{1}{\omega} \cos^{-1}\left(3 - \frac{2}{\cos^2\beta + \sin^2\beta\cos^2\gamma}\right). \tag{85}$$

Inspection of Equations (84) and (75) shows that the (+) sign should be used if $\sin\gamma \geq 0$, i.e., if $\gamma \geq 0$. Otherwise, the (-) sign is used.

In both Equations (83) and (85), the principal values of the inverse cosines should be used.

Of course, from Equations (83) and (85), t_1, t_2 and/or φ_1, φ_2 are simply computed:

$$\begin{aligned} t_1 &= \tfrac{1}{2}(s - d) \\ t_2 &= \tfrac{1}{2}(s + d) \\ \varphi_1 &= \tfrac{1}{2}(s - d)\omega \\ \varphi_2 &= \tfrac{1}{2}(s + d)\omega. \end{aligned} \tag{86}$$

Case B. The Two Fan Beams Propagated from Opposite Sides of the Satellite

This type of antenna mounting would allow the "up" fan beam to be turned off while the "down" fan beam is on. The only change in Figure 5-1 is to assume fan beam a normal as before (beam downward), and fan beam b normal directed oppositely to a (with beam upward). The equation for φ_1 will be exactly as before, Equation (80). Also, Equation (78) for Ψ still holds.

At time t_2,

$$b(t_2) = (-k \cos \varphi_2,\ k,\ k \sin \varphi_2). \tag{87}$$

This leads to

$$r_1\cos\varphi_2 - r_3\sin\varphi_2 = r_2,$$

and

$$\cos(\varphi_2 + \Psi) = \frac{r_2}{\rho},$$

which is of the same form as the corresponding equation for φ_1, Equation (80). (Indeed, when normal a is perpendicular to r, so is normal b.) The negative inverse cosine should be taken to obtain the alternate alignment position:

$$\varphi_2 = -\cos^{-1}\left(\frac{r_2}{\sqrt{1 - r_2^2}}\right) - \Psi. \tag{88}$$

Also,

$$\varphi_1 + \varphi_2 = -2\Psi. \tag{89}$$

If φ_2 from Equation (88) is less than $-\pi$, a time of alignment closer to time $t = 0$ may be obtained by replacing φ_2 by $\varphi_2 + 2\pi$.

Finally,

$$\varphi_2 - \varphi_1 = -2\cos^{-1}\left(\frac{r_2}{\sqrt{1 - r_2^2}}\right). \tag{90}$$

If $r_2 \geq 0$, $|\varphi_2 - \varphi_1| \leq \pi$, or $|t_2 - t_1| \leq \pi/\omega$.

If $r_2 < 0$, $|\varphi_2 - \varphi_1| > \pi$, but by replacing φ_2 by $\varphi_2 + 2\pi$,

$|\varphi_2 + 2\pi - \varphi_1| \leq \pi$. This manipulation corresponds simply to the navigator's choosing, from the sequence of fan beam detections, a pair for which $|t_2 - t_1|$ is minimal.

From the two cases discussed above, an obvious necessary relationship is

$$r_2^2 \leq 1 - r_2^2$$

$$r_2^2 \leq \tfrac{1}{2} \tag{91}$$

$$\sin^2\beta \sin^2\gamma \leq \tfrac{1}{2}.$$

This defines the region of navigator positions which have access to the satellite for navigation.

5.2.3 Differential Relations

To obtain navigator position differentials, refer to Figure 5-2, below.

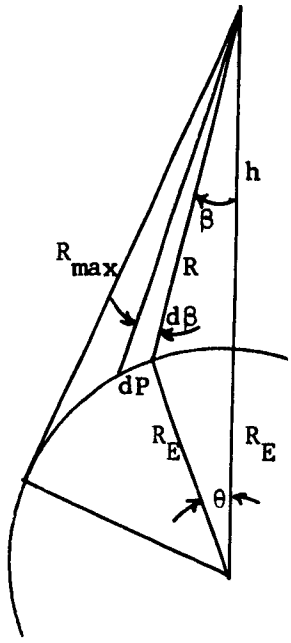

Figure 5-2 Position Vectors

The line R represents the distance from satellite to navigator. Lines R and h are taken in the plane of the paper.

$$R^2 = (R_E + h)^2 + R_E^2 - 2R_E(R_E + h)\cos\theta \qquad (92)$$

$$R_E^2 = (R_E + h)^2 + R^2 - 2R(R_E + h)\cos\beta \qquad (93)$$

$$R\sin\beta = R_E\sin\theta. \qquad (94)$$

Differentiating Equations (92), (93):

$$R\frac{dR}{d\beta} = R_E(R_E + h)\sin\theta\,\frac{d\theta}{d\beta} \qquad (95)$$

$$0 = R\frac{dR}{d\beta} - (R_E + h)\cos\beta\,\frac{dR}{d\beta} + R(R_E + h)\sin\beta \qquad (96)$$

$$R\frac{dR}{d\beta} = \frac{R^2(R_E + h)\sin\beta}{(R_E + h)\cos\beta - R}$$

Using Equations (95), (94):

$$d\theta = \frac{(R_E + h)R^2\sin\beta}{(R_E + h)R_E\sin\theta}\ \frac{1}{(R_E + h)\cos\beta - R}\,d\beta$$

$$= \frac{R}{(R_E + h)\cos\beta - R}\,d\beta$$

Employing Equation (93):

$$d\theta = \frac{2R^2}{(R_E + h)^2 - R_E^2 - R^2}\,d\beta. \qquad (97)$$

Then the position change is

$$dP_1 = R_E d\theta = \frac{2R_E R^2}{(R_E + h)^2 - R_E^2 - R^2}\,d\beta, \qquad (98)$$

which may be written

$$dP_1 = \frac{2R_E}{\left(\frac{R_{max}}{R}\right)^2 - 1}\,d\beta.$$

Recalling the definition of γ, an obvious approximate position change with γ is

$$dP_2 = R\sin\beta\, d\gamma. \qquad (99)$$

For the comparisons with computer output, the differentials of r_1, r_2 and r_3, defined by Equations (75), will be needed.

$$\begin{aligned} dr_1 &= \cos\beta\cos\gamma\, d\beta - \sin\beta\sin\gamma\, d\gamma \\ dr_2 &= \cos\beta\sin\gamma\, d\beta + \sin\beta\cos\gamma\, d\gamma \\ dr_3 &= -\sin\beta\, d\beta. \end{aligned} \qquad (100)$$

5.2.4 Comparisons With NavSat Output

A set of calculations was made using the equations which have been described, for comparison with a NavSat run having the following inputs:

A. Satellite

1.	Altitude	= 5000 nautical miles.
2.	Latitude	= 0 degrees.
3.	Longitude	= 0 degrees.
4.	Velocity Azimuth	= 0 degrees, (polar orbit).
5.	Spin Rate	= 18.849555 radian/second.

B. Navigator

1.	Altitude	= 0 nautical miles.
2.	Latitude	= 0 degrees.
3.	Longitude	= 40 degrees.
4.	Motion Relative to Earth	= 0 nautical miles per hour.

Because of the navigator computation method assumed in NavSat, earth and satellite motion and finite fan beam width caused errors in the navigator's estimation of fan beam passage times. These, of course, led to errors in estimation of position.

Starting with the computer output of position error, the "reverse" calculations were performed to compute the timing errors. The latitude error (corresponding to a γ error) was negligible. The longitude (or β) error was (see Figure 5-2).

$$dP = -2.6575 \text{ km.}$$

Using Equation (92), with $\theta = 40^{\circ}$,

$$R = 11{,}451.201 \text{ km.}$$

Also,

$$R_{max} = 14{,}212.502 \text{ km.}$$

From Equation (98):

$$d\beta = \frac{(1.2411364)^2 - 1}{12756}(-2.6575)$$

$$= -.000112587 \text{ radian.}$$

First, the correct φ_1 and φ_2 are calculated. From Equation

$$\sin\beta = \frac{6378}{11,451.201}(.6427876097)$$

$$= .3580148259$$

$$\cos\beta = .9337159013.$$

Also,

$$\sin\gamma = 1.0$$
$$\cos\gamma = 0.0$$

For r_1, r_2, and r_3, from Equations (75):

$$r_1 = 0$$
$$r_2 = .3580148259$$
$$r_3 = .9337159013.$$

Then, from Equation (78) the phase angle is

$$\Psi = \cot^{-1}\left(\frac{0}{r_3}\right)$$

$$= \frac{\pi}{2},$$

And from Equations (80), (82):

$$\varphi_1 = \cos^{-1}\left(\frac{.3580148259}{.9337159013}\right) - \frac{\pi}{2}$$

$$= \cos^{-1}(.383430147) - \frac{\pi}{2}$$

$$= 67.453684^\circ - 90^\circ.$$

$$= -22.546316^\circ$$

$$\varphi_2 = \pi - \pi - \varphi_1 = 22.546316^\circ.$$

These are the values φ_1 and φ_2 should have. Next, the incorrect values, as used by the navigator are calculated.

For $d\beta = -112.587\mu rad$, from Equation (100):

$$\begin{aligned} dr_1 &= 0 \\ dr_2 &= -.9337159013(.000112587) \\ &= -.000105124 \\ dr_3 &= .3580148259(.000112587) \\ &= .000040308. \end{aligned}$$

The perturbed values of r_1, r_2 and r_3 are

$$\begin{aligned} \tilde{r}_1 &= 0 \\ \tilde{r}_2 &= r_2 + dr_2 = .3579097019 \\ \tilde{r}_3 &= r_3 + dr_3 = .9337562093. \end{aligned}$$

Angle Ψ is not changed:

$$\tilde{\Psi} = \Psi = \frac{\pi}{2}.$$

The perturbed values of φ_1 and φ_2 are

$$\begin{aligned} \tilde{\varphi}_1 &= \cos^{-1}\left(\frac{.3579097019}{.9337562093}\right) - \frac{\pi}{2} \\ &= 67.461695^\circ - 90^\circ \\ &= -22.538305^\circ \\ \tilde{\varphi}_2 &= -\tilde{\varphi}_1 = 22.538305^\circ. \end{aligned}$$

For fan beam a, the rotation error is

$$\begin{aligned} d\varphi_1 = \tilde{\varphi}_1 - \varphi_1 &= -22.538305^\circ + 22.546316^\circ \\ &= .008011^\circ, \end{aligned}$$

and the timing error is

$$\begin{aligned} dt_1 &= \frac{1}{\omega} d\varphi_1 = \frac{.008011(.017453293)}{18.849555} \\ &= .000007418 \text{ second} \\ &= 7.418 \ \mu sec. \end{aligned}$$

Of course, the fan beam b timing error is -7.418 μseconds.

All of the above values agree closely with the values from the NavSat output. A summary is given in the following tabulation (for fan beam a).

ITEM	FROM PRESENT EQUATIONS	FROM NAVSAT OUTPUT
dP		- 2.6575 km
R	11,451.201 km	11,451.302 km
$d\beta$	-112.587 μrad	-112.684 μrad
Ψ	90.0 deg	90.0 deg
φ_1	- 22.546316 deg	-22.546948 deg
$\tilde{\varphi}_1$	- 22.538305 deg	-22.538926 deg
$d\varphi_1$	.008011 deg	.008022 deg
dt_1	7.418 μsec	7.428 μsec

5.2.5 Satellite to Navigator Direction as a Function of Satellite Rotations

Case A. Both Fan Beams Propagated From the Same Side of the Satellite

From Equation (76), and the analogous equation for fan beam b:

$$\begin{aligned} \cos\varphi_1 \frac{r_1}{r_3} - \frac{r_2}{r_3} &= \sin\varphi_1 \\ \cos\varphi_2 \frac{r_1}{r_3} + \frac{r_2}{r_3} &= \sin\varphi_2. \end{aligned} \tag{101}$$

Solving for r_1/r_3 and r_2/r_3 by Cramer's Rule:

$$\frac{r_1}{r_3} = \cot\Psi = \frac{\sin\varphi_1 + \sin\varphi_2}{\cos\varphi_1 + \cos\varphi_2} = \tan\tfrac{1}{2}(\varphi_1 + \varphi_2) \tag{102}$$

$$\Psi = \frac{\pi}{2} - \tfrac{1}{2}(\varphi_2 + \varphi_1) + 2n\pi \tag{103}$$

where n is an integer, chosen to make $0 \le \Psi \le \pi$.

$$\frac{r_2}{r_3} = \frac{\sin(\varphi_2 - \varphi_1)}{\cos\varphi_1 + \cos\varphi_2} = \frac{\sin\tfrac{1}{2}(\varphi_2 - \varphi_1)}{\cos\tfrac{1}{2}(\varphi_2 + \varphi_1)} \tag{104}$$

Then, from Equations (75):

$$\gamma = \tan^{-1}\left(\frac{r_2}{r_1}\right) = \tan^{-1}\left[\frac{\sin(\varphi_2 - \varphi_1)}{\sin\varphi_2 + \sin\varphi_1}\right] = \tan^{-1}\left[\frac{\sin\tfrac{1}{2}(\varphi_2 - \varphi_1)}{\sin\tfrac{1}{2}(\varphi_2 + \varphi_1)}\right] \tag{105}$$

$$\beta = \tan^{-1}\left(\sqrt{\left(\frac{r_1}{r_3}\right)^2 + \left(\frac{r_2}{r_e}\right)^2}\right) = \tan^{-1}\left[\frac{\sqrt{\sin^2\tfrac{1}{2}(\varphi_2+\varphi_1) + \sin^2\tfrac{1}{2}(\varphi_2 - \varphi_1)}}{\cos\tfrac{1}{2}(\varphi_2 + \varphi_1)}\right] \tag{106}$$

$$= \tan^{-1}\left[\pm\sqrt{1 + \tan^2\gamma}\,\tan\tfrac{1}{2}(\varphi_2 + \varphi_1)\right] . \tag{107}$$

Of course, $-\pi \le \gamma \le \pi$, and $0 \le \beta < \pi/2$.

The direction of the navigator may be obtained from Equations (74):

$$a(t_1) \times b(t_2) = \tfrac{1}{2}(\sin\varphi_1 + \sin\varphi_2,\ \sin(\varphi_2 - \varphi_1),\ \cos\varphi_1 + \cos\varphi_2). \tag{108}$$

This may also be written:

$$a(t_1) \times b(t_2) = \cos\tfrac{1}{2}(\varphi_2 - \varphi_1)\left[\sin\tfrac{1}{2}(\varphi_2 + \varphi_1),\ \sin\tfrac{1}{2}(\varphi_2 - \varphi_1),\ \cos\tfrac{1}{2}(\varphi_2 + \varphi_1)\right]. \tag{109}$$

The unit vector is

$$r = \frac{1}{\sqrt{1 + \sin^2\tfrac{1}{2}(\varphi_2 - \varphi_1)}}\left[\sin\tfrac{1}{2}(\varphi_2 + \varphi_1), \sin\tfrac{1}{2}(\varphi_2 - \varphi_1), \cos\tfrac{1}{2}(\varphi_2 + \varphi_1)\right]. \tag{110}$$

Of some interest is the angle between $a(t_1)$ and $b(t_2)$ at the time of fix determination. From Equations (74):

$$a(t_1)\cdot b(t_2) = \tfrac{1}{2}\cos\varphi_1\cos\varphi_2 - \tfrac{1}{2} + \tfrac{1}{2}\sin\varphi_1\sin\varphi_2 = \tfrac{1}{2}\left[\cos(\varphi_2 - \varphi_1) - 1\right] . \quad (111)$$

This also may be expressed in terms of the direction angles β and γ. From Equations (80), (81):

$$\cos(\varphi_2 - \varphi_1) - 1 = -\cos 2\left[\cos^{-1}\left(\frac{r_2}{\sqrt{1 - r_2^2}}\right)\right] - 1.$$

Using the trigonometric identity, $\cos 2x = 2\cos^2 x - 1$:

$$\cos(\varphi_2 - \varphi_1) - 1 = \frac{-2r_2^2}{1 - r_2^2} . \quad (112)$$

Hence, using the definition of r_2, Equations (75):

$$a(t_1) \cdot b(t_2) = \frac{-\sin^2\beta\sin^2\gamma}{1 - \sin^2\beta\sin^2\gamma} \leq 0. \quad (113)$$

It can be seen that the angle between $a(t_1)$ and $b(t_2)$ is always $\geq \pi/2$.

Case B. <u>The Two Fan Beams Propagated from Opposite Sides of the Satellite</u>

In this case, the solution for β and γ can not be found from equations analogous to Equations (101), since the equation involving φ_2 is

identical in form to that involving φ_1. However, the equations for Ψ, β and γ can be obtained easily from the corresponding equations in Case A. The b fan beam normal in Case B leads (or lags) the b fan beam normal in Case A by π. Hence, in Equations (102), (105), and (106), the Case B equations are obtained by adding π to φ_2. Thus:

$$\cot\Psi = \tan\left[\frac{\pi}{2} + \tfrac{1}{2}(\varphi_2 + \varphi_1)\right] = -\cot\tfrac{1}{2}(\varphi_2 + \varphi_1) \tag{114}$$

$$\Psi = -\tfrac{1}{2}(\varphi_2 + \varphi_1) + 2n\pi, \tag{115}$$

where n is an integer, chosen to make $0 \le \Psi \le \pi$.

$$\gamma = \tan^{-1}\left[\frac{\sin(\varphi_2 - \varphi_1)}{\sin\varphi_2 - \sin\varphi_1}\right] = \tan^{-1}\left[\frac{\cos\tfrac{1}{2}(\varphi_2 - \varphi_1)}{\cos\tfrac{1}{2}(\varphi_2 + \varphi_1)}\right] \tag{116}$$

$$\beta = \tan^{-1}\left[\frac{\sqrt{\cos^2\tfrac{1}{2}(\varphi_2 + \varphi_1) + \cos^2\tfrac{1}{2}(\varphi_2 - \varphi_1)}}{-\sin\tfrac{1}{2}(\varphi_2 + \varphi_1)}\right] \tag{117}$$

$$= \tan^{-1}\left[\pm\sqrt{1 + \tan^2\gamma}\,\cot\tfrac{1}{2}(\varphi_2 + \varphi_1)\right]. \tag{118}$$

Of course, $-\pi \le \gamma \le \pi$, and $0 \le \beta < \pi/2$.

The other relations in Case A can also be modified by adding π to angle φ_2 to obtain corresponding relations for Case B. This need not be done explicitly, however. Given a negative Case B φ_2 angle ($-2\pi \le \varphi_2 < 0$), it is only necessary to add π and use the Case A equations. Given a positive Case B φ_2 angle ($0 \le \varphi_2 \le 2\pi$), π should be subtracted.

5.2.6 An Alternate Linear Error Analysis

An alternate approach to the estimation of navigator position error is to consider the satellite to navigator unit vector, Equation (110), and obtain a differential relationship between components of this position vector and the time interval and satellite spin rate errors, i. e.

$$\begin{aligned} dr_1 &= f_1\ (dt_1,\ dt_2,\ d\omega) \\ dr_2 &= f_2\ (dt_1,\ dt_2,\ d\omega) \\ dr_3 &= f_3\ (dt_1 1\ dt_2,\ d\omega) \end{aligned} \tag{119}$$

where f_1, f_2, f_3 are linear functions.

From Equations (105) and (106)

$$\begin{aligned} d\theta &= g_1\ (dr_1,\ dr_2,\ dr_3) \\ d\gamma &= g_2\ (dr_1,\ dr_2,\ dr_3) \end{aligned} \tag{120}$$

and from the Equations (98) and (99) a sensitivity matrix can be derived and the navigator position error components, dp_1 and dp_2, can be computed directly from assumed errors in time interval measurement and spin rate measurement. In other words the matrix H can be found such that:

$$\begin{bmatrix} dP_1 \\ dP_2 \end{bmatrix} = H \begin{bmatrix} dt_1 \\ dt_2 \\ d\omega \end{bmatrix} \tag{121}$$

$$\text{where } H = \begin{bmatrix} \frac{\partial P_1}{\partial t_1} & \frac{\partial P_1}{\partial t_2} & \frac{\partial P_1}{\partial \omega} \\ \frac{\partial P_2}{\partial t_1} & \frac{\partial P_2}{\partial t_2} & \frac{\partial P_2}{\partial \omega} \end{bmatrix} \tag{122}$$

and the actual navigator position error is found from:

$$dP = \sqrt{(dP_1)^2 + (dP_2)^2} \tag{123}$$

Before obtaining the sensitivity matrix H two assumptions are needed. First is that the system has a given set of initial conditions. Second is that the error sources considered in the NavSat system which are listed in Section 2.3 produce the errors dt_1 and dt_2 and that dt_1, dt_2, $d\omega$ are the only errors being considered here. Only a brief outline and the final form of the sensitivity matrix H will be listed.

Again referring to Equation (110), it may be written in the following form:

$$R = \frac{1}{\sqrt{1 + \sin^2 \tfrac{1}{2}\omega d}} \left[r_1, r_2, r_3\right] \tag{124}$$

$$\begin{aligned} \text{where } r_1 &= \sin \tfrac{1}{2}\omega s \\ r_2 &= \sin \tfrac{1}{2}\omega d \\ r_3 &= \cos \tfrac{1}{2}\omega s \\ \text{and } s &= t_2 + t_1, \quad d = t_2 - t_1 \end{aligned} \tag{125}$$

Expressing Equations (119), (120), (121) in matrix form and eliminating dr_1, dr_2, dr_3, $d\beta$, and $d\gamma$ through matrix multiplication leads to the following expressions for the entries of H.

$$\frac{\partial P_1}{\partial t_1} = \frac{-\alpha\omega}{2 \sin \beta} \left[\frac{-\sin \tfrac{1}{2}\omega s}{\sqrt{1 + \sin^2 \tfrac{1}{2}\omega d}} + \frac{\cos \tfrac{1}{2}\omega s \sin \omega d}{2 (1 + \sin^2 \tfrac{1}{2}\omega d)^{3/2}} \right] \tag{126}$$

$$\frac{\partial P_1}{\partial t_2} = \frac{+\alpha\omega}{2 \sin \beta} \left[\frac{+\sin \tfrac{1}{2}\omega s}{\sqrt{1 + \sin^2 \tfrac{1}{2}\omega d}} + \frac{\cos \tfrac{1}{2}\omega s \sin \omega d}{2 (1 + \sin^2 \tfrac{1}{2}\omega d)^{3/2}} \right] \tag{127}$$

$$\frac{\partial P_1}{\partial \omega} = \frac{+\alpha}{2 \sin \beta} \left[\frac{d}{2} \frac{\cos \frac{1}{2}\omega s \sin \omega d}{(1 + \sin^2 \frac{1}{2}\omega d)^{3/2}} + \frac{s \sin \frac{1}{2}\omega s}{\sqrt{1 + \sin^2 \frac{1}{2}\omega d}} \right] \tag{128}$$

$$\frac{\partial P_2}{\partial t_1} = \frac{\omega R}{2} \left[\left(\frac{-\cos \frac{1}{2}\omega d}{\sqrt{1 + \sin^2 \frac{1}{2}\omega d}} + \frac{\sin^2 \frac{1}{2}\omega d \cos \frac{1}{2}\omega d}{(1 + \sin^2 \frac{1}{2}\omega d)^{5/2}} \right) \frac{1}{\cos \gamma} + \frac{\tan \gamma}{\tan \beta} \left(\frac{- \sin \frac{1}{2}\omega s}{\sqrt{1 + \sin^2 \frac{1}{2}\omega d}} + \frac{\cos \frac{1}{2}\omega s \sin \omega d}{2(1 + \sin^2 \frac{1}{2}\omega d)^{3/2}} \right) \right] \tag{129}$$

$$\frac{\partial P}{\partial t_2} = \frac{\omega R}{2} \left[\left(\frac{\sin^2 \frac{1}{2}\omega d \cos \frac{1}{2}\omega d}{(1 + \sin^2 \frac{1}{2}\omega d)^{5/2}} + \frac{\cos \frac{1}{2}\omega d}{\sqrt{1 + \sin^2 \frac{1}{2}\omega d}} \right) \frac{1}{\cos \gamma} + \frac{\tan \gamma}{\tan \beta} \left(\frac{- \sin \frac{1}{2}\omega s}{\sqrt{1 + \sin^2 \frac{1}{2}\omega d}} - \frac{\cos \frac{1}{2}\omega s \sin \omega d}{2(1 + \sin^2 \frac{1}{2}\omega d)^{3/2}} \right) \right] \tag{130}$$

$$\frac{\partial P}{\partial \omega} = \frac{R}{2} \left[\frac{d}{\cos \gamma} \left(\frac{\cos \frac{1}{2}\omega d}{\sqrt{1 + \sin^2 \frac{1}{2}\omega d}} - \frac{\sin^2 \frac{1}{2}\omega d \cos \frac{1}{2}\omega d}{(1 + \sin^2 \frac{1}{2}\omega d)^{5/2}} \right) + \frac{\tan \gamma}{\tan \beta} \left[\left(\frac{- s \sin \frac{1}{2}\omega s}{\sqrt{1 + \sin^2 \frac{1}{2}\omega d}} \right) - \frac{d}{2} \left(\frac{\cos \frac{1}{2}\omega s \sin \omega d}{(1 + \sin^2 \frac{1}{2}\omega d)^{3/2}} \right) \right] \right] \tag{131}$$

where $\alpha = \dfrac{2R_E}{\left[\dfrac{R_{Max}}{R}\right]^2 - 1}$

A set of calculations was made using the following initial conditions.

Altitude = 19311 n. mi.

ω = 10.47195 rad/sec

t_1 = 3.85306 μ sec

t_2 = 14.35783 μ sec

ϕ_1 = 2.311835881°

ϕ_2 = 8.614697577°

The matrix H was determined to be

$$H = \begin{bmatrix} -.0690996 & .4170327 & .0002773 \\ -.1257103 & -.0385699 & .0000433 \end{bmatrix}$$

The table that follows lists the changes in position, for the given time interval and spin rate errors. It follows from the method of determination of dP that the error propagation is assumed linear and the table shows the results for constant multiples of the assumed errors dt_1, dt_2, and $d\omega$.

dt_1 (μ sec)	dt_2 (μ sec)	$d\omega$ (μ rad/sec)	dP (n. mi.)	dP For Errors $k(dt_1, dt_2, d\omega)$			
				k = 2	k = 3	k = 4	k = 5
1	1	10	.38709	.77418	1.16127	1.54836	1.93545
1	1	-10	.38245	.76490	1.14735	1.52980	1.91225
1	-1	10	.49107	.98214	1.47321	1.96428	2.45535
1	-1	-10	.49669	.99338	1.49007	1.98676	2.48345

Table 5-1 Differential Error Relations

Of course the two time interval errors and spin rate error could be considered individually. For example having the time interval errors constant and varying the spin rate error.

By examining the coefficients of $d\omega$ which are the elements in the right column of matrix H , it can be concluded that at least for these initial conditions a logical range of error for the spin rate has little effect on the navigator position error.

5.3 APPROXIMATION OF ANGULAR VELOCITY AND FAN BEAM REFERENCE NORMALS BY CONSTANT VECTORS

5.3.1 Introduction

In Section 4.1.3, comparisons were made of the magnitudes of various errors incurred in Fix computation, under two alternative assumptions upon direction of the satellite angular velocity vector, $\hat{\omega}$:

a. $\hat{\omega}$ along the axis of symmetry, $\hat{e}_2$, as of time t_0.
b. $\hat{\omega}$ along the angular momentum vector, $\vec{h}$.

The angular rate, ω, was assumed known. With an assumed precession cone angle, α, of .1 milliradian (angle between the axis of symmetry and the angular velocity vector), errors in position for case (b) were less than one tenth of those for case (a).

The relationship of errors for case (a) and case (b) depends partly upon the assumed moment of inertia ratio, $\rho = 1.1$, as follows.

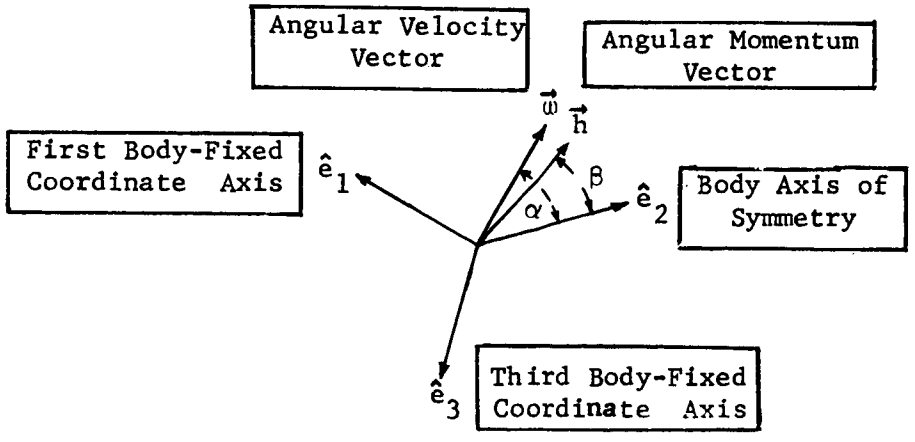

Figure 5-3 Precession Geometry.

From dynamics, referring to Figure 5-3,

$$\rho = \text{moment of inertia ratio}$$

$$\tan \beta = \frac{1}{\rho} \tan \alpha \tag{132}$$

$$\Omega = \frac{\sin \alpha}{\sin \beta} \omega \tag{133}$$

$$C = (\rho - 1) \omega \cos \alpha \tag{134}$$

where Ω is the angular rate of rotation of the $(\hat{e}_2, \vec{\omega})$-plane about $\vec{h}$, and C is the precession rate of $\vec{\omega}$ about $\hat{e}_2$ (as seen by an observer fixed in the body).

For

$\rho = 1.1$ and $\alpha = .1$ m rad:

$$\beta \cong \tan \beta \cong \frac{1}{1.1} .0001$$

$$\beta \cong .0909 \text{ m rad.} \tag{135}$$

$$\alpha - \beta \cong .1 - .0909 = .0091 \text{ m rad.}$$

$$< .1 \alpha.$$

Thus, the $\vec{h}$ vector lies only about one tenth as "far" from $\vec{\omega}$, when compared to the axis of symmetry $\hat{e}_2$.

Of secondary interest:

$$\Omega \cong \frac{.1}{.0909} \omega = 1.1 \omega$$

$$C \cong .1 \omega. \tag{136}$$

Since $\hat{\omega}$ rotates about $\hat{h}$, $\hat{h}$ in a sense represents an "average" $\hat{\omega}$. In Section 5.3.2, a least squares procedure is described which should allow estimation of $\hat{h}$ by a calibration station, using the analytical method of fix determination as described in Section 3.7.2. An estimate of the ω magnitude is also found. At the same time, least squares estimates are obtained for "effective (i.e. average) fan beam normals", $\hat{n}_1(t_o)$ and $\hat{n}_2(t_o)$ at the reference pulse times. More on this in the next section.

5.3.2 Least Squares Procedure

The method to be described probably represents a near minimum attack on the calibration requirements for navigation by use of fan beams. No attempt is made to obtain ω, $\hat{\omega}$, $\hat{n}_1(t_o)$ and $\hat{n}_2(t_o)$ accurately as functions of time. Instead, a best fitting average $\vec{\omega}$ (inertially constant over the calibration interval), and best fitting "effective fan beam normals" at the reference pulse times (recognizing the probability of bent antenna slot arrays), are sought.

The best fitting average $\vec{\omega}$, to be calculated, is fairly easily visualized. The analogous concept for $\hat{n}_1(t_o)$ and $\hat{n}_2(t_o)$ will be described with the aid of Figure 5-4.

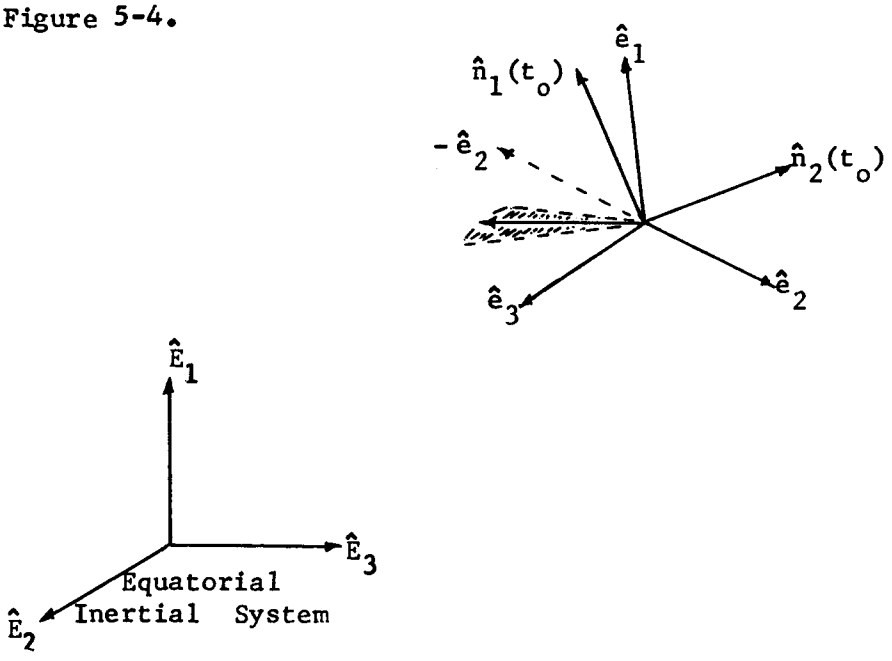

Figure 5-4 Geometry at a Time t_o.

The times t_o, t_1 and t_2 are of course functions of the satellite revolution number, and the least square fitting is to be done over an N-revolution calibration interval. Figure 5-4 represents the geometry at one of the t_o times.

For present purposes, an easily visualized definition of a time t_o is chosen: a time at which the intersection of the two fan beams is perpendicular to the equatorial inertial $\hat{E}_1$- axis. It is assumed that the satellite itself emits a t_o pulse at these times. In Section 5.3.3, the alternative in which the calibration station emits the t_o pulses is described.

Due to precession, this intersection vector at a time t_o will be somewhere in the shaded fan shaped area of Figure 5-4, in a plane parallel to the plane of $\hat{E}_2$ and $\hat{E}_3$. The positions of $\hat{n}_1\ (t_o)$ and $\hat{n}_2\ (t_o)$ on successive revolutions will lie near the positions shown in the figure. An average position for $\hat{n}_1\ (t_o)$ and for $\hat{n}_2\ (t_o)$, in $(\hat{E}_1, \hat{E}_2, \hat{E}_3)$ coordinates, is computed for the calibration interval, by the least squares procedure.

In the following development of the normal equations, all vectors will be assumed written in equatorial inertial coordinates, (E_1, E_2, E_3).

The calibration station is assumed to have accurate knowledge of its geographic location $\vec{r}_n$, and the satellite position $\vec{r}_s$ as a function of time. Hence, at any time t, the satellite-to-station vector $\vec{r}$ is known:

$$\vec{r} = \vec{r}_n - \vec{r}_s \tag{137}$$

The unit vector is

$$\hat{r} = \vec{r}/|\vec{r}| \tag{138}$$

Having a set of values for ω, $\dot{\omega}$, $\hat{n}_1(t_o)$, $\hat{n}_2(t_o)$, the station can compute an <u>apparent</u> $\hat{r}$ using the analytical method of Section 3.7.2, by detecting t_o, t_1 and t_2. This vector will be called $\hat{r}_o$. This computation of the true $\hat{r}$ and apparent $\hat{r}_o$ is repeated for N Revolutions of the satellite. In

this way, two vectors of 2N components each are generated:

$$\vec{s} = \begin{bmatrix} r_{11} \\ r_{12} \\ \hline r_{21} \\ r_{22} \\ \hline \vdots \\ \hline r_{N1} \\ r_{N2} \end{bmatrix} , \qquad \vec{s}_o = \begin{bmatrix} r_{011} \\ r_{012} \\ \hline r_{021} \\ r_{022} \\ \hline \vdots \\ \hline r_{ON1} \\ r_{ON2} \end{bmatrix} \tag{139}$$

(The third components of $\hat{r}$ and $\hat{r}_0$ are not included since they are dependent upon the first and second components.) To simplify notation, define the 7 element state vector σ:

$$\sigma \equiv \begin{bmatrix} \omega \\ \omega_1 \\ \omega_2 \\ n_{11}(t_0) \\ n_{12}(t_0) \\ n_{21}(t_0) \\ n_{22}(t_0) \end{bmatrix} \equiv \begin{bmatrix} \sigma_1 \\ \sigma_2 \\ \sigma_3 \\ \sigma_4 \\ \sigma_5 \\ \sigma_6 \\ \sigma_7 \end{bmatrix} \tag{140}$$

Writing only the linear terms of the Taylor's series, the change in $\vec{s}_o$ due to a change $\Delta\vec{\sigma}$ in $\vec{\sigma}$ is

$$\vec{s}_o(\vec{\sigma}_o + \Delta\vec{\sigma}) \cong \vec{s}_o(\vec{\sigma}_o) + A\Delta\vec{\sigma} , \tag{141}$$

where A is the (2N) x 7 matrix of partial derivatives:

$$A = \begin{bmatrix} \frac{\partial r_{01}}{\partial \sigma_1} & \frac{\partial r_{01}}{\partial \sigma_2} & \frac{\partial r_{01}}{\partial \sigma_3} & \frac{\partial r_{01}}{\partial \sigma_4} & \frac{\partial r_{01}}{\partial \sigma_5} & \frac{\partial r_{01}}{\partial \sigma_6} & \frac{\partial r_{01}}{\partial \sigma_7} \\ \frac{\partial r_{02}}{\partial \sigma_1} & \frac{\partial r_{02}}{\partial \sigma_2} & \frac{\partial r_{02}}{\partial \sigma_3} & \frac{\partial r_{02}}{\partial \sigma_4} & \frac{\partial r_{02}}{\partial \sigma_5} & \frac{\partial r_{02}}{\partial \sigma_6} & \frac{\partial r_{02}}{\partial \sigma_7} \\ \multicolumn{7}{c}{\cdots\cdots\cdots\cdots\cdots\cdots\cdots} \\ & & & \vdots & & & \\ \multicolumn{7}{c}{\cdots\cdots\cdots\cdots\cdots\cdots\cdots} \\ \frac{\partial r_{01}}{\partial \sigma_1} & \frac{\partial r_{01}}{\partial \sigma_2} & \frac{\partial r_{01}}{\partial \sigma_3} & \cdot & \cdot & \cdot & \\ \frac{\partial r_{02}}{\partial \sigma_1} & \frac{\partial r_{01}}{\partial \sigma_2} & \cdot & \cdot & \cdot & & \end{bmatrix}$$

First Satellite Revolution

N'th Satellite Revolution

(142)

Ideally, $\vec{s}_o(\sigma_o + \Delta\sigma) = \vec{s}$. Substituting in **Equation (141)**,

$$A\Delta\vec{\sigma} = (\vec{s} - \vec{s}_o(\vec{\sigma}_o)) + \vec{v}, \tag{143}$$

where a vector of residuals $\vec{v}$ has been included, since in general there is no solution for $\Delta\vec{\sigma}$ with $\vec{v} = \vec{0}$. The least squares solution consists of multiplying **Equation (143) by a diagonal weight matrix B,**

$$BA\Delta\vec{\sigma} = B(\vec{s} - \vec{s}_o(\vec{\sigma}_o)) + B\vec{v}, \tag{144}$$

and finding that $\Delta\vec{\sigma}$ for which the squared length of $B\vec{v}$, is as small as possible. (In the simplest case, B is taken as the identity matrix I.) It may be shown that the solution is given by the "normal equations"

$$(A^T B^2 A)\Delta\vec{\sigma} = A^T B(\vec{s} - \vec{s}_o(\vec{\sigma}_o)) \tag{145}$$

or

$$\Delta\vec{\sigma} = (A^T B^2 A)^{-1} A^T B(\vec{s} - \vec{s}_o(\vec{\sigma}_o)) \tag{146}$$

The solution of Equation (145) is iterated, updating $\vec{\sigma}_o$ each time, until $\Delta\vec{\sigma}$ becomes insignificant.

It remains to show how to compute the partial derivatives for the A-matrix. In the analytical method of Section 3.7.2, within any satellite revolution,

$$\hat{r}_o = \hat{n}_1(t_1) \times \hat{n}_2(t_2)/|\hat{n}_1(t_1) \times \hat{n}_2(t_2)| \tag{147}$$

In Section 3.2 (Equation (13)) it is shown that for constant $\hat{\omega}$ and ω, and for i = 1 and 2:

$$\begin{bmatrix} n_{i1}(t_i) \\ n_{i2}(t_i) \\ n_{i3}(t_i) \end{bmatrix} = \begin{bmatrix} \omega_1 \cos\theta_i, & n_{i1}(t_o)-\omega_1 \cos\theta_i, & \omega_2 n_{i3}(t_o)-\omega_3 n_{i2}(t_o) \\ \omega_2 \cos\theta_i, & n_{i2}(t_o)-\omega_2 \cos\theta_i, & \omega_3 n_{i1}(t_o)-\omega_1 n_{i3}(t_o) \\ \omega_3 \cos\theta_i, & n_{i3}(t_o)-\omega_3 \cos\theta_i, & \omega_i n_{i2}(t_o)-\omega_2 n_{i1}(t_o) \end{bmatrix} \begin{bmatrix} 1 \\ \cos\omega(t_i-t_o) \\ \sin\omega(t_i-t_o) \end{bmatrix} \tag{148}$$

or, in abbreviated notation,

$$\hat{n}_i(t_i) = W_{\hat{\omega}}(\hat{n}_i(t_o))\vec{\tau}_i \tag{149}$$

where

$$\cos\theta_i = \sum_{k=1}^{3} n_{ik}(t_o)\omega_k \tag{150}$$

In Equation (148) it is understood that ω_3 and $n_{i3}(t_o)$ are to be computed from

$$\begin{aligned} \omega_3^2 &= 1-\omega_1^2 - \omega_2^2 \\ n_{i3}^2(t_o) &= 1-n_{i1}^2(t_o) - n_{i2}^2(t_o) \end{aligned} \tag{151}$$

To differentiate Equation (147) note that, for j = 1, ..., 7:

$$|\hat{n}_1(t_1) \times \hat{n}_2(t_2)|^2 = (\hat{n}_1(t_1) \times \hat{n}_2(t_2)) \cdot (\hat{n}_1(t_1) \times \hat{n}_2(t_2))$$

$$\frac{\partial|\hat{n}_1(t_1) \times \hat{n}_2(t_2)|}{\partial\sigma_j} = \hat{f}_o \cdot \frac{\partial(\hat{n}_1(t_1) \times \hat{n}_2(t_2))}{\partial\sigma_j} \tag{152}$$

Then,

$$\frac{\partial\hat{f}_o}{\partial\sigma_j} = \frac{|\hat{n}_1(t_1) \times \hat{n}_2(t_2)|\frac{\partial(\hat{n}_1(t_1) \times \hat{n}_2(t_2))}{\partial\sigma_j} - \hat{f}_o \cdot \frac{\partial(\hat{n}_1(t_1) \times \hat{n}_2(t_2))}{\partial\sigma_j}(\hat{n}_1(t_1) \times \hat{n}_2(t_2))}{|\hat{n}_1(t_1) \times \hat{n}_2(t_2)|^2} \tag{153}$$

(The third components of the vectors $\partial\hat{f}_o/\partial\sigma_j$ are discarded since they are not used in the A-matrix.)

Of course,

$$\frac{\partial(\hat{n}_1(t_1) \times \hat{n}_2(t_2))}{\partial\sigma_j} = \hat{n}_1(t_1) \times \frac{\partial\hat{n}_2(t_2)}{\partial\sigma_j} + \frac{\partial\hat{n}_1(t_1)}{\partial\sigma_j} \times \hat{n}_2(t_2) \tag{154}$$

Finally, from Equation (149) for i = 1 and 2:

$$\frac{\partial\hat{n}_i(t_i)}{\partial\sigma_1} = W_{\hat{\omega}}(\hat{n}_i(t_i))\frac{\partial\vec{r}_i}{\partial\sigma_1}$$

$$\frac{\partial\hat{n}_i(t_i)}{\partial\sigma_j} = \frac{\partial W_{\hat{\omega}}(\hat{n}_i(t_i))}{\partial\sigma_j}\vec{r}_i, \quad j = 2, \ldots, 7 \tag{155}$$

In performing these last differentiations, using Equations (148) and (150), care must be exercised to employ Equations (151) in the case of ω_3 and $n_{i3}(t_o)$:

$$\frac{\partial \omega_3}{\partial \omega_k} = - \frac{\omega_k}{\omega_3} \quad \text{for } k = 1, 2$$

$$\frac{\partial n_{i3}(t_o)}{\partial n_{im}(t_o)} = - \frac{n_{im}(t_o)}{n_{i3}(t_o)} \quad \text{for } m = 1,2 \tag{156}$$

Equations (151) are appropriate for the case of low inclination orbits to assure $\omega_3 \neq 0$ in Equations (156). For high inclinations, ω_1 or ω_2 should be made a dependent variable in Equations (151). This will of course require a modification of the state vector $\vec{\sigma}$.

A few examples of the calculation of the derivatives are:

$$\frac{\partial \vec{\tau}_1}{\partial \sigma_1} \equiv \frac{\partial \vec{\tau}_1}{\partial \omega} = (t_1 - t_o) \begin{bmatrix} 0 \\ - \sin \omega (t_1 - t_o) \\ \cos \omega (t_1 - t_o) \end{bmatrix} \tag{157}$$

$$\frac{\partial \cos \theta_2}{\partial \sigma_3} \equiv \frac{\partial \cos \theta_2}{\partial \omega_2} = n_{22}(t_o) - n_{23}(t_o) \frac{\omega_2}{\omega_3} \tag{158}$$

$$\frac{\partial \hat{n}_1(t_1)}{\partial \sigma_2} = \begin{bmatrix} \cos\theta_1 + n_{11}\omega_1 - n_{13}\dfrac{\omega_1^2}{\omega_3} & , & -\cos\theta_1 - n_{11}\omega_1 + n_{13}\dfrac{\omega_1^2}{\omega_3} & , & n_{12}\dfrac{\omega_1}{\omega_3} \\ n_{11}\omega_2 - n_{13}\dfrac{\omega_1\omega_2}{\omega_3} & , & -n_{11}\omega_2 + n_{13}\dfrac{\omega_1\omega_2}{\omega_3} & , & -n_{11}\dfrac{\omega_1}{\omega_3} - n_{13} \\ -\dfrac{\omega_1}{\omega_3}\cos\theta_1 + n_{11}\omega_3 - n_{13}\omega_1 & , & \dfrac{\omega_1}{\omega_3}\cos\theta_1 - n_{11}\omega_3 + n_{13}\omega_1 & , & n_{12} \end{bmatrix} \vec{\tau}_1 \qquad (159)$$

$$\frac{\partial \hat{n}_2(t_2)}{\partial \sigma_7} = \begin{bmatrix} \omega_1\omega_2 - \dfrac{n_{22}}{n_{23}}\omega_1\omega_3 & , & -\omega_1\omega_2 + \dfrac{n_{22}}{n_{23}}\omega_1\omega_3 & , & -\dfrac{n_{22}}{n_{23}}\omega_2 - \omega_3 \\ \omega_2^2 - \dfrac{n_{22}}{n_{23}}\omega_2\omega_3 & , & 1 - \omega_2^2 + \dfrac{n_{22}}{n_{23}}\omega_2\omega_3 & , & \dfrac{n_{22}}{n_{23}}\omega_1 \\ \omega_2\omega_3 - \dfrac{n_{22}}{n_{23}}\omega_3^2 & , & -\dfrac{n_{22}}{n_{23}} - \omega_2\omega_3 + \dfrac{n_{22}}{n_{23}}\omega_3^2 & , & \omega_1 \end{bmatrix} \vec{\tau}_2 \qquad (160)$$

The symbols n_{ij} are understood to represent $n_{ij}(t_o)$.

Initial approximations for $\hat{\omega}$, $\hat{n}_1(t_o)$ and $\hat{n}_2(t_o)$, to start the least squares iterations, are easily obtained:

- For $\hat{\omega}$, use the normal to the orbit plane.
- For $\hat{n}_1(t_o)$ and $\hat{n}_2(t_o)$ rotate the nominal 45^o vectors fixed in the satellite until their cross product is perpendicular to the equatorial inertial E_1-axis.

The covariance matrix of the state vector $\vec{\sigma}$, $(A^T B^2 A)^{-1}$, may be of use for other purposes.

5.3.3 Two Variations on the Calibration Procedure

The calibration method was presented in terms of data processing by a single calibration station. It may be that the normal equations, Equation (145) so obtained will be numerically ill-conditioned. Least squares normal equations are often ill-conditioned, especially if the data points are closely spaced over a too short total range.

It is not expected that the $A^T B^2 A$ matrix occurring in Equation (145) will be singular (in the mathematical sense) due to use of only one calibration station. Since the angular momentum $\hat{h}$ is essentially fixed in the equatorial inertial coordinate system, the satellite presents a continually changing aspect to the station over N revolutions, because of earth rotation and satellite orbital motion. This should assure a unique solution for the normal equations. (It will be recalled that the elements of the state vector σ are expressed in the equatorial inertial coordinate system.)

The condition of the normal equations, Equation (145), probably may be improved by using data from two (or more) observation stations. No change is needed in the formulation of the normal equations. The $\vec{s}$ and $\vec{s}_o$ vectors are simply extended by inclusion of the elements of the $\hat{r}$ and $\hat{r}_o$ vectors for the additional stations, and the A-matrix is extended by including rows for the additional stations. Of course, the order of the elements in $\vec{s}$ and $\vec{s}_o$, and of the rows of A, is unimportant so long as they are mutually consistent. With multiple stations, perhaps a smaller value of N would be permissible.

Experiment through simulation would show the relative effectiveness of the use of one, two or more stations.

In the formulation of the calibration procedure, it was assumed that the satellite itself would provide a reference pulse each revolution by sensing an inertial reference such as the sun or a star. A method will now be described where in a calibration station may issue the reference pulses. It requires only a very minor change in the basic procedure.

The definition of the reference pulse time $t_o(k)$ for satellite revolution k was shown in Section 3.7.1 to imply periodicity of the $t_o(k)$ pulses (at least in the case of nominal satellite antenna mounting angles):

$$t_o(k) = t_o(0) + 2k\pi/\omega \qquad k = 0, 1, 2, \ldots\ldots \tag{161}$$

where $t_o(0)$ is entirely arbitrary.

In Equation (148), then, wherever the symbol t_o appears, replace it by $t_o(k)$, defined by Equation (161). The only modification of procedure is in the technique of differentiation in Equation (155) as illustrated in Equation (157). It now becomes:

$$\frac{\partial \tau_i}{\partial \sigma_1} = \frac{\partial \tau_i}{\partial \omega} = \left[t_i - t_o(0)\right] \begin{bmatrix} 0 \\ -\sin\omega\left[t_i - t_o(0) - 2k\pi/\omega\right] \\ \cos\omega\left[t_i - t_o(0) - 2k\pi/\omega\right] \end{bmatrix}, \tag{162}$$

for i = 1, 2.

It remains to choose $t_o(0)$. A convenient choice is $t_o(0) = t_1(0)$ for a particular calibration station. At this time, it is known that $\hat{n}_1(t_1)$ is perpendicular to $\hat{r}$. This allows computation of initial approximations for $\hat{n}_1(t_o)$ and $\hat{n}_2(t_o)$ to start the least squares iterations:

- For ω, average several elapsed time differences between successive occurrences of t_1 detections.
- For $\hat{\omega}$, set $\hat{\omega} = \hat{e}_2$ = normal to orbit plane.
- Use $\hat{n}_1(t_1) \cdot \hat{r} = 0$ along with the assumed $\hat{e}_2$ and nominal (45^o) mounting angles to compute guesses for $\hat{n}_1(t_o)$ and $\hat{n}_2(t_o)$. For example,

$$r_1 n_1 + r_2 n_2 + r_3 n_3 = 0$$

$$e_{21} n_1 + e_{22} n_2 + e_{23} n_3 = -.707$$

$$n_1^2 + n_2^2 + n_3^2 = 1.0$$

(or use subrouting ORIENT)

5.3.4 Summary

A method has been given for determining best fitting constant approximations for $\vec{m}$, $\hat{n}_1(t_o)$ and $\hat{n}_2(t_o)$ in the sense of least squares, based upon fan-beam detections by calibration stations, over N satellite revolutions.

The motivation for this development was due mainly to two results from the fan beam study:

a. Considerable bending of the antenna slot arrays is to be expected, even if the arrays are guyed.

b. For a typical moment of inertia ratio, the constant $\hat{h}$ vector lies very close to the varying $\hat{m}$ vector, and yielded acceptable position errors when used as an approximation to $\hat{m}$.

To use the analytical method of fix computation, Section 3.7.2, item (a) above implies a need for "effective fan beam normals" which approximate the bent arrays.

The process described is probably of near minimal complexity, lying a stage below use of the model of a torque-free spinning body with an axis of symmetry. It does not require inclusion of the moment of inertia ratio ρ in the state vector $\vec{\sigma}$. Also, of course, it is not necessary to determine any relationships within the body coordinate system such as fan beam antenna mounting angles or the angular misalignment of $\hat{m}$ with $\hat{e}_2$.

The suitability for navigation purposes, of the reference vectors for $\hat{\omega}$, $\hat{n}_1$ and $\hat{n}_2$ provided by the simple calibration procedure described, depends primarily upon:

- A sufficiently good alignment of the angular velocity vector with the axis of symmetry, accomplished either at spinup or through use of a precession-nutation damper. In cases so far studied a cone angle of .1 milliradian was assumed.

- Requirements as regards navigator distance from the subsatellite point. In the cases studied, when a set of timing data was averaged, the limitation on this distance was about 2000 n. mi. for a satellite altitude of 5000 n. mi., and about 3000 n. mi. for a satellite at synchronous altitude. These figures are based on a "worst case" position determination error of .4 n. mi.

As indicated above, best results are obtained by a navigator when a set of fixes or timing data is averaged. The set should cover one or more precession cycles of the satellite (11 fixes, corresponding to 10 satellite revolutions, for cases studied), to average out periodic bias errors and smooth out noise errors. The calibration stations could easily determine the approximate number of satellite revolutions in a precession cycle by simple experiment.

SECTION 6

REFERENCES

1. Battin, Richard H., Astronomical Guidance, McGraw-Hill Book Company, New York, 1964, pp. 20-21.

2. Synge, John L., and Griffin, Byron A., Principles of Mechanics, McGraw-Hill Book Company, New York, 1959, pp. 380-383.

3. Goldstein, Herbert, Ph. D., Classical Mechanics, Addison-Wesley Publishing Company, Inc., Cambridge, Mass., 1953, pp. 159-163.